Studies in Systems, Decision and Control 78

Chenxiao Cai
Zidong Wang
Jing Xu
Yun Zou

Finite Frequency Analysis and Synthesis for Singularly Perturbed Systems

Springer

Studies in Systems, Decision and Control

Volume 78

Series editor

Janusz Kacprzyk, Polish Academy of Sciences, Warsaw, Poland
e-mail: kacprzyk@ibspan.waw.pl

About this Series

The series "Studies in Systems, Decision and Control" (SSDC) covers both new developments and advances, as well as the state of the art, in the various areas of broadly perceived systems, decision making and control- quickly, up to date and with a high quality. The intent is to cover the theory, applications, and perspectives on the state of the art and future developments relevant to systems, decision making, control, complex processes and related areas, as embedded in the fields of engineering, computer science, physics, economics, social and life sciences, as well as the paradigms and methodologies behind them. The series contains monographs, textbooks, lecture notes and edited volumes in systems, decision making and control spanning the areas of Cyber-Physical Systems, Autonomous Systems, Sensor Networks, Control Systems, Energy Systems, Automotive Systems, Biological Systems, Vehicular Networking and Connected Vehicles, Aerospace Systems, Automation, Manufacturing, Smart Grids, Nonlinear Systems, Power Systems, Robotics, Social Systems, Economic Systems and other. Of particular value to both the contributors and the readership are the short publication timeframe and the world-wide distribution and exposure which enable both a wide and rapid dissemination of research output.

More information about this series at http://www.springer.com/series/13304

Chenxiao Cai · Zidong Wang
Jing Xu · Yun Zou

Finite Frequency Analysis and Synthesis for Singularly Perturbed Systems

Springer

Chenxiao Cai
School of Automation
Nanjing University of Science
and Technology
Nanjing
China

Jing Xu
School of Automation
Nanjing University of Science
and Technology
Nanjing
China

Zidong Wang
Department of Computer Science
Brunel University London
Uxbridge, Middlesex
UK

Yun Zou
School of Automation
Nanjing University of Science
and Technology
Nanjing
China

ISSN 2198-4182 ISSN 2198-4190 (electronic)
Studies in Systems, Decision and Control
ISBN 978-3-319-45404-7 ISBN 978-3-319-45405-4 (eBook)
DOI 10.1007/978-3-319-45405-4

Library of Congress Control Number: 2016948235

Printed on acid-free paper

This Springer imprint is published by Springer Nature
The registered company is Springer International Publishing AG
The registered company address is: Gewerbestrasse 11, 6330 Cham, Switzerland

This book is dedicated to the authors' research teams and families

Preface

From Prandtl's work at the beginning of last century, singular perturbation techniques (SPTs) have become the basic tool of fluid dynamics. Further the approach was extended to other fields of control theory and engineering including aircraft and racket systems, power systems and nuclear reactor systems. The dynamics of singularly perturbed systems (SPSs) contain the interaction of the slow and fast phenomena so that the feedback design often suffers from high dimensionality and ill-posed problem. To alleviate the numerical stiffness, engineers usually use the singular perturbation approach to process the type of system. It lowers the model order by neglecting the fast dynamics and improves the approximation by reintroducing their effects as 'boundary layer' corrections in separate timescales. From the frequency domain perspective, poles farther to imaginary axis are associated with the natural signals that decay faster than those associated with poles closer to the imaginary axis on the left half *s*-plane. The fast modes dominate at the initial stage, and the slow modes are the primary contributors later. The fast/slow dynamics of the state trajectories correspond to the high/low-frequency parts of the system response.

In terms of perspectives of systems and control, Kokotovic and Sannuti had explored the optimal control problem of continuous-time SPSs. Two-point boundary value problem of open-loop systems had been analyzed and been converted controller design problem to solve the Riccati matrix equation of closed-loop systems. The methodology of singular perturbation methods and timescale (SPaTS) techniques, "gifted" with the remedial features of both dimensional reduction and stiffness relief, is considered as a "boon" to systems and control engineers. Thus, the goal of SPaTS techniques is to reduce and simplify the software and hardware implementation. Both the theory and the technique had now attained a maturity level for the continuous-time and discrete-time control systems described by ordinary differential and difference equations, respectively.

However, majority of researches are focused on the time domain state space analysis and synthesis about the SPSs. This book tries to pave a new way to fill the gap between frequency domain transfer function (TF) based results and time domain state space based results. We focus on topics such as H_∞ control, mixed

H_-/H_∞ theory, positive real control, loop-shaping techniques, and quadratic stability, whose specifications are characterized by frequency domain inequalities described by transfer function matrices (TFMs). Due to the existence of the small parasitic parameters in the system model, such control problems usually suffer from high dimensionality and ill-posed problem. Advantage of our results is thereby taken as the unique frequency nature of SPSs to design a combined controller to deal with the original ill-posed problem. We adopt the classical slow–fast decomposition method or descriptor system approaches for SPSs, for convenience of development in the sequel, which is called singular method throughout this monograph, to design ε-independent or ε-dependent controllers for SPSs. It should be noted that our results can be extended to more complex systems with multi-timescale characteristics such as multiagent systems and stochastic systems.

The authors of this monograph are thankful to the whole Singular Perturbation Research Team at Nanjing University of Science and Technology. We would like to thank Dr. Ningfan Zhong, Dr. Ping Mei, Yanlong Huang, Wen Wang, Yan Zhang and Zhaozhen Ding for their contribution and stimulation to write this monograph. We are particularly thankful to Prof. James Lam for his special help when Chenxiao Cai visited the University of Hong Kong.

We owe a debt of gratitude to our families for their sacrifice, understanding and encouragement during the course of preparing this monograph. It is evident that we dedicate this work to our families and to our whole Singular Perturbation Research Team.

All these works in the monograph were supported by the National Natural Science Foundation of China under Grant Nos. 61104064 and 61329301, and by the Fundamental Research Funds for the Central Universities under Grant Nos. 30920140112005 and 30915011105.

Nanjing, China — Chenxiao Cai
London, UK — Zidong Wang
Nanjing, China — Jing Xu
Nanjing, China — Yun Zou
April 2016

Contents

Part II Singularly Perturbed Systems Analysis and Synthesis

Abbreviations

6-DOF	Six-degree-of-freedom
BIBO	Bounded input, bounded output
CKC	Closed kinematic chains
DAE	Differential algebraic equation
DC	Direct current
DOFC	Dynamic output feedback controller
DTC	Direct torque control
FD	Fault detection
FDI	Frequency domain inequality
FF	Finite frequency
FFPR	Finite frequency positive real
FFSPR	Finite frequency strictly positive real
GKYP	General Kalman–Yakubovich–Popov
KYP	Kalman–Yakubovich–Popov
LMI	Linear matrix inequality
LPV	Linear parameter varying
LTI	Linear time invariant
MIMO	Multiple-input and multiple-output
MOFC	Mixed output feedback controller
MPC	Model predictive control
PJA	Prompt jump approximation
PLL	Phase-locked loop
PR	Positive real
SCL	Schur complement lemma
SISO	Single-input and single-output
SOFC	Static output feedback controller
SPaTS	Singular perturbation method and timescale
SPM	Singular perturbation method
SPR	Strictly positive real
SPS	Singularly perturbed system

SPT	Singular perturbation technique
TDI	Time domain inequality
TF	Transfer function
TFM	Transfer function matrix
TTS	Two time-scales
UAV	Unmanned aerial vehicle

Part I
Preliminaries

In this part, some preliminaries will be introduced for the finite frequency control of the SPSs. Here singular perturbation phenomenon and timescale techniques are discussed. The general KYP lemma, the bridge of time domain and frequency domain, is deduced for finite frequency. Some performance indices are confirmed rationally. The preliminaries would serve as a preparation for the analysis and synthesis of the finite frequency SPSs discussed in the next part.

Chapter 1
Singular Perturbation Methods and Time-Scale Techniques

For control engineering, typical tasks can generally be classified into three main categories: optimal regulation, tracking and guidance. To overcome the external disturbances, parameter variations and other uncertainties, control systems should possess a sufficient degree of robustness or insensitivity to extraneous effects. With the development of controller design techniques, oversimplified models cannot accomplish control tasks that require higher precision, such as the taking-off and landing of an unmanned aerial vehicle (UAV). The key feature of SPTs is at the level of modelling, where the system order is increased with both slow and fast dynamics accurately modelled. Using the classical slow-fast decomposition, reduced-order subsystems are obtained, which can attenuate the design difficulty in the oversimplified design. The growth of research activities in the field of SPTs has resulted in the publication of excellent survey papers, reports and proceedings of special conferences, which provides broad space for further applications of SPTs in many fields such as electromechanical networks and power systems, chemical kinetics, nuclear reactors and heat exchangers. In the following, we present some fundamental principles and application methods of SPTs.

1.1 Modelling

Traditional TF and state-space modelling approaches both have been proven to be effective modelling tools for the analysis and design of control systems. The presence of some parasitic parameters may cause some technical difficulties in the traditional modelling methods, which is the source for the increased order and stiffness of systems. The stiffness, resulted from weak coupling among slow and fast modes, gave rise to SPTs, which can be viewed as the basic singular perturbation modelling background [37]. With the development of modelling approaches, some novel SPTs were

C. Cai et al., *Finite Frequency Analysis and Synthesis for Singularly Perturbed Systems*, Studies in Systems, Decision and Control 78,
DOI 10.1007/978-3-319-45405-4_1

developed using δ-operators in [28] and a bond graph model in [17]. For example, Cao introduced a new reduced-order SPS model using the actual value of ε [6]. Next, singularly perturbed phenomena will be discussed in the following.

1.1.1 Singularly Perturbed Phenomena

Let us consider the following system [36] expressed by a linear second-order equation with a parameter $0 < \varepsilon \ll 1$:

$$\varepsilon \ddot{x}(t) + \dot{x}(t) + x(t) = 0,\ x(0) = x_i,\ x(1) = x_f. \tag{1.1}$$

Evidently, as $\varepsilon \to 0$, either from positive or negative values, we can obtain

$$\lim_{\varepsilon \to 0_+} x(t, \varepsilon) = x_f \exp(1 - t),\ 0 < t \leqslant 1,$$
$$\lim_{\varepsilon \to 0_-} x(t, \varepsilon) = x_i \exp(-t),\ 0 \leqslant t < 1.$$

The degeneration problem of the system (1.1) obtained by letting $\varepsilon = 0$ can be formulated by

$$\dot{x}^{(0)}(t) + x^{(0)}(t) = 0.$$

The main characteristics of SPTs are summarized in [36] as follows:

1. The problem (1.1) can be referred to as a singularly perturbed problem. Particularly, it is called degeneration problem when the order of (1.1) is lowered setting $\varepsilon = 0$.
2. Due to existence of the parameter ε, there takes shape a boundary layer, and the solution varies rapidly over there.
3. The reduced-order degeneration problem, or the unperturbed problem cannot satisfy all the given boundary conditions for the original full-order problem (1.1). However, the boundary layer part will compensate the loss for system accuracy.
4. There are two widely separated groups of characteristic roots in SPS (1.1), which results in the simultaneous existence of slow and fast modes in its solution, and makes the problem stiff from the numerical solution point of view. In this sense, the SPS (1.1) possesses a two-time-scale property.

The procedure on how to construct a singular perturbed model for an engineering application problem is demonstrated as follows:

Example 1.1 An inverted pendulum system is shown in Fig. 1.1. As a high-order, multi-variable and nonlinear system, it can be modelled in the singularly perturbed form.

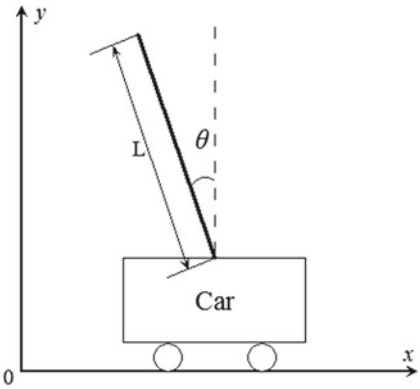

Fig. 1.1 The inverted pendulum system

Using Newton's second law of motion, the model of single inverted pendulum is given as

$$\begin{aligned}\ddot{x} &= (-(J+ml^2)b_1\dot{x}^2 + m^2gl^2\cos\theta\sin\theta - mlb_2\cos\theta\dot{\theta} \\ &\quad - ml\dot{\theta}^2(J+ml^2)\sin\theta + ml\cos\theta w + (J+ml^2)F)/N, \\ \ddot{\theta} &= (-ml\cos\theta b_1\dot{x} + (M+m)mgl\sin\theta - b_2(M+m)\dot{\theta} \\ &\quad - m^2l^2\dot{\theta}^2\cos\theta\sin\theta + (M+m)w + ml\cos\theta F)/N,\end{aligned} \tag{1.2}$$

where $N = (M+m)(J+ml^2) - ml^2\cos^2\theta$. The related parameters are defined in Table 1.1.

Table 1.1 Parameters of the single inverted pendulum

Physical description	Parameter	Value	Unit
Displacement of Car Relative to the Initial Position	x	—	m
Angle of Swinging Rod and Vertical Upward Direction	θ	—	rad
Forces Acting on the Inverted Pendulum System	F	—	N
Disturbance Force on the Swinging Rod	w	—	N
Mass of Car	M	1.06	kg
Mass of the Swinging Rod	m	0.109	kg
Length of the Swinging Rod	L	0.5	m
Distance from the Swinging Rod Centroid to the Axis	l	0.25	m
Moment of Inertia of Swinging Rod	J	0.0034	$\text{kg}\cdot\text{m}^2$
Sliding Friction Coefficient of the Car	b_1	0.1	$\text{N}\cdot\text{s/m}$
Sliding Friction Coefficient of the Swinging Rod	b_2	0.1	$\text{N}\cdot\text{s/rad}$
Gravity Acceleration	g	9.81	m/s^2

The linearization near the operation point $\theta = 0$ is conducted by assuming that $\cos\theta \approx 1,\ \ \sin\theta \approx \theta,\ \dot{\theta}^2 = 0$. The state-space equations after using linearization techniques are represented as

$$\begin{bmatrix} \dot{x} \\ \ddot{x} \\ \dot{\theta} \\ \ddot{\theta} \end{bmatrix} = \begin{bmatrix} 0 & 1 & 0 & 0 \\ 0 & -0.0883 & 0.63 & -0.0024 \\ 0 & 0 & 0 & 1 \\ 0 & -0.2357 & 27.8569 & -0.1042 \end{bmatrix} \begin{bmatrix} x \\ \dot{x} \\ \theta \\ \dot{\theta} \end{bmatrix} + \begin{bmatrix} 0 \\ 2.3566 \\ 0 \\ 104.2072 \end{bmatrix} w + \begin{bmatrix} 0 \\ 0.8822 \\ 0 \\ 2.3566 \end{bmatrix} u,$$

$$\begin{bmatrix} y_1 \\ y_2 \end{bmatrix} = \begin{bmatrix} 1 & 0 & 0 & 0 \\ 0 & 0 & 1 & 0 \end{bmatrix} \begin{bmatrix} x \\ \dot{x} \\ \theta \\ \dot{\theta} \end{bmatrix}.$$

The eigenvalues of the above linear open-loop system is

$$\lambda_1 = 0, \lambda_2 = 0.083, \lambda_3 = -5.3331, \lambda_4 = 5.2235,$$

and the open-loop system is unstable because some of the eigenvalues are located in the right half s-plane. The values of $\lambda_i,\ \ i = 1, 2, 3, 4$ can reflect frequencies of vibration and energy levels of systems. λ_1 and λ_2 are very near the imaginary axis, called fast eigenvalues, and the modes formed by the fast eigenvalues have faster dynamics than the modes formed by the eigenvalues λ_3 and λ_4, called slow eigenvalues. The fast dynamics will disappear soon. We will enlarge time-scales, in order that what happened over there during the short initial period. Then, we define the small parameter ε which will have the effect of magnifying glass. One special choice is $\varepsilon = 0.01$, according to the absolute magnitude of all eigenvalues. Through the introduction of ε, or the stretching in time-scales, fast eigenvalues can virtually be moved close to slow eigenvalues, and both of them can be handles in a similar dynamic characteristics.

Remark 1.1 Provided all fast modes, formed by fast eigenvalues, located in the left half $s-$plane, in some sense, the fast modes can be treated "less important", and the design should focus on stabilizing slow modes, formed by slow eigenvalues which are also dominant poles of the system.

Then, from another perspective, we analyze the characteristics of the system. Let state matrix, input matrix and output matrix of the above inverted pendulum system be defined as follows:

$$A = \begin{bmatrix} 0 & 1 & 0 & 0 \\ 0 & -0.0883 & 0.63 & -0.0024 \\ 0 & 0 & 0 & 1 \\ 0 & -0.2357 & 27.8569 & -0.1042 \end{bmatrix},\ B = \begin{bmatrix} 0 \\ 0.8822 \\ 0 \\ 2.3566 \end{bmatrix},\ C = \begin{bmatrix} 1 & 0 & 0 & 0 \\ 0 & 0 & 1 & 0 \end{bmatrix}.$$

Controllability matrix, observability matrix and their ranks can easily be calculated,

$$\text{rank}\left[\begin{array}{cccc} B & AB & A^2B & A^3B \end{array}\right] = 4, \quad \text{rank}\left[\begin{array}{c} C \\ CA \\ CA^2 \\ CA^3 \end{array}\right] = 4.$$

Thus, the single inverted pendulum is completely controllable and observable. Using the singular value decomposition method in [14], the singular values of the state matrix are

$$\sigma_1 = 0, \quad \sigma_2 = 1, \quad \sigma_3 = 1.024, \quad \sigma_4 = 27.8716.$$

The degree of controllability, reciprocal of the largest singular value, can then be derived,

$$\delta = 1/27.8716 = 0.0359,$$

which easily leads to numerical stiffness in control design.

The singularly perturbed model of the single inverted pendulum is shown as follows:

$$\left[\begin{array}{c} \dot{x} \\ \ddot{x} \\ \varepsilon\dot{\theta} \\ \varepsilon\ddot{\theta} \end{array}\right] = \left[\begin{array}{cccc} 0 & 1 & 0 & 0 \\ 0 & -0.0883 & 0.63 & -0.0024 \\ 0 & 0 & 0 & 0.001 \\ 0 & -0.002357 & 0.278569 & -0.001042 \end{array}\right] \left[\begin{array}{c} x \\ \dot{x} \\ \theta \\ \dot{\theta} \end{array}\right] + \left[\begin{array}{c} 0 \\ 2.3566 \\ 0 \\ 1.04 \end{array}\right] w + \left[\begin{array}{c} 0 \\ 0.8822 \\ 0 \\ 0.023566 \end{array}\right] u,$$

$$\left[\begin{array}{c} y_1 \\ y_2 \end{array}\right] = \left[\begin{array}{cccc} 1 & 0 & 0 & 0 \\ 0 & 0 & 1 & 0 \end{array}\right] \left[\begin{array}{c} x \\ \dot{x} \\ \theta \\ \dot{\theta} \end{array}\right].$$

The state matrix is corrected into

$$A_\varepsilon = \left[\begin{array}{cccc} 0 & 1 & 0 & 0 \\ 0 & -0.0883 & 0.63 & -0.0024 \\ 0 & 0 & 0 & 0.001 \\ 0 & -0.002357 & 0.278569 & -0.001042 \end{array}\right],$$

with its eigenvalues in different time-scales as

$$\lambda_1 = 0, \quad \lambda_2 = -0.0886, \quad p_3 = -0.0165, \quad p_4 = 0.0158,$$

singular values as

$$\sigma_1 = 0, \quad \sigma_2 = 0.001, \quad \sigma_3 = 0.6846, \quad \sigma_4 = 1.0068,$$

and the degree of controllability is

$$\delta_\varepsilon = 1/1.0068 = 0.9932.$$

From Example 1.1, we find that there are typical singularly perturbed phenomena in the inverted pendulum system. The SPTs reduced numerical stiffness and improved controllability for the system.

1.1.2 Linear Time-Invariant Singularly Perturbed Systems

Let us now describe the idea of singular perturbation from the system and control perspective. A linear time-invariant (LTI) SPS as below considered,

$$\begin{aligned} \dot{x}_1(t) &= A_{11}x_1(t) + A_{12}x_2(t) + B_1u(t),\ x_1(t_0) = x_1^0, \\ \varepsilon\dot{x}_2(t) &= A_{21}x_1(t) + A_{22}x_2(t) + B_2u(t),\ x_2(t_0) = x_2^0, \end{aligned} \tag{1.3}$$

where $x_1(t) \in \mathbf{R}^{n_1}$ and $x_2(t) \in \mathbf{R}^{n_2}$ are slow and fast state vectors, respectively, $n_1 + n_2 = n$. $u(t) \in \mathbf{R}^p$ is the control vector, and ε is a small positive scalar parameter, called singularly perturbed parameter. A_{ij} and B_i $(i, j = 1, 2)$ are matrices of appropriate dimensions.

The stretched system can be obtained by using the transformation $\tau = t/\varepsilon$

$$\begin{aligned} \frac{dx_1}{d\tau} &= \varepsilon A_{11}x_1 + \varepsilon A_{12}x_2 + \varepsilon B_1u, \\ \frac{dx_2}{d\tau} &= A_{21}x_1 + A_{22}x_2 + B_2u, \end{aligned} \tag{1.4}$$

which can be used to distinguish the fast states from the slow states.

Remark 1.2 For the SPSs, slow states and fast states are relative concepts.

Remark 1.3 The standard and nonstandard singularly perturbed problem.

Assume that the matrix A_{22} is nonsingular, which is customarily referred to the standard singular perturbation problem. For the case that A_{22} is singular, it is called nonstandard singular perturbation problem [27, 33]. In general, throughout the monograph, we will discuss standard singular perturbation problem.

Setting $\varepsilon = 0$ in the system (1.3), the degeneration system can be represented by

$$\begin{aligned} \dot{x}_1^{(0)}(t) &= A_{11}x_1^{(0)}(t) + A_{12}x_2^{(0)}(t) + B_1u(t),\ x_1(t_0) = x_1^0, \\ 0 &= A_{21}x_1^{(0)}(t) + A_{22}x_2^{(0)}(t) + B_2u(t),\ x_2(t_0) \neq x_2^0, \end{aligned} \tag{1.5}$$

which is combination of "differential" system in $x^{(0)}(t)$ with order n_1 and "algebraic" system in $x_2^{(0)}(t)$ with order n_2, where $n = n_1 + n_2$. The limited form (1.5) is called singular system or differential algebraic equation (DAE).

The function of degeneration is not only to "cripple" the order of the system from n to n_1 by "dethroning" $x_2(t)$ from its original state variable status, but also to "desert" its initial conditions $x_2^0(t)$. This is a harsh limitation on $x_2(t)$, which is closely related with the singular perturbation parameter ε.

In [51], a larger bound of ε, was provided which was a gauge on the validity of the Chang transformation defined in [24]. Gauss-Seidel iteration method was used to investigate the exponential stability of singularly perturbed LTI systems in [8]. A set of ε-dependent inequalities were proposed to compute the upper bound of ε which ensured the system was exponential stable.

1.1.3 Nonlinear Singularly Perturbed Systems

A nonlinear SPS can be described by the following equations,

$$\begin{aligned} \dot{x}_1(t) &= f(x_1(t), x_2(t), u(t), \varepsilon, t), \ x_1(t_0) = x_1^0, \\ \varepsilon \dot{x}_2(t) &= g(x_1(t), x_2(t), u(t), \varepsilon, t), \ x_2(t_0) = x_2^0. \end{aligned} \tag{1.6}$$

As a special case of the nonlinear SPS (1.6), we can develop a class of nonlinear singularly perturbed model, which is linear with states vector $x_2(t)$,

$$\begin{aligned} \dot{x}_1(t) &= f_1(x_1(t)) + A_{12}x_2(t), \ x_1(t_0) = x_1^0, \\ \varepsilon \dot{x}_2(t) &= g_1(x_1(t)) + A_{22}x_2(t), \ x_2(t_0) = x_2^0, \end{aligned} \tag{1.7}$$

where A_{12} and A_{22} can be either matrices of appropriate dimensions or functions of states vector $x_1(t)$.

As for more advanced modelling methods of SPSs, bond graph model for a nonlinear SPS was presented in [1], and a new discretization scheme for two-time-scale nonlinear continuous-time systems was proposed based on Euler's methodology in [3]. For singularly perturbed Hodgkin-Huxley systems, Neumann boundary conditions were given from [4]. In [9], gain scheduling control was designed for a nonlinear singularly perturbed time-varying system. In [29], a class of nonlinear memoryless controllers was synthesized for a class of imperfectly known nonlinear SPSs with discrete and distributed delays. In [38], a holographic explanation was given to show how the renormalization group approach to singular perturbations in nonlinear differential equations.

1.1.4 Hybrid Singularly Perturbed Systems

If an SPS includes both the continuous and discrete states, or both the continuous-time and discrete-time, or both the time-driven and event-trigger properties, then such system can be referred to as a hybrid SPS.

The stability of hybrid SPSs was analyzed in [7, 44, 48]. The oscillation conditions of a second-order singularly perturbed hybrid linear delay dynamic equation were discussed on different time-scales in [12]. In [47, 48], the solutions of a class of

singularly perturbed hybrid linear delay dynamic equations were discussed. In [18], singular perturbation theory was used to decompose a hybrid system and the global bifurcations of the forced Van der Pol equation were studied based on the reduced systems. Similarly, SPT in [10, 45, 52] was used to deal with hybrid systems. Also, see [30, 53] for further results on this topic.

1.2 Time-Scale and Frequency-Scale Analysis

A fundamental problem in the control theory is the mathematical modelling of a real physical system. The occurrence of some parasitic parameters, such as small time constants, resistances, inductances, capacitances, moments of inertia and Reynolds number, may increase model order and stiffness of control systems [23, 25]. In the frequency domain, an SPS with two widely separated characteristic roots, which arouses high-frequency and low-frequency oscillations. The corresponding system has slow and fast components in its time domain solutions. In the control theory, we can see that poles further to imaginary axis on the left half s-plane are associated with natural signals that decay faster than those associated with poles closer to the imaginary axis. The fast modes dominate response of states in initial time instants and disappear soon with the system into the steady state. And the slow modes are the primary contributors with the vibration disappearance due to the fast modes. Thus, the singularly perturbed problem possess a two-time-scale or two-frequency-scale property. To capture the dominant phenomena, scaling techniques are used via a separation of time-scales or frequency-scales such that the numerical stiffness is eliminated, which leads to a more efficient implementation of the controller design of SPSs.

1.2.1 Time-Scale and Multiple Time-Scales

The concept of time-scale comes from the SPS model which contains small parameters. These small parameters lead to high dimensionality and ill-posed problem of the practical system. Aiming at the class of systems, the SPTs can more accurately control the system than the general reduce-order methods.

Supposing that t is properly scaled for the slow phenomena, and a new time variable τ is introduced and scaled for the fast phenomena. If t is in hours scale, for instance, τ can be defined in seconds. The ratio of the time-scales can be characterized as a small positive parameter ε, which is the main tool for the asymptotic analysis of the SPS. Define τ as

$$\tau = \frac{t - t_0}{\varepsilon},$$

and its initial instant $\tau = 0$ corresponds to a particular instant t_0 in t time-scale.

Generally, the above forms (1.3) or (1.6) are also known as two-time-scale systems. In addition, some practical SPSs show the multiple time-scales properties.

Considering LTI systems on arbitrary time-scales, necessary and sufficient conditions for the existence of uniform exponential stability were derived in [11], also the uniform exponential stability was characterized using spectrum of its matrix. In [21], a class of second-order nonlinear dynamic equations on time domain was considered, and a condition was developed to ensure the existence and uniqueness of solutions. In [43], a novel time-frequency method to analyze the phase-locked loops (PLLs) was presented.

For the time-scale analysis of a linear system, Chang transformation is introduced to decompose the two-time-scale system into two low-order subsystems [24]. Time-scale analysis is introduced by the following simple linear SPS without control inputs,

$$\begin{aligned} \dot{x}_1(t) &= A_{11}x_1(t) + A_{12}x_2(t), \\ \varepsilon\dot{x}_2(t) &= A_{21}x_1(t) + A_{22}x_2(t), \end{aligned} \tag{1.8}$$

or the matrix equation form

$$\begin{bmatrix} \dot{x}_1(t) \\ \varepsilon\dot{x}_2(t) \end{bmatrix} = \begin{bmatrix} A_{11} & A_{12} \\ A_{21} & A_{22} \end{bmatrix} \begin{bmatrix} x_1(t) \\ x_2(t) \end{bmatrix}, \tag{1.9}$$

under the initial conditions $x_1(t_0) = x_1^0,\ x_2(t_0) = x_2^0$, where $x_1(t) \in \mathbf{R}^{n_1}$ and $x_2(t) \in \mathbf{R}^{n_2}$ are state vectors, respectively, $n_1 + n_2 = n$, and ε is a small scalar parameter satisfying $0 < \varepsilon \ll 1$. A_{ij} $(i, j = 1, 2)$ are of appropriate dimensions matrices.

When $\varepsilon \to 0$, the degenerate system of (1.8) or (1.9) is obtained as

$$\begin{bmatrix} \dot{x}_1^{(0)}(t) \\ 0 \end{bmatrix} = \begin{bmatrix} A_{11} & A_{12} \\ A_{21} & A_{22} \end{bmatrix} \begin{bmatrix} x_1^{(0)(t)} \\ x_2^{(0)(t)} \end{bmatrix}. \tag{1.10}$$

The procedure of degeneration can reduce the system order from n to n_1 by forcing $x_2(t)$ away from its original state variable status. Thus, the initial state values for the degenerate system (1.10) are represented by

$$x_1^{(0)}(t_0) = x_1^0, \quad x_2^{(0)}(t_0) \neq x_2^0.$$

Assuming A_{22} is nonsingular, the degenerate system (1.10) can be rewritten in a more simplified way:

$$\begin{aligned} \dot{x}_1^{(0)}(t) &= (A_{11} - A_{12}A_{22}^{-1}A_{21})x_1^0(t), \\ x_2^{(0)}(t) &= -A_{22}^{-1}A_{21}x_1^{(0)}(t), \end{aligned} \tag{1.11}$$

with the initial conditions x_1^0 and $x_2^0 = -A_{22}^{-1}A_{21}x_1^0$. The degenerate problem, also referred to as the unperturbed problem, is of reduced order and cannot meet all of the given boundary requirements of the original singularly perturbed problem (1.8). There is a boundary layer where the solution changes rapidly. In the simplified model

(1.11), the boundary condition x_2^0 is buried inside the boundary layer in the process of degeneration. The key problem is to find the conditions to ensure that the solution of the full problem (1.8) tends to the solution of the degenerate problem (1.11) in the boundary layer.

A lemma concerning degeneration in [46] was represented here.

Lemma 1.1 *The exact solutions $x_1(t,\varepsilon)$ and $x_2(t,\varepsilon)$ of the full problem (1.8) are related to the solutions $x_1^{(0)}(t)$ and $x_2^{(0)}(t)$ of the degenerate problem (1.11)*

$$\lim_{\varepsilon\to 0}[x_1(t,\varepsilon)] = x_1^{(0)}(t),\ 0 \leqslant t \leqslant T,$$

$$\lim_{\varepsilon\to 0}[x_2(t,\varepsilon)] = x_2^{(0)}(t),\ 0 \leqslant t \leqslant T,$$

under the assumptions in [35, 49]. Here, T is any number such that quasi-steady-state solution $x_2^{(0)}(t)$ is an isolated stable root of (1.8) for $0 \leqslant t \leqslant T$. $x_1(t,\varepsilon)$ is uniform convergence in $0 \leqslant t \leqslant T$ and $x_2(t,\varepsilon)$ is also uniform convergence in interval $t_1 \leqslant t \leqslant T$ for any $0 < t_1 \ll T$, but $x_2(t,\varepsilon)$ will usually be nonuniform at $t = 0$.

Remark 1.4 Note that the reduced-order system is not the standard limit as $\varepsilon \to 0$. To conquer that, invariant measurements of parameterized fast flow are employed to describe the limit behaviour [36].

In order to recover the lost initial conditions, the boundary layer is stretched by using the transformation

$$\tau = t/\varepsilon. \tag{1.12}$$

Substituting (1.12) into the second equation of (1.8), the original system can be represented in the two-time-scale form,

$$\begin{aligned} \frac{dx_1}{dt} &= A_{11}x_1 + A_{12}x_2, \\ \frac{dx_2}{d\tau} &= A_{21}x_1 + A_{22}x_2. \end{aligned} \tag{1.13}$$

System (1.13) is a representation of system (1.8) in different time-scales.

Applying the block diagonalization transformation in the continuous-time systems given by (1.8), the original state variables $x_1(t)$ and $x_2(t)$ can be expressed in terms of the decoupled system consisting of slow and fast variables $x_{1s}(t)$ and $x_{2f}(\tau)$.

Example 1.2 Consider the following autonomous SPS:

$$\begin{bmatrix} \dot{x}_1 \\ \varepsilon\dot{x}_2 \end{bmatrix} = \begin{bmatrix} -1 & -2 \\ 3 & -4 \end{bmatrix} \begin{bmatrix} x_1 \\ x_2 \end{bmatrix}. \tag{1.14}$$

The state responses of this SPS and its degeration system are in Fig. 1.2.

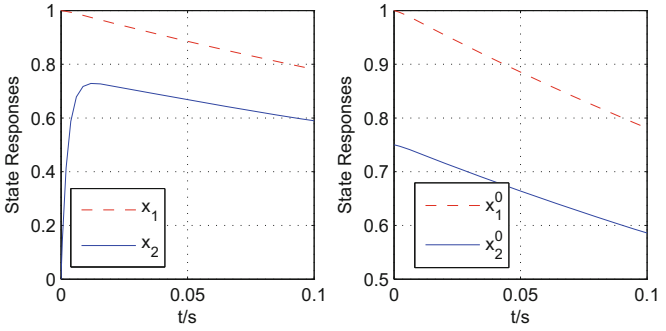

Fig. 1.2 Basic concepts of singularly perturbations and time-scales

Compare the two systems and corresponding state responses, we have

1. For $\varepsilon = 0.01$, the eigenvalues for the system (1.14) are $\lambda_s = -2.5095$ and $\lambda_f = -398.4905$ corresponding to slow and fast solutions.
2. The boundary layer exists near the initial point $t = 0$ in the SPS, but it is disappeared in the degeration system.
3. As $\varepsilon \to 0$, the initial condition x_2^0 is destroyed in the process of degeneration.

Some researchers have made much progress in the field of time-scale analysis in control design. In [43], a novel time-frequency method to analyze the phase-locked loops was presented. Singular perturbation method was used for diagnosability of linear two time-scales (TTS) systems in [16], and reduction of the order of unstable linear time-invariant systems was done in [50]. Also see [39–41] for works on two-time-scale discrete-time systems. Further, for multiparameter (multi-time-scale) deterministic and stochastic systems, we decomposed a full-order system with several small parameters into one low-order slow subsystem and several low-order fast subsystems. See [2, 5, 34, 42] for recent results on multi-time-scale method.

Multi-time-scale method was applied to the network of livestock movements and the dynamics of diseases [22], fractal dynamics in physiology [15], a small set of plant, animal, and abiotic processes structure ecosystems [20]. In multiparameter (multi-time-scale) deterministic and stochastic systems, we decomposed a full-order system with several small parameters into one low-order slow subsystem and several low-order fast subsystems. The method in [42] was proposed to transform multi time-scale singularly perturbed linear systems into N independent subsystems. In [34], multi-time-scale method was used to analyze the dynamics of a neural network and the existence, and the uniqueness of the equilibrium were proved. The relationship between the network of livestock movements in the UK and the dynamics of two diseases: foot-and-mouth disease on different time-scales were analyzed [**?**]. Scaling techniques were applied to analyzed fractal dynamics in physiology in [13]. The proposition was tested that a small set of plant, animal, and abiotic processes structure ecosystems across scales in time and space [19]. For a class of multi-time-scale systems, control of nondegenerate diffusions with infinite horizon risk-sensitive

criterion was studied in [5]. In [2], considering a class of differential equations in which both the slow and fast variables were perturbed by noise, it can be shown that sample paths of the stochastic system were concentrated in a neighbourhood of the slow manifold when the deterministic system admitted a uniformly asymptotically stable slow manifold.

1.2.2 Multiple Frequency-Scales

As mentioned above, an SPS usually achieves the multi-time-scale property corresponding to the multi-frequency-scale property in the frequency domain. It is more intuitive for the multi-time-scale phenomena to be observed in real applications. The phenomenon of two widely separated groups of eigenvalues is a key feature of the two-frequency-scale property, and the small positive parameter ε can be calculated based on the locations of eigenvalues.

Consider the linear SPS (1.8), and introduce the new variable as follows:

$$\eta(t) = x_2(t) + Lx_1(t). \tag{1.15}$$

Then, system (1.8) can be rewritten by

$$\begin{bmatrix} \dot{x}_1(t) \\ \varepsilon\dot{\eta}(t) \end{bmatrix} = \begin{bmatrix} F_1 & A_{12} \\ 0 & F_2 \end{bmatrix} \begin{bmatrix} x_1(t) \\ \eta(t) \end{bmatrix}, \tag{1.16}$$

where L is selected to satisfy the following the equations

$$A_{22}L - A_{21} - \varepsilon L A_{11} + \varepsilon L A_{12} L = 0, \tag{1.17}$$

and

$$F_1 = A_{11} - A_{12}L, \ F_2 = A_{22} + \varepsilon L A_{12}. \tag{1.18}$$

Based on the substitution, the system (1.8) has been partially decoupled into (1.16) to obtain a separate fast subsystem

$$\varepsilon\dot{\eta}(t) = (A_{22} + \varepsilon L A_{12})\eta(t). \tag{1.19}$$

In addition, set the variable

$$\xi(t) = x_1(t) - \varepsilon H\eta(t) \tag{1.20}$$

and substituting (1.20) into (1.16), we have

$$\begin{bmatrix} \dot{\xi}(t) \\ \varepsilon\dot{\eta}(t) \end{bmatrix} = \begin{bmatrix} F_1 & 0 \\ 0 & F_2 \end{bmatrix} \begin{bmatrix} \xi(t) \\ \eta(t) \end{bmatrix}, \tag{1.21}$$

where

$$HA_{22} - A_{12} - \varepsilon A_{11}H + \varepsilon A_{12}LH + \varepsilon HLA_{12} = 0. \tag{1.22}$$

Here, the slow subsystem can be represented by

$$\dot{\xi}(t) = (A_{11} - A_{12}L)\xi(t). \tag{1.23}$$

If A_{22} is invertible, solutions for (1.18) and (1.22) are shown as follows:

$$L = A_{22}^{-1}A_{21} + O(\varepsilon),\ H = A_{12}A_{22}^{-1} + O(\varepsilon). \tag{1.24}$$

Substituting (1.24) into (1.18),

$$F_1 = A_0 + O(\varepsilon),\ F_2 = A_{22} + O(\varepsilon), \tag{1.25}$$

where $A_0 = A_{11} - A_{12}A_{22}^{-1}A_{21}$. Hence, the SPS (1.8) has n_1 poles located around the eigenvalues of A_0, and n_2 poles are approximately determined by A_{22}/ε. The two-time-scale characteristics, t and τ, are corresponding to two-frequency-scale characteristics, s and p, in the frequency domain for the system (1.8).

Lemma 1.2 *[26] If A_{22} is invertible, as $\varepsilon \to 0$, the first n_1 eigenvalues of the system (1.8) tend to fixed positions in the s-plane defined by the eigenvalues of A_0, namely, $\lambda_i(A_0),\ i = 1, 2, \ldots, n_1$. While the remaining n_2 eigenvalues of the system (1.8) tend to infinity, with the rate $1/\varepsilon$, along asymptotes defined by the eigenvalues of A_{22}, namely, $(1/\varepsilon)\lambda_j(A_{22}),\ j = n_1 + 1, n_1 + 2, \ldots, n$.*

Furthermore, if the n eigenvalues of the SPS (1.8) are all distinct, where $\lambda_i(A_0) = \lambda_j(A_{22})$ is allowed, then the eigenvalues of the original system are approximated as

$$\lambda_i = \lambda_i(A_0) + O(\varepsilon),\ i = 1, 2, \ldots, n_1; \tag{1.26}$$

$$\lambda_i = [\lambda_j(A_{22}) + O(\varepsilon)]/\varepsilon,\ i = n_1 + j,\ j = 1, \ldots, n_2. \tag{1.27}$$

Applying Laplace transformation with initial conditions, (1.8) can be converted into the following frequency model:

$$\begin{aligned} sX_1(s) - x_1^0 &= A_{11}X_1(s) + A_{12}X_2(s), \\ \varepsilon sX_2(s) - x_2^0 &= A_{21}X_1(s) + A_{22}X_2(s). \end{aligned} \tag{1.28}$$

Through the stretching transformation $p = \varepsilon s$, (1.28) can be converted into a two-frequency-scale version,

$$\begin{aligned} sX_1(s) - x_1^0 &= A_{11}X_1(s) + A_{12}X_2(s), \\ px_2(p) - x_2^0 &= A_{21}X_1(p) + A_{22}X_2(p). \end{aligned} \tag{1.29}$$

In summary, an SPS has two time-scales (TTS) t and τ, which is corresponding to two frequency-scales p and s in the frequency domain. Their relationships are as follows:

$$\tau = t/\varepsilon, \tag{1.30}$$

$$p = \varepsilon s. \tag{1.31}$$

Let $s = j\omega$ and $p = j\bar{\omega}$, then $\bar{\omega} = \varepsilon\omega$.

1.3 Slow-Fast Decomposition Method

In this section, we present some basic definitions and mathematical preliminaries of SPTs. Singular perturbation approach provides a tool to overcome the lack of system stiffness to improve the quasi-steady-state approximation that characterize the conventional reduction-order techniques. Via the slow-fast decomposition method, the reduced-order subsystems can be obtained within a specified precision, based on which the composite control strategy is utilized to solve the ill-conditioned problem.

1.3.1 Decoupling Transformation

According to the transformation in Sect. 1.2.2, we obtain the separate fast subsystem (1.19) with the initial condition $\eta_0 = x_2^0 + Lx_1^0$.

A feasible solution of L can be approximated as

$$L = A_{22}^{-1}A_{21} + \varepsilon A_{22}^{-2}A_{21}A_0 + O(\varepsilon^2), \tag{1.32}$$

where $A_0 = A_{11} - A_{12}A_{22}^{-1}A_{21}$.

We should point out that the Eq. (1.17) has several real solutions, and only one of them is represented by (1.32). Differentiating (1.32) with respect to ε, it is obtained that

$$\frac{dL}{d\varepsilon}|_{\varepsilon=0} = A_{22}^{-2}A_{21}A_0.$$

The margin of ε is of great importance to control design because it determines the range of application of the singular perturbed model. In other words, the mathematical model fail to be effective if ε exceeds the upper bound ε^*. The upper bound ε^* can be estimated by the following formula [26]

$$\varepsilon^* = \frac{1}{\|A_{22}^{-1}\|(\|A_0\| + \|A_{12}\|\|A_{22}^{-1}A_{21}\| + 2(\|A_0\|\|A_{12}\|\|A_{22}^{-1}A_{21}\|)^{1/2})}. \tag{1.33}$$

1.3.2 Construction of Slow and Fast Subsystems

Consider the following LTI SPS:

$$\begin{aligned}\begin{bmatrix}\dot{x}_1(t)\\ \varepsilon\dot{x}_2(t)\end{bmatrix} &= \begin{bmatrix}A_{11} & A_{12}\\ A_{21} & A_{22}\end{bmatrix}\begin{bmatrix}x_1(t)\\ x_2(t)\end{bmatrix} + \begin{bmatrix}B_1\\ B_2\end{bmatrix}u(t) + \begin{bmatrix}B_{w1}\\ B_{w2}\end{bmatrix}w(t),\\ y(t) &= \begin{bmatrix}C_1 & C_2\end{bmatrix}\begin{bmatrix}x_1(t)\\ x_2(t)\end{bmatrix} + D_1u(t) + D_2w(t),\end{aligned} \tag{1.34}$$

where $x_1(t) \in \mathbf{R}^{n_1}$ and $x_2(t) \in \mathbf{R}^{n_2}$ are the slow and fast state variables, respectively, and $n = n_1 + n_2$ is the system dimension. $u(t) \in \mathbf{R}^p$ is the control input, $w(t) \in \mathbf{R}^r$ is the external disturbance, and $y(t) \in \mathbf{R}^q$ is the measurement output. The small positive constant $\varepsilon \in (0,\ \varepsilon^*]$, ε^* is upper bound of ε from the formula (1.33).

Remark 1.5 The small positive constant ε serves as a measure of the separation in "speed" of the slow and fast dynamics in the sense that $dx/d\tau$ is $O(\varepsilon)$ (a function $f(\varepsilon)$ is said to be $O(\varepsilon)$ if $|f(\varepsilon)| \leqslant K\varepsilon$, for $\varepsilon < \varepsilon^*$, where K is a positive constant independent of ε), whereas $dz/d\tau$ is $O(1)$.

Recall that we have already defined two time variables: t, which is assumed to be properly scaled for the slow phenomena and τ, which is related with the fast phenomena. The ratio of these time scales is defined as $\varepsilon = t/\tau$, which indicates that the dynamics of the fast states $x_2(t)$ are $1/\varepsilon$ times faster than the slow states $x_1(t)$.

With the singular perturbation method, system (1.34) may be decoupled into two subsystems under the assumption that A_{22} is invertible. The procedure of the construction of the slow and fast subsystems is shown below.

The slow subsystem Σ_s, obtained by formally setting $\varepsilon = 0$, is

$$\begin{aligned}\dot{x}_{1s}(t) &= A_s x_{1s}(t) + B_{us}u_s(t) + B_{ws}w(t),\\ y_s(t) &= C_s x_{1s}(t) + D_{us}u(t) + D_{ws}w(t),\end{aligned} \tag{1.35}$$

with

$$\begin{aligned}&A_s = A_{11} - A_{12}A_{22}^{-1}A_{21},\ B_{us} = B_1 - A_{12}A_{22}^{-1}B_2,\\ &B_{ws} = B_{w1} - A_{12}A_{22}^{-1}B_{w2},\ C_s = C_1 - C_2A_{22}^{-1}A_{21},\\ &D_{us} = D_1 - C_2A_{22}^{-1}B_2,\ D_{ws} = D_2 - C_2A_{22}^{-1}B_{w2},\end{aligned}$$

where the quasi-steady-state $x_{2s}(t)$ is

$$x_{2s}(t) = A_{22}^{-1}A_{21}x_{1s}(t) + A_{22}^{-1}B_2u(t) + A_{22}^{-1}B_{w2}w(t).$$

The open-loop TFM of the slow subsystem Σ_s from the external disturbance $w(t)$ to the measurement output $y_s(t)$ is a function of s:

$$G_s(s) = C_s(sI_{n_1} - A_s)^{-1}B_{ws} + D_{ws}.$$

To obtain the fast parts of $x_1(t)$ and $x_2(t)$, the subsystem, denoted by Σ_f, in the fast time-scale τ is rewritten as

$$\begin{aligned}\begin{bmatrix}\dot{x}_1(\tau)\\ \dot{x}_2(\tau)\end{bmatrix} &= \begin{bmatrix}\varepsilon A_{11} & \varepsilon A_{12}\\ A_{21} & A_{22}\end{bmatrix}\begin{bmatrix}x_1(\tau)\\ x_2(\tau)\end{bmatrix} + \begin{bmatrix}\varepsilon B_1\\ B_2\end{bmatrix}u(\tau) + \begin{bmatrix}\varepsilon B_{w1}\\ B_{w2}\end{bmatrix}w(\tau),\\ y(\tau) &= \begin{bmatrix}C_1 & C_2\end{bmatrix}\begin{bmatrix}x_1(\tau)\\ x_2(\tau)\end{bmatrix} + D_1u(\tau) + D_2w(\tau).\end{aligned} \tag{1.36}$$

Denote $x_{2f}(\tau) = x_2(\tau) - x_{2s}(\tau)$. As $\varepsilon \to 0$, the fast subsystem is represented as

$$\begin{aligned}\dot{x}_{2f}(\tau) &= A_{22}x_{2f}(\tau) + B_2u_f(\tau) + B_{w2}w(\tau),\\ y_f(\tau) &= C_2x_{2f}(\tau) + D_1u_f(\tau) + D_2w(\tau).\end{aligned} \tag{1.37}$$

In this case, $x_1(\tau)$ is assumed to be constant in the fast time-scale, and only fast variations, are the derivations of $x_2(\tau)$ from its quasi-steady-state. The approximation for $x_1(t)$ and $x_2(t)$ are then given as

$$x_1(t) \cong x_{1s}(t),\ x_2(t) \cong x_{2s}(t) + x_{2f}(t/\varepsilon).$$

An SPS (1.8) is equivalent to parallel connection of slow subsystem and fast subsystem in Fig. 1.3.

The corresponding open-loop TFM of the fast subsystem Σ_f from the external disturbance w to the measurement output y_f is a function of p:

$$G_f(p) = C_2(pI_{n_2} - A_{22})^{-1}B_2 + D_2.$$

As mentioned before, the high-frequency scale $p = \varepsilon s$ in frequency domain corresponds to the fast time-scale $\tau = t/\varepsilon$ in the time domain. Let $s = j\omega,\ p = j\bar{\omega}$, we have the relationship between ω and $\bar{\omega}$ is $\bar{\omega} = \varepsilon\omega$.

The open-loop TFM $G(s)$ of the whole system (1.34) is given by the sum of the slow and fast TFMs,

$$y(s,\varepsilon) = G(s,\varepsilon)w(s) = [G_s(s) + G_f(p/\varepsilon)]w(s).$$

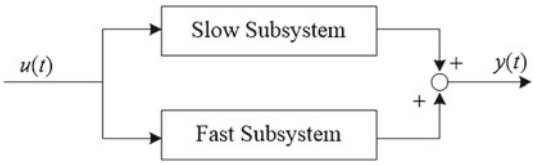

Fig. 1.3 Construction of subsystems

Here, the TF for the open-loop full-dimensional system (1.34), omitting initial conditions, is

$$G(s,\varepsilon) = \begin{bmatrix} C_1 & C_2 \end{bmatrix} \left(sI - \begin{bmatrix} A_{11} & A_{12} \\ A_{21}/\varepsilon & A_{22}/\varepsilon \end{bmatrix} \right)^{-1} \begin{bmatrix} B_{w1} \\ B_{w2}/\varepsilon \end{bmatrix} + D_2,$$

which can be converted into the following form after introducing the decoupling transformation,

$$G(s,\varepsilon) = \begin{bmatrix} C_s & C_2 \end{bmatrix} \begin{bmatrix} (sI_{n_1} - A_s)^{-1} & 0 \\ 0 & (sI_{n_2} - A_{22}/\varepsilon)^{-1} \end{bmatrix} \begin{bmatrix} B_{ws} \\ B_{w2}/\varepsilon \end{bmatrix} + (D_{ws} + D_2),$$

It is obvious that $G(s,\varepsilon)$ has two-frequency-scale characteristic. The TFs $G_{\text{low}}(s)$ and $G_{\text{high}}(p)$ are defined as the corresponding low-frequency and high-frequency approximations of $G(s,\varepsilon)$, respectively.

The external relation between the external disturbance $w(t)$ and output $y(t)$ is described by $y(s,\varepsilon) = G(s,\varepsilon)w(s)$ in which

$$G(s,\varepsilon) = G_s(s) + G_f(p/\varepsilon).$$

By using the classical singular perturbation methods, the whole system (1.34) is decoupled into the slow and fast subsystems. Correspondingly, the system TF will be decomposed into the low-frequency and high-frequency blocks. From the frequency domain perspective, the slow subsystem is established based on the low-frequency components, and the fast subsystem is used to extract the high-frequency modes from the whole dynamics.

In this sense, the related subsystems ought to work in the disjoint frequency ranges to avoid the unnecessary frequency overlap. Based on this concept, we introduce the cut-frequency subsystems to describe the dominant modes in the corresponding frequency range. Considering the fact that the slow dynamics are sensitive to low-frequency signals while the fast ones are easily affected by signals associated with the high-frequency oscillators, the slow (fast) subsystem in the low (high) frequency range is used to represent the low (high) frequency characteristic of SPS.

For low frequencies $\Lambda_l = \{\omega | |\omega| < \omega_c\}$, where ω_c is cut-frequency which can differentiate high-low dominant modes obviously, the fast TFM $G_f(p)$ can be approximated by its DC-gain, that is, $G_f(0) = -C_2 A_{22}^{-1} B_{w2} + D_2$. Thus, the low-frequency approximation of $G(s,\varepsilon)$ is estimated as

$$\begin{aligned} G_{\text{low}}(s) &= G_s(s) + G_f(0) \\ &= C_s(sI_{n_1} - A_s)^{-1} B_{ws} + E_{ws}, \end{aligned}$$

where $E_{ws} = D_{ws} - C_2 A_{22}^{-1} B_{w2} + D_2$. The corresponding high-frequency approximation of $G(s,\varepsilon)$ in the high-frequency range $\Lambda_h = \{\bar{\omega} | |\bar{\omega}| > \varepsilon\omega_c\}$ is a function of p:

$$G_{\text{high}}(p) = \lim_{s\to\infty} G_s(s) + G_f(p)$$
$$= C_2(pI_{n_2} - A_{22})^{-1}B_{w2} + E_{wf},$$

where $E_{wf} = D_{ws} + D_2$. To avoid the mixed impacts of state feedback design of the fast (slow) subsystems sensitive to high-frequency (low-frequency) signals in the low (high) frequency range, the approximation of the TFM $G(s, \varepsilon)$ is represented as

$$G(s, \varepsilon) = \begin{cases} G_{\text{low}}(s), & 0 < \omega < \omega_c, \\ G_{\text{high}}(\varepsilon s), & \omega > \omega_c. \end{cases}$$

The unitization of related cut-off subsystems is the approximation of the TFM $G(s, \varepsilon)$. It should be highlighted that the precision α of the approximation of $G(s, \varepsilon)$ is lowest in the neighbourhood of the cut-frequency ω_c because α increases as ω gradually leaves away from ω_c. The control switch frame is demonstrated in Fig. 1.4 for the equivalent model of (1.8).

Applying the state feedback controllers, K_s and K_f, respectively into the related subsystems (1.36), (1.37), the closed-loop systems of slow and fast subsystems can be derived,

$$\begin{aligned} \dot{x_{1s}}(t) &= (A_s + B_{us}K_s)x_{1s}(t) + B_{ws}w(t), \\ y_s(t) &= (C_s + D_{us}K_s)x_{1s}(t) + D_{ws}w(t), \end{aligned} \tag{1.38}$$

and

$$\begin{aligned} \dot{x}_{2f}(\tau) &= (A_{22} + B_2K_f)x_{2f}(\tau) + B_{w2}w(\tau), \\ y_f(\tau) &= (C_2 + D_1K_f)x_{2f}(\tau) + D_2w(\tau). \end{aligned} \tag{1.39}$$

The state feedback controller gains K_s and K_f are designed, respectively, based on the stability requirement and some control performance specifications. However, these two sub-controllers can only be applied to the related subsystems rather than the original ill-conditioned system. Next, we discuss the method to design the composite state feedback controller K, the sum of slow and fast controllers, to solve the original SPS within a specified order-of-ε accuracy.

Assuming, for the moment, that we have successfully designed K_s and K_f, a composite controller is formulated as

$$K = \left[K_s + K_f A_{22}^{-1} A_{21} + K_f A_{22}^{-1} B_2 K_s \;\; K_f \right].$$

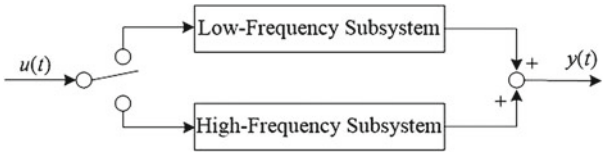

Fig. 1.4 The finite-frequency switch approach

Lemma 1.3 *[32] Let $G(s,\varepsilon)$ be a two frequency-scale TF with $G_s(s) = G(s,0)$ and $G_f(p) = G(p/\varepsilon,\varepsilon)|_{\varepsilon=0}$ as its slow and fast TFs, respectively. Suppose that $G_s(s)$ and $G_f(p)$ are stable, $G(s,\varepsilon)$ has no unstable lost poles, and $\|G_s(s)\|_\infty < \gamma$, $\|G_f(p)\|_\infty < \gamma$. Then $\|G(s,\varepsilon)\|_\infty < \gamma + o(\varepsilon)$, for sufficiently small $\varepsilon > 0$.*

Remark 1.6 Lost poles represent poles that disappear in the limiting process as $\varepsilon \to 0$. Lost poles were defined in [31] using parameter-dependent system matrices.

It follows from Lemma 1.3 that, for sufficiently small ε, $u(t) = K\begin{bmatrix} x_1(t) \\ x_2(t) \end{bmatrix}$ is an internally stabilizing controller, and $\|G(s,\varepsilon)\|_{zw} < \gamma + O(\varepsilon)$ is satisfied for SPS (1.34).

With almost the same case, we can develop slow and fast subsystems for nonlinear systems that are linear in the vector $x_2(t)$, that is, for

$$\begin{aligned} \dot{x}_1(t) &= h(x_1(t)) + A_{12}x_2(t), \\ \varepsilon\dot{x}_2(t) &= g(x_1(t)) + A_{22}x_2(t). \end{aligned} \tag{1.40}$$

In this case, we have that the quasi-steady-state of the slow dynamic $x_2(t)$ is

$$x_{2s}(t) = -A_{22}^{-1}g(x_1(t)),$$

as $\varepsilon \to 0$.

Substitute $x_{2s}(t)$ into (1.40), and we can obtain the slow subsystem as follows:

$$\dot{x}_{1s}(t) = h(x_1(t)) - A_{12}A_{22}^{-1}g(x_1(t)). \tag{1.41}$$

Similarly, the fast subsystem is represented as

$$\dot{x}_{2f}(\tau) = A_{22}x_2(\tau). \tag{1.42}$$

From the subsystems (1.41), (1.42), it can be seen that, in systems with slow nonlinearities, the linearity of the fast phenomena is preserved.

1.4 Controllability and Observability

Now, let us turn to analyze the controllability and observability of the system (1.34). It is well known that controllability and observability are two important concepts in modern control theory, which are used to characterize the general property of a system.

For notational convenience, let us define the following notations:

$$\zeta(t) = \begin{bmatrix} x_1(t) \\ x_2(t) \end{bmatrix},\ A_\varepsilon = \begin{bmatrix} A_{11} & A_{12} \\ A_{21}/\varepsilon & A_{22}/\varepsilon \end{bmatrix},\ B_\varepsilon = \begin{bmatrix} B_1 \\ B_2/\varepsilon \end{bmatrix},\ C = \begin{bmatrix} C_1 & C_2 \end{bmatrix}.$$

An SPS (1.34) can be represented in the form of an ordinary system

$$\begin{aligned} \dot{\zeta}(t) &= A_\varepsilon \zeta(t) + B_\varepsilon u(t) + B_{w\varepsilon} w(t), \\ y(t) &= C\zeta(t) + D_1 u(t) + D_2 w(t). \end{aligned} \tag{1.43}$$

Controllability is a property of the coupling between the input and the state, which involves the matrices $A_\varepsilon,\ B_\varepsilon$.

Definition 1.1 (Controllable) A state-space representation of a LTI system is

$$\dot{x}(t) = Ax(t) + Bu(t).$$

A initial state $x(t_0)$ is **controllable** at time t_0 if for some finite time t_1 there exists an input $u(t)$ that transfers the $x(t)$ from x_0 to the origin at time t_1. The system $\dot{x}(t) = Ax(t) + Bu(t)$ is called **completely controllable** at the time t_0 if every state $x(t_0)$ in the state-space is controllable.

It should be highlighted that

1. Initial state is arbitrary finite non-zero in the state-space. The control object is zero state.
2. When all initial states are observable, the system is controllable.
3. When there exists external disturbance that does not rely on the input u, namely,

$$\dot{x}(t) = Ax(t) + Bu(t) + B_w w(t),$$

it will not change the controllability of the system.

In other words, a system is said to be controllable at time t_0 if it is possible by means of an unconstrained control vector to transfer the system from initial state $x(t_0)$ to any final state in a finite time interval.

Observability is a property of the coupling between the state and the output, and thus involves the matrices A_ε and C.

Definition 1.2 (*Observable*) A system with an initial state $x(t_0)$, is **observable** if and only if the value of the initial state can be determined from the system output $y(t)$ that has been observed through the time interval $[t_0, t_1]$. If the initial state cannot be so determined, the system is **unobservable**. A system is said to be **completely observable** if all the possible initial states of the system can be observed.

It should be noted that if a system is not completely observable, the initial state $x(t_0)$ cannot be determined from the output, no matter how long the output is observed.

Lemma 1.4 *[26] A necessary and sufficient condition for the ith eigenvalue λ_i of the system (1.43) to be controlled is*

$$rank[\lambda_i I_n - A_\varepsilon\ B_\varepsilon] = n,\ i = 1, 2, \ldots, n, \tag{1.44}$$

and that for the ith eigenvalue λ_i of the system (1.43) to be observable is

$$rank\begin{bmatrix} \lambda_i I_n - A_\varepsilon \\ C \end{bmatrix} = n,\ i = 1, 2, \ldots, n. \tag{1.45}$$

In addition, the system (1.43) is completely controllable or completely observable if and only if (1.44) or (1.45) is satisfied for all its eigenvalues λ_i. The system (1.43) is stabilizable or detectable if and only if all its eigenvalues with nonnegative real parts are controllable or observable.

Considering the fact that controllability and observability are invariant with regard to similarity transformation, these properties can be analyzed based on the equivalent models. Via the following similarity transformation

$$\zeta(t) = \begin{bmatrix} x_1(t) \\ x_2(t) \end{bmatrix} = \begin{bmatrix} I_{n_1} & \varepsilon H \\ -L & I_{n_2} - \varepsilon LH \end{bmatrix} \begin{bmatrix} \xi(t) \\ \eta(t) \end{bmatrix} = T \begin{bmatrix} \xi(t) \\ \eta(t) \end{bmatrix},$$

the system (1.43) can be transformed to the equivalent system

$$\begin{bmatrix} \dot{\xi}(t) \\ \dot{\eta}(t) \end{bmatrix} = A_e \begin{bmatrix} \xi(t) \\ \eta(t) \end{bmatrix} + B_e u(t), \tag{1.46}$$

$$y(t) = C_e \begin{bmatrix} \xi(t) \\ \eta(t) \end{bmatrix}, \tag{1.47}$$

where

$$A_e = \begin{bmatrix} A_{s\varepsilon} & 0 \\ 0 & A_{f\varepsilon}/\varepsilon \end{bmatrix},\ B_e = \begin{bmatrix} B_{s\varepsilon} \\ B_{f\varepsilon}/\varepsilon \end{bmatrix},\ C = \begin{bmatrix} C_{s\varepsilon} & C_{f\varepsilon} \end{bmatrix}$$

and

$$\begin{aligned} A_{s\varepsilon} &= A_{11} - A_{12}L,\ A_{f\varepsilon} = A_{22} + \varepsilon LA_{12}, \\ B_{s\varepsilon} &= B_1 - HB_2 - \varepsilon HLB_1,\ B_{f\varepsilon} = B_2 + \varepsilon LB_1, \\ C_{s\varepsilon} &= C_1 - C_2L,\ C_{f\varepsilon} = C_2 + \varepsilon(C_1 - C_2L)H. \end{aligned}$$

Based on the similarity transformation, the whole system (1.34) can be decoupled into two subsystems with reduced order. Based on the associated subsystems, more simplified results are obtained. Noting that controllability and observability do not vary with the similarity transformation, the following lemmas are obtained, which can be derived based on the slow-fast decomposition method.

Lemma 1.5 *[26] Let $\lambda_i^0,\ i = 1, 2, \ldots, n_1$, be the eigenvalue of $A_s = A_{11} - A_{12}A_{22}^{-1}A_{21}$ approximating the slow eigenvalue λ_i in A_ε. If*

$$\text{rank}[\lambda_i^0 I_{n_1} - A_s\ B_s] = n_1,$$

where $B_s = B_1 - A_{12}A_{22}^{-1}B_2$, *then there exists a positive scalar* ε^* *such that* λ_i *is controllable for all* $\varepsilon \in (0, \varepsilon^*]$.

Similarly, let π_j^0, $j = 1, 2, \ldots, n_2$, *be the eigenvalue of* A_{22} *approximating the fast eigenvalue* λ_i *of* A_ε *according to* $\lambda_i = \pi_j/\varepsilon$, $i = n_1 + j$. *If*

$$\text{rank}[\pi_j^0 I_{n_2} - A_{22}\ B_2] = n_2,$$

then there exists a positive scalar ε^* *such that* λ_i *is controllable for all* $\varepsilon \in (0, \varepsilon^*]$.

The observability criterion is as follows:

Lemma 1.6 *[26] Let* λ_i^0, i=1, 2, ..., n_1, *be the eigenvalue of* A_s=$A_{11} - A_{12}A_{22}^{-1}A_{21}$ *approximating the slow eigenvalue* λ_i *in* A_ε. *If*

$$\text{rank}\begin{bmatrix} \lambda_i^0 I_{n_1} - A_s \\ C_s \end{bmatrix} = n_1,$$

where $C_s = C_1 - C_2A_{22}^{-1}A_{21}$, *then there exists a positive scalar* ε^* *such that* λ_i *is observable for all* $\varepsilon \in (0, \varepsilon^*]$.

Similarly, let π_j^0, $j = 1, 2, \ldots, n_2$, *be the eigenvalue of* A_{22} *approximating the fast eigenvalue* λ_i *according to* $\lambda_i = \pi_j/\varepsilon$, $i = n_1 + j$. *If*

$$\text{rank}\begin{bmatrix} \pi_j^0 I_{n_2} - A_{22} \\ C_2 \end{bmatrix} = n_2,$$

then there exists a positive scalar ε^* *such that* λ_i *is observable for all* $\varepsilon \in (0, \varepsilon^*]$.

1.5 Conclusion

In this chapter, some background knowledge and preliminaries have been presented. The modelling methodology for the construction of SPSs has been proposed in linear, nonlinear and hybrid forms in Sect. 1.1. Time-scale and frequency-scale analysis of linear SPSs has been investigated to characterize slow and fast systems in different time-scales in Sects. 1.2 and 1.3. We further put forward the concepts of cut-off subsystems to avoid the conflicts of subsystems in different frequency ranges. To best of our knowledge, it has been the first time that the idea of cut-off subsystems has been put forward for SPSs. In Sect. 1.4, the controllability and observability of SPSs has been introduced. We should point out only single-parameter perturbations, i.e., TTS systems, are taken into consideration in this book.

References

1. Avalos, G.G., Gallegos, N.B.: Quasi-steady state model determination for systems with singular perturbations modelled by bond graphs. Math. Comput. Modell. Dyn. Syst. **19**(5), 483–503 (2013)
2. Berglund, N., Gentz, B.: Geometric singular perturbation theory for stochastic differential equations. J. Differ. Equ. **191**(1), 1–54 (2003)
3. Bidani, M., Djemai, M.: A multirate digital control via a discrete-time observer for non-linear singularly perturbed continuous-time systems. Int. J. Control **75**(8), 591–613 (2002)
4. Bonfoh, A.: Dynamics of Hodgkin-Huxley systems revisited. Appl. Anal. **89**(8), 1251–1269 (2010)
5. Borkar, V.S., Kumar, K.S.: Singular perturbations in risk-sensitive stochastic control. SIAM J. Control Optim. **48**(6), 3675–3697 (2010)
6. Cao, L., Schwartz, H.M.: Output feedback stabilization of linear systems with a singular perturbation model. Proc. Am. Control Conf. **2**, 1627–1632 (2002)
7. Chen, W.H., Yuan, G., Zheng, W.X.: Robust stability of singularly perturbed impulsive systems under nonlinear perturbation. IEEE Trans. Autom. Control **58**(1), 1–6 (2012)
8. Chen, W.H., Fu, W., Du, R., Lu, X.M.: Exponential stability of a class of linear time-varying singularly perturbed systems. In: Proceedings of the International Conference on Information Science and Technology, pp. 778–783 (2011)
9. Choi, H.L., Lim, J.T.: Gain scheduling control of nonlinear singularly perturbed time-varying systems with derivative information. Int. J. Syst. Sci. **36**(6), 357–364 (2005)
10. Costa, O.L.V., Dufour, F.: Singular perturbation for the discounted continuous control of piecewise deterministic markov processes. In: Proceedings of the 49th IEEE Conference on Decision and Control, pp. 1436–1441 (2010)
11. Doan, T.S., Kalauch, A., Siegmund, S.: Exponential stability of linear time-invariant systems on time scales. Nonlinear Dyn. Syst. Theory **9**(1), 37–50 (2009)
12. Erbe, L., Hassan, T.S., Peterson, A., Saker, S.H.: Oscillation criteria for half-linear delay dynamic equations on time scales. J. Math. Anal. Appl. **345**(1), 176–185 (2009)
13. J. M. Ginoux, J. L., Chua, L. O.: Canards from chuas circuit. Int. J. Bifur. Chaos Appl. Sci. Eng., **23**(4), 1–13 (2013)
14. Golub, G.H., Reinsch, C.: Singular value decomposition and least squares solutions. Numerische mathematik **14**(5), 403–420 (1970)
15. Goldberger, A.L., Amaral, L.A.N., Hausdorff, J.M., Ivanov, PCh., Peng, C.K., Stanley, H.E.: Fractal dynamics in physiology: Alterations with disease and aging. Proc. Natl. Acad. Sci. U.S.A. **99**, 2466–2472 (2002)
16. Gong, F., Khorasani, K.: Fault diagnosis of linear singularly perturbed systems. In: Proceedings of the 44th IEEE Conference on Decision and Control, and the European Control Conference, pp. 2415–2420 (2005)
17. Gonzalez-A, G., N. Barrera-G. Quasy steady state model determination using bond graph for a singularly perturbed lti system. In: Proceedings of the 16th International Conference on Methods and Models in Automation and Robotics, pp. 194–199 (2011)
18. Guckenheimer, J., Hoffman, K., Weckesser, W.: The forced van der pol equation I: The slow flow and its bifurcations. SIAM J. Appl. Dyn. Syst. **2**(1), 1–35 (2003)
19. Heldt, T., Chang, J.L., Chen, J.J.S., Verghese, G.C., Mark, R.G.: Cycle-averaged dynamics of a periodically driven, closed-loop circulation model. Control Eng. Pr. **13**(9), 1163–1171 (2005)
20. Holling, C.S.: Cross-scale morphology, geometry, and dynamics of ecosystems. Ecol. Monogr. **62**(4), 447–502 (1992)
21. Huseynov, A.: On solutions of a nonlinear boundary value problem on time scales. Nonlinear Dyn. Syst. Theory **9**(1), 69–76 (2009)
22. Kao, R.R., Green, D.M., Johnson, J., Kiss, I.Z.: Disease dynamics over very different time-scales: foot-and-mouth disease and scrapie on the network of livestock movements in the UK. J. R. Soc. Interface **4**(16), 907–916 (2007)

23. Kokotović, P.V.: Applications of singular perturbation techniques to control problems. SIAM Rev. **26**(4), 501–550 (1984)
24. Kokotovic, P.V., Haddad, A.H.: Controllability and time-optimal control of systems with slow and fast modes. IEEE Trans. Autom. Control **20**(1), 111–113 (1975)
25. Kokotović, P.V., O'Malley Jr., R.E., Sannuti, P.: Singular perturbations and order reduction in control theory-an overview. Automatica **12**(2), 123–132 (1976)
26. Kokotovic, P.V., Khalil, H.K., OReilly, J.: Singular Perturbation Methods in Control: Analysis and Design. Academic Press, New York (1986)
27. Krishnan, H., McClamroch, N.H.: On the connection between nonlinear differential-algebraic equations and singularly perturbed systems in nonstandard form. IEEE Trans. Autom. Control **39**(5), 1079–1084 (1994)
28. Lee, K., Shim, K.H., Sawan, M.E.: Unified modeling for singular perturbed systems by delta operator: Pole assignment case. In: Kim, Tag (ed.) Artificial Intelligence and Simulation, vol. 3397, pp. 24–32. Springer, Berlin, Heidelberg (2005)
29. Lin-Chen, Y.Y., Goodall, D.P.: Stabilizing feedbacks for imperfectly known, singularly perturbed nonlinear systems with discrete and distributed delays. Int. J. Syst. Sci. **35**(15), 869–887 (2004)
30. Li, J., Lu, K., Bates, P.: Normally hyperbolic invariant manifolds for random dynamical systems: Part I-persistence. Trans. Am. Math. Soc. **365**(11), 5933–5966 (2013)
31. Luse, D.W., Khalil, H.: Frequency domain results for systems with slow and fast dynamics. IEEE Trans. Autom. Control **30**(12), 1171–1179 (1985)
32. Luse, D.W., Ball, J.A.: Frequency-scale decomposition of H_∞ disk problems. SIAM J. Control Optim. **27**(4), 814–835 (1989)
33. McClamroch, N.H., Krishnan, H.: Nonstandard singularly perturbed control systems and differential-algebraic equations. Int. J. Control **55**(2), 1239–1253 (1992)
34. Meyer-Baese, A., Pilyugin, S.S., Chen, Y.: Global exponential stability of competitive neural networks with different time scales. IEEE Trans. Neural Netw. **14**(3), 716–719 (2003)
35. Naidu, D.S.: Singular Perturbation Methodology in Control Systems. IEE Control Engineering Series, vol. 34. Peter Peregrinus Limited, Stevenage Herts, UK (1988)
36. Naidu, D.S.: Singular perturbations and time scales in control theory and applications: overview. Dyn. Contin. Discr. Impuls. Syst. (DCDIS) J. **9**(2), 233–278 (2002)
37. Naidu, D.S.: Singular perturbations and time scales in control theory and applications: overview. Dyn. Contin. Discret. Impuls. Syst. J. **9**(2), 233–278 (2002)
38. Nakayama, Y.: Holographic interpretation of renormalization group approach to singular perturbations in non-linear differential equations. Phys. Rev. D **88**(10), 1845–1858 (2013)
39. Oloomi, H., Shafai, B.: Realization theory for two-time-scale distributions through approximation of markov parameters. Int. J. Syst. Sci. **39**(2), 127–138 (2008)
40. Park, K.S., Lim, J.T.: Time-scale separation of nonlinear singularly perturbed discrete systems. In: Proceedings of the 2010 International Conference on Control Automation and Systems, pp. 892–895 (2010)
41. Potzsche, C.: Slow and fast variables in non-autonomous difference equations. J. Differ. Equ. Appl. **9**(5), 473–487 (2003)
42. Prljaca, N., Gajic, Z.: General transformation for block diagonalization of multitime-scale singularly perturbed linear systems. IEEE Trans. Autom. Control **53**(5), 1303–1305 (2008)
43. Sancho, S., Suarez, A., Chuan, J.: General envelope-transient formulation of phase-locked loops using three time scales. IEEE Trans. Microwave Theory Tech. **52**(4), 1310–1320 (2004)
44. Sanfelice, R.G., Teel, A.R.: On singular perturbations due to fast actuators in hybrid control systems. Automatica **47**(4), 692–701 (2011)
45. Sedghi, B., Srinivasan, B., Longchamp, R.: Control of hybrid systems via dehybridization. Proc. Am. Control Confer. **1**, 692–697 (2002)
46. Tikhonov, A.N., Vasil'eva, A.B., Sveshnikov, A.G.: Differential Equations. Springer, Berlin (1980)
47. Wang, W., Teel, A.R., Nesic, D.: Averaging tools for singularly perturbed hybrid systems. In: Australian Control Conference, pp. 88–93 (2011)

48. Wang, W., Teel, A.R., Nesic, D.: Analysis for a class of singularly perturbed hybrid systems via averaging. Automatica **48**(6), 1057–1068 (2012)
49. Wasow, W.: Asymptotic Expansions for Ordinary Differential Equations. Wiley-Interscience, New York, NY, 1965. Unabridged and unaltered publication by Dover Publications, Inc., New York, NY, in 1987 of the corrected and slightly enlarged publication by Robert E. Krieger Publishing Company, Huntington, NY, in 1976
50. Widowati, R. Bambang, R. Saragih, and S.M. Nababan. Model reduction for unstable LPV systems based on coprimend factorizations and singular perturbation. In: Proceedings of the 5th Asian Control Conference, vol. 2, pp. 963–970 (2004)
51. Yang, X.J., Zhu, J.J.: A generalization of chang transformation for linear time-varying systems. In: Proceedings of the 49th IEEE Conference on Decision and Control, pp. 6863–6869 (2010)
52. Yin, G., Zhang, J.F.: Hybrid singular systems of differential equations. Sci. China Ser. F: Inform. Sci. **45**(4), 241–258 (2002)
53. Yin, G., Zhang, H.Q.: Discrete-time markov chains with two-time scales and a countable state space: limit results and queueing applications. Stochastics: Int. J. Prob. Stoch. Process, **80**(4), 339–369 (2008)

Chapter 2
Theoretical Foundation of Finite Frequency Control

Finite frequency control strategy has been proven to be an important method for modern control system. Combined with the particular frequency characteristics of the plant, many control specifications in the full frequency domain can be simplified into finite frequency ones. Commonly used tools in the frequency division are the weighting function and general Kalman-Yakubovich-Popov (GKYP) Lemma. In this chapter, some background information and useful lemmas in the field of finite frequency control have been investigated in detail.

2.1 The Laplace Transform

The Laplace transform is used to solve linear constant coefficient differential equations, which acts as a function of a positive real variable t (often time) to a function of a complex variable s (frequency). On the other hand, the inverse Laplace transform is used to obtain a solution in terms of the original variables, which takes a function of a complex variable s to a positive real variable t. This techniques can be applied to both single differential equation and simultaneous differential equations. The Laplace transform can be used to produce TFMs to describe the elements of an engineering system. As the system elements, blocks are connected together to form the closed-loop diagram and to represent the characteristics of systems. Through decomposing a system in this way, it is much easier to visualize that how the various parts of the system interact. As a result, a TF model can be used to describe a time-domain model, which is particularly important in the control system design.

Definition 2.1 (*Laplace Transform*) Let $f(t)$ be a function of time t. The **Laplace transform** of $f(t)$ is $F(s)$, which is defined by

$$F(s) = \int_0^\infty e^{-st} f(t) dt.$$

C. Cai et al., *Finite Frequency Analysis and Synthesis for Singularly Perturbed Systems*, Studies in Systems, Decision and Control 78,
DOI 10.1007/978-3-319-45405-4_2

Table 2.1 The Laplace transform of some common functions

$f(t)$	$F(s)$	$f(t)$	$F(s)$
1	$\frac{1}{s}$	$\sinh bt$	$\frac{b}{s^2-b^2}$
t	$\frac{1}{s^2}$	$\cosh bt$	$\frac{s}{s^2-b^2}$
t^2	$\frac{2}{s^3}$	$e^{-at}\sinh bt$	$\frac{b}{(s+a)^2-b^2}$
t^n	$\frac{n!}{s^{n+1}}$	$e^{-at}\cosh bt$	$\frac{s+a}{(s+a)^2-b^2}$
e^{at}	$\frac{1}{s-a}$	$t\sin bt$	$\frac{2bs}{s^2+b^2}$
e^{-at}	$\frac{1}{s+a}$	$t\cos bt$	$\frac{s^2-b^2}{s^2+b^2}$
$t^n e^{-at}$	$\frac{n!}{(s+a)^{n+1}}$	$1(t)$	$\frac{1}{s}$
$\sin bt$	$\frac{b}{s^2+b^2}$	$1(t-d)$	$\frac{e^{-sd}}{s}$
$\cos bt$	$\frac{s}{s^2+b^2}$	$\delta(t)$	1
$e^{-at}\sin bt$	$\frac{b}{(s+a)^2+b^2}$	$\delta(t)$	e^{-sd}
$e^{-at}\cos bt$	$\frac{s+a}{(s+a)^2+b^2}$		

To find the Laplace transform of a function $f(t)$, we multiply it by e^{-st} and integrate between the limits 0 and ∞. Determining the Laplace transform of a given functions $f(t)$ is essentially an exercise in integration. In Table 2.1, we have listed some common functions and their corresponding Laplace transform.

There are some useful properties of the Laplace transform that can be exploited, which are namely listed as follows.

1. Linearity:
   Let $f(t)$ and $g(t)$ be two functions of time t, and k be a constant which may be negative, and then

$$\mathscr{L}\{f(t)+g(t)\} = \mathscr{L}\{f(t)\} + \mathscr{L}\{g(t)\},$$
$$\mathscr{L}\{kf(t)\} = k\mathscr{L}\{f(t)\}.$$

2. Shift theorems:
   If $\mathscr{L}\{f(t)\} = F(s)$, then

$$\mathscr{L}\{e^{-at}f(t)\} = F(s+a),$$

   where a is a constant.
   If $\mathscr{L}\{f(t)\} = F(s)$, then

$$\mathscr{L}\{u(t-d)f(t-d)\} = e^{-sd}F(s),\ d>0.$$

3. Final value theorem:

$$\lim_{s\to 0} sF(s) = \lim_{t\to\infty} f(t).$$

It is possible to obtain a mathematical model of an engineering system that consists of one or more differential equations. We have already seen that the solution of differential equations can be found using the Laplace transform, which naturally leads to the concept of a TF.

Consider a first-order differential equation

$$\frac{dx(t)}{dt} + x(t) = f(t),\ x(0) = x_0, \tag{2.1}$$

where $f(t)$ represents the control input of system (2.1), and $x(t)$ is the output or the response of the system. Taking the Laplace transform of (2.1), we obtain

$$sX(s) - x_0 + X(s) = F(s). \tag{2.2}$$

Assuming $x_0 = 0$, the equivalent form of (2.2) can be formulated by

$$\frac{X(s)}{F(s)} = \frac{1}{1+s}. \tag{2.3}$$

The function (2.3) is also referred to as a TF, which is the ratio of the Laplace transform of the output to the Laplace transform of the input for the single-input and single-output (SISO) system. Therefore, the TF for the system (2.1) from $f(t)$ to the output $x(t)$ is

$$G(s) = \frac{1}{1+s}.$$

The concept of a TF is very useful in engineering applications, which provides a simple algebraic relationship between the input and the output. In other words, it allows the analysis of dynamic system based on the differential equation to proceed in a relatively straightforward manner. Earlier we noted that it was necessary to assume zero initial conditions in order to form the TF. Without the assumption, the relationship between the input and the output would have been more complicated, and the relationship would vary depending on how much energy is stored in the system at $t = 0$. Assuming the zero initial conditions, the TF depends purely on the system characteristics.

Let $R(s) = \mathscr{L}\{r(t)\}$ be the Laplace transform of the input signal, and $Y(s) = \mathscr{L}\{y(t)\}$ be the Laplace transform of the output signal. It can be seen from Fig. 2.1 that

$$Y(s) = G(s)R(s).$$

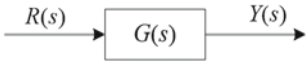

Fig. 2.1 Block diagram

(a) A summing point **(b)** A take-off point

Fig. 2.2 Two components of block diagram

Block diagram consists of two basic components in Fig. 2.2. A summing point adds together the incoming signals to the summing point and produces an outgoing signal. A take-off point is the place where a signal is tapped. The process of tapping the signal has no effects on the signal value.

There are several rules governing the manipulation of block diagrams as follows:

1. Cascade (Series) connection. The TF equivalent to a series connection of 2 blocks with TFs $G_1(s)$ and $G_2(s)$, represented in Fig. 2.3, is given by

$$G_c(s) = G_1(s)G_2(s).$$

2. Parallel connection. The equivalent TF for such a connection representing a summation of signals, given in Fig. 2.4, is obtained as

$$G_c(s) = G_1(s) + G_2(s).$$

3. Feedback connection. The simplest form of a feedback control system is given in Fig. 2.5. For such a system connection the TF is given by

$$G_c(s) = \frac{G(s)}{1 + KG(s)}.$$

Fig. 2.3 Series connection

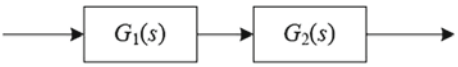

Fig. 2.4 Parallel connection

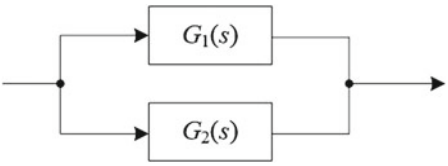

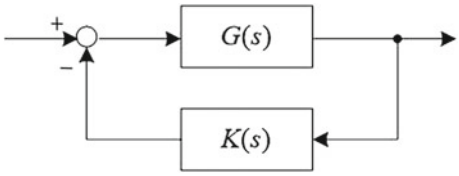

Fig. 2.5 Feedback connection

2.2 Frequency Division Strategies

2.2.1 Weighting Functions

Up till now, much progress has been made in terms of synthesizing H_∞ controllers. However, the selection method of appropriate weighting function is still very much an art. In this subsection, we consider how to formulate some performance objectives in finite frequency ranges using the weighting functions. For example, the finite frequency performance represented in the form of a TF $G(s)$ can be specified as

$$\begin{cases} \|G(j\omega)\|_\infty \leqslant \alpha < 1, \ \forall \omega \leqslant \omega_0, \\ \|G(j\omega)\|_\infty \leqslant \beta > 1, \ \forall \omega > \omega_0. \end{cases} \tag{2.4}$$

where ω_0 is the cut-frequency of high-low frequency ranges. We generally reflect the system performance objectives via the appropriate selection of weighting functions. On this basis, the finite frequency control specifications, such as the H_∞ performance index (2.4) can be obtained the following weighted form,

$$\|W_s(j\omega)G(j\omega)\| \leqslant 1,$$

with

$$\|W_s(j\omega)G(j\omega)\|_\infty = \begin{cases} \alpha^{-1}, \ \forall \omega \leqslant \omega_0, \\ \beta^{-1}, \ \forall \omega > \omega_0. \end{cases}$$

The meaning of weighted performance specifications can be shown as follows:

1. Some particular frequency components of a signal usually play very important roles in the control design.
2. Each of the signal component may not be measured in the same metric.

Note that weighting functions are essential to identify particular frequency components. On this basis, control design may be regarded as a process of choosing a controller such that certain weighted control specification are satisfied in some sense. In addition, we can see that low-frequency and high-frequency components of a plant can be extracted by band-pass filters. The TF of a band-pass filter can be used as a weighting function to form a weighted control specification.

Consider a weighting function $W(s)$ after normalization in the form of

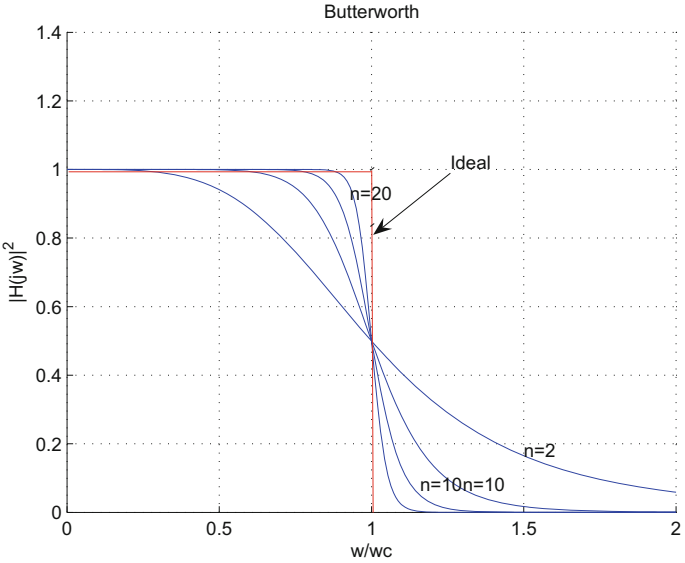

Fig. 2.6 Amplitude-frequency characteristic of butterworth low-pass filter

$$W(s) = \frac{b_m s^m + b_{m-1} s^{m-1} + \cdots + b_0}{s^n + a_{n-1} s^{n-1} + \cdots + a_0}.$$

If $n > m$, that is $W(s)$ is rational fraction, $W(s)$ has the low-pass property. If $n \leqslant m$, then $W(s)$ achieves the high-pass property. One of the most commonly used filter is the Butterworth LC filter. There are two classes Butterworth filter as follows:

- Butterworth low-pass filter

$$H_l(s) = \frac{b_0}{s^n + a_{n-1} s^{n-1} + \cdots + a_1 s + a_0}$$

where $b_0 = \omega_c^n$. Setting $\omega_c = 1$ rad/s, the normalized results of the butterworth low-pass filter are obtained. The amplitude response, denoted by $|H_l(j\omega)|$, is

$$|H_l(j\omega)| = \frac{1}{\sqrt{1 + (\frac{\omega}{\omega_c})^n}}.$$

Its amplitude-frequency characteristics are in Fig. 2.6.
This type of filter has some specific characteristics.

1. For all n, $|H_l(j0)|^2 = 1$, if $\omega = 0$.
2. For all n, $|H_l(j\omega_c)|^2 = 1/2$, if $\omega = \omega_c$, such that there exists 3 dB amplitude attenuation at $\omega = \omega_c$.

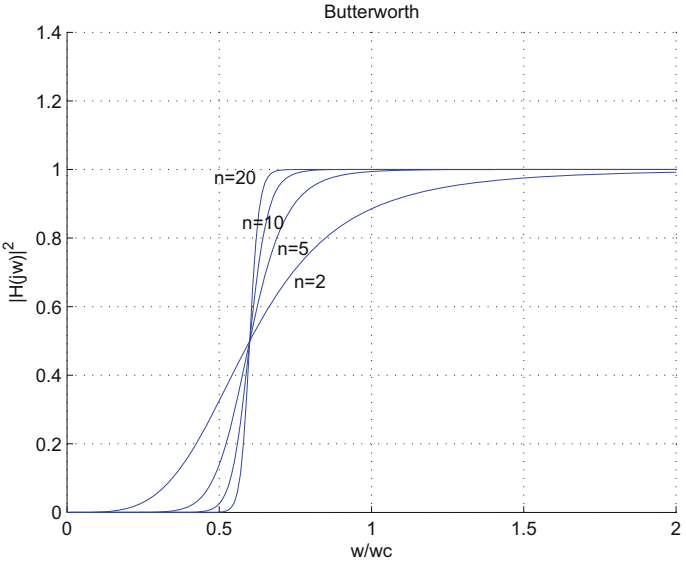

Fig. 2.7 Amplitude-frequency characteristic of butterworth high-pass filter

3. $|H_l(j\omega)|^2$ is a monotonically decreasing and continuous function about ω.
4. When $n \to +\infty$, the butterworth low-pass filter can be viewed as a perfect low-pass filter.
5. When $\omega = 0$, all levels of the derivative of $|H_l(j\omega)|^2$ are zero so that $|H_l(j\omega)|^2$ gets the maximum value and achieves the largest plain features at this point.

- Butterworth high-pass filter

$$H_h(s) = \frac{s^n}{s^n + a_{n-1}s^{n-1} + \cdots + a_1 s + a_0}$$

The amplitude response, denoted by $|H_h(j\omega)|$, is

$$|H_h(j\omega)| = \frac{1}{\sqrt{1 + (\frac{\omega_c}{\omega})^n}}.$$

Its amplitude-frequency characteristics are in Fig. 2.7.

This type of filter has some specific characteristics.

1. For all n, $|H_h(j0)|^2 = 0$, if $\omega = 0$.
2. For all n, $|H_h(j\omega_c)|^2 = 1/2$, if $\omega = \omega_c$, such that there exists 3 dB amplitude attenuation at $\omega = \omega_c$.
3. $|H_h(j\omega)|^2$ is a monotonically increasing and continuous function about ω.

4. When $n \to +\infty$, the butterworth high-pass filter can be viewed as an ideal high-pass filter.
5. When $\omega = +\infty$, all levels of the derivative of $|H_h(j\omega)|^2$ are zero so that $|H_h(j\omega)|^2$ gets the maximum value and achieves the largest plain features at this point.

Remark 2.1 We would emphasize that the weighing function method is particularly suitable for SISO systems. It is difficult for control engineers to construct satisfied weighing function matrices for multiple-input and multiple-output (MIMO) systems, which leads to the wide application of the general Kalman-Yakubovivh-Popov (GKYP) lemma.

2.2.2 General Kalman-Yakubovich-Popov Lemma

Up till now, a wide range of state-space approaches for controller design problems adopt the Kalman-Yakubovich-Popov (KYP) lemma that transforms a frequency domain inequality (FDI) into a numerically tractable linear matrix inequality (LMI) [4, 6, 8, 9]. Although that the standard KYP lemma specifies FDIs in the entire frequency range, practical requirements are usually described by multiple FDIs in finite frequency ranges. For example, usually, small sensitivity in a low-frequency range and control roll-off in a high-frequency range are utilized to ensure desired tracking performance and disturbance attenuation capability. As a result, some sort of adaptors, such as the weighting functions, have been adopted to the requirements into the KYP framework. However, the design costs to search for the suitable weighting functions would be tedious and time-consuming, and the controller complexity tends to increase with respect to the complexity of the weighting functions, which leads to the development of GKYP lemma.

The purpose of this section is to develop the state-space design theory that is capable of directly treating multiple FDI specifications in various frequency ranges. The GKYP lemma has been proven to be effective tools to handle inequalities on curves in the complex plane defined as [9, 18],

$$\Lambda(\Phi, \Psi) = \{\lambda \in \mathbf{C} | \begin{bmatrix} \lambda \\ 1 \end{bmatrix}^* \Phi \begin{bmatrix} \lambda \\ 1 \end{bmatrix} = 0, \ \begin{bmatrix} \lambda \\ 1 \end{bmatrix}^* \Psi \begin{bmatrix} \lambda \\ 1 \end{bmatrix} \geqslant 0\}, \tag{2.5}$$

with $\Phi, \ \Psi \in \mathbf{H}_2$, where $\mathbf{H}_n$ stands for $n \times n$ Hermitian matrices set and $[\cdot]^*$ denotes the conjugate transpose. The set $\Lambda(\Phi, \Psi)$ represents a curve in the complex plane if and only if [16]

1. $\det(\Phi) < 0$, so that $\Lambda(\Phi, 0)$ corresponds to a circle or a straight line.
2. Φ and Ψ satisfy an additional condition that excludes empty or singleton sets.

The latter condition is most easily expressed with the help of a congruence transformation introduced. It can be demonstrated in [9] that if $\det(\Phi) < 0$, there exists a nonsingular $T \in \mathbf{C}^{2\times 2}$ such that

$$\Phi = T^* \Phi_0 T, \ \Psi = T^* \Psi_0 T,$$

where $\Phi_0 = \begin{bmatrix} 0 & 1 \\ 1 & 0 \end{bmatrix}$, $\Psi_0 = \begin{bmatrix} \alpha & \beta \\ \beta & \gamma \end{bmatrix}$ and $\alpha,\ \beta,\ \gamma \in \mathbf{R}$ with $\alpha \leqslant \gamma$. In the former case, $\Lambda(\Phi, \Psi)$ coincides with the circle or straight line given by $\Lambda(\Phi, 0)$, while in the latter case it is a segment of this circle or line. The imaginary axis and the unit circle are special cases of (2.5) with $\Psi = 0$, and Φ equal to

$$\Phi_c = \begin{bmatrix} 0 & 1 \\ 1 & 0 \end{bmatrix},\ \Phi_d = \begin{bmatrix} 1 & 0 \\ 0 & -1 \end{bmatrix}$$

for the imaginary axis and the unit circle, respectively.

Next, we present a dual version of the GKYP lemma which is more suitable than the original GKYP lemma for feedback synthesis. A multiplier method is then developed to render the synthesis conditions convex through a simple substitution of variable, in the static gain feedback setting.

Consider a TF for a given system with state-space matrix (A, B, C, D),

$$G(\lambda) = C(\lambda I - A)^{-1}B + D,$$

where λ is the frequency variable.

In order to more clearly describe GKYP lemma, we give the following function definition. For $G \in \mathbf{C}^{s\times r}$ and $\Pi \in \mathbf{H}_{s+r}$, a function $\sigma : \mathbf{C}^{s\times r} \times \mathbf{H}_{s+r} \to \mathbf{H}_r$ is defined by

$$\sigma(G(\lambda), \Pi) = \begin{bmatrix} G(\lambda) \\ I_r \end{bmatrix}^* \Pi \begin{bmatrix} G(\lambda) \\ I_r \end{bmatrix} < 0,$$

for all $\lambda \in \Lambda(\Phi, \Psi)$. The formulation of the performance matrix Π will be introduced detailedly in Sect. 2.3.3.

In the extended definition, the set $\Lambda(\Phi, \Psi)$ can be interpreted as the integration of elements (u, v),

$$\Sigma(\Phi, \Psi) = \{(u, v) \in \mathbf{C} \times \mathbf{C} | (u, v) \neq 0, \begin{bmatrix} u \\ v \end{bmatrix}^* \Phi \begin{bmatrix} u \\ v \end{bmatrix} = 0,\ \begin{bmatrix} u \\ v \end{bmatrix}^* \Psi \begin{bmatrix} u \\ v \end{bmatrix} \geqslant 0\}.$$

If $v \neq 0$, then $\lambda \neq u/v$ is a finite point in $\Lambda(\Phi, \Psi)$ and if $v = 0$, then $\Lambda(\Phi, \Psi)$ extends $\lambda = \infty$.

Lemma 2.1 (The GKYP Lemma) *Let $A \in \mathbf{C}^{n\times n}$, $B \in \mathbf{C}^{n\times r}$, and $\Theta \in \mathbf{H}_{n+r}$, Suppose $\Phi,\ \Psi \in \mathbf{H_2}$. Define a curve $\Lambda(\Phi, \Psi)$ in the complex plane, the following two statements are equivalent.*

(1) *If $\lambda \in \Lambda(\Phi, \Psi)$,*

$$\begin{bmatrix} u \\ v \end{bmatrix}^* \Theta \begin{bmatrix} u \\ v \end{bmatrix} < 0,$$

for all nonzero $(u, v) \in \Sigma(\Phi, \Psi)$.

(2) *There exist $P, Q \in \mathbf{H}_n$, that satisfy*

$$Q > 0,\ \begin{bmatrix} A & B \\ I_n & 0 \end{bmatrix}^* (\Phi \otimes P + \Psi \otimes Q) \begin{bmatrix} A & B \\ I_n & 0 \end{bmatrix} + \Theta < 0.$$

If A has no eigenvalues in $\Lambda(\Phi, \Psi)$, the first statement reduces to the FDI

$$\begin{bmatrix} (\lambda I_n - A)^{-1} B \\ I_r \end{bmatrix}^* \Theta \begin{bmatrix} (\lambda I_n - A)^{-1} B \\ I_r \end{bmatrix} < 0,\ \forall \lambda \in \Lambda(\Phi, \Psi).$$

For the sake of brevity, we point out that only strict FDIs are considered in this monograph. The GKYP lemma readily extends to non-strict inequalities if a regularity condition is imposed.

Two critical lemmas in [8] are presented, which are treated as efficient mathematical tools throughout the following discussion.

Lemma 2.2 *Let $\Phi,\ \Psi \in \mathbf{H}_2,\ \Pi \in \mathbf{H}_{s+r}$, and the system*

$$\begin{bmatrix} \dot{x}(t) \\ z(t) \\ y(t) \end{bmatrix} = \begin{bmatrix} A & B_1 & B_2 \\ C_1 & D_{11} & D_{12} \\ C_2 & D_{21} & 0 \end{bmatrix} \begin{bmatrix} x(t) \\ w(t) \\ u(t) \end{bmatrix}, \tag{2.6}$$

where $x(t) \in \mathbf{R}^n$ is state vector, $w(t) \in \mathbf{R}^r$ is the external disturbance, $u(t) \in \mathbf{R}^p$ is the control input, $y(t) \in \mathbf{R}^q$ is the measurement output, and $z(t) \in \mathbf{R}^s$ is the controlled output. $A,\ B_i,\ C_i$ and D_{ij} $(i,\ j = 1, 2)$ are all appropriate dimensions matrices. The system (2.6) can be given with TFM from $w(t)$ to $z(t)$ formulated by

$$G(s) = C_1(sI - A)^{-1} B_1 + D_{11}.$$

Consider $\Lambda(\Phi, \Psi)$ defined by (2.5). Suppose $\Lambda(\Phi, \Psi)$ represents curves on the complex plane and A has no eigenvalues in $\Lambda(\Phi, \Psi)$. The following statements are equivalent:

(1) $\sigma(G(\lambda)^*, \Pi) < 0$ *holds for all* $\lambda \in \overline{\Lambda}(\Phi^T, \Psi^T)$, *where* $\overline{\Lambda} = \Lambda$ *if* Λ *is bounded and* $\overline{\Lambda} = \Lambda \cup \{\infty\}$ *if unbounded.*

(2) *There exist* $P = P^*$ *and* $Q = Q^* > 0$ *such that*

$$N \begin{bmatrix} \Phi \otimes P + \Psi \otimes Q & 0 \\ 0 & \Pi \end{bmatrix} N^* < 0,$$

where $N = \begin{bmatrix} M & I_{n+s} \end{bmatrix} T,\ M = \begin{bmatrix} A & B_1 \\ C_1 & D_{11} \end{bmatrix}$, *and T is the permutation matrix such that for arbitrary matrices $M_1,\ M_2,\ M_3$ and M_4*

$$\begin{bmatrix} M_1 & M_2 & M_3 & M_4 \end{bmatrix} T = \begin{bmatrix} M_1 & M_3 & M_2 & M_4 \end{bmatrix},$$

where matrices $M_1,\ M_2,\ M_3$ and M_4 have column dimensions n, r, n and s, respectively.

Define $G(\lambda) * K$ as the closed-loop TF from $w(t)$ to $z(t)$. A synthesis problem may be formulated as the search for the parameters $Q > 0$, P and K with $\mathscr{M}$ defined to be the state-space matrices of $G(\lambda) * K$ as

$$\mathscr{M} = \mathscr{A} + \mathscr{B}K\mathscr{C} = \begin{bmatrix} A & B_1 \\ C_1 & D_{11} \end{bmatrix} + \begin{bmatrix} B_2 \\ D_{12} \end{bmatrix} K \begin{bmatrix} C_2 & D_{21} \end{bmatrix}.$$

The resulting condition is not convex due to the existence of the product term. Lemma 2.2 in [8] is developed as a multiplier method to re-parameterize the condition so that the problem becomes convex which can be further transformed into LMIs.

Lemma 2.3 *Let $R \in \mathbf{C}^{q\times(2n+r+s)}$, Φ, $\Psi \in \mathbf{H}_2$, $\Pi \in \mathbf{H}_{r+s}$, P, $Q \in \mathbf{H}_n$ and the system (2.6) be given. The following statements are equivalent.*

(1) *There exist a feedback gain K and a real scalar $\mu > 0$ such that*

$$NXN^* < 0,\ S(TXT^* - \mu R^* R)S^* < 0,$$

where $S = \begin{bmatrix} \mathscr{M} & I_{n+s} \\ \mathscr{C} & 0 \end{bmatrix}$, $X = \begin{bmatrix} \Phi \otimes P + \Psi \otimes Q & 0 \\ 0 & \Pi \end{bmatrix}$, *and $\mathscr{M}$ is defined in Lemma 2.2.*

(2) *There exist matrices $\chi \in W(\mathscr{C}, R)$ and κ such that*

$$T \begin{bmatrix} \Phi \otimes P + \Psi \otimes Q & 0 \\ 0 & \Pi \end{bmatrix} T^* < \mathrm{He} \begin{bmatrix} -\chi \\ \mathscr{A}\chi + \mathscr{B}\kappa R \end{bmatrix}.$$

If (2) *holds, the gain in* (1) *can be given by $K = \kappa W^{-1}$.*

To make the problem trackable, the multiplier χ can be specified by

$$W(\mathscr{C}, R) = \{\mathscr{C}^\dagger WR + (I - \mathscr{C}^\dagger\mathscr{C})V | W \in \mathbf{C}^{q\times q},\ \det(W) \neq 0,\ V \in \mathbf{C}^{(n+r)\times(2n+r+s)}\},$$

where W and V are matrices to be solved, and superscript † denotes the Moore-Penrose inverse of matrix.

Remark 2.2 Here, for notational convenience throughout the monograph, the Hermitian part of a square matrix M is denoted by $\mathrm{He}(M) = M + M^*$.

The condition in statement (2) of Lemma 2.3 has been characterized in terms of LMIs, which can thereby be numerically solved by semi-definite programming. Up till now, many commercial software packages are now available for solving this task. We strongly believe that it is beneficial for most engineers to have one of these computer programs. Software to synthesize H_∞ controllers has been available sometimes, such as the Robust Control Toolbox in MATLAB®. Recently, a LMI Toolbox for MATLAB has been widely used, which includes LMI solving program, alternative

H_∞ software, and μ-analysis and synthesis. All computation presented in this monograph has been done employing such toolbox.

Then, we will give particular choices of R that lead to LMI synthesis conditions which are nonconservative. Please see [8] for detailed explanation. Later, we will discuss some heuristic choices of R leading to sufficient conditions for synthesis:

1. For continuous-time, small gain condition and low-frequency case, R can be chosen as
$$R_l = \begin{bmatrix} 0 & 0 & I & (D_{11}B_1^\dagger)^* \end{bmatrix}.$$
2. For continuous-time, small gain condition and high-frequency case, R can be chosen as
$$R_h = \begin{bmatrix} I & 0 & 0 & 0 \end{bmatrix}.$$

2.3 Characterization of Control Performance Index

2.3.1 Characterization of Finite Frequency Ranges

Denote the frequency variable as (2.5) with its properties. The continuous-time and discrete-time variable frequency variables are, respectively, shown as

$$\Lambda_c = \{j\omega | \omega \in \Omega_c\},\ \ \Lambda_d = \{e^{j\theta} | \theta \in \Omega_d\},$$

where Ω_c and Ω_d are subsets of real numbers specified by an additional choice of Ψ in Tables 2.2 and 2.3, respectively, Φ in $\Lambda(\Phi,\ \Psi)$ is selected as

$$\Phi_c = \begin{bmatrix} 0 & 1 \\ 1 & 0 \end{bmatrix}, \quad \Phi_d = \begin{bmatrix} 1 & 0 \\ 0 & -1 \end{bmatrix},$$

for the imaginary axis and the unit circle, respectively.

For convenience presentation of main results, we divide the frequency range in the continuous-time case into the following three parts. For low frequencies, the frequency set Λ is specified by

$$\Lambda_{cl} = \{\omega | \ | \ \omega \ | < \omega_l\},$$

and for middle frequencies, Λ can be represented by

$$\Lambda_{cm} = \{\omega | \omega_1 < \omega < \omega_2\},$$

in the similar way, the high frequencies can be characterized by

$$\Lambda_{ch} = \{\omega | \ | \ \omega \ | > \omega_h\}$$

Table 2.2 The choice of Ψ in continuous-time case

Cont.	Ω_c	Ψ
LF	Λ_{cl}	$\begin{bmatrix} -1 & 0 \\ 0 & \omega_l^2 \end{bmatrix}$
MF	Λ_{cm}	$\begin{bmatrix} -1 & j\omega_c \\ -j\omega_c & -\omega_1\omega_2 \end{bmatrix}$
HF	Λ_{ch}	$\begin{bmatrix} 1 & 0 \\ 0 & -\omega_h^2 \end{bmatrix}$

Table 2.3 The choice of Ψ for the discrete-time case

Disc.	Ω_d	Ψ
LF	Λ_{dl}	$\begin{bmatrix} 0 & 1 \\ 1 & -2\cos\theta_l \end{bmatrix}$
MF	Λ_{dm}	$\begin{bmatrix} 0 & e^{j\theta_c} \\ e^{-j\theta_c} & -2\cos\theta_w \end{bmatrix}$
HF	Λ_{dh}	$\begin{bmatrix} 0 & -1 \\ -1 & 2\cos\theta_h \end{bmatrix}$

and the related Ψ in frequency division is summarized in Table 2.2, where $\omega_c = (\omega_1 + \omega_2)/2$ and LF, HF, and MF stand for low, high, and middle-frequency ranges, respectively.

Similarly, for the discrete-time system, the selection method of Ψ is stated as follows. Consider the low-frequency condition with

$$\Lambda_{dl} = \{e^{j\theta} \mid\mid \theta \mid < \theta_l\}.$$

Noting that $\mid \theta \mid \leqslant \theta_l$ if and only if $z = e^{j\theta}$ satisfies

$$z + \bar{z} \geqslant 2\cos\theta_l = \gamma,$$

we choose

$$\Psi = \begin{bmatrix} 0 & 1 \\ 1 & -2\cos\theta_l \end{bmatrix}.$$

The middle-frequency condition is considered with

$$\Lambda_{dm} = \{e^{j\theta} \mid \theta_1 \leqslant \mid \theta \mid \leqslant \theta_2\}.$$

Note that the frequency interval condition can be written as

$$\mid \theta - \theta_c \mid \leqslant \theta_w$$

or

$$\cos(\theta - \theta_c) \geqslant \cos\theta_w,$$

where $0 \leqslant \theta_w \leqslant \pi$ and

$$\theta_c = \frac{\theta_2 + \theta_1}{2},\ \theta_w = \frac{\theta_2 - \theta_1}{2},$$

which can be rewritten as $\sigma(e^{j\theta}, \Psi) \geqslant 0$ with

$$\Psi = \begin{bmatrix} 0 & e^{j\theta_c} \\ e^{-j\theta_c} & -2\cos\theta_w \end{bmatrix}.$$

Finally, the high-frequency condition with

$$\Lambda_{dh} = \{e^{j\theta} \mid \theta_h \leqslant |\ \theta\ | \leqslant \pi\}$$

can be treated similarly. In this case, we have

$$\Psi = \begin{bmatrix} 0 & -1 \\ -1 & 2\cos\theta_h \end{bmatrix}.$$

The work above can be summarized in Table 2.3.

2.3.2 Window Norm

One natural extension is then to directly specify important frequency domain properties such as bandwidth and magnitude of resonance peaks on certain TFM. All the work related with the TFM of a system is established in the finite frequency range rather than the entire frequency so that the conservativeness of frequency domain constraints is much reduced. Such property is described by using window norm.

A TF in terms of state-space model is denoted as

$$E(s) = \left[\begin{array}{c|c} A & B \\ \hline C & D \end{array}\right] = C(sI - A)^{-1}B + D.$$

This section reviews some mathematical preliminaries, in particular, the computation of H_2 and H_∞ norm of a TFM $E(s)$.

Definition 2.2 (*Finite Frequency H_∞ Norm*) For a stable TFM $E(s)$, the H_∞ **norm** is given by

$$\|E\|_\infty = \sup_\omega \sigma(E(j\omega)),\ \omega \in \Lambda,$$

where $\sigma(\cdot)$ denotes the singular value of a matrix, and $\sup_{\omega}\sigma(E(j\omega))$ denotes the peak singular value in finite frequency set Λ.

The H_∞ norm can be viewed as a direct generalization of frequency domain specifications used in classical control for systems. For instance, it can be used to minimize the weighted sensitivity function, and select $E = \omega_p S$, where sensitivity function $S = (I + GC)^{-1}$. The following proposition provides an equivalent condition for the H_∞ norm of a rational matrix.

Proposition 2.1 *Let $E(s)$ be a rational matrix, which does not have poles on the closed right half complex plane. Then, it can be obtained that*

$$\|E(s)\|_\infty = \sup_s\{\sigma_{\max}(E(s)|\mathrm{Re}(s) > 0),\ \mathrm{Im}(s) \in \Lambda\}.$$

Likewise, H_2 norm is also defined for rational matrix. The strict definition is as follows.

Definition 2.3 (*Finite Frequency H_2 Norm*) The H_2 **norm** of a TF $E(s)$, namely $\|E(s)\|_2$, which also corresponds to the impulse response energy $\|e(t)\|_2$, or L_2 norm of a real signal $e(t)$, can be formulated in either time or frequency domain as follows:

$$\|e(t)\|_2^2 = \int_0^\infty e(t)e(t)dt = \|E(s)\|_2^2 = \frac{1}{\pi}\int_0^\infty E(j\omega)E(-j\omega)d\omega.$$

The change from time domain to frequency domain is justified using Plancherels theorem (which discrete version is known as Parsevals theorem). H_2 norm can be used to characterize the input energy of signal $u(t)$.

Remark 2.3 If $U(s)$, the Laplace transform of input signal $u(t)$, is a vector function such that the integral $\int_{-\infty}^{\infty} U^*(j\omega)U(j\omega)d\omega$ exists, then, obviously the H_2 norm of $U(s)$ reduces to

$$\|U(s)\|_2 = (\mathrm{trace}(\frac{1}{2\pi}\int_{-\infty}^{\infty} U^*(j\omega)U(j\omega)d\omega))^{\frac{1}{2}}.$$

To investigate H_-/H_∞ performance of continuous-time control systems in local frequency range, a new conception of window H_-/H_∞ norm is presented based on traditional H_-/H_∞ norm, and it is stated that traditional H_-/H_∞ norm is a special case of window H_-/H_∞ norm.

Definition 2.4 (*Finite Frequency H_-/H_∞ Norm*) The H_- index of a TFM $E(s)$ over the finite frequency range $[\omega_1, \omega_2]$ is defined as

$$\|E(s)\|_-^{[\omega_1,\omega_2]} = \inf_{\omega\in[\omega_1,\omega_2]} \underline{\sigma}\left[E(j\omega)\right],$$

where $\underline{\sigma}$ denotes the minimum singular value of the matrix $E(j\omega)$.

The H_∞ norm of a TFM $E(s)$ over the finite frequency range $[0, \omega_l] \cup [\omega_h, \infty)$ is defined as

$$\|E(s)\|_\infty^{[0,\omega_l]\cup[\omega_h,\infty)} = \sup_{\omega\in[0,\omega_l]\cup[\omega_h,\infty)} \bar{\sigma}[E(j\omega)],$$

where $\bar{\sigma}$ denotes the maximum singular value of the matrix $E(j\omega)$.

To indicate the dependency on the finite frequency range $[\omega_1, \omega_2]$, we define the window H_- norm as $\|E(s)\|_-^{[\omega_1,\omega_2]}$, which is simplified into $\|E(s)\|_-$ when the frequency range is made with certainty. H_- norm is used as the worst-case fault sensitivity measure.

2.3.3 Frequency Domain Inequalities

Much of the recent work on robustness has been focused on frequency domain characterizations. The significant results in system and control literature, such as design specifications for practical control synthesis, depend on the characterizations of system in terms of FDIs. Classical FDIs are specified in the full frequency range. However, recent developments have demonstrated that finite frequency FDIs can increase flexibility in system analysis and synthesis because that system usually works in the specific frequency range due to the limits of external conditions or nature of pumping signals.

If the designs of the structure and the controller are integrated, control performance of mechanical structures can be significantly enhanced. In this subsection, we also present how to formulate the performance matrix Π. Generally, some characterizations of the system $G(s)$ are considered as follows:

1. Positive real property:

$$G(j\omega)^* + G(j\omega) > 0,$$

which is an important requirement for mechanical structure design to guarantee the existence of controllers that achieve high servo-bandwidth, where $G(j\omega)$ is the TF of the mechanical system to be designed. In this case, the performance matrix can be selected by

$$\Pi = \begin{bmatrix} 0 & -I \\ -I & 0 \end{bmatrix}.$$

2. Bounded real property:

$$G(j\omega)^* G(j\omega) < \gamma^2 I,$$

is an important requirement for mechanical structure design to guarantee the existence of controllers that achieves good disturbance attenuation ability with Π as

$$\Pi = \begin{bmatrix} I & 0 \\ 0 & -\gamma^2 I \end{bmatrix}.$$

3. Sensitivity shaping:
   A typical control design with specifications on the closed-loop TF: a plant $G(s)$ and a controller $K(s)$. The sensitivity and the complementary sensitivity functions are defined by

$$S(j\omega) = (1 - G(j\omega)K(j\omega))^{-1},$$
$$T(j\omega) = G(j\omega)(1 - G(j\omega)K(j\omega))^{-1}.$$

   The sensitivity-shaping problem typically consists of the following requirements:

$$\|S(j\omega)\|_\infty < \alpha_1, \ \omega \in \Lambda_l,$$
$$\|T(j\omega)\|_\infty < \alpha_2, \ \omega \in \Lambda_h,$$

   where $\alpha_1 > 0$ and $\alpha_2 > 0$. These FDIs can be further represented in terms of open-loop TF, and the performance matrix Π can be formulated hereinafter.

Remark 2.4 There are close relationships between FDIs and TDIs. Most the significant results in systems and control literature generally characterize control system performances using FDIs and/or time domain inequalities. Certain system properties are characterized in terms of an inequality condition on the TF. Time domain interpretations of FDIs can provide more flexibility to capture various engineering requirements. For instance, we can see that the bounded-realness with gain bound γ is equivalent to the L_2 gain being less than or equal to $\sqrt{\gamma}$ in the time domain:

$$\int_0^\infty y^T(t)y(t)dt < \gamma \int_0^\infty u^T(t)u(t)dt, \ \ u(t) \in L_2.$$

where the nonnegative number $\|u(t)\| = (\int_0^\infty u^T(t)u(t)dt)^{\frac{1}{2}}$ is the L_2 gain of $u(t)$, $y(t)$ is the response output with the input $u(t)$ for the system $G(s)$, and the space $L_2[0, \infty)$ is the space of all piecewise-continuous inputs defined on $[0, \infty)$ satisfying $\int_0^\infty \|u(t)\|^2 < \infty$. With this interpretation, the FDI for bounded-realness can encompass the worst-case disturbance attenuation (or tracking error, etc.) level in the L_2 sense, rather than the peak amplification factor with respect to a fixed sinusoidal input. Likewise, the positive-realness of $G(s)$ is equivalent to the passivity of the system in the time domain:

$$\int_0^\infty u^T(t)y(t)dt > 0, \ \ u(t) \in L_2.$$

This interpretation allows for the concept of energy to be treated within the FDI framework for formalizing specifications.

In addition, some recent results [1, 3, 5, 7, 9, 14] have addressed this issue and generalized the standard KYP lemma [15, 19] to characterize FDIs within (semi)finite

frequency ranges in terms of LMIs. These results are based on the idea of the S-procedure, and are in connection with the literature on integral quadratic constraints [10, 12], indefinite linear quadratic control [19], and power distribution inequality [13]. These references demonstrated that structures of practical significance can be designed to achieve the specific property by solving LMI feasibility problem with the aid of an existing version of the finite frequency KYP lemma. To convert FDI to LMI, the following lemma is useful.

Lemma 2.4 (Schur Complement Lemma (SCL)) *The following statements are equivalent:*

(1) $\begin{bmatrix} Q & S \\ S^* & R \end{bmatrix} > 0;$

(2) $Q > 0,\ R - S^* Q^{-1} S > 0;$

(3) $R > 0,\ Q - S R^{-1} S^* > 0.$

SCL can be extended into semi-definite program.

Lemma 2.5 (Semi-Definite Case of SCL) *The following statements are equivalent:*

(1) $\begin{bmatrix} Q & S \\ S^* & R \end{bmatrix} \geqslant 0;$

(2) $R \geqslant 0,\ Q - S R^{-1} S^* \geqslant 0.$

2.4 Conclusion

This chapter mainly introduces a few of mathematical analysis and useful lemmas, which will be used throughout the manuscript. In Sect. 2.1, the definition of the Laplace Transform has been presented, and some commonly used forms are given. In Sect. 2.2, we explain that both the weighting functions and the GKYP lemma are useful methods in the frequency division, where the former one is particularly suitable for SISO systems, and the latter one used in both SISO and MIMO systems enjoy wider application ranges. In Sect. 2.3, we present two methods to characterize system performances, namely window norm and FDIs. Concluding remarks are given in Sect. 2.4.

References

1. Davidson, T., Luo, Z., Sturm, J.: Linear matrix inequality formulation of spectral mask constraints. In: Proceedings of IEEE International Conference on Acoustics, Speech, and Signal Processing, vol. 6, pp. 3813–3816 (2001)
2. Fradkov, A.L.: Duality theorems for certain nonconvex extremal problems. Siberian Math. J. **14**(2), 357–383 (1973)

3. Genin, Y., Hachez, Y., Nesterov, Y., Van Dooren, P.: Convex optimization over positive polynomials and filter design. In: Proceedings of UKACC International Conference on Control (2000)
4. Hara, S., Iwasaki, T.: Robust PID control using generalized KYP synthesis. IEEE Control Syst. Mag. **26**(1), 80–91 (2006)
5. Iwasaki, T., Hara, S., Yamauchi, H.: Dynamical system design from a control perspective: finite frequency positive realness approach. IEEE Trans. Autom. Control **48**(8), 1337–1354 (2003)
6. Iwasaki, T., Hara, S., Fradkov, A.L.: Time domain interpretations of frequency domain inequalities on finite ranges. Syst. Control Lett. **54**(7), 681–691 (2005)
7. Iwasaki, T., Meinsma, G., Fu, M.: Generalized S-procedure and finite frequency KYP lemma. Math. Prob. Eng. **6**(2–3), 305–320 (2009)
8. Iwasaki, T., Hara, S.: Robust control synthesis with general frequency domain specifications: static gain feedback case. Proc. Am. Control Conf. **5**, 4613–4618 (2004)
9. Iwasaki, T., Hara, S.: Generalized KYP lemma: unified frequency domain inequalities with design applications. IEEE Trans. Autom. Control **50**(1), 41–59 (2005)
10. Jonsson, U.: Robustness analysis of uncertain and nonlinear systems. Ph.D. Dissertation, Department of Automatic Control, Lund Institute of Technology (1996)
11. Luse, D.W., Ball, J.A.: Frequency-scale decoposition of H_∞ disk problems. SIAM J. Control Optimization **27**, 814–835 (1989)
12. Megretski, A., Rantzer, A.: System analysis via integral quadratic constraints. IEEE Trans. Autom. Control **42**(6), 819–830 (1997)
13. Megretski, A., Treil, S.: Power distribution inequalities in optimization and robustness of uncertain systems. J. Math. Syst. Estim. Control **3**(3), 301–319 (1993)
14. Nesterov, Y.: Squared functional systems and optimization problems. In: Frenk, H., et al. (eds.) High Performance Optimization, pp. 405–440. Kluwer Academic Publishers, Dordrecht (2000)
15. Oloomi, H., Shafai, B.: A system theory criterion for positive real matrices. SIAM J. Control **5**(171–182), 2008 (1967)
16. Pipeleers, G., Vandenberghe, L.: Generalized KYP lemma with real data. IEEE Trans. Autom. Control **56**(12), 2942–2946 (2011)
17. Rantzer, A.: On the Kalman–Yakubovich–Popov lemma. Systems and Control Letters **28**(1), 7–10 (1996)
18. Scherer, C.W.: LMI relaxations in robust control. Eur. J Control **12**(1), 3–29 (2006)
19. Willems, J.C.: Least squares stationary optimal control and the algebraic Riccati equation. IEEE Trans. Autom. Control **16**(6), 621–634 (1971)
20. Yakubovich, V.A.: The S-procedure in nonlinear control theory. Vestn. Leningrad Univ. **1**, 62–77 (1971)
21. Yakubovich, V.A.: Nonconvex optimization problem: the infinite-horizon linear-quadratic control problem with quadratic constraints. Syst. Control Lett. **19**(1), 13–22 (1992). (2010)

Part II
Singularly Perturbed Systems Analysis and Synthesis

In this part, analysis and synthesis problems for finite frequency control of SPSs are discussed. Stability theory is studied using fast-slow decomposition method and descriptor system method in time domain for the SPSs. Finite frequency H_∞ control is emphatically discussed, including state feedback control, output feedback control, shaping H_∞ control, H_∞ tracking problem and H_∞ model matching problem, for the SPSs. Finite frequency positive real control and sensitive-shaping problem are also introduced in Chaps. 5 and 6, respectively.

Chapter 3
Stabilization of Singularly Perturbed Systems

Stability analysis and controller design are significant problems of dynamic systems in theory and practice that have attracted the interest of many investigators [4]. In recent decades, researchers have focused on the problem of stability analysis and stabilization for SPSs, and these approaches can improve the control precision of system. In this chapter, we first discuss the concept of stability in general, and then present four techniques for assessing the stability of a system: (1) introducing Lyapunov functions; (2) finding the eigenvalues for state-space notation; (3) finding the location of the poles in the complex frequency plane of the closed-loop TF; and (4) providing a descriptor-system method to stabilize the SPSs. Note that the stability of the system should be guaranteed in the entire frequency range, while the related control system specifications should be specified in the finite frequency ranges to reduce their conservatism.

3.1 Stability Analysis of Dynamical Systems

Let us begin to discuss the stability and instability of systems informally. For an unstable system, there may be a huge shock with small inputs or small initial state variation in states.

Consider the LTI continuous-time system

$$\dot{x}(t) = Ax(t) + bu(t), \quad x(0) = x^{(0)}, \tag{3.1}$$

which is known as the state transition equation, and then an equilibrium is a state $\bar{x}(t)$ satisfying $A\bar{x}(t) + bu(t) = 0$ for all $t \geqslant 0$.

C. Cai et al., *Finite Frequency Analysis and Synthesis for Singularly Perturbed Systems*, Studies in Systems, Decision and Control 78,
DOI 10.1007/978-3-319-45405-4_3

Definition 3.1 (*Equilibrium* [4]) A vector $\bar{x}(t)$ is **equilibrium state** of a dynamic system with an input function $u(t)$, if it has the property that once the state reaches $\bar{x}(t)$ it remains at $\bar{x}(t)$ for all future time.

Next, we give out definitions of stability for a general system. We consider four types of stability in this chapter, namely internal stability, quadratical stability, exponential stability and Hurwitz stability.

Definition 3.2 (*State Stability/Internal Stability*)

1. An equilibrium state $\bar{x}(t)$ is **stable** if there exists an μ_0 with the following property: for all μ_1 satisfying $0 < \mu_1 < \mu_0$, there is an μ such that if $\|\bar{x}(t) - x_0(t)\| < \mu$, then $\|\bar{x}(t) - x(t)\| < \mu_1$, for all $t > t_0$;
2. An equilibrium state $\bar{x}(t)$ is **asymptotically stable** if it is stable and there is an $\mu > 0$ such that whenever $\|\bar{x}(t) - x(t)\| < \mu$, then $x(t) \to \bar{x}(t)$ as $t \to \infty$;
3. An equilibrium state $\bar{x}(t)$ is **globally asymptotically stable** if it is stable and with arbitrary initial state $x_0(t) \in X$, $x(t) \to \bar{x}(t)$ as $t \to \infty$.

It is worth pointing out that these stability concepts are referred to as internal stability, which represent properties of the system states involving the qualitative behaviours of the zero-input state response, i.e., the response of a related homogeneous state equation that relies solely on the initial states.

Definition 3.3 (*Exponential Stability*) System (3.1) is **globally uniformly exponentially stable** if there exist constants $c > 0$ and $\mu > 0$ such that the solution of (3.1) satisfies

$$\|x(t)\| \leqslant \exp^{-\mu t} \|x(0)\|, \quad t > 0,$$

for any initial state $x^{(0)}$, where $\|\cdot\|$ denotes the standard Euclidean norm in $\mathbf{R}^n$.

Remark 3.1 Asymptotic stability and exponential stability are equivalent concepts for the LTI cases.

We also present an energy-based stability analysis which origins in the work of Lyapunov. Lyapunov function methods can be conducted in both linear and nonlinear systems. However, we focus on its specialization to linear systems.

Definition 3.4 (*Lyapunov Function*) A real-valued function $V(x(t))$ defined on Ω is called a **Lyapunov function**, if the following conditions are satisfied,

1. $V(x(t))$ is continuous;
2. $V(x(t))$ has a unique global minimum at $\bar{x}(t)$ subject to all other points in Ω;
3. $V(x(t))$ is non-increasing in time t, for any state trajectory $x(t)$ contained in Ω.

Remark 3.2 The Lyapunov function can be considered as the generalization of the energy function in control systems. The first requirement simply means that the graph of $V(x(t))$ has no discontinuities. The second requirement means that the graph of $V(x(t))$ has its lowest point at the equilibrium. Moreover, the third requirement generalizes the well-known fact that the energy in a control system should always decrease.

Remark 3.3 For the linear state equation (3.1), the stability analysis using the Lyapunov function can be made more explicit. First, we can focus on energy-like functions in the quadratic form,

$$V(x) = x^T P x = \Sigma_{i,j=1}^{n} p_{ij} x_i x_j,$$

in which, without loss of generality, the matrix $P = [p_{ij}]$ is assumed to be symmetric, i.e., its elements satisfy the constraint $p_{ij} = p_{ji}$. A quadratic Lyapunov function is positive-definite overall of $\mathbf{R}^n$ if and only if P is a positive-definite symmetric matrix. In general, the constraint that $\dot{V}(x(t)) < 0$, or $\Delta V(x(t)) < 0$ is sufficient to guarantee the stability of linear and nonlinear systems, even if $V(x(t))$ is constrained to match a quadratic form.

Quadratic stability is a special class of exponential stability, which implies asymptotic stability, and has attracted the attention of many researchers due to its importance in practice. Note that the sufficient conditions for the existence of quadratic Lyapunov functions can be expressed in terms of LMIs. The following lemmas are useful throughout this section.

Lemma 3.1 (Quadratic Stability Condition) *There exist a positive definite symmetric matrix P, such that*

$$A^T P + P A < 0, \tag{3.2}$$

for the continuous-time case, or

$$A^T P A - P < 0, \tag{3.3}$$

for the discrete-time case, hold.

Definition 3.5 (*System Stability*) Consider a continuous-time linear system

$$\dot{x}(t) = Ax(t). \tag{3.4}$$

It is said to be **stable** if all the eigenvalues of the matrix A have non-positive real parts; in this case, we also say that the matrix A is Hurwitz critically stable, and it is said to be asymptotically stable if all the eigenvalues of the matrix A have negative real parts, and in this case we also say that the matrix A is **Hurwitz stable**.

Lemma 3.2 *There are the following properties of eigenvalues for the linear system (3.4):*

(1) *If at least one eigenvalue of A, $\mathrm{Re}(\lambda_i) > 0$, then the system is unstable; and*
(2) *The stability is asymptotic if and only if for all i, $\mathrm{Re}(\lambda_i) < 0$.*

3.2 Stability Analysis and Integration

Stability is a crucial requirement in control system design and other fields. It is desirable to construct a state feedback controller K for the LTI SPS analyzed in Sect. 1.3.2:

$$\begin{aligned}\begin{bmatrix}\dot{x}_1(t)\\ \varepsilon\dot{x}_2(t)\end{bmatrix} &= \begin{bmatrix}A_{11} & A_{12}\\ A_{21} & A_{22}\end{bmatrix}\begin{bmatrix}x_1(t)\\ x_2(t)\end{bmatrix} + \begin{bmatrix}B_1\\ B_2\end{bmatrix}u(t) + \begin{bmatrix}B_{w1}\\ B_{w2}\end{bmatrix}w(t),\\ y(t) &= \begin{bmatrix}C_1 & C_2\end{bmatrix}\begin{bmatrix}x_1(t)\\ x_2(t)\end{bmatrix} + D_1u(t) + D_2w(t).\end{aligned} \tag{3.5}$$

where $x_1(t) \in \mathbf{R}^{n_1}$ and $x_2(t) \in \mathbf{R}^{n_2}$ are the slow and fast states, respectively, and $n = n_1 + n_2$ is the system dimension. $u(t) \in \mathbf{R}^p$ is the control input, $w(t) \in \mathbf{R}^r$ is the external disturbance and $y(t) \in \mathbf{R}^q$ is the measurement output. The small positive constant $\varepsilon \in (0,\ \varepsilon^*]$, where ε^* is upper bound of ε from the formula (1.33). Using the forced singular perturbation method, the SPS (3.5) can be decoupled into a n_1-dimensional slow subsystem and a n_2-dimensional fast subsystem.

The slow subsystem, denoted by Σ_s, is represented as

$$\begin{aligned}\dot{x_s}(t) &= A_s x_s(t) + B_{us}u_s(t) + B_{ws}w(t),\\ y_s(t) &= C_s x_s(t) + D_{us}u(t) + D_{ws}w(t),\end{aligned} \tag{3.6}$$

and the fast subsystem, denoted by Σ_f, is expressed as

$$\begin{aligned}\dot{x}_f(\tau) &= A_{22}x_f(\tau) + B_2u_f(\tau) + B_{w2}w(\tau),\\ y_f(\tau) &= C_2x_f(\tau) + D_1u_f(\tau) + D_2w(\tau).\end{aligned} \tag{3.7}$$

It is appropriate to consider the following decomposition of feedback controls where

$$u_s(t) = K_s x_s(t), \quad u_f(\tau) = K_f x_f(\tau).$$

Then, the closed-loop subsystem using the above feedback can formulate the closed-loop slow closed-loop subsystem:

$$\begin{aligned}\dot{x_s}(t) &= (A_s + B_{us}K_s)x_s(t) + B_{ws}w(t),\\ y_s(t) &= (C_s + D_{us}K_s)x_s(t) + D_{ws}w(t),\end{aligned} \tag{3.8}$$

and the closed-loop fast subsystem,

$$\begin{aligned}\dot{x}_f(\tau) &= (A_{22} + B_2K_f)x_f(\tau) + B_{w2}w(\tau),\\ y_f(\tau) &= (C_2 + D_1K_f)x_f(\tau) + D_2w(\tau).\end{aligned} \tag{3.9}$$

Internal stability is a basic requirement for a practical feedback system. The reason behind this is that all interconnected subsystems may be unavoidably subject to

some initial conditions and some (possibly small) errors, and it cannot be tolerated in practice that such errors at some locations will lead to unbounded signals at some other locations in the closed-loop system. Internal stability guarantees that all signals in a system are bounded provided that the injected signals (at any locations) are bounded.

In the following sections, we provide the sufficient conditions for the stability property of the system (3.5) based on a LMI approach, we develop the state feedback controller that guarantees the following:

1. The states of linear SPSs achieves the internal stability;
2. The poles of the closed-loop SPS are within a pre-specified region.

In order to alleviate the ill-conditioning of SPSs resulting from the interaction of slow and fast dynamic modes, the high-order LMIs are decomposed into ε-independent and ε-dependent LMIs. The ε-independent LMIs derived in Sect. 3.3.1 are not ill-conditioned, and the ε-dependent LMIs in Sect. 3.3.2 approximate to zero when ε is small enough. It can be shown that when ε is sufficiently small, the original ill-conditioned LMIs are solvable if and only if the ε-independent LMIs are solvable. The proposed approach does not involve the separation of states into slow and fast ones, which can be applied in both standard and nonstandard SPSs.

3.3 Stability Theory on Time Domain

3.3.1 Method Based on Slow and Fast Subsystems

In this subsection, we will discuss the design of stabilizing controllers for SPSs on the basis of simplified models. For the stability analysis problem, the first question is whether the whole system is stable. It is necessary to require that both the slow and the fast subsystems are asymptotically stable.

According to Lemma 1.3, the stability of the slow subsystem and the fast subsystem can guarantee the stability of the original SPS for $\varepsilon \in (0, \varepsilon^*]$, where ε^* is the upper bounded of ε. The following work is done based on this concept.

Lemma 3.3 [1] (Projection Lemma) *Let $Q \in \mathbf{R}^{n_1 \times n_1}$, $\zeta \in \mathbf{R}^{n_1}$ and $\Gamma \in \mathbf{R}^{n_1 \times n_2}$. Let $\zeta^\perp$ be any vector such that $\zeta^\perp \zeta = 0$, i.e., the superscript $\perp$ denotes the projection of the vector. Then, the following statements are equivalent:*

(1) $\zeta^* Q \zeta < 0$, *for any* $\Gamma^* \zeta = 0$, $\zeta \neq 0$;
(2) $\Gamma^\perp Q \Gamma^{\perp *} < 0$;
(3) *Exist* $\chi \in \mathbf{R}^{n_2 \times n_1}$, *such that* $Q + \mathrm{He}(\Gamma \chi) < 0$.

Theorem 3.1 *For given scalars p_1, q_1, p_2 and q_2 satisfying $p_1 q_1 > 0$ and $p_2 q_2 > 0$, the closed-loop SPS (3.5) can achieve the internal stability for any $\varepsilon \in (0, \varepsilon^*]$, if there exist symmetric matrices W_s, $P_s > 0$, W_f and $P_h > 0$, and matrices κ_s, κ_f such that the following LMIs hold:*

$$\begin{bmatrix} 0 & P_s \\ P_s & 0 \end{bmatrix} < \mathrm{He}\begin{bmatrix} -W_s \\ A_s W_s + B_{us}\kappa_s \end{bmatrix}\begin{bmatrix} q_1 I_{n_1} \\ p_1 I_{n_1} \end{bmatrix}^T, \tag{3.10}$$

$$\begin{bmatrix} 0 & P_f \\ P_f & 0 \end{bmatrix} < \mathrm{He}\begin{bmatrix} -W_f \\ A_{22} W_f + B_2\kappa_f \end{bmatrix}\begin{bmatrix} q_2 I_{n_2} \\ p_2 I_{n_2} \end{bmatrix}^T. \tag{3.11}$$

The state feedback sub-controller gain can be solved as $K_s = \kappa_s W_s^{-1}$, $K_f = \kappa_f W_f^{-1}$. *Hence, the composite state feedback controller gain is given as*

$$K = \begin{bmatrix} K_s + K_f A_{22}^{-1} A_{21} + K_f A_{22}^{-1} B_2 K_s & K_f \end{bmatrix}.$$

Proof First, the stability of the closed-loop subsystems is investigated.

Consider the following Lyapunov function:

$$V_s = x_s^T P_s x_s, \ P_s > 0.$$

Differentiating V_s with respect to t along the trajectories of Eq. (3.8), it is obtained

$$\begin{aligned} \dot{V}_s &= \dot{x}_s^T P_s x_s + x_s^T P_s \dot{x}_s, \\ &= x_s^T [(A_s + B_{us} K_s)^T P_s + P_s (A_s + B_{us} K_s)] x_s < 0, \end{aligned}$$

which is equivalent to

$$(A_s + B_{us} K_s)^T P_s + P_s (A_s + B_{us} K_s) < 0.$$

In the same way, the Lyapunov condition for the dual system of (3.8) is represented as

$$(A_s + B_{us} K_s) P_s + P_s (A_s + B_{us} K_s)^T < 0,$$

which can be rewritten as

$$\begin{bmatrix} A_s + B_{us} K_s & I_{n_1} \end{bmatrix}\begin{bmatrix} 0 & P_s \\ P_s & 0 \end{bmatrix}\begin{bmatrix} (A_s + B_{us} K_s)^T \\ I_{n_1} \end{bmatrix}^T < 0. \tag{3.12}$$

According to Lemma 3.3, (3.12) can be converted to the following feasible LMI:

$$\begin{bmatrix} 0 & P_s \\ P_s & 0 \end{bmatrix} < \mathrm{He}\begin{bmatrix} -W_s \\ A_s W_s + B_{us}\kappa_s \end{bmatrix} \mathrm{R_s}. \tag{3.13}$$

Taking $R_s = \begin{bmatrix} q_1 I_{n_1} & p_1 I_{n_1} \end{bmatrix}$ with the constraint that $p_1 q_1 > 0$ and substituting it into (3.13) can yield

$$\begin{bmatrix} 0 & P_s \\ P_s & 0 \end{bmatrix} < \mathrm{He}\begin{bmatrix} -W_s \\ A_s W_s + B_{us}\kappa_s \end{bmatrix}\begin{bmatrix} q_1 I_{n_1} & p_1 I_{n_1} \end{bmatrix}.$$

Similar results can be derived for the corresponding fast subsystem, which is omitted here.

Second, design the composite state feedback controller:

Based on Lemma 1.3, we have the internal stability property for the whole SPS (3.5) can be guaranteed by the stabilization of its related subsystems (3.8) and (3.9) for all ε satisfying $\varepsilon \in (0, \varepsilon^*]$. In other words, the establishment of LMIs (3.10) and (3.11) can ensure the internal stability of the whole system (3.5).

Considering that $u_s = K_s x_s,\ u_f = K_f x_f$, a composite control for the full SPS (3.5) might then be taken as

$$u = u_s + u_f = K_s x_s + K_f x_f.$$

It should be pointed out that a realizable composite control requires the system states $x_1,\ x_2$ rather than $x_s,\ x_f$. The substitution of $x_s = x_1,\ x_f = x_2 - x_{2s}$, the composite control can be converted into the realizable feedback form

$$u = K_s x_1 + K_f[x_2 + A_{22}^{-1}(A_{21}x_1 + B_2 K_s x_1)] := K_1 x_1 + K_f x_2, \tag{3.14}$$

where $K_1 = K_s + K_f A_{22}^{-1} B_2 K_s + K_f A_{22}^{-1} A_{21}$.

Remark 3.4 The associated degree of conservatism of Theorem 3.1 depends on the selection of the real scalars p_1, q_1, p_2 and q_2. Compared with results in [3], Theorem 3.1 can be treated as a special case of pole-placement, which guarantees that all poles of SPSs should locate in the left half of s-plane.

3.3.2 A Descriptor-System Method

Deficiencies of classical slow-fast decomposition method is that more than one sub-controllers should be designed, and a gain schedule should be provided to produce a full-dimensional state feedback controller based on sub-controllers. In this subsection, methods from descriptor systems are introduced to provide a general framework on how to handle the ε-dependent Lyapunov function of SPSs. Contrast with methods in Sect. 3.3.1, the proposed methods are utilized to avoid the slow-fast decomposition, and the designed controller can be applied directly in the original SPS.

For notational convenience, let us define the following notions:

$$\zeta(t) = \begin{bmatrix} x_1(t) \\ x_2(t) \end{bmatrix},\ A_\varepsilon = \begin{bmatrix} A_{11} & A_{12} \\ A_{21}/\varepsilon & A_{22}/\varepsilon \end{bmatrix},\ B_\varepsilon = \begin{bmatrix} B_1 \\ B_2/\varepsilon \end{bmatrix},\ B_{w\varepsilon} = \begin{bmatrix} B_{w1} \\ B_{w2}/\varepsilon \end{bmatrix}$$

and $C = \begin{bmatrix} C_1 & C_2 \end{bmatrix}$, then the SPS (3.5) can be represented as

$$\begin{aligned} \dot{\zeta}(t) &= A_\varepsilon \zeta(t) + B_\varepsilon u(t) + B_{w\varepsilon} w(t), \\ y(t) &= C\zeta(t) + D_1 u(t) + D_2 w(t). \end{aligned} \tag{3.15}$$

Applying the state feedback controller $u(t) = K\zeta(t)$ into the system (3.15), the closed-loop system is obtained,

$$\begin{aligned} \dot{\zeta}(t) &= (A_\varepsilon + B_\varepsilon K)\zeta(t) + B_{w\varepsilon} w(t), \\ y(t) &= (C + D_1 K)\zeta(t) + D_2 w(t). \end{aligned} \tag{3.16}$$

Theorem 3.2 *For given scalars p, q satisfying $pq > 0$, the closed-loop SPS (3.5) can achieve the internal stability property, if there exist symmetric matrices W_g, $P_\varepsilon = \begin{bmatrix} P_{11} & \varepsilon P_{12} \\ \varepsilon P_{12}^* & \varepsilon P_{22} \end{bmatrix} > 0$ and κ_g such that the following LMI holds:*

$$\begin{bmatrix} 0 & \begin{bmatrix} P_{11} & \varepsilon P_{12} \\ P_{12}^T & P_{22} \end{bmatrix} \\ \begin{bmatrix} P_{11} & P_{12} \\ \varepsilon P_{12}^T & P_{22} \end{bmatrix} & 0 \end{bmatrix} < \mathrm{He} \begin{bmatrix} -W_g \\ AW_g + B\kappa_g \end{bmatrix} \begin{bmatrix} qI_n & pI_n \end{bmatrix}. \tag{3.17}$$

The state feedback sub-controller gain can be solved by $K = \kappa_g W_g^{-1}$.

Proof As for the stability analysis of the system (3.16), we consider the following ε-dependent Lyapunov function

$$V(\zeta(t)) = \zeta(t)^* P_\varepsilon \zeta(t),$$

where $P_\varepsilon = \begin{bmatrix} P_{11} & \varepsilon P_{12} \\ \varepsilon P_{12}^T & \varepsilon P_{22} \end{bmatrix} > 0$.

Then, the derivative of $V(\zeta(t))$ along the trajectories of Eq. (3.16) is

$$\dot{V}(\zeta(t)) = \zeta(t)^T [(A_\varepsilon + B_\varepsilon K)^T P_\varepsilon + P_\varepsilon (A_\varepsilon + B_\varepsilon K)]\zeta(t) < 0,$$

which is equivalent to

$$(A + BK)^T \begin{bmatrix} P_{11} & \varepsilon P_{12} \\ P_{12}^T & P_{22} \end{bmatrix} + \begin{bmatrix} P_{11} & P_{12} \\ \varepsilon P_{12}^T & P_{22} \end{bmatrix} (A + BK) < 0,$$

where $A = \begin{bmatrix} A_{11} & A_{12} \\ A_{21} & A_{22} \end{bmatrix}$, $B = \begin{bmatrix} B_1 \\ B_2 \end{bmatrix}$.

Similarly, the Lyapunov condition for the dual system of Eq. (3.16) is shown as

$$(A + BK) \begin{bmatrix} P_{11} & \varepsilon P_{12} \\ P_{12}^T & P_{22} \end{bmatrix} + \begin{bmatrix} P_{11} & P_{12} \\ \varepsilon P_{12}^T & P_{22} \end{bmatrix} (A + BK)^* < 0,$$

which can be rewritten as

$$\begin{bmatrix} A+BK & I_n \end{bmatrix} \begin{bmatrix} 0 & \begin{bmatrix} P_{11} & \varepsilon P_{12} \\ P_{12}^T & P_{22} \end{bmatrix} \\ \begin{bmatrix} P_{11} & P_{12} \\ \varepsilon P_{12}^T & P_{22} \end{bmatrix} & 0 \end{bmatrix} \begin{bmatrix} (A+BK)^T \\ I_n \end{bmatrix} < 0. \tag{3.18}$$

Based on Lemma 3.3, it can be seen that (3.18) can be converted to the following feasible LMI

$$\begin{bmatrix} 0 & \begin{bmatrix} P_{11} & \varepsilon P_{12} \\ P_{12}^T & P_{22} \end{bmatrix} \\ \begin{bmatrix} P_{11} & P_{12} \\ \varepsilon P_{12}^T & P_{22} \end{bmatrix} & 0 \end{bmatrix} < \mathrm{He} \begin{bmatrix} -W_g \\ AW_g + B\kappa_g \end{bmatrix} \begin{bmatrix} qI_n & pI_n \end{bmatrix}. \tag{3.19}$$

Remark 3.5 We point out that the associated degree of conservatism in Theorem 3.2 depends on the selection of the real scalars p and q, which indicates the locations of poles of SPSs in the left half of s-plane.

Remark 3.6 Theorem 3.1 involving slow-fast decomposition may bring in more conservatism than Theorem 3.2. Theorem 3.2 does not require the separation of states into slow and fast ones, which can be applied in both standard and nonstandard SPSs.

3.4 Stability Theory on Frequency Domain

This section proposes a new method to decompose the SPSs. The low-frequency and high-frequency subsystems are obtained by the low-pass filter and the high-pass filter detaching respectively. The new composed rule has been studied for the SPSs. It is verified conciseness of the decomposition method and effectiveness of the proposed composite controller on frequency domain.

Classical slow-fast decomposition methods are conducted by separating the SPS into slow and fast subsystems in different time-scales t and τ. Slow and fast sub-controllers are designed to realize the control specifications of slow and fast subsystems, respectively. A composite controller has been designed based on the sub-controllers [2]. Contrast with the existing methods, we discuss the decomposition of the SPSs in the frequency domain. The low/high-frequency model is extracted by the low/high-pass filter, and the composite controller is formulated by sum of the related sub-controllers.

Consider an SPS in the form of

$$\begin{aligned} \begin{bmatrix} \dot{x}_1(t) \\ \varepsilon \dot{x}_2(t) \end{bmatrix} &= \begin{bmatrix} A_{11} & A_{12} \\ A_{21} & A_{22} \end{bmatrix} \begin{bmatrix} x_1(t) \\ x_2(t) \end{bmatrix} + \begin{bmatrix} B_1 \\ B_2 \end{bmatrix} u(t), \\ y(t) &= \begin{bmatrix} C_1 & C_2 \end{bmatrix} \begin{bmatrix} x_1(t) \\ x_2(t) \end{bmatrix}, \end{aligned} \tag{3.20}$$

where $x_1(t) \in \mathbf{R}^{n_1}$ and $x_2(t) \in \mathbf{R}^{n_2}$ are the slow and fast states, respectively, and $n = n_1 + n_2$ is the system dimension. $u(t) \in \mathbf{R}^p$ is the control input, $w(t) \in \mathbf{R}^r$ is the external disturbance, and $y(t) \in \mathbf{R}^q$ is the measurement output. The TFM of (3.20) from $u(t)$ to $y(t)$ is

$$G(s) = C(sE_\varepsilon - A)^{-1}B,$$

where

$$E_\varepsilon = \begin{bmatrix} I_{n_1} & 0 \\ 0 & \varepsilon I_{n_2} \end{bmatrix}, \quad A = \begin{bmatrix} A_{11} & A_{12} \\ A_{21} & A_{22} \end{bmatrix}, \quad B = \begin{bmatrix} B_1 \\ B_2 \end{bmatrix}, \quad C = \begin{bmatrix} C_1 & C_2 \end{bmatrix}.$$

Assuming that the weighting function $W(s)$ is equivalent to the low-pass or high-pass filter to accomplish the frequency decomposition of the SPS (3.20) in the corresponding frequency range. In this concept, the TF for the related frequency subsystem is denoted by $G(s)W(s)$.

It has been proven that the addition of inertial element to the TFM $G(s)$ corresponds to add a new pole to $G(s)$ such that the amplitude response of $G(s)$ decreases faster, which benefits the low-frequency characteristic of $G(s)$. Conversely, an additional differentiation element is equivalent to add a new zero to $G(s)$ such that the amplitude response of $G(s)$ increases faster, which can be used to change the high-frequency characteristic of $G(s)$. Thus, we can improve the frequency characteristic of the SPS (3.20) by changing zeros and poles of $G(s)$.

Here, the Butterworth filters are used to extract the low- or high-frequency components of the system (3.20) the low-frequency Butterworth filter in the following form:

$$W_l(s) = \frac{b_0}{s^n + a_{n-1}s^{n-1} + \cdots + a_0},$$

and the high-frequency Butterworth filter in the form of

$$W_h(s) = \frac{s^n}{s^n + a_{n-1}s^{n-1} + \cdots + a_0}.$$

The TF for the low-pass Butterworth filter shown in Fig. 3.1 is

$$G_{Bl}(s) = \frac{1}{C_1C_2R_1R_2s^2 + (C_1R_2 + C_2R_2)s + 1},$$

where the quality factor, $Q = \frac{1}{2}\sqrt{\frac{C_1}{C_2}}$, and the related parameters are

$$R_f = R_1 = R_2, \ f_c = \frac{1}{2\pi R_f C_f}, \ C_1 = 2QC_f, \ C_2 = C_f/2Q.$$

Based on the low trade-off frequency ω_l, $\omega_l = \frac{1}{R_f C_f}$, we can calculate R_f, C_f.

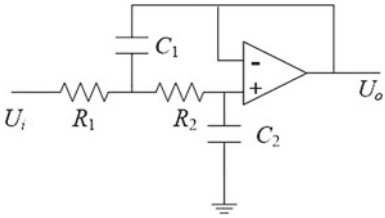

Fig. 3.1 The structure of low-pass Butterworth filter

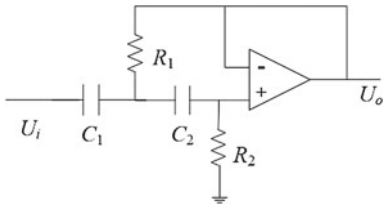

Fig. 3.2 The structure of high-pass Butterworth filter

Similarly, the TF for the high-pass Butterworth filter shown in Fig. 3.2 is

$$G_{Bh}(s) = \frac{C_1C_2R_1R_2s^2}{C_1C_2R_1R_2s^2 + (C_1R_2 + C_2R_2)s + 1},$$

where the quality factor $Q = \frac{1}{2}\sqrt{\frac{R_2}{R_1}}$, and the related parameters are

$$C_f = C_1 = C_2,\ f_c = \frac{1}{2\pi R_f C_f},\ R_1 = R_f/2Q,\ C_2 = 2QR_f.$$

Based on the high trade-off frequency ω_h, R_f, C_f are easily obtained.

In addition, the following theorems are useful to keep the stability of the SPS (3.20).

Theorem 3.3 *Consider the system (3.20) with the TFM $G(s)$. The TFMs for the slow subsystem and fast subsystem are denoted as $G_s(s)$ and $G_f(s)$, respectively. If $G_{sc}(s)$ and $G_{fs}(s)$ are the stabilizing controllers for the two subsystems, then the composite control to stabilize the whole system (3.20) can be formed as*

$$G_c(s) = \frac{\Theta(s)}{1 - G_s(s)G_{sc}(s)G_f(s)G_{fc}(s)G(s),}$$

where $\Theta(s) = 2G_s(s)G_f(s)G_{sc}(s)G_{fc}(s) + G_s(s)G_{sc}(s) + G_f(s)G_{fc}(s)$.

Proof The SPS (3.20) is paralleled by the low-frequency subsystem and the high-frequency subsystem such that the following expression is set up:

$$\frac{G_s(s)G_{sc}(s)}{G_s(s)G_{sc}(s) + 1} + \frac{G_f(s)G_{fc}(s)}{G_f(s)G_{fc}(s) + 1} = \frac{G_s(s)G_{sc}(s)}{G_s(s)G_{sc}(s) + 1}. \tag{3.21}$$

The sub-controller $G_{sc}(s)$ is used to stabilize the slow subsystem such that all the poles of

$$\frac{G_s(s)G_{sc}(s)}{G_s(s)G_{sc}(s)+1}$$

are located in the left half s-plane. Similarly, all the poles of the closed-loop high-frequency subsystem are located in the left half s-plane, too.

From Lemma 1.2, the poles of the whole system can be estimated by the sum of poles of related slow and fast subsystems. All the poles of

$$\frac{G(s)G_c(s)}{G(s)G_c(s)+1}$$

should be placed in the left half s-plane to guarantee the internal stability of the whole system.

By solving (3.21), we have

$$\frac{\Theta(s)}{(G_s(s)G_{sc}(s)+1)(G_f(s)G_{fc}(s)+1)}=\frac{G(s)G_c(s)}{G(s)G_c(s)+1},$$

which gives

$$G_c(s)=\frac{\Theta(s)}{1-G_s(s)G_{sc}(s)G_f(s)G_{fc}(s)G(s)}.$$

Example 3.1 Consider the following SPS:

$$\begin{aligned}\dot{x}_1(t) &= x_1(t)+2x_2(t)+2u(t),\\ \varepsilon\dot{x}_2(t) &= x_1(t)+2x_2(t)+2u(t),\\ y(t) &= x_1(t)+x_2(t).\end{aligned}\tag{3.22}$$

Taking $\varepsilon=0.001$, the TF for the system (3.22) is shown as

$$G(s)=\frac{2.002s-6}{0.001s^2-5.001s+3}.$$

The trade-off frequencies are given as $\omega_l=0.5\,\text{rad/s}$, $\omega_h=100\,\text{rad/s}$. We can get the low-frequency subsystem in Fig. 3.3, if

$$W_l(s)=\frac{1}{4s^2+4.242s+1}.$$

And, the high-frequency subsystem is in Fig. 3.4, if

$$W_l(s)=\frac{0.0001s^2}{0.0001s^2+0.02121s+1}.$$

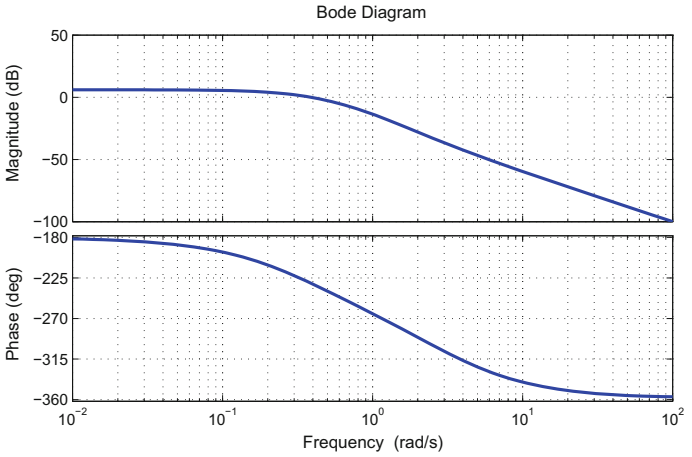

Fig. 3.3 The bode diagram of low-frequency subsystem

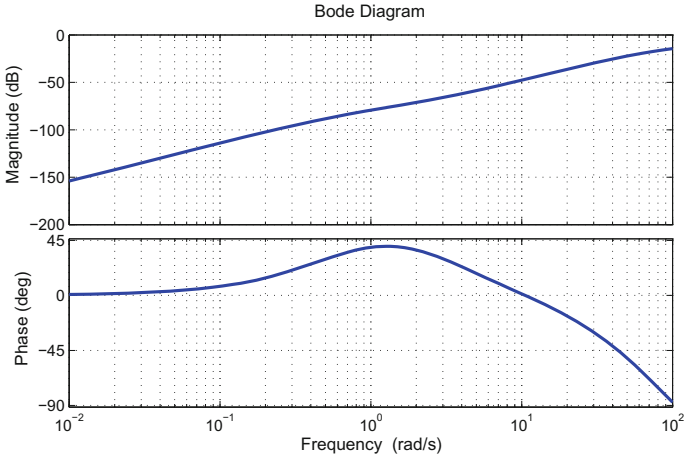

Fig. 3.4 The bode diagram of high-frequency subsystem

Based on Theorem 3.3, the sub-controllers for slow and fast subsystems are shown by

$$G_{cs}(s) = \frac{s^4 - 5000s^3 - 535.4s^2 + 870.8s + 750}{s^4 + 2.5s^3 + 1267s^2 + 1081.5s + 5379},$$

and

$$G_{cf}(s) = \frac{s^4 - 4788.9s^3 - 1.048 * 10^6 s^2 - 4.932 * 10^7 s + 3 * 10^7}{s^4 - 1999.85s^3 + 10704s^2 + 5026s + 19490}.$$

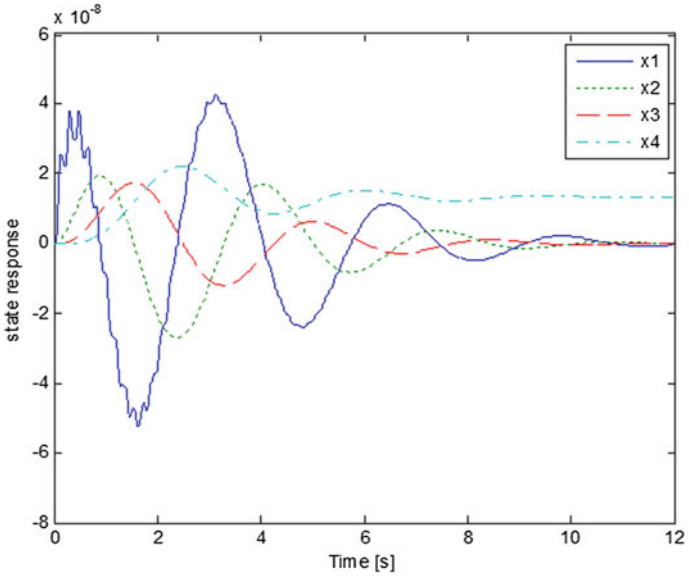

Fig. 3.5 Dynamics response of an SPS

The composite controller is given by

$$G_c(s) = \frac{(s-3)^2(s^2-0.2s+1.22)}{(s-1995)(s-6)(s-0.6)(s^2-0.4s+2)}.$$

The effectiveness of the composite controller is revealed in Fig. 3.5.

3.5 Conclusion

In this chapter, we give out definitions of stability of control systems in Sect. 3.1, and conduct the stability analysis of SPSs hereinafter. For SPSs with stable fast modes, the high-order SPS can be stabilized via the stabilization of the degenerate system [2]. As for SPSs with some unstable fast modes, Lyapunov methods have been proven to be effective tools to stabilize SPSs. The stability analysis of SPSs is performed based on Lyapunov function in Sects. 3.2 and 3.3, where both ε-independent and ε-dependent Lyapunov functions are constructed. Conservatism of these methods have been presented and compared to show their effectiveness and merits. In Sect. 3.4, slow-fast decomposition has been conducted in the frequency domain with slow/fast modes extracted via low/fast filter, and a new composite controller for SPSs has been presented. Finally, we need to point out that the stability should be guaranteed in the entire frequency range, that is why GKYP lemma is not used in this chapter.

References

1. Gahinet, P., Apkarian, P.: A linear matrix inequality approach to H_∞ control. Int. J. Robust Nonlinear Control **4**(4), 421–448 (1994)
2. Kokotovic, P.V., Khalil, H.K., OReilly, J.: Singular Perturbation Methods in Control: Analysis and Design. Academic Press, New York (1986)
3. Peaucelle, D., Arzelier, D., Bachelier, O., Bernussou, J.: A new robust D-stability condition for real convex polytopic uncertainty. Syst. Control Lett. **40**(1), 21–30 (2000)
4. Szidarovszky, F., Bahill, A.T.: Linear System Theory. Carlos Esser and Gary Bennet. CRC Press, Boca Raton (1997)

Chapter 4
Finite Frequency H_∞ Control for Singularly Perturbed Systems

In this chapter, we consider the finite frequency H_∞ methodologies of SPSs based on a dual version of GKYP lemma approach, which is more suitable for feedback synthesis. Two different methods are mainly utilized, namely the classical slow-fast decomposition method and the descriptor-system method for SPSs. The classical slow-fast decomposition method aims at applying this dual GKYP lemma in slow and fast subsystems, respectively, to achieve the desired performance characteristics for the closed-loop SPSs. The descriptor-system method for SPSs is intended to solve the problem as a whole to avoid the degradation of model accuracy resulted from the forced decomposition method. A multiplier method is then developed to render the synthesis conditions convex through the change of variable, in the state feedback or output feedback setting.

4.1 Background Information for H_∞ Control of Singularly Perturbed Systems

In this section, we first state the background information for H_∞ control of linear SPSs. A general linear system is represented by

$$\begin{aligned} \dot{x}(t) &= Ax(t) + B_1 w(t) + B_2 u(t), \\ z(t) &= C_1 x(t) + D_{11} w(t) + D_{12} u(t), \\ y(t) &= C_2 x(t) + D_{21} w(t) + D_{22} u(t), \end{aligned} \tag{4.1}$$

where $x(t) \in \mathbf{R}^n$ is state vector, $w(t) \in \mathbf{R}^r$ is the external disturbance, $u(t) \in \mathbf{R}^p$ is the control input, $y(t) \in \mathbf{R}^q$ is the measurement output, and $z(t) \in \mathbf{R}^s$ is the controlled output. A, B_i, C_i and D_{ij} $(i, j = 1, 2)$ are all appropriate dimensions matrices. The standard block diagram of the system (4.1) is shown in Fig. 4.1.

The TFMs $G(s)$ and $K(s)$ are, by assumption, real-rational and proper. The TFM from the external disturbance $w(t)$ to the measurement output $z(t)$, denoted by

C. Cai et al., *Finite Frequency Analysis and Synthesis for Singularly Perturbed Systems*, Studies in Systems, Decision and Control 78,
DOI 10.1007/978-3-319-45405-4_4

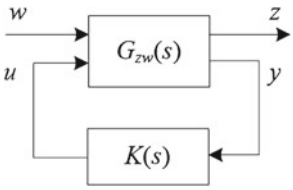

Fig. 4.1 The standard block diagram

$G_{zw}(s)$, has the following partition

$$G_{zw}(s) = \left[\begin{array}{c|c} G_{11}(s) & G_{12}(s) \\ \hline G_{21}(s) & G_{22}(s) \end{array}\right].$$

Recalling the results in Chap. 2, it can be seen that $\|G_{zw}(s)\|_\infty$ can be used to perform the function of an amplifier from disturbance to the system output. Then, the following H_∞ problem of linear systems can be formulated.

Problem 4.1 For the linear system (4.1), we design a state feedback control law or an output feedback law under the internal stability constraint such that the following requirement,

$$\|G_{zw}(s)\|_\infty < \gamma,$$

holds for a given positive scalar γ.

Remark 4.1 Internal stability is a fundamental property of a dynamic system, which is merely dependent on the state-space matrix A. Moreover, H_∞ control also discusses a type of external stability called bounded-input, bounded-output (BIBO) stability, which requires the gain from external disturbance to measurement output is restrained,

$$\|G_{zw}(s)\|_\infty < \gamma.$$

Following are two examples of the standard H_∞ problem.

1. **Model Matching Problem**
   In Fig. 4.2, the block T_1 represents a model to be matched by the cascade connection of three blocks T_2, T_3 and Q. Here, T_i $(i = 1, 2, 3)$ are given, and the controller Q is to be designed. Assume that $T_i \in \mathbf{RH}_\infty, i = 1, 2, 3$ and $Q \in \mathbf{RH}_\infty$ should be required, where $\mathbf{RH}_\infty$ denotes $\mathbf{R}$ space which satisfies H_∞ condition. For this purposes, the model matching criterion is represented by

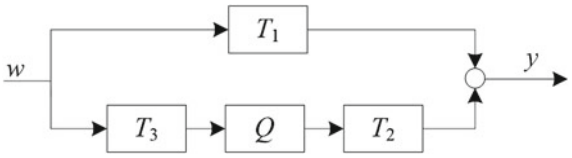

Fig. 4.2 Model matching

$$\sup\{\|y(t)\|_2 : w(t) \in \mathbf{H_2},\ \|w(t)\|_2\} < \gamma.$$

Thereby, the energy of the error $y(t)$ can be minimized for the worst input $w(t)$ of unit energy. On this basis, an equivalent criterion is thereby given as

$$\|T_1 - T_2 Q T_3\|_\infty < \gamma.$$

The model matching problem can be recast as a standard problem by defining

$$G := \begin{bmatrix} T_1 & T_2 \\ T_3 & 0 \end{bmatrix},\ K := -Q.$$

2. **Tracking problem**
Figure 4.3 reveals that the block P is the plant to be controlled, and the output $v(t)$ ought to track a reference signal $r(t)$. Controlled input $u(t)$ is produced by passing $r(t)$ and $v(t)$ through controllers C_1 and C_2, respectively. Note that $r(t)$ is an unknown fixed signal. Here, P and W are given, and C_1, C_2 are the blocks to be designed. The tracking error signal can be formulated by $r(t) - v(t)$, and the cost function is thereby defined as

$$(\|r(t) - v(t)\|_2^2 + \|\rho u(t)\|_2^2)^{1/2},$$

where ρ is a positive scalar representing weighing factor. Including $\rho u(t)$ in the cost function is to ensure the existence of an optimal proper controller. It should be noted that the cost function is equal to the H_2 norm of

$$y(t) := \begin{bmatrix} r(t) - v(t) \\ \rho u(t) \end{bmatrix}.$$

Therefore, the tracking criterion is taken to be

$$\|y(t)\|_\infty < \gamma.$$

Over the past few years, researches on SPSs in the H_∞ sense has been highly recognized in the control area due to its great practical importance [2–6, 12, 13, 16, 21, 22, 25, 27]. Luse and Ball [16] solved the H_∞ problem in the frequency domain. Pan and Baser [21, 22] used the theory of differential games and obtain necessary and sufficient conditions for the existence of a suboptimal solution as well as the construction of the suboptimal solution. Khail and Chen [12] had solved a

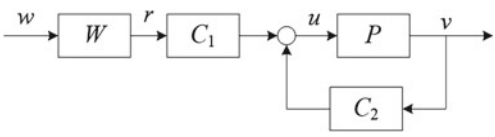

Fig. 4.3 Tracking problem

more general version of the H_∞ problem using the state-space algorithm. Dragan [2] studied the asymptotic expansions for game theoretic Riccati equations and showed how they may be used in singularly perturbed H_∞ control. More recently, Fridman [4] also considered a construction of high-order approximations to a controller that guaranteed a desired performance level on the basis of the exact decomposition of the full-order Riccati equations to the reduced order slow and fast equations. However, all these papers consider the H_∞ optimization over an entire frequency range. This, in a certain sense, does not take advantage of the special frequency characteristics analysis, which may result in some conservativeness in the designs.

The KYP lemma [23], one of the most fundamental results in control and signal processing, established the equivalence between a FDI characterized by the TF and a LMI associated with its state-space realization. The standard KYP lemma, however, is only applicable for the infinite frequency range. A very significant development made by Iwasaki and Hara [8–11] was the GKYP lemma, which established the equivalence between a frequency-domain property and a LMI over a finite frequency (FF) range, and enabled designers to impose performance requirements over chosen finite or infinite frequency ranges. Hence, it is very suitable for analysis and synthesis problems in practical applications, where different specifications over different frequency ranges are usually required.

4.2 Finite Frequency H_∞ State Feedback Control

In this section, H_∞ control synthesis of linear time-invariant SPSs based on a GKYP lemma is investigated. By employing the GKYP lemma on low-frequency and high-frequency ranges of SPSs, respectively, a slow (low-frequency) sub-controller and a fast (high frequency) sub-controller are designed to stabilize slow and fast subsystems, and satisfy individual H_∞ performance specifications. A composite controller for the full-order SPS is constructed via the two well-defined lower order sub-controllers. The problem of designing stabilizing controllers for SPSs is discussed based on simplified models. For this problem, it is necessary to require that the slow and the fast subsystems are asymptotically stable with some prescribed H_∞ constraints.

In Chaps. 1 and 2, a singularly perturbed model has already been given. Consider an LTI SPS, which is expressed by

$$\begin{aligned} \dot{x}_1(t) &= A_{11}x_1(t) + A_{12}x_2(t) + B_1u(t) + B_{w1}w(t), \\ \varepsilon\dot{x}_2(t) &= A_{21}x_1(t) + A_{22}x_2(t) + B_2u(t) + B_{w2}w(t), \\ y(t) &= C_1x_1(t) + C_2x_2(t), \end{aligned} \tag{4.2}$$

where $\varepsilon > 0$ is a small perturbation parameter, $x_1(t) \in \mathbf{R}^{n_1}$ and $x_2(t) \in \mathbf{R}^{n_2}$ are the slow and fast states, respectively, and $n = n_1 + n_2$ is the system dimension. $y(t) \in \mathbf{R}^q$ is measured output vector, $u(t) \in \mathbf{R}^p$ is the control input, and $w(t) \in \mathbf{R}^r$ is the external disturbance. The matrices A_{ij}, B_i, B_{wi} and C_i $(i, j = 1, 2)$ are of appropriate dimensions.

The assumption in the following is established throughout the section,

Assumption 4.1 *A_{22} is nonsingular.*

Remark 4.2 As mentioned in Chap. 1, Assumption 4.1 is widely used in SPSs, which guarantees the existence of A_{22}^{-1}, and is the requirement for the classical decomposition method of singular perturbations. With certain conditions, the high-order complicated system (4.2) could be reduced to two low-order subsystems that are called a reduced model (slow subsystem) and a boundary layer model (fast subsystem).

With the assumption, the SPS (4.2) is customarily referred to as a standard singularly perturbed model [13].

Hence, by decomposing the SPS (4.2), we get slow and fast subsystems, namely the slow subsystem Σ_s,

$$\begin{aligned} \dot{x}_{1s}(t) &= A_s x_{1s}(t) + B_{us} u_s(t) + B_{ws} w(t), \\ y_s(t) &= C_s x_{1s}(t) + D_{us} u_s(t) + D_{ws} w(t), \end{aligned} \tag{4.3}$$

where $A_s = A_{11} - A_{12}A_{22}^{-1}A_{21}$, $B_{us} = B_1 - A_{12}A_{22}^{-1}B_2$, $B_{ws} = B_{w1} - A_{12}A_{22}^{-1}B_{w2}$, $C_s = C_1 - C_2A_{22}^{-1}A_{21}$, $D_{us} = -C_2A_{22}^{-1}B_2$, $D_{ws} = -C_2A_{22}^{-1}B_{w2}$, and the fast subsystem, denoted by Σ_f,

$$\begin{aligned} \dot{x}_{2f}(\tau) &= A_{22} x_{2f}(\tau) + B_2 u_f(\tau) + B_{w2} w(\tau), \\ y_f(\tau) &= C_2 x_{2f}(\tau). \end{aligned} \tag{4.4}$$

We focus on the application of state feedback control laws of the form

$$u_s(t) = K_s x_{1s}(t), \quad u_f(\tau) = K_f x_{2f}(\tau),$$

with the goal of achieving desired H_∞ performance characteristics for subsystems Σ_s and Σ_f. Then, the closed-loop subsystems are shown as follows, the slow closed-loop subsystem,

$$\begin{aligned} \dot{x}_{1s}(t) &= (A_s + B_{us}K_s) x_{1s}(t) + B_{ws} w(t), \\ y_s(t) &= (C_s + D_{us}K_s) x_{1s}(t) + D_{ws} w(t), \end{aligned} \tag{4.5}$$

and the fast closed-loop subsystem,

$$\begin{aligned} \dot{x}_{2f}(\tau) &= (A_{22} + B_2K_f) x_{2f}(\tau) + B_{w2} w(\tau), \\ y_f(\tau) &= C_2 x_{2f}(\tau). \end{aligned} \tag{4.6}$$

It has been shown in [15–17] that $G(s, \varepsilon)$ has a two-frequency-scale TFM with

$$\begin{aligned} G_s(s) &= C_s(sI_{n_1} - A_s)^{-1}B_{ws} + D_{ws}, \\ G_f(p) &= C_2(pI_{n_2} - A_{22})^{-1}B_{w2}, \end{aligned}$$

if an SPS is a minimal analytic realization for $G(s, \varepsilon)$.

Here, the TFs $G_s(s)$ and $G_f(p)$ are mentioned as the low-frequency (slow) and high-frequency (fast) approximations of $G(s,\varepsilon)$, respectively. The high-frequency scale $p = \varepsilon s$ corresponds to the fast timescale $\tau = t/\varepsilon$ in the time domain. Thus, the problem under discussions can be described as follows.

Problem 4.2 (H_∞ *Control Problem*) Find a state feedback $u(t) = Kx(t)$, such that the closed loop of SPS (4.2) satisfies:

1. Internal stability;
2. For a given $\gamma > 0$, $\|G(s,\varepsilon)\|_\infty < \gamma$, for sufficient small parameter $\varepsilon > 0$.

Problem 4.3 (*Slow* H_∞ *Control Problem*) For the slow subsystem (4.5), the problem is summarized as follows: the state feedback sub-controller gain K_s is designed such that for a given ω_l the following requirements are satisfied:

1. $\|G_s(s)\|_\infty^{\Omega_l} < \gamma, \quad \Omega_l := \{\omega | |\omega| < \omega_l\}$;
2. The closed-loop system (4.5) is stable.

Note that here the H_∞ norm optimization is restricted in a specific regional Ω_l. For convenience of later development, define M_s the state-space matrices of $G_s * K_s$, that is

$$M_s := \begin{bmatrix} A_s & B_{ws} \\ C_s & D_{ws} \end{bmatrix} + \begin{bmatrix} B_{us} \\ D_{us} \end{bmatrix} K_s \begin{bmatrix} I_{n_1} & 0 \end{bmatrix}.$$

Theorem 4.1 *Let scalars p_1 and q_1 satisfying $p_1 q_1 > 0$, and $\gamma > 0$, and matrix $R_l \in \boldsymbol{R}^{n_1 \times (2n_1 + r + q)}$ be given. The closed-loop system of the slow subsystem (4.5) is stable and satisfies that for a given $\omega_l > 0$, when $|\omega| < \omega_l$, $\|G_s(s)\|_\infty^{\Omega_l} < \gamma$ holds, if there exist symmetric matrices $P_s \in \boldsymbol{R}^{n_1 \times n_1} > 0$, $P_l \in \boldsymbol{R}^{n_1 \times n_1}$, $Q_l \in \boldsymbol{R}^{n_1 \times n_1} > 0$ and $W_s \in \boldsymbol{R}^{n_1 \times n_1}$, and matrices $\mathscr{K}_s \in \boldsymbol{R}^{p \times n_1}$ and $V_l \in \boldsymbol{R}^{r \times (2n_1 + r + q)}$ such that the following LMIs are satisfied:*

$$\begin{bmatrix} 0 & P_s \\ P_s & 0 \end{bmatrix} < \mathrm{He} \begin{bmatrix} -W_s \\ A_s W_s + B_{us} \mathscr{K}_s \end{bmatrix} \begin{bmatrix} q_1 I_{n_1} & p_1 I_{n_1} \end{bmatrix}, \tag{4.7}$$

$$\begin{bmatrix} -Q_l & 0 & P_l & 0 \\ 0 & I_r & 0 & 0 \\ P_l & 0 & \omega_l^2 Q_l & 0 \\ 0 & 0 & 0 & -\gamma^2 I_q \end{bmatrix} < \mathrm{He} \begin{bmatrix} -I_{n_1} & 0 & 0 \\ 0 & -I_r & 0 \\ A_s & B_{ws} & B_{us} \\ C_s & D_{ws} & D_{us} \end{bmatrix} \begin{bmatrix} W_s R_l \\ V_l \\ \mathscr{K}_s R_l \end{bmatrix}. \tag{4.8}$$

With the conditions, a feasible state feedback gain is then given by $K_s = \mathscr{K}_s W_s^{-1}$.

Proof By [9], the matrices associated with the frequency separation can be selected by

$$\Phi = \begin{bmatrix} 0 & 1 \\ 1 & 0 \end{bmatrix}, \quad \Psi = \begin{bmatrix} -1 & 0 \\ 0 & \omega_l^2 \end{bmatrix}.$$

In this sense, the set $\Lambda(\Phi, \Psi)$ can be specialized to define a low-frequency range of variable ω.

On the other hand,

$$\|G_s(s)\|_\infty^{\Omega_l} < \gamma \iff \sigma(G_s(j\omega), \Pi) := \begin{bmatrix} G_s(j\omega) \\ I_q \end{bmatrix}^* \Pi \begin{bmatrix} G_s(j\omega) \\ I_q \end{bmatrix} < 0,$$

where $\Pi = \begin{bmatrix} I_r & 0 \\ 0 & -\gamma^2 I_q \end{bmatrix}$.

According to Lemma 2.2, we know that the above inequality holds if and only if there exist symmetric matrices $P_l = P_l^T$ and $Q_l = Q_l^T > 0$ such that the following inequality holds,

$$N \begin{bmatrix} \Phi \otimes P_l + \Psi \otimes Q_l & 0 \\ 0 & \Pi \end{bmatrix} N^T < 0, \tag{4.9}$$

where $N := \begin{bmatrix} M_s & I_{n_1+q} \end{bmatrix}$.

Note that the condition (4.9) is not convex due to the product terms between the parameters P_l, Q_l and $\mathscr{K}_s$. To solve it, a multiplier method is developed in [8], which reparameterizes the condition so that the problem becomes convex. To be specific, a sufficient condition based on the multiplier method is given in [8] to make condition (4.9) hold. If there exist matrices $W_s \in \mathscr{W}(\mathscr{C}_s, R_l)$, and $\mathscr{K}_s$ such that the following LMI holds

$$T \begin{bmatrix} \Phi \otimes P_l + \Psi \otimes Q_l & 0 \\ 0 & \Pi \end{bmatrix} T^T < \mathrm{He} \begin{bmatrix} -I_{n_1} & 0 & 0 \\ 0 & -I_r & 0 \\ A_s & B_{ws} & B_{us} \\ C_s & D_{ws} & D_{us} \end{bmatrix} \begin{bmatrix} W_s R_l \\ V_l \\ \mathscr{K}_s R_l \end{bmatrix}, \tag{4.10}$$

then the inequality (4.9) is satisfied.

On the other hand, we take the closed-loop stability into account, and a feasible stability condition taken also from [8] is given as follows: if there exist matrices W_s, $P_s > 0$, and K_s such that the following LMI holds:

$$\begin{bmatrix} 0 & P_s \\ P_s & 0 \end{bmatrix} < \mathrm{He} \begin{bmatrix} -W_s \\ A_s W_s + B_{us} \mathscr{K}_s \end{bmatrix} \begin{bmatrix} q_1 I_{n_1} & p_1 I_{n_1} \end{bmatrix},$$

then the closed-loop system (4.5) is stable. This completes the proof.

Remark 4.3 Theorem 4.1 gives a sufficient condition for the existence of a static feedback gain that achieves H_∞ performance for the slow problem. The conditions are given in terms of LMIs and can be solved numerically. The associated conservativeness is dependent upon the choice of R_l. In the state feedback setting, a reasonable choice has been proposed in [9]. In the case of the continuous-time, small gain condition, a feasible choice of R_l in the low-frequency range can be chosen as

$$R_l = \begin{bmatrix} 0 & 0 & I_{n_1} & (D_{11} B_1^\dagger)^T \end{bmatrix},$$

which, however, presents some potentially conservativeness.

Remark 4.4 Without loss of generality, if A_s, B_{ws}, B_{us}, C_s, D_{us} and D_{ws} are all real matrices, then P_s, P_l and Q_l in Theorem 4.1 are restricted to real matrices.

Problem 4.4 (*Fast H_∞ Control Problem*) For the fast subsystem (4.6), the following problem aims to find a state feedback gain K_f such that the following requirements are satisfied for a given ω_h:

1. When $\omega_h \in \Omega_h := \{\omega | |\omega| > \omega_h\}$, $\|G_f(p)\|_\infty^{\Omega_h} < \gamma$ is satisfied;
2. The closed-loop fast subsystem (4.6) can achieve the internal stability with $w = 0$.

Define M_f as the state-space matrix of system $G_f * K_f$,

$$M_f := \begin{bmatrix} A_{22} & B_{w2} \\ C_2 & 0 \end{bmatrix} + \begin{bmatrix} B_2 \\ 0 \end{bmatrix} K_f \begin{bmatrix} I_{n_2} & 0 \end{bmatrix}.$$

Similarly, here the H_∞ norm optimization is restricted on a specific regional Ω_h. One of our main results is given as follows.

Theorem 4.2 *Let $R_h \in \boldsymbol{R}^{n_2 \times (2n_2+r+q)}$ and p_2, q_2, $\gamma > 0$ be given, with $p_2 q_2 > 0$. The closed-loop system of fast subsystem (4.6) is internally stable and satisfies that for a given crossover frequency $\omega_h > 0$, $\|G_f(p)\|_\infty^{\Omega_h} < \gamma^2$, $|\omega| > \omega_h$, if there exist symmetric matrices $P_f \in \boldsymbol{R}^{n_2 \times n_2} > 0$, $P_h \in \boldsymbol{R}^{n_2 \times n_2}$, $Q_h \in \boldsymbol{R}^{n_2 \times n_2} > 0$ and $W_f \in \boldsymbol{R}^{n_2 \times n_2}$, and the matrices $\mathscr{K}_f \in \boldsymbol{R}^{p \times n_2}$ and $V_h \in \boldsymbol{R}^{r \times (2n_2+r+q)}$ such that the following LMIs are satisfied,*

$$\begin{bmatrix} 0 & P_f \\ P_f & 0 \end{bmatrix} < \mathrm{He} \begin{bmatrix} -W_f \\ A_f W_f + B_2 \mathscr{K}_f \end{bmatrix} \begin{bmatrix} q_2 I_{n_2} & p_2 I_{n_2} \end{bmatrix}, \tag{4.11}$$

$$\begin{bmatrix} Q_h & 0 & P_h & 0 \\ 0 & I_r & 0 & 0 \\ P_h & 0 & -\omega_h^2 Q_h & 0 \\ 0 & 0 & 0 & -\gamma^2 I_q \end{bmatrix} < \mathrm{He} \begin{bmatrix} -I_{n_2} & 0 & 0 \\ 0 & -I_r & 0 \\ A_f & B_{wf} & B_{uf} \\ C_f & D_{wf} & D_{uf} \end{bmatrix} \begin{bmatrix} W_f R_h \\ V_h \\ \mathscr{K}_f R_h \end{bmatrix}. \tag{4.12}$$

And with these conditions, a feasible state feedback gain is given by $K_f = \mathscr{K}_f W_f^{-1}$.

Proof From [9], we know that the set $\Lambda(\Phi, \Psi)$ can be specialized to define a high-frequency range of frequency variable by an appropriate choice of Φ and Ψ,

$$\Phi = \begin{bmatrix} 0 & 1 \\ 1 & 0 \end{bmatrix}, \quad \Psi = \begin{bmatrix} 1 & 0 \\ 0 & -\omega_h^2 \end{bmatrix}.$$

In this case, $\Lambda(\Phi, \Psi) = \{j\omega : \omega \in \Omega_h\}$. The following is similar to the proof of Theorem 4.1, and is omitted here.

Remark 4.5 Theorem 4.2 gives a sufficient condition for the existence of static feedback gain that achieves H_∞ performance for the fast problem. The condition is given in terms of LMIs and can be solved numerically. The associated conservativeness is

dependent upon the choice of R_h. In the state feedback setting, a reasonable choice has been proposed for the high-frequency continuous-time, small-gain condition,

$$R_h = \begin{bmatrix} I_{n_2} & 0 & 0 & 0 \end{bmatrix}.$$

Based on the composite strategy shown in Fig. 4.4, the gain of a composite state feedback controller is given as

$$K = \begin{bmatrix} K_s + K_f A_{22}^{-1} A_{21} + K_f A_{22}^{-1} B_2 K_s & K_f \end{bmatrix}. \tag{4.13}$$

Remark 4.6 The composite controller undertaken in this section has already been utilized in Chap. 3 to discuss the stability for SPS, which is different from the previous literature [4, 12, 21, 22], where the composite controller in the sense is just taken as the connection of K_s and K_f, that is, $K = \begin{bmatrix} K_s & K_f \end{bmatrix}$. The main reason behind this is that the states of slow and fast subsystems are x_{1s} and x_{2f}, respectively, and the sub-controllers K_s and K_f are used to control x_{1s} and x_{2f}, respectively. The states of the original SPS (4.2) are (x_1, x_2) rather than (x_{1s}, x_{2f}), which are controlled by the composite controller K.

The potential explanation for this difference is that we consider the H_∞ control in a FF range rather than in an entire frequency range. Here, the composite controller form (4.13) is more effective to solve the ill-posed problem of an SPS.

Note that cross-over frequencies ω_l and ω_h are closely related with the conservatism of Theorems. Next, we present how to effectively choose the cross-over frequencies ω_l and ω_h.

Algorithm 4.1 *The prescribed values of ω_l and ω_h are given as the following algorithm.*

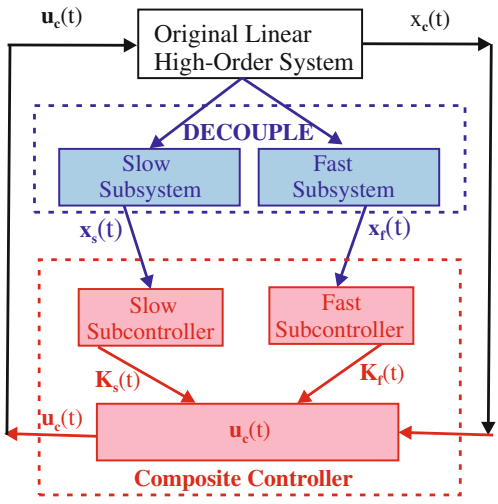

Fig. 4.4 The composite strategy

Step1. *Calculate the module of low-frequency TF* $G_s(j\omega)$ *and high-frequency TF* $G_f(\varepsilon j\omega)$.
Step2. *Given error accuracy* $e = 0.01$ *and sufficient small parameter* ε, *for* $\omega = 0 : 0.0001 : 100$, *if* $\|G_s(j\omega)\| - \|G_f(\varepsilon j\omega)\| < e$, *then* ω *is achieved.*
Step3. *Choose* $\omega_l \in [0, \omega]$ *and* $\omega_h \in (\omega, +\infty)$.

To summarize, we have solved the H_∞ controller design problem of SPSs in the specific frequency domain, and we have shown how to decompose the H_∞ control problem into slow and fast subproblems in each frequency scale.

4.3 Finite Frequency H_∞ Output Feedback Control

To the best of the authors' knowledge, methods to realize FF H_∞ control of SPSs remain as an open research area in the literature. This section presents approaches for the design of static and dynamic output feedback controllers according to the frequency characteristics of SPSs. A novel strategy for the design of mixed output feedback controller (MOFC) is proposed in the sum of the static output feedback controller (SOFC) and dynamic output feedback controller (DOFC), where the numerical stiffness of the whole SPS is alleviated. In this sense, the original ill-conditioned control problem can be solved within a specified order-of-ε accuracy.

Consider the following linear SPS with n-dimensional dynamics representing the fast and slow phenomena:

$$\begin{aligned} \dot{x}_1(t) &= A_{11}x_1(t) + A_{12}x_2(t) + B_{w1}w(t) + B_1u(t), \\ \varepsilon\dot{x}_2(t) &= A_{21}x_1(t) + A_{22}x_2(t) + B_{w2}w(t) + B_2u(t), \\ y(t) &= C_{11}x_1(t) + C_{12}x_2(t) + D_{11}w(t) + D_{12}u(t), \\ z(t) &= C_{21}x_1(t) + C_{22}x_2(t) + D_{21}w(t) + D_{22}u(t), \end{aligned} \tag{4.14}$$

where ε is a perturbation parameter and $0 < \varepsilon \ll 1$; $x_1(t) \in \mathbf{R}^{n_1}$ and $x_2(t) \in \mathbf{R}^{n_2}$ are the slow and fast states, respectively, $n_1 + n_2 = n$. $u(t) \in \mathbf{R}^p$ is the control input, $w(t) \in \mathbf{R}^r$ is the external disturbance, $y(t) \in \mathbf{R}^q$ is the measurement output, and $z(t) \in \mathbf{R}^s$ is the controlled output. Matrices A_{ij}, B_{wi}, B_i, C_{ij} and D_{ij} $(i, j = 1, 2)$ are constant matrices with appropriate dimensions.

Applying Laplace transform with zero initial condition, the system (4.14) can be converted into the following frequency model:

$$\begin{bmatrix} \lambda x_1(s) \\ \varepsilon\lambda x_2(s) \\ y(s) \\ z(s) \end{bmatrix} = \begin{bmatrix} A_{11} & A_{12} & B_{w1} & B_1 \\ A_{21} & A_{22} & B_{w2} & B_2 \\ C_{11} & C_{12} & D_{11} & D_{12} \\ C_{21} & C_{22} & D_{21} & 0 \end{bmatrix} \begin{bmatrix} x_1(s) \\ x_2(s) \\ w(s) \\ u(s) \end{bmatrix}, \tag{4.15}$$

where λ is the frequency variable.

Consider the linear SOFC:

$$u(t) = Kz(t), \quad K \in \mathbf{R}^{p\times s}. \tag{4.16}$$

Substituting (4.16) into (4.14) yields

$$\begin{aligned}
\dot{x}_1 &= (A_{11} + B_1KC_{21})x_1 + (A_{12} + B_1KC_{22})x_2 + (B_{w1} + B_1KD_{21})w,\\
\varepsilon\dot{x}_2 &= (A_{21} + B_2KC_{21})x_1 + (A_{22} + B_2KC_{22})x_2 + (B_{w2} + B_2KD_{21})w,\\
y &= (C_{11} + D_{12}KC_{21})x_1 + (C_{12} + D_{12}KC_{22})x_2 + (D_{11} + D_{12}KD_{21})w.
\end{aligned} \tag{4.17}$$

Take the DOFC into consideration,

$$\begin{aligned}
\dot{\hat{x}} &= A_k\hat{x} + B_kz,\\
u &= C_k\hat{x} + D_kz,
\end{aligned} \tag{4.18}$$

where $\hat{x} \in \mathbf{R}^{n_k}$ is the state vector, and A_k, B_k, C_k, D_k, are uncertain matrices to be identified. Denoting $\xi = \left[x_1{}^T \ \hat{x}^T\right]^T$, $\xi \in \mathbf{R}^{n_1+n_k}$, the closed-loop system for (4.14) can be expressed as

$$\begin{aligned}
\dot{\xi} &= \hat{A}_{11}\xi + \hat{A}_{12}z + \hat{B}_{w1}w,\\
\varepsilon\dot{x}_2 &= \hat{A}_{21}\xi + \hat{A}_{22}x_2 + \hat{B}_{w2}w,\\
y &= \hat{C}_{11}\xi + \hat{C}_{12}x_2 + \hat{D}_ww,
\end{aligned} \tag{4.19}$$

where

$$\begin{aligned}
\hat{A}_{11} &= \begin{bmatrix} A_{11} + B_1D_kC_{21} & B_1C_k \\ B_kC_{21} & A_k \end{bmatrix}, \quad \hat{A}_{12} = \begin{bmatrix} A_{12} + B_1D_kC_{22} \\ B_kC_{22} \end{bmatrix},\\
\hat{A}_{21} &= \begin{bmatrix} A_{21} + B_2D_kC_{21} \\ B_2C_k \end{bmatrix}^T, \quad \hat{A}_{22} = A_{22} + B_2D_kC_{22},\\
\hat{B}_{w1} &= \begin{bmatrix} B_{w1} + B_1D_kD_{21} \\ B_kD_{21} \end{bmatrix}, \quad \hat{B}_{w2} = B_{w2} + B_2D_kD_{21},\\
\hat{C}_{11} &= \begin{bmatrix} C_{11} + D_{12}D_kC_{21} \\ D_{12}C_k \end{bmatrix}^T, \quad \hat{C}_{12} = C_{12} + D_{12}D_kC_{22},\\
\hat{D}_w &= D_{11} + D_{12}D_kD_{21}.
\end{aligned}$$

Remark 4.7 (*The characteristics of SOFC and DOFC*) SOFC is simple and practical, but its response rate is much slower than DOFC. Considering the dynamic performances of output feedback controllers, the SOFC is effective to suppress the low-frequency disturbances, while the DOFC can detect the high-frequency interferences immediately to restrain them to a large extent. Note that the DOFC using here should be of lower order than the fast subsystem to facilitate the practical implementation of the proposed control scheme.

Definition 4.1 (*Slow and Fast Transfer Function Matrix (TFM)*) The TFM $G(\varepsilon, s)$ from the input $u(s)$ to the output $y(s, \varepsilon)$ is given by the sum of the slow and fast TFMs [13],

$$y(s, \varepsilon) = G(s, \varepsilon)u(s) = [G_s(s, \varepsilon) + G_f(p, \varepsilon)]u(s).$$

The **slow TFM** is a function of s:

$$G(s, \varepsilon) = C_s(sI_{n_1} - A_s)^{-1}B_s + D_s,$$

and the **fast TFM** is a function of p:

$$G_f(p, \varepsilon) = C_f(pI_{n_2} - A_f)^{-1}B_f + D_f.$$

The TFMs from the external disturbance to measurement output of slow and fast subsystems are denoted as $T_{yws}(s)$ and $T_{ywf}(p)$, respectively.

To derive the main results, the following definition of FF H_∞ control of SPSs is needed.

Definition 4.2 (*FF H_∞ Control of SPSs*) The LTI SPS is said to have H_∞ **property** if, for any initial values $x_1(0)$ and $x_2(0)$, there exists an output feedback controller in form of (4.16) or (4.18) such that

1. the closed-loop systems of the slow and fast subsystems are asymptotically stable when $w(t) = 0$;
2. H_∞ norms of the closed-loop slow and fast TFMs, $T_{yws}(s)$ and $T_{ywf}(p)$, satisfy the constraints below.

$$\left\| T_{yws}(s) \right\|_\infty < \gamma, \ \omega \in \{\omega | \, |\omega| \leq \omega_l\}, \tag{4.20}$$

$$\left\| T_{ywf}(p) \right\|_\infty < \gamma, \ \bar{\omega} \in \{\bar{\omega} | \, |\bar{\omega}| \geqslant \omega_h\}. \tag{4.21}$$

Remark 4.8 The full-frequency H_∞ control is a special case for the FF H_∞ control when the symmetric matrix Q in the GKYP lemma is set to zero.

Hence, the aim of the section is to derive the sufficient conditions in terms of ε-independent LMIs, and design output feedback controllers to realize the performance indexes (4.20) and (4.21) hereinafter.

Using the classical SPMs in [13], system (4.14) can be separated into slow and fast subsystems, with the slow subsystem established as

$$\begin{aligned} \dot{x}_1 &= A_s x_1 + B_{ws} w + B_s u, \\ y &= C_s x_1 + D_{ws} w + D_s u, \\ z &= Y_{s1} x_1 + Y_{s2} w + Y_{s3} u, \end{aligned} \tag{4.22}$$

where

$$A_s = A_{11} - A_{12}A_{22}^{-1}A_{21},\ B_{ws} = B_{w1} - A_{12}A_{22}^{-1}B_{w2},\ B_s = B_1 - A_{12}A_{22}^{-1}B_2,$$
$$C_s = C_{11} - C_{12}A_{22}^{-1}A_{21},\ D_{ws} = D_{11} - C_{12}A_{22}^{-1}B_{w2},\ D_s = D_{12} - C_{12}A_{22}^{-1}B_2,$$
$$Y_{s1} = C_{21} - C_{22}A_{22}^{-1}A_{21},\ Y_{s2} = D_{21} - C_{22}A_{22}^{-1}B_{w2},\ Y_{s3} = -C_{22}A_{22}^{-1}B_2.$$

The open-loop TF of system (4.22) with $u = 0$, denoted by $G_{yws}(s)$, is

$$G_{yws}(s) = C_s(sI_{n_1} - A_s)^{-1}B_{ws} + D_{ws}. \tag{4.23}$$

Plugging (4.16) into (4.22), the closed-loop slow subsystem via the SOFC is

$$\begin{aligned} \dot{x}_1 &= (A_s + B_sKY_{s1})x_1 + (B_{ws} + B_sKY_{s2})w, \\ y &= (C_s + D_sKY_{s1})x_1 + (D_{ws} + D_sKY_{s2})w, \end{aligned} \tag{4.24}$$

and $M_{ss} = \bar{A}_s + \bar{B}_sK\bar{C}_s = \begin{bmatrix} A_s & B_{ws} \\ C_s & D_{ws} \end{bmatrix} + \begin{bmatrix} B_s \\ D_s \end{bmatrix} K \begin{bmatrix} Y_{s1} & Y_{s2} \end{bmatrix}$.

Plugging (4.18) into (4.22), the closed-loop slow subsystem via the DOFC is

$$\begin{aligned} \dot{\xi} &= A_{sd}\xi + B_{sd}w, \\ y &= C_{sd}\xi + D_{sd}w, \end{aligned} \tag{4.25}$$

where

$$A_{sd} = \begin{bmatrix} A_{11} - A_{12}A_{22}^{-1}A_{21} & (B_1 - A_{12}A_{22}^{-1}B_2)C_k \\ B_k(C_{21} - C_{22}A_{22}^{-1}A_{21}) & A_k - B_kC_{22}A_{22}^{-1}B_2C_k \end{bmatrix},\ B_{sd} = \begin{bmatrix} B_{w1} - A_{12}A_{22}^{-1}B_{w2} \\ B_k(D_{21} - C_{22}A_{22}^{-1}B_{w2}) \end{bmatrix},$$
$$C_{sd} = \begin{bmatrix} C_{11} - C_{12}A_{22}^{-1}A_{21} \\ (D_{12} - C_{12}A_{22}^{-1}B_2)C_k \end{bmatrix}^T,\ D_{sd} = D_{11} - C_{12}A_{22}^{-1}B_{w2}.$$

The state-space realization of the closed-loop system (4.18) is represented as

$$M_{sd} = \bar{A}_{sd} + \bar{B}_{sd}K_{sd}\bar{C}_{sd}\ (D_k = 0),$$

where

$$\bar{A}_{sd} = \begin{bmatrix} A_{11} - A_{12}A_{22}^{-1}A_{21} & 0 & B_{w1} - A_{12}A_{22}^{-1}B_{w2} \\ 0 & 0 & 0 \\ C_{11} - C_{12}A_{22}^{-1}A_{21} & 0 & D_{11} - C_{12}A_{22}^{-1}B_{w2} \end{bmatrix},\ \bar{B}_{sd} = \begin{bmatrix} 0 & B_1 - A_{12}A_{22}^{-1}B_2 \\ I_{n_k} & 0 \\ 0 & D_{12} - C_{12}A_{22}^{-1}B_2 \end{bmatrix},$$
$$\bar{C}_{sd} = \begin{bmatrix} 0 & I_{n_k} & 0 \\ C_{21} - C_{22}A_{22}^{-1}A_{21} & 0 & D_{21} - C_{22}A_{22}^{-1}B_{w2} \end{bmatrix},\ K_{sd} = \begin{bmatrix} A_k - B_kC_{22}A_{22}^{-1}B_2C_k & B_k \\ C_k & 0 \end{bmatrix},$$

and K_{sd} is the unknown parameter matrix to be determined.

The resulting description of the fast subsystem is demonstrated as

$$\begin{aligned} \dot{x}_2 &= A_{22}x_2 + B_{w2}w + B_2u, \\ y &= C_{12}x_2 + D_{11}w + D_{12}u, \\ z &= C_{22}x_2 + D_{21}w. \end{aligned} \tag{4.26}$$

The open-loop TF of the fast subsystem, defined by $G_{ywf}(p)$, is

$$G_{ywf}(p) = C_{12}(pI_{n_2} - A_{22})^{-1}B_{w2} + D_{11}. \tag{4.27}$$

Substituting (4.16) into system (4.26) gives us that

$$\begin{aligned} \dot{x}_2 &= (A_{22} + B_2KC_{22})x_2 + (B_{w2} + B_2KD_{21})w, \\ y &= (C_{12} + D_{12}KC_{22})x_2 + (D_{11} + D_{12}KD_{21})w, \end{aligned} \tag{4.28}$$

and

$$M_{fs} = \bar{A}_f + \bar{B}_fK\bar{C}_f = \begin{bmatrix} A_{22} & B_{w2} \\ C_{12} & D_{11} \end{bmatrix} + \begin{bmatrix} B_2 \\ D_{12} \end{bmatrix} K \begin{bmatrix} C_{22} & D_{21} \end{bmatrix}.$$

Plugging (4.18) into (4.26) gives

$$\begin{aligned} \dot{x}_2 &= (A_{22} + B_2D_kC_{22})x_2 + (B_{w2} + B_2D_kD_{21})w, \\ y &= (C_{12} + D_{12}D_kC_{22})x_2 + (D_{11} + D_{12}D_kD_{21})w, \end{aligned} \tag{4.29}$$

and

$$M_{fd} = \bar{A}_{fd} + \bar{B}_{fd}D_k\bar{C}_{fd} = \begin{bmatrix} A_{22} & B_{w2} \\ C_{12} & D_{11} \end{bmatrix} + \begin{bmatrix} B_2 \\ D_{12} \end{bmatrix} D_k \begin{bmatrix} C_{22} & D_{21} \end{bmatrix}.$$

Remark 4.9 (*The Frequency Domain Nature of SPSs*) With the aid of the classical SPMs, the whole system is decoupled into the slow and fast subsystems. From the frequency-domain perspective, the slow (fast) subsystem is composed of low-frequency (high-frequency) components. To avoid the unnecessary frequency overlap, the related subsystems should work in the disjoint frequency bands. In other words, the slow (fast) subsystem in the low (high) frequency range is used to represent the low (high) frequency characteristic of SPS.

In addition, the assumption in the following is established throughout the section.

Assumption 4.2 *$T_{yws}(s)$ and $T_{ywf}(p)$ have no unstable lost poles.*

Remark 4.10 Lost poles are defined in [17] through the usage of parameter-dependent system matrices. Assumption 4.2 guarantees the stability of the uncontrollable and unobservable part of the whole system, which essentially guarantees that there are no singularities induced by unstable lost poles.

Next, sufficient conditions for bounded realness with the stability constraints of the related subsystems are given in terms of LMIs. Methods to design the composite SOFC and DOFC for SPSs are stated. Then, the entire frequency range are divided into three parts: the low-, middle- and high-frequency ranges. Different frequency ranges lead to different control strategies. Furthermore, the MOFC is constructed comprising of the composite SOFC and DOFC to achieve better control effectiveness of the whole system.

4.3.1 The Slow Subsystem and Associated H_∞ Controller in the Low-Frequency Domain

Theorem 4.3 *Let weighing matrices $R_l \in \mathbf{R}^{s\times(2n_1+r+q)}$ and $R_s \in \mathbf{R}^{s\times 2n_1}$, crossover frequency ω_l, and the disturbance attenuation index $\gamma > 0$ be given. If there exist positive definite matrices $P_s \in \mathbf{R}^{n_1\times n_1}$ and $Q_l \in \mathbf{R}^{n_1\times n_1}$, symmetrical matrices $P_l \in \mathbf{R}^{n_1\times n_1}$ and $W_s \in \mathbf{R}^{s\times s}$, and matrices $V_s \in \mathbf{R}^{n_1\times 2n_1}$, $V_l \in \mathbf{R}^{(n_1+r)\times(2n_1+r+q)}$, and $\mathscr{K}_{ss} \in \mathbf{R}^{p\times s}$ such that the following LMIs are satisfied,*

$$\begin{bmatrix} 0 & P_s \\ P_s & 0 \end{bmatrix} < \mathrm{He}\begin{bmatrix} -Y_{s1}^\dagger & -(I_{n_1} - Y_{s1}^\dagger Y_{s1}) & 0 \\ A_s Y_{s1}^\dagger & A_s(I_{n_1} - Y_{s1}^\dagger Y_{s1}) & B_s \end{bmatrix}\begin{bmatrix} W_s R_s \\ V_s \\ \mathscr{K}_{ss} R_s \end{bmatrix}, \tag{4.30}$$

$$\begin{bmatrix} -Q_l & 0 & P_l & 0 \\ 0 & I_r & 0 & 0 \\ P_l & 0 & \omega_l^2 Q_l & 0 \\ 0 & 0 & 0 & -\gamma^2 I_q \end{bmatrix} < \mathrm{He}\begin{bmatrix} -\bar{C}_s^\dagger & -(I_{n_1+r} - \bar{C}_s^\dagger \bar{C}_s) & 0 \\ \bar{A}_s \bar{C}_s^\dagger & \bar{A}_s(I_{n_1+r} - \bar{C}_s^\dagger \bar{C}_s) & \bar{B}_s \end{bmatrix}\begin{bmatrix} W_s R_l \\ V_l \\ \mathscr{K}_{ss} R_l \end{bmatrix}, \tag{4.31}$$

then the closed-loop slow subsystem (4.24) is stable and satisfies Eq. (4.20) for a given ω_l. With these conditions, a feasible SOFC gain is given by $K_{ss} = \mathscr{K}_{ss} W_s^{-1}$.

Proof (1) First, the stability of the slow subsystem is proven.

Provided that $w = 0$, we select the Lyapunov function of the slow subsystem,

$$V(x(t)) = x^T(t) P_s x(t),\ P_s \in \mathbf{R}^{n_1\times n_1} > 0.$$

Taking the derivative of $V(x(t))$, we have

$$\dot{V}(x(t)) = x^T P_s \dot{x} + \dot{x}^T P_s x = x^T P_s(A_s + B_s K_{ss} Y_{s1})x + x^T (A_s + B_s K_{ss} Y_{s1})^T P_s x.$$

Since a matrix has the same eigenvalues as its transposition, it is established that

$$(A_s + B_s K_{ss} Y_{s1}) P_s + P_s (A_s + B_s K_{ss} Y_{s1})^T < 0,$$

which can be represented as

$$\left[\begin{array}{cc} A_s + B_s K_{ss} Y_{s1} & I_{n_1} \end{array}\right] \left[\begin{array}{cc} 0 & P_s \\ P_s & 0 \end{array}\right] \left[\begin{array}{c} (A_s + B_s K_{ss} Y_{s1})^T \\ I_{n_1} \end{array}\right] < 0.$$

and by Lemma 2.3, can be simplified by setting $\mathscr{K}_{ss} = K_{ss} W_s$,

$$\left[\begin{array}{cc} 0 & P_s \\ P_s & 0 \end{array}\right] < \mathrm{He} \left[\begin{array}{c} -\chi_s \\ A_s \chi_s + B_s \mathscr{K}_{ss} R_s \end{array}\right], \tag{4.32}$$

with $\chi_s = Y_{s1}^\dagger W_s R_s + (I_{n_1} - Y_{s1}^\dagger Y_{s1}) V_s$.

Substituting χ_s into (4.32) implies

$$\left[\begin{array}{cc} 0 & P_s \\ P_s & 0 \end{array}\right] < \mathrm{He} \left[\begin{array}{ccc} -Y_{s1}^\dagger & -(I_{n_1} - Y_{s1}^\dagger Y_{s1}) & 0 \\ A_s Y_{s1}^\dagger & A_s (I_{n_1} - Y_{s1}^\dagger Y_{s1}) & B_s \end{array}\right] \left[\begin{array}{c} W_s R_s \\ V_s \\ \mathscr{K}_{ss} R_s \end{array}\right]. \tag{4.33}$$

(2) Realize the FF bounded realness for the slow subsystems.

To get the target frequency set Ω_l, we select

$$\Phi = \left[\begin{array}{cc} 0 & 1 \\ 1 & 0 \end{array}\right], \quad \Psi = \left[\begin{array}{cc} -1 & 0 \\ 0 & \omega_l^2 \end{array}\right].$$

The low-frequency bounded-real property of the slow subsystem can be formulated by letting

$$\Pi = \left[\begin{array}{cc} I_r & 0 \\ 0 & -\gamma^2 I_q \end{array}\right],$$

and the inequality hereinafter can be derived from Lemma 2.3,

$$NT \left[\begin{array}{cc} \Phi \otimes P_l + \Psi \otimes Q_l & 0 \\ 0 & \Pi \end{array}\right] T^T N^T < 0, \tag{4.34}$$

where $N = \left[\begin{array}{cccc} A_s + B_s K_{ss} Y_{s1} & B_{ws} + B_s K_{ss} Y_{s2} & I_{n_1} & 0 \\ C_s + D_s K_{ss} Y_{s1} & D_{ws} + D_s K_{ss} Y_{s1} & 0 & I_q \end{array}\right] = [\, M_{ss} \;\; I_{n_1+q} \,]$.

For a certain R_l satisfying conditions in Lemma 2.2, we have

$$T \left[\begin{array}{cc} \Phi \otimes P_l + \Psi \otimes Q_l & 0 \\ 0 & \Pi \end{array}\right] T^T < \mathrm{He} \left[\begin{array}{c} -\chi_l \\ \bar{A}_s \chi_l + \bar{B}_s \mathscr{K}_{ss} R_l \end{array}\right], \tag{4.35}$$

where $\mathscr{K}_{ss} = K_{ss} W_s$. Here, the multiplier χ_l belongs to the class of

$$\chi_l \in W\left(\bar{C}_s, R_l\right) = \{\bar{C}_s^\dagger W_s R_l + (I_{n_1+r} - \bar{C}_s^\dagger \bar{C}_s) V_l \,|\, W_s \in \mathbf{R}^{s \times s}, V_l \in \mathbf{R}^{(n_1+r)\times(2n_1+r+q)}\}.$$

Hence, (4.35) can be rewritten as

$$T\begin{bmatrix}\Phi\otimes P_l+\Psi\otimes Q_l & 0\\ 0 & \Pi\end{bmatrix}T^T<\mathrm{He}\begin{bmatrix}-\bar{C}_s^\dagger & -(I_{n_1+r}-\bar{C}_s^\dagger\bar{C}_s) & 0\\ \bar{A}_s\bar{C}_s^\dagger & \bar{A}_s(I_{n_1+r}-\bar{C}_s^\dagger\bar{C}_s) & \bar{B}_s\end{bmatrix}\begin{bmatrix}W_sR_l\\ V_l\\ \mathscr{K}_{ss}R_l\end{bmatrix}, \tag{4.36}$$

where $\bar{A}_s$, $\bar{B}_s$ and $\bar{C}_s$ are defined in M_{ss}, and T is the permutation matrix such that

$$\begin{bmatrix}M_1 & M_2 & M_3 & M_4\end{bmatrix}T=\begin{bmatrix}M_1 & M_3 & M_2 & M_4\end{bmatrix}.$$

It can be seen that (4.36) can be represented in the compact form,

$$\begin{bmatrix}-Q_l & 0 & P_l & 0\\ 0 & I_r & 0 & 0\\ P_l & 0 & \omega_l^2Q_l & 0\\ 0 & 0 & 0 & -\gamma^2I_q\end{bmatrix}<\mathrm{He}\begin{bmatrix}-\bar{C}_s^\dagger & -(I_{n_1+r}-\bar{C}_s^\dagger\bar{C}_s) & 0\\ \bar{A}_s\bar{C}_s^\dagger & \bar{A}_s(I_{n_1+r}-\bar{C}_s^\dagger\bar{C}_s) & \bar{B}_s\end{bmatrix}\begin{bmatrix}W_sR_l\\ V_l\\ \mathscr{K}_{ss}R_l\end{bmatrix}. \tag{4.37}$$

This completes the proof.

For the system (4.25), we can get the following result.

Theorem 4.4 *Let matrices $R_{ld}\in\mathbf{R}^{(s+n_k)\times[2(n_1+n_k)+r+q]}$ and $R_{sd}\in\mathbf{R}^{(s+n_k)\times2(n_1+n_k)}$, the crossover frequency ω_l, and the disturbance attenuation index $\gamma>0$ be given. If there exist positive definite matrices $P_{sd}\in\mathbf{R}^{(n_1+n_k)\times(n_1+n_k)}$ and $Q_{ld}\in\mathbf{R}^{(n_1+n_k)\times(n_1+n_k)}$, symmetrical matrices $P_{ld}\in\mathbf{R}^{(n_1+n_k)\times(n_1+n_k)}$ and $W_{sd}\in\mathbf{R}^{(s+n_k)\times(s+n_k)}$, and matrices $V_{sd}\in\mathbf{R}^{(n_1+n_k)\times2(n_1+n_k)}$ and $V_{ld}\in\mathbf{R}^{(n_1+n_k+r)\times[2(n_1+n_k)+r+q]}$, such that the following LMIs are satisfied,*

$$\begin{bmatrix}0 & P_{sd}\\ P_{sd} & 0\end{bmatrix}<\mathrm{He}\begin{bmatrix}-C_{sd}^\dagger & -(I_{n_1+n_k}-C_{sd}^\dagger C_{sd}) & 0\\ A_{sd}C_{sd}^\dagger & A_{sd}(I_{n_1+n_k}-C_{sd}^\dagger C_{sd}) & B_{sd}\end{bmatrix}\begin{bmatrix}W_{sd}R_{sd}\\ V_{sd}\\ \kappa_{sd}R_{sd}\end{bmatrix}, \tag{4.38}$$

$$\begin{bmatrix}-Q_{ld} & 0 & P_{ld} & 0\\ 0 & I_r & 0 & 0\\ P_{ld} & 0 & \omega_l^2Q_{ld} & 0\\ 0 & 0 & 0 & -\gamma^2I_q\end{bmatrix}<\mathrm{He}\begin{bmatrix}-\bar{C}_{sd}^\dagger & -(I_{n_1+n_k+r}-\bar{C}_{sd}^\dagger\bar{C}_{sd}) & 0\\ \bar{A}_{sd}\bar{C}_{sd}^\dagger & \bar{A}_{sd}(I_{n_1+n_k+r}-\bar{C}_{sd}^\dagger\bar{C}_{sd}) & \bar{B}_{sd}\end{bmatrix}\begin{bmatrix}W_{sd}R_{ld}\\ V_{ld}\\ \kappa_{sd}R_{ld}\end{bmatrix}, \tag{4.39}$$

then the closed-loop slow subsystem (4.25) is stable and satisfies (4.20) for a given ω_l.

Thus, the parameter matrices of the DOFC (4.18) can be calculated by the following formula,

$$\tilde{A}_kW_{sd1}+B_kW_{sd2}=\kappa_{sd1},\ C_kW_{sd1}=\kappa_{sd2},$$

where

$$\kappa_{sd}=\begin{bmatrix}\kappa_{sd1}\\ \kappa_{sd2}\end{bmatrix},\ \kappa_{sd1}\in\mathbf{R}^{n_k\times(n_k+s)},\ \kappa_{sd2}\in\mathbf{R}^{s\times(n_k+s)},$$

$$W_{sd}=\begin{bmatrix}W_{sd1}\\ W_{sd2}\end{bmatrix},\ W_{sd1}\in\mathbf{R}^{n_k\times(n_k+s)},\ W_{sd2}\in\mathbf{R}^{s\times(n_k+s)},$$

$$\tilde{A}_k=A_k-B_kC_{22}A_{22}^{-1}B_2C_k.$$

Proof (1) Realize the stability and FF bounded realness for the slow subsystems.

Using the DOFC (4.18), the closed-loop system can be represented by (4.25). To eliminate the coupling part in (4.25), we set $D_k = 0$ compulsively, which makes it possible to convert the conditions into the LMI form. In this sense, it is easy to verify that $\hat{A}_{22} = A_{22}$. Thus, the slow subsystem (4.25) can be rewritten by

$$\begin{aligned} \dot{\xi} &= A_{sd}\xi + B_{sd}w, \\ z &= C_{sd}\xi + D_{sd}w, \end{aligned} \tag{4.40}$$

where

$$A_{sd} = \begin{bmatrix} A_{11} - A_{12}A_{22}^{-1}A_{21} & (B_1 - A_{12}A_{22}^{-1}B_2)C_k \\ B_k(C_{21} - C_{22}A_{22}^{-1}A_{21}) & A_k - B_kC_{22}A_{22}^{-1}B_2C_k \end{bmatrix}, B_{sd} = \begin{bmatrix} B_{w1} - A_{12}A_{22}^{-1}B_{w2} \\ B_k(D_{21} - C_{22}A_{22}^{-1}B_{w2}) \end{bmatrix},$$
$$C_{sd} = \begin{bmatrix} C_{11} - C_{12}A_{22}^{-1}A_{21} & (D_{12} - C_{12}A_{22}^{-1}B_2)C_k \end{bmatrix}, \ D_{sd} = D_{11} - C_{12}A_{22}^{-1}B_{w2}.$$

The state-space matrix can be written in the standard form in Lemma 2.3,

$$M_{sd} := \bar{A}_{sd} + \bar{B}_{sd}K_{sd}\bar{C}_{sd},$$

where

$$\bar{A}_{sd} = \begin{bmatrix} A_{11} - A_{12}A_{22}^{-1}A_{21} & 0 & B_{w1} - A_{12}A_{22}^{-1}B_{w2} \\ 0 & 0 & 0 \\ C_{11} - C_{12}A_{22}^{-1}A_{21} & 0 & D_{11} - C_{12}A_{22}^{-1}B_{w2} \end{bmatrix}, \bar{B}_{sd} = \begin{bmatrix} 0 & B_1 - A_{12}A_{22}^{-1}B_2 \\ I_{n_k} & 0 \\ 0 & D_{12} - C_{12}A_{22}^{-1}B_2 \end{bmatrix},$$
$$\bar{C}_{sd} = \begin{bmatrix} 0 & I_{n_k} & 0 \\ C_{21} - C_{22}A_{22}^{-1}A_{21} & 0 & D_{21} - C_{22}A_{22}^{-1}B_{w2} \end{bmatrix}, K_{sd} = \begin{bmatrix} A_k - B_kC_{22}A_{22}^{-1}B_2C_k & B_k \\ C_k & 0 \end{bmatrix}.$$

Note that $\hat{A}_{22}$ contains no uncertain parts in the case of $D_k = 0$ and $\hat{A}_{22}^{-1} = A_{22}^{-1}$. In this way, the integral quadratic constraints can be transformed into LMIs. The next procedure is similar as that of Theorem 4.3, which is omitted here.

(2) Calculate the parameters of the DOFC.

Partition κ_{sd} into two parts, namely

$$\kappa_{sd} = \begin{bmatrix} \kappa_{sd1} \\ \kappa_{sd2} \end{bmatrix}, \ \kappa_{sd1} \in \mathbf{R}^{n_k \times (n_k+s)}, \ \kappa_{sd2} \in \mathbf{R}^{s \times (n_k+s)}.$$

Simultaneously, we can see that W_{sd} can be separated into two parts in corresponding dimensions with κ_{sd1} and κ_{sd2},

$$W_{sd} = \begin{bmatrix} W_{sd1} \\ W_{sd2} \end{bmatrix}, W_{sd1} \in \mathbf{R}^{n_k \times (n_k+s)}, W_{sd2} \in \mathbf{R}^{s \times (n_k+s)}.$$

Then, $\kappa_{sd} = K_{sd} W_{sd}$ can be rewritten as

$$\begin{bmatrix} \kappa_{sd1} \\ \kappa_{sd2} \end{bmatrix} = \begin{bmatrix} \tilde{A}_k & B_k \\ C_k & 0 \end{bmatrix} \begin{bmatrix} W_{sd1} \\ W_{sd2} \end{bmatrix} = \begin{bmatrix} \tilde{A}_k W_{sd1} + B_k W_{sd2} \\ C_k W_{sd1} \end{bmatrix},$$

where $\tilde{A}_k = A_k - B_k C_{22} A_{22}^{-1} B_2 C_k$.

It is obvious that $\tilde{A}_k$ and B_k are uncertain because any $\tilde{A}_k$, B_k satisfying $\tilde{A}_k W_{sd1} + B_k W_{sd2} = \kappa_{sd1}$ are the feasible solutions. For the convenience of calculation, we assume $\tilde{A}_k$ is known beforehand or selected artificially to meet the engineering requirements. Then, the parameter matrices of the DOFC can be given by

$$\begin{aligned} A_k &= \tilde{A}_k + B_k C_{22} A_{22}^{-1} B_2 C_k, \\ B_k &= (\kappa_{sd1} - \tilde{A}_k W_{sd1}) {W_{sd2}}^{\dagger}, \\ C_k &= \kappa_{sd2} {W_{sd1}}^{\dagger}. \end{aligned}$$

This completes the proof.

In addition, for a certain R, we can derive the controller to minimize the disturbance of the closed-loop system through searching for γ. Hence, the concept of FF H_∞ suboptimal control is put forward.

Corollary 4.1 *There exists a SOFC (4.16) to stabilize the slow subsystem (4.17) and to satisfy (4.20) if (4.30) and (4.31) are feasible and*

$$\min_{P_s Q_l, P_l, W_s, V_l} \gamma \tag{4.41}$$

where the parameters required are defined in Theorem 4.3.

Corollary 4.2 *There exists a DOFC (4.18) to stabilize the slow subsystem (4.19) and to satisfy (4.20) if (4.38) and (4.39) are feasible and*

$$\min_{P_{sd}, Q_{ld}, P_{ld}, W_{sd}, V_{ld}} \gamma \tag{4.42}$$

where the parameters are referred to in Theorem 4.4.

Remark 4.11 It should be noted that the minimum value of γ relates to the selection of weighing matrices. In other words, the disturbance attenuation index $\gamma_{\min}$ obtained by Corollary 4.1 or 4.2 can be further optimized with a better choice of R, which is the concept of design of the FF H_∞ suboptimal controller. However, due to the fact that $\gamma_{\min}$ is a bit bigger but gradually tends to the real value of $\gamma_{\min}$, this method can be used to obtain the estimation of $\gamma_{\min}$. In fact, consequences in Corollary 4.1 or 4.2 are more useful in engineering applications to estimate the disturbance attenuation degree of the closed-loop system.

4.3.2 The Fast Subsystem and Associated Controller in the High-Frequency Domain

For a system (4.28), the following results are established.

Theorem 4.5 *Let weighing matrices $R_f \in \mathbf{R}^{s\times 2n_2}$ and $R_h \in \mathbf{R}^{s\times(2n_2+r+q)}$, the crossover frequency ω_h, and a scalar $\gamma > 0$ be given. If there exist positive definite matrices $P_f \in \mathbf{R}^{n_2\times n_2}$ and $Q_h \in \mathbf{R}^{n_2\times n_2}$, symmetrical matrices $P_h \in \mathbf{R}^{n_2\times n_2}$ and $W_f \in \mathbf{R}^{s\times s}$, and matrices $V_h \in \mathbf{R}^{(n_2+r)\times(2n_2+r+q)}$ and $V_f \in \mathbf{R}^{n_2\times 2n_2}$, and $\mathscr{K}_{fs} \in \mathbf{R}^{p\times s}$ such that LMIs below are satisfied,*

$$\begin{bmatrix} 0 & P_f \\ P_f & 0 \end{bmatrix} < \mathrm{He}\begin{bmatrix} -C_{22}^\dagger & -(I_{n_2} - C_{22}^\dagger C_{22}) & 0 \\ A_{22}C_{22}^\dagger & A_{22}(I_{n_2} - C_{22}^\dagger C_{22}) & B_2 \end{bmatrix}\begin{bmatrix} W_f R_f \\ V_f \\ \mathscr{K}_{fs} R_f \end{bmatrix}, \tag{4.43}$$

$$\begin{bmatrix} Q_h & 0 & P_h & 0 \\ 0 & I_r & 0 & 0 \\ P_h & 0 & -\omega_h^2 Q_h^2 & 0 \\ 0 & 0 & 0 & -\gamma^2 I_q \end{bmatrix} < \mathrm{He}\begin{bmatrix} -\bar{C}_f^\dagger & -(I_{n_2+r} - \bar{C}_f^\dagger \bar{C}_f) & 0 \\ \bar{A}_f \bar{C}_f^\dagger & \bar{A}_f(I_{n_2+r} - \bar{C}_f^\dagger \bar{C}_f) & \bar{B}_f \end{bmatrix}\begin{bmatrix} W_f R_h \\ V_h \\ \mathscr{K}_{fs} R_h \end{bmatrix}, \tag{4.44}$$

then the closed-loop fast subsystem (4.28) is stable and satisfies (4.20) for a given $\bar{\omega}_h$. A feasible SOFC gain is given by $K_{sf} = \mathscr{K}_{sf} {W_f}^{-1}$.

Proof Through an appropriate choice of $\Phi = \begin{bmatrix} 0 & 1 \\ 1 & 0 \end{bmatrix}$, $\Psi = \begin{bmatrix} 1 & 0 \\ 0 & -\omega_h^2 \end{bmatrix}$, the set $\Lambda(\Phi, \Psi)$ can be specialized in a high-frequency range of the frequency-scale $\bar{\omega}$. Here, $\Lambda(\Phi, \Psi) = \Omega_h$. The part to follow is similar to the proof of Theorem 4.3 and is therefore ignored here. This completes the proof.

In system (4.29), we have the following result.

Theorem 4.6 *For given weighing matrices $R_{fd} \in \mathbf{R}^{s\times 2n_2}$ and $R_{hd} \in \mathbf{R}^{s\times(2n_2+r+q)}$, and disturbance attenuation index $\gamma > 0$, if there exist positive definite matrices $P_{fd} \in \mathbf{R}^{n_2\times n_2}$ and $Q_{hd} \in \mathbf{R}^{n_2\times n_2}$, symmetrical matrices $P_{hd} \in \mathbf{R}^{n_2\times n_2}$ and $W_{fd} \in \mathbf{R}^{s\times s}$, and matrices $V_{hd} \in \mathbf{R}^{(n_2+r)\times(2n_2+r+q)}$, $V_{fd} \in \mathbf{R}^{n_2\times 2n_2}$, and $\mathscr{K}_{fd} \in \mathbf{R}^{p\times s}$ such that LMIs below hold*

$$\begin{bmatrix} 0 & P_{fd} \\ P_{fd} & 0 \end{bmatrix} < \mathrm{He}\begin{bmatrix} -C_{22}^\dagger & -(I_{n_2} - C_{22}^\dagger C_{22}) & 0 \\ A_{22}C_{22}^\dagger & A_{22}(I_{n_2} - C_{22}^\dagger C_{22}) & B_2 \end{bmatrix}\begin{bmatrix} W_{fd} R_{fd} \\ V_{fd} \\ \mathscr{K}_{fd} R_{fd} \end{bmatrix}, \tag{4.45}$$

$$\begin{bmatrix} Q_{hd} & 0 & P_{hd} & 0 \\ 0 & I_r & 0 & 0 \\ P_{hd} & 0 & -\omega_h^2 Q_{hd}^2 & 0 \\ 0 & 0 & 0 & -\gamma^2 I_q \end{bmatrix} < \mathrm{He}\begin{bmatrix} -\bar{C}_{fd}^\dagger & -(I_{n_2+r} - \bar{C}_{fd}^\dagger \bar{C}_{fd}) & 0 \\ \bar{A}_{fd} \bar{C}_{fd}^\dagger & \bar{A}_{fd}(I_{n_2+r} - \bar{C}_{fd}^\dagger \bar{C}_{fd}) & \bar{B}_{fd} \end{bmatrix}\begin{bmatrix} W_{fd} R_{hd} \\ V_{hd} \\ \mathscr{K}_{fd} R_{hd} \end{bmatrix}, \tag{4.46}$$

then the closed-loop fast subsystem (4.29) is stable and satisfies (4.21) for a given $\bar{\omega}_h$. Moreover, the parameter matrices of the DOFC can be given by $D_d = \mathscr{K}_{fd} {W_{fd}}^{-1}$ with A_d, B_d and C_d being any matrices of corresponding dimensions.

Proof Using the DOFC (4.18), the closed-loop fast subsystem can be represented by (4.29). Considering that ξ is rather slow compared with the fast state x_2, we have

$$M_{fd} = \bar{A}_{fd} + \bar{B}_{fd} D_k \bar{C}_{fd} = \begin{bmatrix} A_{22} & B_{w2} \\ C_{12} & D_{11} \end{bmatrix} + \begin{bmatrix} B_2 \\ D_{12} \end{bmatrix} D_k \begin{bmatrix} C_{22} & D_{21} \end{bmatrix},$$

which is similar to M_{fs} in Theorem 4.5.

It is obvious that parameters of the DOFC, A_k, B_k and C_k, are less related with fast dynamics, which can be chosen as arbitrary matrices of corresponding appropriate dimensions. When the composite DOFC is designed to realize specifications of two subsystem at the same time, the properties of the slow subsystem are mainly determined by A_k, B_k and C_k. This completes the proof.

Similarly, the concept of the suboptimal H_∞ control for the fast subsystem is stated.

Corollary 4.3 *There exists a SOFC (4.16) to stabilize the fast subsystem (4.26) and satisfy the high-frequency control system specification (4.21) if LMIs (4.43) and (4.44) are satisfied with*

$$\min_{P_f, Q_f, P_h, W_h, V_h} \gamma,$$

where the parameters above are defined in Theorem 4.5.

Corollary 4.4 *There exists a DOFC (4.18) to stabilize the fast subsystem (4.26) and satisfy the high-frequency control system specification (4.21) if LMIs (4.45) and (4.46) are satisfied with*

$$\min_{P_{fd}, Q_{fd}, P_{hd}, W_{hd}, V_{hd}} \gamma,$$

where the parameters referred to are defined in Theorem 4.6.

To reduce the conservativeness, the cut-off frequencies ω_l and $\bar{\omega}_h$ are determined, which are related with three factors: the parameters of the open-loop system, the desired external disturbance attenuation degree γ and the general frequency range of the external noise Ω_n. The strategy to obtain ω_l and $\bar{\omega}_h$ is presented below.

Algorithm 4.2 *The prescribed values of ω_l and $\bar{\omega}_h$ are given as the following algorithm.*

Step1. *Calculate the module of open-loop low-frequency TFM $G_{zws}(j\omega)$ and open-loop high-frequency TFM $G_{zwf}(j\bar{\omega})$.*

Step2. *Given error accuracy e, γ and sufficient small singular perturbation parameter ε, for ω_l, if $\|G_{zws}(j\omega_l) - \gamma\| < e$, then ω_l is obtained. Similarly, for $\bar{\omega}_h$, if $\|G_{zwf}(j\bar{\omega}_h) - \gamma\| < e$, $\bar{\omega}_h$ is obtained.*

Step3. *Choose $\omega_l \in [0, \omega_l]$ and $\bar{\omega}_h \in [\bar{\omega}_h, +\infty]$. Also, $\omega_h = \bar{\omega}_h/\varepsilon$.*

Then, the entire frequency range can be divided into three parts, namely the low-frequency range $\tilde{\Omega}_l$, the middle-frequency range $\tilde{\Omega}_m$ and the high-frequency range $\tilde{\Omega}_h$,

$$\tilde{\Omega}_l = \{\omega | 0 < |\omega| \leqslant \omega_l\},\ \tilde{\Omega}_m = \{\omega | \omega_l < |\omega| < \omega_h\},\ \tilde{\Omega}_h = \{\omega | |\omega| \geqslant \omega_h\}.$$

Remark 4.12 (*The design of the stabilizing controller*) The feasibility of LMIs (4.30)–(4.43) can ensure that the internal stability of slow and fast subsystems. As mentioned in [14], if there exists a scalar $\varepsilon^* > 0$ such that, for any $\varepsilon \in (0, \varepsilon^*]$, the stability of the two related subsystem, then the stability of the original SPS can be guaranteed. Then, we put forward the design method of the stabilizing controller.

$$\begin{bmatrix} 0 & P_s \\ P_s & 0 \end{bmatrix} < \mathrm{He} \begin{bmatrix} -Y_{s1}^{\dagger} & -(I_{n_1} - Y_{s1}^{\dagger} Y_{s1}) & 0 \\ A_s Y_{s1}^{\dagger} & A_s (I_{n_1} - Y_{s1}^{\dagger} Y_{s1}) & B_s \end{bmatrix} \begin{bmatrix} W R_s \\ V_s \\ \mathscr{K} R_s \end{bmatrix},$$

$$\begin{bmatrix} 0 & P_f \\ P_f & 0 \end{bmatrix} < \mathrm{He} \begin{bmatrix} -C_{22}^{\dagger} & -(I_{n_2} - C_{22}^{\dagger} C_{22}) & 0 \\ A_{22} C_{22}^{\dagger} & A_{22} (I_{n_2} - C_{22}^{\dagger} C_{22}) & B_2 \end{bmatrix} \begin{bmatrix} W R_f \\ V_f \\ \mathscr{K} R_f \end{bmatrix},$$

where the related parameters have been mentioned in Theorems 4.3 and 4.5. It follows that the stabilizing controller gain is $K = \mathscr{K} W^{-1}$.

Remark 4.13 (*The design of the composite SOFC*) To realize the control system specifications (4.20) and (4.21) by using the SOFC (4.16), it is necessary to find the static gain K that satisfies Ineqs. (4.30), (4.31), (4.43) and (4.44) simultaneously.

Remark 4.14 (*The design of the composite DOFC*) Apparently, the DOFC can be separated into two parts,

$$\kappa_{sd} = \begin{bmatrix} A_k - B_k C_{22} A_{22}^{-1} B_2 C_k & B_k \\ C_k & 0 \end{bmatrix}, \quad \mathscr{K}_{fd} = \begin{bmatrix} 0 & 0 \\ 0 & D_k \end{bmatrix}.$$

The controller gain κ_{sd} have significant impacts on the slow dynamics, while the gain $\mathscr{K}_{fd}$ is mainly used to control the fast modes. When D_k is rather small, the composite dynamic output feedback controller gain can be roughly chosen as $\kappa_d = \kappa_{sd} + \mathscr{K}_{fd}$.

Different controllers are designed to attenuate different types of disturbances. As the measurement techniques developed, the frequency range of external noises can be estimated. For example, a frequency metre can be used to determine the general frequency band that external disturbances operate. On the other hand, the SPSs contain abundant dynamics with different rates of convergence with fast (slow) modes dominating the early (late) part of the time history, such that a SOFC can be adopted to suppress the low-frequency disturbances while the DOFC can be utilized to restrain the high-frequency interferences.

Next, the approach for designing the MOFC is proposed.

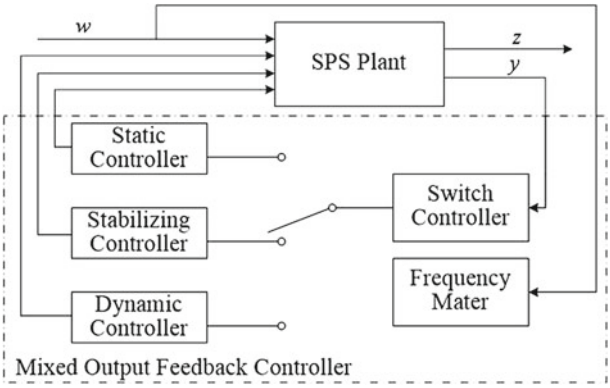

Fig. 4.5 Design of the mixed output feedback controller

Remark 4.15 (*The Design of the MOFC*) The MOFC shown in Fig. 4.5 is composed of three parts, namely the measurement unit, the decision-making unit and the executing unit. The frequency range of the external disturbances, ω_n, can be tested by the measurement unit. Then, the decision-making unit derives the control strategy which is stated as follows. Finally, according to the control strategy, the executing unit works to get the best system performances.

The decision strategy. In case of no disturbance or middle-frequency disturbance exists, the stabilizing controller plays a role such that the designed system can work stably, which is also the initial state of the mixed controller; If the external disturbances are in the low-frequency range, $\omega_n \in \tilde{\Omega}_l$, the SOFC is chosen; when the external disturbances are in the high-frequency range, $\omega_n \in \tilde{\Omega}_h$, the decision-making unit switches to the DOFC to increase the response rate to track the fast dynamics and decreases the effects of the high-frequency disturbances. Hence, the MOFC is a piecewise controller.

Remark 4.16 An abrupt switch between controllers may cause unacceptable closed-loop behaviours such as transients or bumps. A high-gain feedback F can be activated in the switching time to drive the off-line signal to be close to the online signal, and be removed when the switching process ends.

Example 4.1 Consider the SPS with parameters given by

$$A_{11} = \begin{bmatrix} 1 & 3 \\ 2 & 1 \end{bmatrix},\ A_{12} = \begin{bmatrix} 2 \\ -2 \end{bmatrix},\ A_{21} = \begin{bmatrix} 1 \\ 2 \end{bmatrix}^T,\ A_{22} = [-3],\ B_{w1} = \begin{bmatrix} 2 \\ 1 \end{bmatrix},$$
$$B_{w2} = 3,\ B_1 = \begin{bmatrix} -1 & -3 \\ 1 & 1 \end{bmatrix},\ B_2 = \begin{bmatrix} 1.5 \\ 1.5 \end{bmatrix}^T,\ C_{11} = \begin{bmatrix} 2 \\ 1.5 \end{bmatrix}^T,\ C_{12} = [0.8],$$
$$C_{21} = \begin{bmatrix} 1 \\ 1 \end{bmatrix}^T,\ C_{22} = [1.5],\ D_{11} = [-1.5],\ D_{12} = \begin{bmatrix} -1 \\ 1 \end{bmatrix}^T,\ D_{21} = [-2].$$

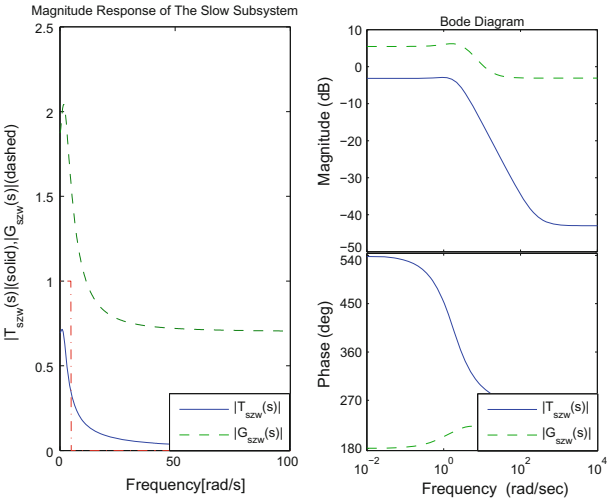

Fig. 4.6 FF H_∞ of slow subsystem via static output feedback controller

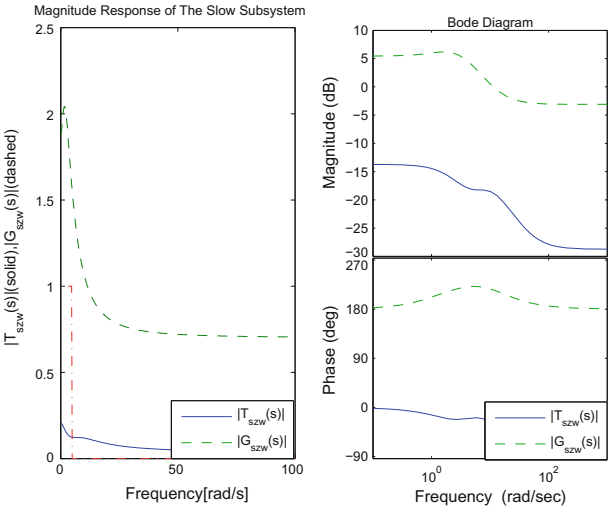

Fig. 4.7 FF H_∞ control of slow subsystem via DOFC

According to Figs. 4.6, 4.7, 4.8 and 4.9, it can be seen that $\omega_l = 12$ rad/s and $\bar{\omega}_h = 185$ rad/s. Based on Algorithm 4.2, the whole frequency range can be divided into three parts: the low-frequency range: $\tilde{\Omega}_l = \{\omega | 0 < |\omega| < 12\}$, the middle-frequency range: $\tilde{\Omega}_m = \{\omega | 12 \leqslant |\omega| \leqslant 185\}$ and the high-frequency range: $\tilde{\Omega}_h = \{\bar{\omega} | |\bar{\omega}| > 185\}$.

In Figs. 4.6, 4.7, 4.8 and 4.9, the left side shows the relationship between 2 norm of the TFM of the closed-loop system and the frequency variable ω. Meanwhile, the

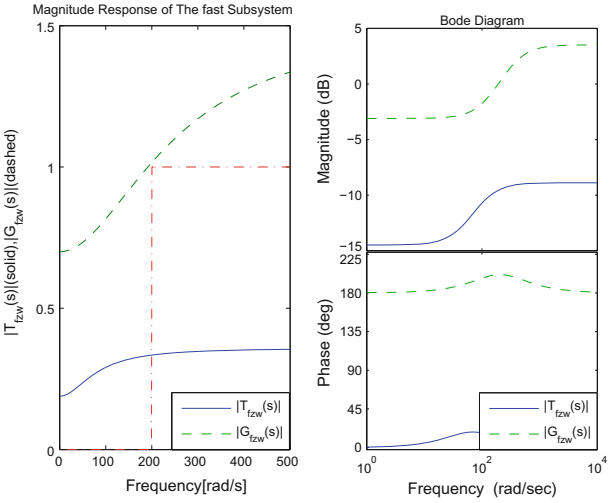

Fig. 4.8 FF H_∞ control of fast subsystem via SOFC

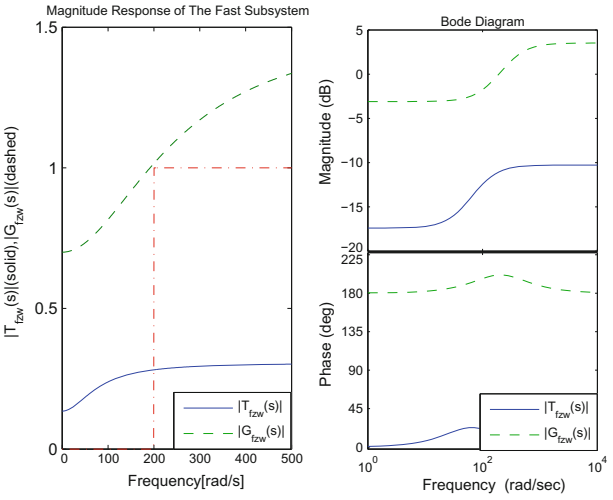

Fig. 4.9 FF H_∞ control of fast subsystem via DOFC

right side represents the bode diagram of the closed-loop system with log magnitude-frequency characteristics and log phase-frequency characteristics shown. Specially, the phase-frequency diagram reflects the response rate of the whole system.

In the slow subsystem, ω_l, γ, ε are chosen as $\omega_l = 5$ rad/s, $\gamma = 1$ and $\varepsilon = 0.01$. With aid of the MATLAB® LMI Toolbox, a feasible solution to Ineqs. (4.30) and (4.31) can be obtained

$$W_s = [1.2470],\ P_s = \begin{bmatrix} 157.0954 & -27.9568 \\ -27.9568 & 66.0124 \end{bmatrix},\ P_l = \begin{bmatrix} 12.3234 & -3.2853 \\ -3.2853 & 3.1487 \end{bmatrix},$$

$$\mathscr{K}_s = \begin{bmatrix} 7.4679 \\ 1.9662 \end{bmatrix},\ Q_l = \begin{bmatrix} 0.1578 & -0.0518 \\ -0.0518 & 0.0255 \end{bmatrix},$$

$$V_s = \begin{bmatrix} 27.3760 & 30.0588 & -4.4518 & -14.7617 \\ 30.0588 & -47.7531 & -14.7617 & -42.0719 \end{bmatrix},$$

$$V_l = \begin{bmatrix} -44.3155 & -585.7411 & 524.8048 & 244.9483 & -229.7876 & 874.5 \\ -33.4304 & -791.3471 & 751.0901 & 109.4174 & -294.8302 & 1155.7 \\ 27.6860 & 177.7587 & -191.7318 & 1.2475 & 45.8796 & 304.9 \end{bmatrix}.$$

From Theorem 4.3, we can find the SOFC gain as

$$K_s = \begin{bmatrix} 5.9889 \\ 1.5768 \end{bmatrix}.$$

According to Theorem 4.3, we can conclude that the slow subsystem (4.17) has FF H_∞ property in the low-frequency range. The simulation result is shown in Fig. 4.6 where the dotted box indicates the bound on the gain of the TFMs.

Similarly, we can validate Theorem 4.4. Solving (4.38) and (4.39), the following feasible results are obtained.

$$W_{sd} = \begin{bmatrix} -0.0086 & -0.0002 \\ -0.0002 & -0.0928 \end{bmatrix},\ P_{sd} = \begin{bmatrix} 929.0617 & -681.1686 & -0.9183 \\ -681.1686 & 514.0504 & 0.6444 \\ -0.9183 & 0.6444 & 0.0920 \end{bmatrix},$$

$$P_{ld} = \begin{bmatrix} -9.2908 & -1.7119 & -2.3380 \\ -1.7119 & 3.1227 & 0.2594 \\ -2.3380 & 0.2594 & -0.0979 \end{bmatrix},\ Q_{ld} = \begin{bmatrix} 9.1082 & -0.5993 & 0.3612 \\ -0.5993 & 0.0728 & -0.0132 \\ 0.3612 & -0.0132 & 0.0413 \end{bmatrix},$$

$$V_{sd} = \begin{bmatrix} -306.4979 & 640.6144 & 57.8813 & -108.8448 & 221.4955 & 18.4215 \\ 469.9120 & 192.6315 & 77.4581 & 86.6957 & -157.8142 & 23.8542 \\ 0 & 0 & 0 & 0 & 0 & 0 \end{bmatrix}.$$

$$V_{ld} = \begin{bmatrix} 105.8 & 3390.3 & -2164.9 & -600.8654 & 230.3230 & 866.1944 & 616.5531 & -1500.6 \\ 547.6 & 4260.1 & -2886.6 & -603.2756 & -54.7234 & 715.8236 & 822.1322 & -2267.0 \\ 0 & 0 & 0 & 0 & 0 & 0 & 0 & 0 \\ 146.7 & -1066.4 & 721.2 & 113.3871 & 198.8414 & -203.6730 & -207.3898 & 567.0 \end{bmatrix}.$$

The controller gain of the DOFC is calculated as

$$K_{sd} = \kappa_{sd} W_{sd}^{-1} = \begin{bmatrix} -5.2201 & -0.4746 \\ -63.8668 & 14.0588 \\ -27.5465 & 4.9730 \end{bmatrix}.$$

According to Theorem 4.4, it is obvious that the slow subsystem achieves FF H_∞ performance in the finite low-frequency range via using the DOFC. The simulation is demonstrated in Fig. 4.7.

Obviously, comparing the two phase-frequency diagrams in Figs. 4.6 and 4.7, we can see the response rate of the slow subsystem via DOFC is much faster than that of the SOFC. In this case, we set $\tilde{A}_k = 10$ to determine the parameters.

$$A_k = [-22.9280],\ B_k = [-0.5035],\ C_k = \begin{bmatrix} -60.7568 \\ -26.4464 \end{bmatrix},\ D_k = \begin{bmatrix} 0 \\ 0 \end{bmatrix}.$$

By virtue of Theorems 4.5 and 4.6, we can get the results of the fast subsystem in the high-frequency range when choosing $\omega_h = 200$ rad/s and $\gamma = 1$. Based on Theorem 4.5, the following feasible solutions are derived:

$$W_f = [17.6185],\ P_f = [47.2767],\ P_h = [-2.7423],\ Q_h = [0.0048],$$
$$V_f = \begin{bmatrix} 0 & 0 \end{bmatrix},\ V_h = \begin{bmatrix} 196.4597 & -214.7538 & 56.5945 & -391.6568 \\ -253.4059 & 146.4538 & 65.0159 & 577.1747 \end{bmatrix},\ \mathscr{K}_f = \begin{bmatrix} 16.1927 \\ -0.1871 \end{bmatrix}.$$

The simulation results are shown in Fig. 4.8, where the dotted box indicates the bound on the gain of the TFMs. Moreover, the SOFC gain is represented by

$$K_f = \begin{bmatrix} 0.9191 \\ -0.0106 \end{bmatrix}.$$

By Theorem 4.6, the resulting frequency responses can be seen in Fig. 4.9, where the solid one is for the open-loop system and the dashed is for the closed-loop one. In addition, the bode diagrams are also shown in Fig. 4.9. The simulations are shown below,

$$W_{fd} = [3.7337],\ P_{fd} = [12.4260],\ P_{hd} = [-2.3141],\ Q_h = [0.0013],\ V_f = \begin{bmatrix} 0 & 0 \end{bmatrix},$$
$$V_{hd} = \begin{bmatrix} 847.1 & -752.7460 & -17.3874 & -1083.5 \\ -1127.9 & 973.2321 & 65.7611 & 1462.2 \end{bmatrix},\ \mathscr{K}_{fd} = \begin{bmatrix} 3.4116 \\ -0.4195 \end{bmatrix}.$$

Likewise, the parameters of the DOFC are

$$\mathrm{A}_k = [0],\ B_k = [0],\ C_k = \begin{bmatrix} 0 \\ 0 \end{bmatrix},\ D_k = \begin{bmatrix} 0.9137 \\ -0.1124 \end{bmatrix}.$$

According to Remark 4.12, the stabilizing controller is

$$K = \begin{bmatrix} -0.2326 \\ 1.3790 \end{bmatrix}.$$

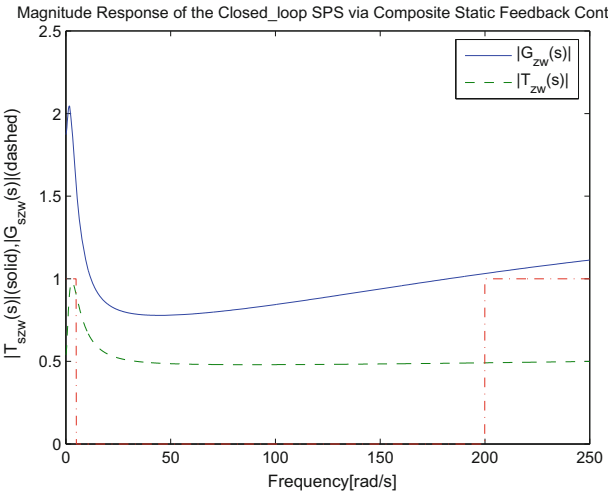

Fig. 4.10 The effectiveness of the composite via SOFC

The gain of the composite SOFC can be calculated, which is shown as

$$K_{sc} = \begin{bmatrix} -0.3550 \\ -0.7962 \end{bmatrix},$$

with the effectiveness demonstrated in Fig. 4.10.

Similarly, the gain of the composite DOFC is

$$K_{dc} = \begin{bmatrix} A_k & B_k \\ C_k & D_k \end{bmatrix} = \begin{bmatrix} -22.9280 & -0.5035 \\ -60.757 & 0.9137 \\ -26.446 & -0.1124 \end{bmatrix},$$

with the effectiveness revealed in Fig. 4.11. To realize the control system specifications of slow and fast subsystems simultaneously, we remove the constraint $D_k = 0$ in Theorem 4.4 and hence sacrifices part of the performance of the closed-loop slow subsystem to balance that of the fast subsystem. The equilibrium point of the composite gain should be selected carefully. Due to the approximation method mentioned above, the DOFC is less effective than the static one when stabilizing and realizing the H_∞ norm properties of the whole system. This problem needs to be improved in the future work.

On this basis, we can design the MOFC according to Remark 4.15. The simulation result is revealed in Fig. 4.12 respectively. The effectiveness of the MOFC is apparent because the H_∞ norm of $T_{zw}(s)$ is restrained in a fixed region, and we can give considerations to both the response rate and design cost. To better show the effectiveness of the MOFC, we do the time-domain simulations. The external disturbances are chosen as $w_l(t) = \sin(t)$ and $w_h(t) = \sin(300t)$. The interference responses of the closed-loop SPSs are suppressed to some extent, which is shown in

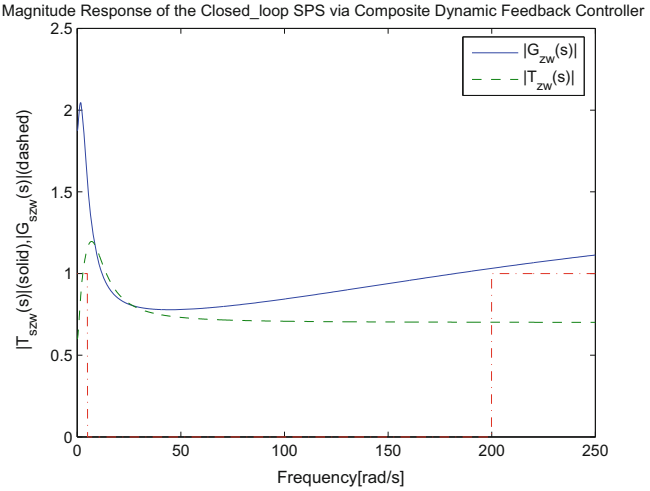

Fig. 4.11 The effectiveness of the composite DOFC

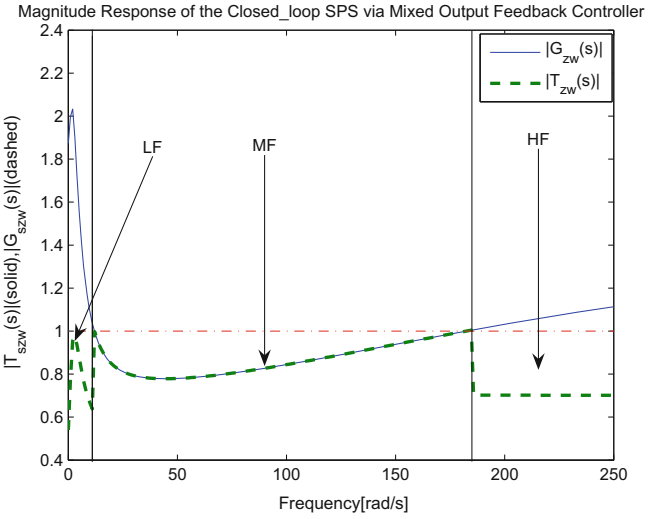

Fig. 4.12 The effectiveness of the MOFC

Fig. 4.13. We observe that the amplitude of the measurement output is restrained in a fixed region.

By setting $Q = 0$, Theorems 4.3–4.6 provide full-frequency conditions for control system specifications (4.20) and (4.21). In Fig. 4.14, $\gamma_{\min}$(full frequency) $>$ $\gamma_{\min}$(finite frequency) when R is set equal. It is obvious that the FF cases achieve better performances and have less conservatism when compared with the existing full-frequency approaches.

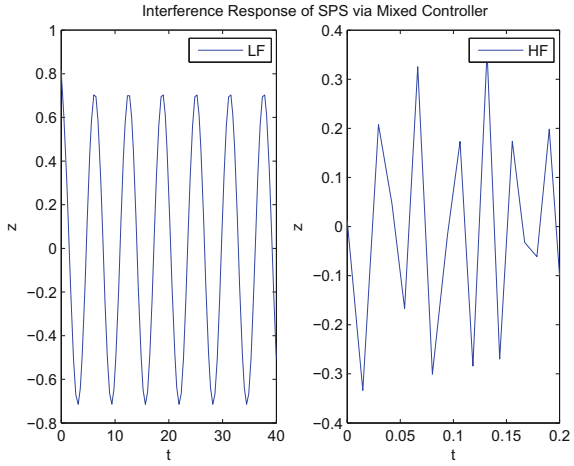

Fig. 4.13 The interference response of the external disturbances via MOFC

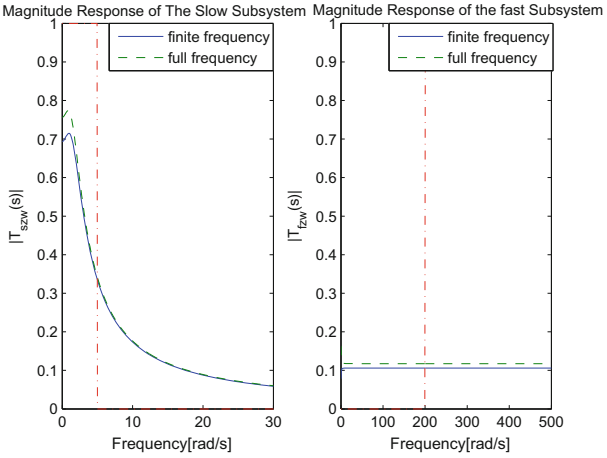

Fig. 4.14 Comparison between the full-frequency and FF approaches

4.4 A Descriptor-System Approach for H_∞ Control of Singularly Perturbed Systems

In this section, a descriptor-system method originating in singular (or descriptor) systems is introduced here to solve the ill-conditioning H_∞ control problem of SPSs, which avoid the degradation of model accuracy in the classical SPTs. This method can be applied in both standard and nonstandard SPSs. It is worth pointing out that the formulation of high-order composite controller is not needed in this method.

Singular systems have been proven to be the limiting models of SPSs. As $\varepsilon \to 0$, two different singular systems are obtained, which could be viewed as the slow limiting model and fast limiting model, respectively. Such limiting models can achieve the slowest speed and fastest speed, respectively. The basic concept of this method is to use the slow (fast) limiting model to describe the low-frequency (high-frequency) characteristics of an SPS. Through specifying the finite frequency control specifications of corresponding limiting models, the original SPS can achieve the desired frequency characteristics.

A LTI SPS in the fast timescale τ is represented by

$$\begin{aligned} \begin{bmatrix} \dot{x}_1(\tau) \\ \dot{x}_2(\tau) \end{bmatrix} &= \begin{bmatrix} \varepsilon A_{11} & \varepsilon A_{12} \\ A_{21} & A_{22} \end{bmatrix} \begin{bmatrix} x_1(\tau) \\ x_2(\tau) \end{bmatrix} + \begin{bmatrix} \varepsilon B_1 \\ B_2 \end{bmatrix} u(\tau) + \begin{bmatrix} \varepsilon B_{w1} \\ B_{w2} \end{bmatrix} w(\tau), \\ y(\tau) &= \begin{bmatrix} C_1 & C_2 \end{bmatrix} \begin{bmatrix} x_1(\tau) \\ x_2(\tau) \end{bmatrix} + D_1 u(\tau) + D_2 w(\tau), \end{aligned} \tag{4.47}$$

where $x_1(\tau) \in \mathbf{R}^{n_1}$ is the slow state vector, $x_2(\tau) \in \mathbf{R}^{n_2}$ is the fast state vector with $n_1 + n_2 = n$ representing the system dimension, $u(\tau) \in \mathbf{R}^p$ is the control input, $w(\tau) \in \mathbf{R}^r$ is the external disturbance, and $y(\tau) \in \mathbf{R}^q$ is the measurement output. The small positive constant ε serves as a measurement of the separation in "speed" of the slow and fast dynamics in the sense that $dx_1/d\tau$ is $O(\varepsilon)$ (a function $f(\varepsilon)$ is said to be $O(\varepsilon)$ if $|f(\varepsilon)| \leqslant \mu\varepsilon$, for $\varepsilon < \varepsilon^*$, where μ is a positive constant independent of ε), whereas $dx_2/d\tau$ is $O(1)$.

In the literature of SPSs, it is common to represent the system in a slow timescale that $t = \varepsilon\tau$,

$$\begin{aligned} \begin{bmatrix} \dot{x}_1(t) \\ \varepsilon\dot{x}_2(t) \end{bmatrix} &= \begin{bmatrix} A_{11} & A_{12} \\ A_{21} & A_{22} \end{bmatrix} \begin{bmatrix} x_1(t) \\ x_2(t) \end{bmatrix} + \begin{bmatrix} B_1 \\ B_2 \end{bmatrix} u(t) + \begin{bmatrix} B_{w1} \\ B_{w2} \end{bmatrix} w(t), \\ y(t) &= \begin{bmatrix} C_1 & C_2 \end{bmatrix} \begin{bmatrix} x_1(t) \\ x_2(t) \end{bmatrix} + D_1 u(t) + D_2 w(t). \end{aligned} \tag{4.48}$$

In the mathematical modelling of a physical system, both of the state-space equations (4.47) and (4.48) can be used to describe the simultaneous occurrence of slow and fast phenomena. For a small parameter ε, SPSs (4.47) and (4.48) can possess a two-timescale property, where the eigenvalues generally cluster into two widely separated groups.

Remark 4.17 In practical applications, the presence of some parasitic parameters such as small constants, resistances, inductances, capacitances and moment of inertia, is often the source of singular perturbation phenomena, which gives rise to timescale techniques. In the process control, such as some chemical changes, the control system specification is mainly associated with the performance of the slow-varying dynamics. For this case, the representation (4.48) is used. However, in the higher accuracy control, such as the attitude control of UAV, the fast varying modes cannot be neglected directly. They are scaled in the fast timescale τ in order to facilitate the design of control strategy.

Remark 4.18 Denoting the invertible transform $T = \begin{bmatrix} \varepsilon I_{n_1} & 0 \\ 0 & I_{n_2} \end{bmatrix}$, we have

$$T\begin{bmatrix} \dot{x}_1(t) \\ \varepsilon\dot{x}_2(t) \end{bmatrix} = T\begin{bmatrix} A_{11} & A_{12} \\ A_{21} & A_{22} \end{bmatrix}\begin{bmatrix} x_1(t) \\ x_2(t) \end{bmatrix} + T\begin{bmatrix} B_1 \\ B_2 \end{bmatrix}u(t) + T\begin{bmatrix} B_{w1} \\ B_{w2} \end{bmatrix}w(t),$$
$$y(t) = \begin{bmatrix} C_1 & C_2 \end{bmatrix}\begin{bmatrix} x_1(t) \\ x_2(t) \end{bmatrix} + D_1u(t) + D_2w(t),$$

which can be rewritten as

$$\begin{aligned} \begin{bmatrix} \varepsilon\dot{x}_1(t) \\ \varepsilon\dot{x}_2(t) \end{bmatrix} &= \begin{bmatrix} \varepsilon A_{11} & \varepsilon A_{12} \\ A_{21} & A_{22} \end{bmatrix}\begin{bmatrix} x_1(t) \\ x_2(t) \end{bmatrix} + \begin{bmatrix} \varepsilon B_1 \\ B_2 \end{bmatrix}u(t) + \begin{bmatrix} \varepsilon B_{w1} \\ B_{w2} \end{bmatrix}w(t), \\ y(t) &= \begin{bmatrix} C_1 & C_2 \end{bmatrix}\begin{bmatrix} x_1(t) \\ x_2(t) \end{bmatrix} + D_1u(t) + D_2w(t), \end{aligned} \tag{4.49}$$

Defining the fast timescale τ as $\tau = t/\varepsilon$, we can see that Eq. (4.49) can be represented in the fast timescale version as (4.47). Thus, through some elementary transformations, Eqs. (4.47) and (4.48) can be converted mutually.

As $\varepsilon \to 0$, the limiting models in the form of Eqs. (4.47) and (4.48) are obtained as follows:

$$\begin{aligned} \begin{bmatrix} \dot{x}_1^{(0)}(\tau) \\ \dot{x}_2^{(0)}(\tau) \end{bmatrix} &= \begin{bmatrix} 0 & 0 \\ A_{21} & A_{22} \end{bmatrix}\begin{bmatrix} x_1^{(0)}(\tau) \\ x_2^{(0)}(\tau) \end{bmatrix} + \begin{bmatrix} 0 \\ B_2 \end{bmatrix}u(\tau) + \begin{bmatrix} 0 \\ B_{w2} \end{bmatrix}w(\tau), \\ y(\tau) &= \begin{bmatrix} C_1 & C_2 \end{bmatrix}\begin{bmatrix} x_1^{(0)}(\tau) \\ x_2^{(0)}(\tau) \end{bmatrix} + D_1u(\tau) + D_2w(\tau). \end{aligned} \tag{4.50}$$

In Eq. (4.50), the slow variable $x_1^{(0)}$ is simplified into be known values, and the fast variable $x_2^{(0)}$ is modelled accurately, which can be considered as the fastest model for the SPS (4.47). Hence, system (4.50) is derived such that the high-frequency components are extracted, with the slow components simplified into the algebraic constraints, i.e., $x_1 =$ constant. Thus, Eq. (4.50) can be used to represent the SPS in the high-frequency range.

Setting $\varepsilon \to 0$ causes the fast dynamics $x_2^{(0)}$ to become algebraic, which implies that the dynamics $x_2^{(0)}$ respond instantaneously in the slow timescale t,

$$\begin{aligned} \begin{bmatrix} \dot{x}_1^{(0)}(t) \\ 0 \end{bmatrix} &= \begin{bmatrix} A_{11} & A_{12} \\ A_{21} & A_{22} \end{bmatrix}\begin{bmatrix} x_1^{(0)}(t) \\ x_2^{(0)}(t) \end{bmatrix} + \begin{bmatrix} B_1 \\ B_2 \end{bmatrix}u(t) + \begin{bmatrix} B_{w1} \\ B_{w2} \end{bmatrix}w(t), \\ y(t) &= \begin{bmatrix} C_1 & C_2 \end{bmatrix}\begin{bmatrix} x_1^{(0)}(t) \\ x_2^{(0)}(t) \end{bmatrix} + D_1u(t) + D_2w(t). \end{aligned} \tag{4.51}$$

The limiting model (4.51) can be viewed as the slowest model for the original system (4.48) with the fast modes simplified into algebraic constraints such that the initial condition $x_2^{(0)}$ is lost. In this case, the low-frequency modes are picked out.

For notational convenience, we define

$$\eta(t) = \begin{bmatrix} x_1(t) \\ x_2(t) \end{bmatrix}, \ \mathbf{A}_1(\varepsilon) = \begin{bmatrix} \varepsilon A_{11} & \varepsilon A_{12} \\ A_{21} & A_{22} \end{bmatrix}, \ \mathbf{B}_1(\varepsilon) = \begin{bmatrix} \varepsilon B_1 \\ B_2 \end{bmatrix}, \ \mathbf{E}_1(\varepsilon) = \begin{bmatrix} \varepsilon B_{w1} \\ B_{w2} \end{bmatrix},$$
$$E(\varepsilon) = \begin{bmatrix} I_{n_1} & 0 \\ 0 & \varepsilon I_{n_2} \end{bmatrix}, \ \mathbf{A}_2 = \begin{bmatrix} A_{11} & A_{12} \\ A_{21} & A_{22} \end{bmatrix}, \ \mathbf{B}_2 = \begin{bmatrix} B_1 \\ B_2 \end{bmatrix}, \ \mathbf{E}_2 = \begin{bmatrix} B_{w1} \\ B_{w2} \end{bmatrix}, C = \begin{bmatrix} C_1 & C_2 \end{bmatrix},$$

and then the continuous-time SPSs (4.47) and (4.48) can be rewritten in the following compact form: the high-frequency model,

$$\begin{aligned} \dot{\eta}(\tau) &= \mathbf{A}_1(\varepsilon)\eta(\tau) + \mathbf{B}_1(\varepsilon)u + \mathbf{E}_1(\varepsilon)w(\tau), \\ y(\tau) &= C\eta(\tau) + D_1u(\tau) + D_2w(\tau), \end{aligned} \tag{4.52}$$

and the low-frequency model,

$$\begin{aligned} E(\varepsilon)\dot{\eta}(t) &= \mathbf{A}_2\eta(t) + \mathbf{B}_2u(t) + \mathbf{E}_2w(t), \\ y(t) &= C\eta(t) + D_1u(t) + D_2w(t). \end{aligned} \tag{4.53}$$

Introducing the state feedback controller $u = K\eta$, the closed-loop system of SPS (4.52) is represented as

$$\begin{aligned} \dot{\eta}(\tau) &= \mathbf{A}_{1c}(\varepsilon)\eta(\tau) + \mathbf{E}_1(\varepsilon)w(\tau), \\ y(\tau) &= C_c\eta(\tau) + D_2w(\tau), \end{aligned} \tag{4.54}$$

where $\mathbf{A}_{1c}(\varepsilon) = \mathbf{A}_1(\varepsilon) + \mathbf{B}_1(\varepsilon)K$ and $C_c = C + D_1K$.

The closed-loop system for the SPS (4.53) is described as

$$\begin{aligned} E(\varepsilon)\dot{\eta}(t) &= \mathbf{A}_{2c}\eta(t) + \mathbf{E}_2w(t), \\ y(t) &= C_c\eta(t) + D_2w(t). \end{aligned} \tag{4.55}$$

in which $\mathbf{A}_{2c} = \mathbf{A}_2 + \mathbf{B}_2K$.

The TFM for the SPSs (4.52) and (4.53) from the disturbances w to the output y are described by $y(p) = G_h(p)u(p)$ and $y(s) = G_l(s)u(s)$, respectively, where

$$\begin{aligned} G_h(p) &= C_c(pI_n - \mathbf{A}_{1c}(\varepsilon))^{-1}\mathbf{E}_1(\varepsilon) + D_2, \\ G_l(s) &= C_c(sE(\varepsilon) - \mathbf{A}_{2c})^{-1}\mathbf{E}_2 + D_2. \end{aligned}$$

Next, we will present method to shape the frequency characteristics of an SPS based on the limiting models.

4.4.1 Shaping the High-Frequency Characteristics of a Singularly Perturbed Systems

The high limiting model, comprising of accurate fast modes and approximate slow modes, possesses the fastest variation rates of states. Such model can be used to shape the high-frequency characteristics of an SPS. In this subsection, H_∞ control design is demonstrated as an example. According to the inequality techniques, it should be pointed out that an SPS can achieve the high-frequency H_∞ property if the limiting model (4.50) exhibits the H_∞ property in the high-frequency range.

Problem 4.5 (*High-frequency H_∞ control problem*) For the fast limiting model (4.50), the state feedback sub-controller gain K_f is searched such that, for a given ω_h, the following requirements are satisfied,

1. When $\omega_h \in \Omega_h := \{\omega || \omega| > \omega_h\}$, $\|G_h(p)\|_\infty^{\Omega_h} < \gamma$;
2. The closed-loop system (4.54) is stable.

By solving the high-frequency H_∞ control problem, the controller gain K_f is obtained so that the amplitude response of the high-frequency model (4.54) in the high-frequency range can be suppressed below γ. In addition, the same K_f can also restrain the high-frequency amplitude response of the original SPS (4.47) below γ.

Theorem 4.7 *For a given matrix R_h, and scalars γ, p_1 and q_1 satisfying $\gamma > 0$ and $p_1 q_1 > 0$, the closed-loop system of SPS (4.47) possesses the FF H_∞ property with stability constraint in the high-frequency range Λ_h, if there exist matrices V_{bh} and κ_h, and symmetric matrices $P_{sh} > 0$, P_h, $Q_h > 0$ and W_h such that the following LMIs hold,*

$$\begin{bmatrix} 0 & P_{sh} \\ * & 0 \end{bmatrix} < \mathrm{He}\begin{bmatrix} W_{sh} \\ \mathbf{A}_1(0)W_{sh} + \mathbf{B}_1(0)\kappa_h \end{bmatrix}\begin{bmatrix} q_1 I_n & p_1 I_n \end{bmatrix}, \tag{4.56}$$

$$\begin{bmatrix} Q_h & 0 & P_h & 0 \\ * & I_r & 0 & 0 \\ * & * & -\omega_h^2 Q_h & 0 \\ * & * & * & -\gamma^2 I_q \end{bmatrix} < \mathrm{He}\begin{bmatrix} -I_n & 0 & 0 \\ 0 & -I_r & 0 \\ \mathbf{A}_1(0) & \mathbf{E}_1(0) & \mathbf{B}_1(0) \\ C & D_2 & D_1 \end{bmatrix}\begin{bmatrix} W_h R_h \\ V_{bh} \\ \kappa_h R_h \end{bmatrix}. \tag{4.57}$$

Then, the controller gain is given by $K_f = \kappa_h W_{sh}^{-1}$.

Proof When the external disturbance is in the high-frequency range, the fast timescale version (4.47) is adopted in which the fast dynamics are modelled accurately rather than neglected directly.

(1) Stability analysis.

Select the Lyapunov function as $V_1 = \eta^T P_{sh}\eta$, $P_{sh} = P_{sh}^T > 0 \in \mathbf{R}^{n\times n}$. The derivative of V_1 is given by

$$\begin{aligned} \dot{V}_1 &= \eta^T P_{sh}\dot{\eta} + \dot{\eta}^T P_{sh}\eta, \\ &= \eta^T (P_{sh}\mathbf{A}_{1c} + \mathbf{A}_{1c}^T P_{sh})\eta < 0, \end{aligned} \tag{4.58}$$

which guarantees the internal stability of the closed-loop system (4.47). The Lyapunov condition for the dual system of (4.47) is written as

$$P_{sh}\mathbf{A}_{1c}(\varepsilon)^T + \mathbf{A}_{1c}(\varepsilon)P_{sh} < 0,$$

or

$$\begin{bmatrix} \mathbf{A}_{1c}(\varepsilon)^T \\ I_n \end{bmatrix}^T \begin{bmatrix} 0 & P_{sh} \\ P_{sh} & 0 \end{bmatrix} \begin{bmatrix} \mathbf{A}_{1c}(\varepsilon)^T \\ I_n \end{bmatrix} < 0. \tag{4.59}$$

Partitioning $\mathbf{A}_{1c}(\varepsilon)$ into two parts indicates that

$$\mathbf{A}_{1c}(\varepsilon)^T = \rho_{h1} + \varepsilon\rho_{h2},$$

where $\rho_{h1} = \mathbf{A}_1(0) + \mathbf{B}_1(0)KI_n$ and $\rho_2 = \begin{bmatrix} A_{11} & A_{12} \\ 0 & 0 \end{bmatrix} + \begin{bmatrix} B_1 \\ 0 \end{bmatrix} KI_n$.

Plugging ρ_{h1}, ρ_{h2} into (4.59), it is derived that

$$\begin{aligned} &\begin{bmatrix} \rho_{h1}^T \\ I_n \end{bmatrix}^T \begin{bmatrix} 0 & P_{sh} \\ P_{sh} & 0 \end{bmatrix} \begin{bmatrix} \rho_{h1}^T \\ I_n \end{bmatrix} \\ &+ \varepsilon \left(\begin{bmatrix} \rho_{h1}^T \\ I_n \end{bmatrix}^T \begin{bmatrix} 0 & P_{sh} \\ P_{sh} & 0 \end{bmatrix} \begin{bmatrix} \rho_{h2}^T \\ I_n \end{bmatrix} + \begin{bmatrix} \rho_{h2}^T \\ I_n \end{bmatrix}^T \begin{bmatrix} 0 & P_{sh} \\ P_{sh} & 0 \end{bmatrix} \begin{bmatrix} \rho_{h1}^T \\ I_n \end{bmatrix} \right) \\ &+ \varepsilon^2 \begin{bmatrix} \rho_{h2}^T \\ I_n \end{bmatrix}^T \begin{bmatrix} 0 & P_{sh} \\ P_{sh} & 0 \end{bmatrix} \begin{bmatrix} \rho_{h2}^T \\ I_n \end{bmatrix} < 0, \end{aligned} \tag{4.60}$$

which is equivalent to

$$\begin{bmatrix} \rho_{h1}^T \\ I_n \end{bmatrix}^T \begin{bmatrix} 0 & P_{sh} \\ P_{sh} & 0 \end{bmatrix} \begin{bmatrix} \rho_{h1}^T \\ I_n \end{bmatrix} < 0. \tag{4.61}$$

Based on Lemma 2.2, it can be seen that (4.61) can be converted into the following LMI,

$$\begin{bmatrix} 0 & P_{sh} \\ * & 0 \end{bmatrix} < \mathrm{He} \begin{bmatrix} -I_n \\ \mathbf{A}_1(0) + \mathbf{B}_1(0)K \end{bmatrix} \mathrm{W_{sh}R_{sh}}. \tag{4.62}$$

Taking $R_{sh} = \begin{bmatrix} -q_1 I_n & p_1 I_n \end{bmatrix}$ and substituting R_{sh} into (4.62) yields

$$\begin{bmatrix} 0 & P_{sh} \\ * & 0 \end{bmatrix} < \mathrm{He} \begin{bmatrix} W_{sh} \\ \mathbf{A}_1(0)W_{sh} + \mathbf{B}_1(0)\kappa_h \end{bmatrix} \begin{bmatrix} q_1 I_n & p_1 I_n \end{bmatrix}. \tag{4.63}$$

(2) Disturbance attenuation capability.

To suppress the effects form the external disturbance $w(t)$ to the measurement output $y(t)$ to a preserved extent, the constraint below characterized by the FDI in the specified frequency range should be satisfied,

$$G_h^T(p)G_h(p) < \gamma^2 I_r,\ \ p \in \Lambda_h. \tag{4.64}$$

Based on the linear system theory, it is easy to verify that (4.64) can be derived from the similar disturbance attenuation condition of the dual system of (4.47), which is represented as

$$G_h(p)G_h^T(p) < \gamma^2 I_q,\ \ p \in \Lambda_h,$$

or equivalently,

$$\begin{bmatrix} G_h^T(p) \\ I_q \end{bmatrix}^T \Pi \begin{bmatrix} G_h^T(p) \\ I_q \end{bmatrix} < 0,\ \ p \in \Lambda_h, \tag{4.65}$$

where $\Pi = \begin{bmatrix} I_r & 0 \\ 0 & -\gamma^2 I_q \end{bmatrix}$.

According to the GKYP lemma, we can see that (4.65) can be converted into the following form,

$$N_1 \Theta_1 N_1^T < 0, \tag{4.66}$$

where

$$\Theta_1 = T \begin{bmatrix} \Phi \otimes P_l + \Psi \otimes Q_h & 0 \\ 0 & \pi \end{bmatrix}, \quad N_1 = \begin{bmatrix} \mathbf{A}_{1c}(\varepsilon) & \mathbf{E}_1(\varepsilon) & I_n & 0 \\ C_c & D_2 & 0 & I_q \end{bmatrix}.$$

Note that N_1 can be partitioned into two parts,

$$\begin{aligned} N_1 &= \begin{bmatrix} \mathbf{A}_1(0) + \mathbf{B}_1(0)K & \mathbf{E}_1(0) & I_n & 0 \\ C + D_1 * K & D_2 & 0 & I_q \end{bmatrix} \\ &\quad + \varepsilon \begin{bmatrix} \begin{bmatrix} A_{11} & A_{12} \\ 0 & 0 \end{bmatrix} + \begin{bmatrix} B_1 \\ 0 \end{bmatrix} K \begin{bmatrix} B_{w1} \\ 0 \end{bmatrix} & \begin{matrix} 0 & 0 \\ 0 & 0 \end{matrix} \\ 0 & \begin{matrix} 0 & 0 \end{matrix} \end{bmatrix}, \\ &:= N_{11} + \varepsilon N_{12}. \end{aligned}$$

Using N_{11} and N_{12} in (4.66), it gives

$$N_{11}\Theta_1 N_{11}^T + \varepsilon(N_{12}\Theta_1 N_{11}^T + N_{11}\Theta_1 N_{12}) + \varepsilon^2 N_{12}\Theta_1 N_{12}^T < 0. \tag{4.67}$$

Based on Lemma 2.3, it can be seen that (4.67) is equivalent to

$$N_{11}\Theta_1 N_{11}^T < 0 \tag{4.68}$$

where $N_{11} = \begin{bmatrix} M_1 & I_{n+q} \end{bmatrix}$, and M_1 can be rewritten into the standard form as

$$M_1 = \begin{bmatrix} \mathbf{A}_1(0) + \mathbf{B}_1(0)K & \mathbf{E}_1(0) \\ C + D_1 K & D_2 \end{bmatrix} = \begin{bmatrix} \mathbf{A}_1(0) & \mathbf{E}_1(0) \\ C & D_2 \end{bmatrix} + \begin{bmatrix} \mathbf{B}_1(0) \\ D_1 \end{bmatrix} K \begin{bmatrix} I_n & 0 \end{bmatrix}.$$

From Lemma 2.2, we can transform (4.68) into the following feasible LMI form

$$\Theta_1 < \mathrm{He}\begin{bmatrix} -I_n & 0 & 0 \\ 0 & -I_r & 0 \\ \mathbf{A}_1(0) & \mathbf{E}_1(0) & \mathbf{B}_1(0) \\ C & D_2 & D_1 \end{bmatrix}\begin{bmatrix} W_h R_h \\ V_{bh} \\ \kappa_h R_h \end{bmatrix}, \tag{4.69}$$

where $\kappa_h = W_h K_h$, and the state feedback gain can be calculated by $K_h = \kappa_h W_h^{-1}$.

In the high-frequency range, we can formulate Θ_1 as

$$\Theta_1 = \begin{bmatrix} Q_h & 0 & P_h & 0 \\ * & I_r & 0 & 0 \\ * & * & -\omega_h^2 Q_h & 0 \\ * & * & * & -\gamma^2 I_q \end{bmatrix}.$$

Substituting Θ_1 into (4.68) yields

$$\begin{bmatrix} Q_h & 0 & P_h & 0 \\ * & I_r & 0 & 0 \\ * & * & -\omega_h^2 Q_h & 0 \\ * & * & * & -\gamma^2 I_q \end{bmatrix} < \mathrm{He}\begin{bmatrix} -I_n & 0 & 0 \\ 0 & -I_r & 0 \\ \mathbf{A}_1(0) & \mathbf{E}_1(0) & \mathbf{B}_1(0) \\ C & D_2 & D_1 \end{bmatrix}\begin{bmatrix} W_h R_h \\ V_{bh} \\ \kappa_h R_h \end{bmatrix}.$$

This completes the proof.

4.4.2 *Shaping the Low-frequency Characteristics of a Singularly Perturbed Systems*

Similarly, we obtain the low-frequency counterpart.

Problem 4.6 (*Low-Frequency H_∞ Control Problem*) For the slow limiting model (4.51), a state feedback sub-controller gain K_s is searched such that for a given ω_l the following requirements are satisfied:

1. when $\omega_l \in \Omega_l := \{\omega | |\omega| < \omega_l\}$, $\|G_l(s)\|_\infty^{\Omega_l} < \gamma$;
2. the closed-loop system (4.53) is stable.

By solving the low-frequency H_∞ control problem, the controller gain K_s is obtained such that the amplitude response of the low-frequency model (4.54) in the low-frequency range can be suppressed below γ. In addition, the same K_s can also restrain the low-frequency amplitude response of the original SPS (4.47) below γ.

Theorem 4.8 *For a given weighing matrix R_l, and scalars γ, p_2, q_2 satisfying $\gamma > 0$ and $p_2 q_2 > 0$, if there exist symmetric matrices $P_{sl} > 0$, P_l, $Q_l > 0$ and W_l, and matrices V_{bl}, κ_l, $P_{sl}^* = P_{sl}E(0)$, $P_l^\star = P_l E(0)$ and $Q_l^\star = E(0)Q_l E(0)$ such that if the following LMIs are feasible:*

$$\begin{bmatrix} 0 & P_{sl}^{\star} \\ * & 0 \end{bmatrix} < \mathrm{He}\begin{bmatrix} -W_l \\ \mathbf{A}_2 W_{sl} + \mathbf{B}_2 \kappa_{sl} \end{bmatrix}\begin{bmatrix} q_2 I_n & p_2 I_n \end{bmatrix}. \tag{4.70}$$

$$\begin{bmatrix} -Q_l & 0 & P_l^{\star} & 0 \\ * & I_r & 0 & 0 \\ * & * & Q_l^{\star} & 0 \\ * & * & * & -\gamma^2 I_q \end{bmatrix} < \mathrm{He}\begin{bmatrix} -I_n & 0 & 0 \\ 0 & -I_r & 0 \\ \mathbf{A}_2 & \mathbf{E}_2 & \mathbf{B}_2 \\ C & D_2 & D_1 \end{bmatrix}\begin{bmatrix} W_l R_l \\ V_{bl} \\ \kappa_l R_l \end{bmatrix}, \tag{4.71}$$

Then, the closed-loop system (4.48) has FF H_∞ property with stability constraint in Λ_l. The controller gain is $K_s = \kappa_l W_l^{-1}$.

Proof When the external disturbance is in the low-frequency range, the slow timescale version (4.48) is adopted, where the slow dynamics are modelled with fast modes represented by algebraic conditions.

(1) First, we do the stability analysis of system (4.48).

Select the Lyapunov function as $V_2 = \eta^T E(\varepsilon) P_{sl} E(\varepsilon) P_{sl} \eta,\ P_{sl} = P_{sl}^T > 0$. The derivation of V_2 is represented as

$$\begin{aligned} \dot{V}_2 &= \eta^T E(\varepsilon) P_{sl} E(\varepsilon) \dot{\eta} + (E(\varepsilon)\dot{\eta})^T P_{sl} E(\varepsilon) \eta, \\ &= \eta^T (E(\varepsilon) P_{sl} A_{2c} + A_{2c}^T P_{sl} E(\varepsilon)) \eta < 0. \end{aligned} \tag{4.72}$$

The Lyapunov condition for the dual system of (4.48) is

$$E(\varepsilon) P_{sl} A_{2c}^T + A_{2c} P_{sl} E(\varepsilon) < 0,$$

which can be rewritten as

$$\begin{bmatrix} A_{2c}^T \\ I_n \end{bmatrix}^T \begin{bmatrix} 0 & \begin{bmatrix} P_{sl11} & \varepsilon P_{sl12} \\ P_{sl12}^T & P_{sl22} \end{bmatrix} \\ * & 0 \end{bmatrix} \begin{bmatrix} A_{2c}^T \\ I_n \end{bmatrix} < 0, \tag{4.73}$$

where $P_{sl} = \begin{bmatrix} P_{sl11} & \varepsilon P_{sl12} \\ P_{sl12}^T & P_{sl22} \end{bmatrix}$.

Based on Lemma 2.2, (4.73) can be converted into the following form, namely

$$\begin{bmatrix} 0 & \begin{bmatrix} P_{sl11} & \varepsilon P_{sl12} \\ P_{sl12}^T & P_{sl22} \end{bmatrix} \\ * & 0 \end{bmatrix} < \mathrm{He}\begin{bmatrix} -I_n \\ \mathbf{A}_2 + \mathbf{B}_2 K \end{bmatrix} W_l R_{sl}. \tag{4.74}$$

Taking $R_{sl} = \begin{bmatrix} -q_2 I_n & p_2 I_n \end{bmatrix}$, it can be seen that (4.74) can be simplified into

$$\begin{bmatrix} 0 & \begin{bmatrix} P_{sl11} & \varepsilon P_{sl12} \\ P_{sl12}^T & P_{sl22} \end{bmatrix} \\ * & 0 \end{bmatrix} < \mathrm{He}\begin{bmatrix} -W_l \\ \mathbf{A}_2 W_l + \mathbf{B}_2 \kappa_{sl} \end{bmatrix}\begin{bmatrix} q_2 I_n & p_2 I_n \end{bmatrix}. \tag{4.75}$$

According to Lemma 2.3, the sufficient condition for the establishment of (4.76) for certain $\varepsilon \in (0, \varepsilon^*]$ is

$$\begin{bmatrix} 0 & P_{sl}^{\star} \\ * & 0 \end{bmatrix} < \mathrm{He}\left[\begin{bmatrix} -W_l \\ \mathbf{A}_2 W_l + \mathbf{B}_2 \kappa_{sl} \end{bmatrix} \begin{bmatrix} q_2 I_n & p_2 I_n \end{bmatrix} \right]. \tag{4.76}$$

where $P_{sl}^{\star} = \begin{bmatrix} P_{sl11} & 0 \\ P_{sl12}^T & P_{sl22} \end{bmatrix}$.

(2) Then, we deal with the disturbance attenuation capability of system (4.48).

To restrain the effects from the external disturbance $w(t)$ in the low-frequency range to the measurement output $y(t)$ to a preserved extent, the requirement below characterized by the FDI in the specified frequency range should be satisfied,

$$G_l^T(s) G_l(s) < \gamma^2 I_r, \ s \in \Lambda_l, \tag{4.77}$$

which implies

$$\begin{bmatrix} G_l^T(s) \\ I_q \end{bmatrix}^T \Pi \begin{bmatrix} G_l^T(s) \\ I_q \end{bmatrix} < 0, \ s \in \Lambda_l, \tag{4.78}$$

and can be rewritten in the following form based on Lemma 2.2,

$$\begin{bmatrix} \mathbf{A}_{2c} & \mathbf{E}_2 & E(\varepsilon) & 0 \\ C_c & D_2 & 0 & I_q \end{bmatrix} T \Theta_2 T^T \begin{bmatrix} \mathbf{A}_{2c}^T & C_c \\ \mathbf{E}_2^T & D_2 \\ E(\varepsilon) & 0 \\ 0 & I_q \end{bmatrix} < 0, \tag{4.79}$$

where $\Theta_2 = \begin{bmatrix} \Phi \otimes P_l + \Psi \otimes Q_l & 0 \\ 0 & \Pi \end{bmatrix}$.

Setting

$$N_2 = \begin{bmatrix} \mathbf{A}_{2c} & \mathbf{E}_2 & I_n & 0 \\ C_c & D_2 & 0 & I_q \end{bmatrix},$$

and using it in (4.79) can yield

$$N_2 \begin{bmatrix} I_n & 0 & 0 & 0 \\ * & I_r & 0 & 0 \\ * & * & E(\varepsilon) & 0 \\ * & * & * & I_q \end{bmatrix} T \Theta_2 T^T \begin{bmatrix} I_n & 0 & 0 & 0 \\ * & I_r & 0 & 0 \\ * & * & E(\varepsilon) & 0 \\ * & * & * & I_q \end{bmatrix} N_2^T < 0. \tag{4.80}$$

which, according to Lemma 2.2, can be represented by

$$\begin{bmatrix} -Q_l & 0 & P_l E(\varepsilon) & 0 \\ * & I_r & 0 & 0 \\ * & * & E(\varepsilon) Q_l E(\varepsilon) & 0 \\ * & * & * & -\gamma^2 I_q \end{bmatrix} < \mathrm{He}\left[\begin{bmatrix} -I_n & 0 & 0 \\ 0 & -I_r & 0 \\ \mathbf{A}_2 & \mathbf{E}_2 & \mathbf{B}_2 \\ C & D_2 & D_1 \end{bmatrix} \begin{bmatrix} W_l R_l \\ V_{bl} \\ \kappa_l R_l \end{bmatrix} \right]. \tag{4.81}$$

A special choice of P_l can be given by

$$P_l = \begin{bmatrix} P_{l11} & P_{l12} \\ * & \frac{1}{\varepsilon} P_{l22} \end{bmatrix},$$

and applying it in (4.80) gives

$$\begin{bmatrix} -Q_l & 0 & P_l^\star & 0 \\ * & I_r & 0 & 0 \\ * & * & Q_l^\star & 0 \\ * & * & * & -\gamma^2 I_q \end{bmatrix} < \mathbf{He} \begin{bmatrix} -I_n & 0 & 0 \\ 0 & -I_r & 0 \\ \mathbf{A}_2 & \mathbf{E}_2 & \mathbf{B}_2 \\ C & D_2 & D_1 \end{bmatrix} \begin{bmatrix} W_l R_l \\ V_{bl} \\ \kappa_l R_l \end{bmatrix}, \tag{4.82}$$

where $P_l^\star = \begin{bmatrix} P_{l11} & 0 \\ P_{l12}^T & P_{l22} \end{bmatrix}$ and $Q_l^\star = E(0) Q_l E(0)$. This completes the proof.

4.5 Finite Frequency H_∞ Tracking Problem

In this section, we will apply our proposed method to the tracking problem of the system (4.2). The problem under investigation is to design a state feedback controller $u = K\eta$ such that the output y tracks a reference signal r, which can be characterized by a polynomial $\Psi(s) = 1/s$ without static error.

Note that the solution of this problem requires inclusion of an internal mode of $\Psi(s) = 1/s$ in the feedback loop [1]. The polynomial $\Psi(s)$ is not dependent on ε that represents a situation where the roots of $\Psi(s)$ are of the same order as the slow poles of the plant, which means that the low-frequency loop shaping is needed. To make use of H_∞ control of SPS demonstrated in the previous sections, it is necessary to convert the tracking problem into a standard H_∞ control problem [24].

To be specific, in the first step we consider the fast model (4.4). The control problem for the fast closed-loop system is simply to stabilize system (4.4) and realize the high-frequency H_∞ control system performance. Next, the low-frequency H_∞ control problem of slow closed-loop system is considered. To include an internal model of the reference, the modified slow model is taken as

$$\begin{aligned} \dot{\bar{x}}_s &= \bar{A}\bar{x}_s + \bar{B}u_s + \bar{F}w_s + \begin{bmatrix} 0 \\ 1 \end{bmatrix} r, \\ \bar{y}_s &= \bar{C}\bar{x}_s + D_s u_s + E_s w_s. \end{aligned}$$

Here,

$$\bar{x}_s = \begin{bmatrix} x_s & x_c \end{bmatrix}, \; x_c = e = r - y_s, \; \bar{A} = \begin{bmatrix} A_s & 0 \\ -C_s & 0 \end{bmatrix}, \; \bar{B} = \begin{bmatrix} B_s \\ C_s \end{bmatrix}, \; \bar{F} = \begin{bmatrix} F_s \\ E_s \end{bmatrix}, \; \bar{C} = \begin{bmatrix} C_s & 0 \end{bmatrix}.$$

In this case, the control problem can be converted to stabilize the modified slow model (4.3), and to meet H_∞ performance in the low-frequency domain.

The results and discussions of the previous sections are now summarized as follows.

Step 1. Following Theorem 4.2, a stabilizing fast controller $u_f = K_f x_f$ is designed to stabilize the fast model and meet H_∞ performance specifications in the high-frequency domain.

Step 2. Following Theorem 4.1, a stabilizing slow controller $u = K(s)\bar{x}$ is designed to stabilize the modified slow model and meet H_∞ performance specifications in the low-frequency domain. Here $K(s) = [K_s \ \frac{1}{s}k]$.

Step 3. The composite controller is achieved based on the strategy described in Fig. 4.4 for the full-order SPS.

Next, an example is given to show the efficiency.

Example 4.2 Now consider an SPS,

$$E_\varepsilon \dot{x}(t) = \begin{bmatrix} 1 & 2 \\ 1 & 5 \end{bmatrix} x + \begin{bmatrix} 2 \\ 2 \end{bmatrix} u + \begin{bmatrix} 1 \\ 3 \end{bmatrix} w,$$
$$z = \begin{bmatrix} 1 & 1 \end{bmatrix} x.$$

From the procedure mentioned above, one has $\omega = 2.674$ rad/s with crossover frequencies ω_l and ω_h selected as $\omega_h = 100$ rad/s and $\omega_l = 2.5$ rad/s. It can be seen that K_f, K_s can be solved following Theorems 4.1 and 4.2 respectively. Then,

$$K_s(s) = \begin{bmatrix} -74.7643 & 111.3440/s \end{bmatrix}, \quad K_f = -5.5359,$$
$$K(s) = \begin{bmatrix} 89.6843 & -136.3198/s & -5.5359 \end{bmatrix}.$$

Figure 4.15 reveals the comparison between H_∞ design in the FF domain (FFD)and the entire frequency domain (EFD). How the values of ω_l and ω_h affect the tracking results is shown in Figs. 4.16 and 4.17.

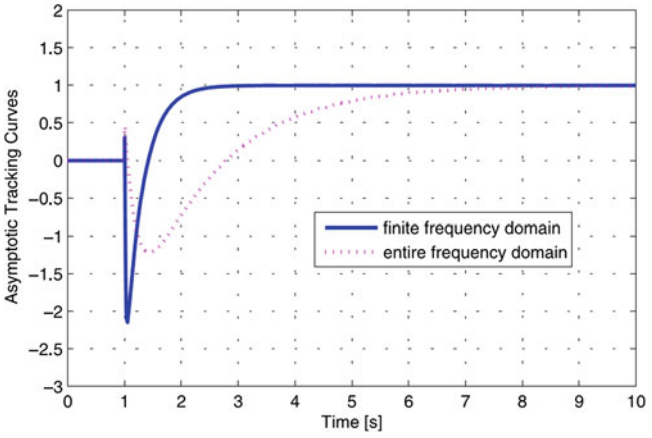

Fig. 4.15 Design results comparison between FFD and EFD

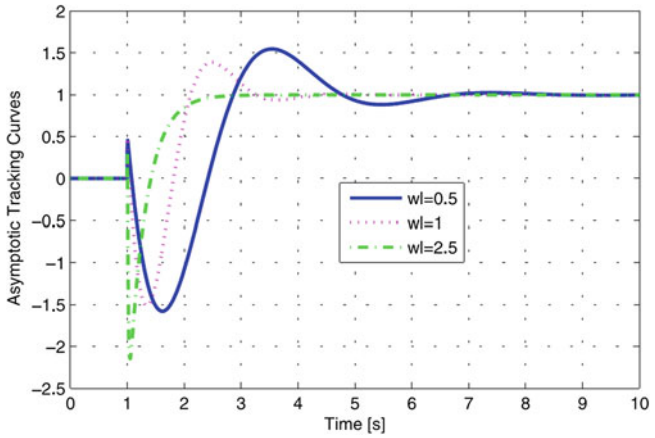

Fig. 4.16 Design results with $\omega_l = 0.5,\ 1,\ 2.5$ rad/s

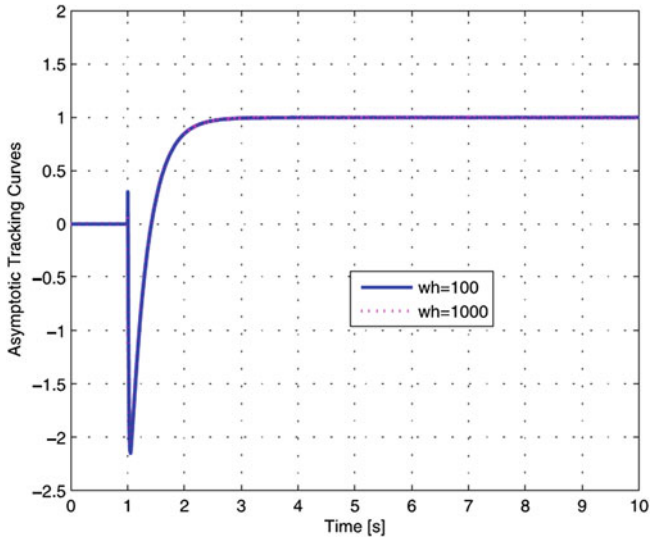

Fig. 4.17 Design results with $\omega_h = 100,\ 1000$ rad/s

4.6 Finite Frequency H_∞ Model Matching Problem

To the best of the authors' knowledge, H_∞ model matching problem has been a heat research topic in the literature, which has been studied in [4, 12, 18–22, 26]. Oloomi and Sawan [19] studied the suboptimal matching problem for SISO systems and obtained a suboptimal H_∞ solution through solving the model matching problems for the low and high-frequency models, respectively. Tan et al. [26] have derived a set of ε-independent sufficient and necessary conditions for the existence of an

H_∞ suboptimal controller in a different and simple way. Pan and Basar [21, 22] have solved the H_∞ model matching problem for MIMO SPSs via using the theory of differential games, and then presented an ε-independent two-stage procedure for the construction of a suboptimal solution. However, their results were based on the entire frequency, without considering the frequency characteristics of subsystems sufficiently in some sense.

This section is concerned with the model matching problem for SISO SPSs in (semi)finite frequency ranges. Sufficient and necessary conditions for the existence of an H_∞ suboptimal controller are derived based on the GKYP lemma. The controller is particularly designed in the singularly perturbed form, which is obtained through designing its fast and slow parts, and the composite controller is then constructed based on.

It has been shown that the slow and fast subsystems could be interpreted as the descriptions of the full-order system at low and high frequencies respectively. The main method in the literature for solving control problem of SPS is that: (1) decompose the ill-conditioned problem into slow and fast parts; (2) design slow and fast sub-controllers respectively; and (3) lay out the composite control strategy. The method in this section adopts such framework to design a full-dimensional controller for the SPS.

The SPS $G_p(s)$ is the plant to be controlled, which can be represented as

$$\begin{aligned} \dot{x} &= A_{11}x_1 + A_{12}x_2 + B_1u, \\ \varepsilon\dot{x}_2 &= A_{21}x_1 + A_{22}x_2 + B_2u, \\ y_p &= C_1x_1 + C_2x_2 + Du, \end{aligned} \tag{4.83}$$

where $x_1 \in \mathbf{R}^{n_1}$ and $x_2 \in \mathbf{R}^{n_2}$ are, respectively the slow and the fast state vectors, $u \in \mathbf{R}$ is the input to be designed, and $y \in \mathbf{R}$ is the output. The matrix A_{22} is assumed to be nonsingular.

The target SPS, defined by $G_m(s)$, is given by

$$\begin{aligned} \dot{\tilde{x}}_1 &= \tilde{A}_{11}\tilde{x}_1 + \tilde{A}_{12}\tilde{x}_2 + \tilde{B}_1e, \\ \varepsilon\dot{\tilde{x}}_2 &= \tilde{A}_{21}\tilde{x}_1 + \tilde{A}_{22}\tilde{x}_2 + \tilde{B}_2u, \\ y_t &= \tilde{C}_1\tilde{x}_1 + \tilde{C}_2\tilde{x}_2 + \tilde{D}u, \end{aligned} \tag{4.84}$$

where $\tilde{x}_1 \in \mathbf{R}^{n_1}$ and $\tilde{x}_2 \in \mathbf{R}^{n_2}$ are the target slow and the fast state vectors with e defined as the error signal, $e = y_p - y_t$, and $\tilde{A}_{22}$ is assumed to be nonsingular.

We aim at finding (if possible) a controller $G_c(s) \in \varphi_\varepsilon$ such that

1. $\|G_p(s)G_c(s) - G_m(s)\|_\infty < \gamma_0 : |\omega| < \omega_l$;
2. $\|G_p(s)G_c(s) - G_m(s)\|_\infty < \gamma_0 : |\omega| > \omega_h$,

where $\omega_l < \omega_h$.

The following assumptions will be made throughout the section, where the subscripts s and f represent the slow and fast models respectively.

Assumption 4.3 (1) $G_{ps}(s), G_{pf}(s), G_{ms}(s), G_{mf}(s) \in \mathbf{RH}_\infty$;
(2) $G_{ps}(j\omega) \neq 0$ *for* $|\omega| < \omega_l$;
(3) $G_{pf}(j\omega) \neq 0$ *for* $|\omega| > \omega_h$;
(4) $G_p(s)$ *and* $G_m(s)$ *have no unstable lost poles.*

The following lemma is introduced to derive the main results.

Lemma 4.1 *Let $G(s)$ be a two-frequency-scale rational matrix. Suppose that $G_s(s)$ and $G_f(s)$ have no pure imaginary poles, or $G(s)$ has no pure imaginary lost poles. Then*

$$\sup_{s\in D} \left\| G(s) - G_s(s) - G_f(s) + V \right\| = O(\varepsilon), \tag{4.85}$$

where $V = G_s(s)|_{s=\infty} = G_f(s)\big|_{\varepsilon s=0}$, $\|\cdot\|$ is some matrix norm, and D is the imaginary axis.

Using SPTs, slow and fast subsystems of $G_p(s)$ have the state-space realizations

$$G_{ps} := \left[\begin{array}{c|c} A_s & B_s \\ \hline C_s & D_s \end{array}\right], \quad G_{pf} := \left[\begin{array}{c|c} A_{22}/\varepsilon & B_2/\varepsilon \\ \hline C_2 & D \end{array}\right],$$

where $A_s = A_{11} - A_{12}A_{22}^{-1}A_{21}$, $B_s = B_1 - A_{12}A_{22}^{-1}B_2$, $C_s = C_1 - C_2A_{22}^{-1}A_{21}$ and $D_s = D - C_2A_{22}^{-1}B_2$.

Similarly, we have

$$G_{ms} := \left[\begin{array}{c|c} \tilde{A}_0 & \tilde{B}_0 \\ \hline \tilde{C}_0 & \tilde{D}_0 \end{array}\right], \; G_{mf} := \left[\begin{array}{c|c} \tilde{A}_{22}/\varepsilon & \tilde{B}_2/\varepsilon \\ \hline \tilde{C}_2 & \tilde{D} \end{array}\right],$$

where $\tilde{A}_s = \tilde{A}_{11} - \tilde{A}_{12}\tilde{A}_{22}^{-1}\tilde{A}_{21}$, $\tilde{B}_s = \tilde{B}_1 - \tilde{A}_{12}\tilde{A}_{22}^{-1}\tilde{B}_2$, $\tilde{C}_s = \tilde{C}_1 - \tilde{C}_2\tilde{A}_{22}^{-1}\tilde{A}_{21}$ and $\tilde{D}_s = \tilde{D} - \tilde{C}_2\tilde{A}_{22}^{-1}\tilde{B}_2$.

Design a singularly perturbed controller $G_c(s)$,

$$G_c : \begin{cases} \dot{p} = E_{11}p + E_{12}q + F_1e, \\ \varepsilon\dot{q} = E_{21}p + E_{22}q + F_2e, \\ u = G_1p + G_2q + He, \end{cases}$$

where $p \in \mathbf{R}^{n_1}$ is the slow state vector, $q \in \mathbf{R}^{n_2}$ is the fast state vector, e is the error, u is the single input to be designed, and E_{22} is assumed to be nonsingular.

The slow and fast parts of $G_c(s)$ have the state-space realizations:

$$G_{cs} := \left[\begin{array}{c|c} E_s & F_s \\ \hline G_s & H_s \end{array}\right], \quad G_{cf} := \left[\begin{array}{c|c} E_{22}/\varepsilon & F_2/\varepsilon \\ \hline G_2 & H \end{array}\right],$$

where $E_0 = E_{11} - E_{12}E_{22}^{-1}E_{21}$, $F_0 = F_1 - E_{12}E_{22}^{-1}F_2$, $G_0 = G_1 - G_2E_{22}^{-1}E_{21}$ and $H_0 = H - G_2E_{22}^{-1}F_2$.

The PID controller is applied to direct open-loop shaping in multiple frequency ranges in [7], whereas, this controller has a pure imaginary pole, which is not suitable in the following discussion. We make a simple improvement of PID controller such that $G_{cs}(s)$ and $G_{cf}(s)$ have the following forms:

$$G_{cs}(s) = k_p + \frac{k_i}{s+a} + \frac{k_d s}{T_d s + 1}, \quad G_{cf}(s) = \tilde{k}_p + \frac{\tilde{k}_i}{\varepsilon s + a} + \frac{\tilde{k}_d \varepsilon s}{T_d \varepsilon s + 1},$$

with the constraint $G_{cs}(s)|_{s=\infty} = G_{cf}(s)\big|_{\varepsilon s=0}$, that means

$$k_p + \frac{k_d}{T_d} = \tilde{k}_p + \frac{\tilde{k}_i}{a},$$

where $k_p,\ k_i,\ k_d$ and $\tilde{k}_p,\ \tilde{k}_i,\ \tilde{k}_d$ are PID parameters, and $T_d > 0$ and $a > 0$ are both small constants. The state-space realizations of $G_{cs}(s),\ G_{cf}(s)$ are chosen such that $F_0,\ H_0,\ F_2$ and H are affine functions of the design parameters (k_p, k_i, k_d) and $(\tilde{k}_p, \tilde{k}_i, \tilde{k}_d)$ respectively.

Denote

$$\left[\begin{array}{c|c} E_0 & F_0 \\ \hline G_0 & H_0 \end{array}\right] = \left[\begin{array}{cc|c} -a & 0 & k_i \\ 0 & -\frac{1}{T_d} & -\frac{k_d}{T_d^2} \\ \hline 1 & 1 & k_p + \frac{k_d}{T_d} \end{array}\right], \tag{4.86}$$

$$\left[\begin{array}{c|c} \frac{E_{22}}{\varepsilon} & \frac{F_2}{\varepsilon} \\ \hline G_2 & H \end{array}\right] = \left[\begin{array}{cc|c} -\frac{a}{\varepsilon} & 0 & \frac{\tilde{k}_i}{\varepsilon} \\ 0 & -\frac{1}{T_d \varepsilon} & -\frac{\tilde{k}_d}{T_d^2 \varepsilon} \\ \hline 1 & 1 & \tilde{k}_p + \frac{\tilde{k}_d}{T_d} \end{array}\right], \tag{4.87}$$

and

$$\begin{aligned} G(s) &= G_p(s)G_c(s) - G_m(s), \\ G_s(s) &= G_{ps}(s)G_{cs}(s) - G_{ms}(s), \\ G_f(s) &= G_{pf}(s)G_{cf}(s) - G_{mf}(s). \end{aligned}$$

It is easy to verify that $G_s(s)$ and $G_f(s)$ are slow and fast subsystems of $G(s)$ respectively. As an extension of Lemma 4.1, the following result is obtained.

Theorem 4.9 *Under assumptions in Lemma 4.1, for given* $W_1 = \{\omega \in \mathrm{R} : |\omega| \le \omega_l\}$ *and* $W_2 = \{\omega \in \mathrm{R} : |\varepsilon\omega| \ge \omega_h\}$, *we define*

$$V = G_s(s)|_{s=\infty} = G_f(s)\big|_{\varepsilon s=0},$$

where $\varepsilon\omega_l < \omega_h$. *Suppose that*

$$\|G_s(s) - V\|_\infty \le O(\varepsilon), \quad \forall \omega \in W_2,$$

and

$$\left\|G_f(s) - V\right\|_\infty \le O(\varepsilon), \quad \forall \omega \in W_1.$$

If

$$\|G_s(s)\|_\infty \le \gamma, \ \forall \omega \in W_1, \quad \left\|G_f(s)\right\|_\infty \le \gamma, \ \forall \omega \in W_2,$$

then

$$\|G(s)\|_\infty \le \gamma + O(\varepsilon), \ \forall \omega \in W_0, \ W_0 = W_1 \cup W_2.$$

Proof According to Lemma 4.1, we have

$$\left\|G(s) - G_s(s) - G_f(s) + V\right\|_\infty \le O(\varepsilon),$$

which is established for any $\omega \in W_2$.

By virtue of the norm characteristics, one can obtain

$$\|G(s)\|_\infty \le \|G_s(s) - V\|_\infty + \left\|G_f(s)\right\|_\infty + O(\varepsilon), \tag{4.88}$$

for all $\omega \in W_2$.

Suppose that the following inequalities hold,

$$\|G_s(s) - V\|_\infty \le O(\varepsilon), \ \forall \omega \in W_2, \text{ and } \left\|G_f(s)\right\|_\infty < \gamma, \ \forall \omega \in W_2. \tag{4.89}$$

Substituting (4.89) into (4.88) yields $\|G(s)\|_\infty \le \gamma + O(\varepsilon)$ for any $\omega \in W_2$.

Similarly, if constraints,

$$\left\|G_f(s) - V\right\|_\infty \le O(\varepsilon), \ \forall \omega \in W_1, \quad \text{and } \|G_s(s)\|_\infty \le \gamma, \ \forall \omega \in W_1,$$

hold, then it is easy to obtain that

$$\|G(s)\|_\infty \le \gamma + O(\varepsilon), \ \forall \omega \in W_1.$$

Summing up all above gives that

$$\|G(s)\|_\infty \le \gamma + O(\varepsilon), \ \forall \omega \in W_0 = W_1 \cup W_2.$$

This completes the proof.

In fact, it is easy to satisfy the following assumptions,

$$\|G_s(s) - V\|_\infty \le O(\varepsilon), \ \forall \omega \in W_2,$$

and

$$\left\| G_f(s) - V \right\|_\infty \le O(\varepsilon),\ \forall \omega \in W_1,$$

in the corresponding high and low-frequency ranges, respectively.

In this sense, crossover frequencies of low and high-frequency ranges, $\omega_{l\max}$ and $\omega_{h\min}$, are defined by

$$\omega_{l\max} = \max\left\{ \omega_l > 0 | \left\| G_f(s) - G_s(\infty) \right\|_\infty \le O(\varepsilon),\quad |\omega| \le \omega_l \right\},$$

$$\omega_{h\min} = \min\left\{ \omega_h > 0 | \left\| G_s(s) - G_s(\infty) \right\|_\infty \le O(\varepsilon),\quad |\omega| \ge \omega_h \right\}.$$

According to Theorem 4.9, the model matching problem for a full-order SPS in (semi)finite frequency ranges can be converted into two lower order model matching problems.

Denote

$$\tilde{G}_c(s) := G_{cs}(s) + G_{cf}(s) - G_{cs}(\infty).$$

It thereby follows from Lemma 4.1 that the composite controller $G_c(s)$ can be approximated by $\tilde{G}_c(s)$, namely

$$\left\| G_c(s) - \tilde{G}_c(s) \right\|_\infty = O(\varepsilon).$$

The following result of the slow subsystem can be derived based on [9].

Theorem 4.10 *Let* $W_1 = \{\omega \in \mathrm{R} : |\omega| \le \omega_l\}$ *be given. Suppose that* $\det(j\omega I - A) \ne 0$, *for any* $\omega \in W_1$. *Then, the constraint that* $\|G_s(s)\|_\infty < \gamma$, *for any* $\omega \in W_1$ *holds if there exist real symmetric matrices* P *and* Q, *such that* $Q > 0$, *and*

$$\begin{bmatrix} AP + PA^T - AQA^T + \omega_l^2 Q & -AQC^T + PC^T & B \\ -CQA^T + CP & -CQC^T - \gamma^2 & D_1 \\ B^T & D_1^T & -1 \end{bmatrix} < 0,$$

where

$$A = \begin{bmatrix} A_0 & B_0 G_0 & 0 \\ 0 & E_0 & 0 \\ 0 & 0 & \tilde{A}_0 \end{bmatrix},\quad B = \begin{bmatrix} B_0 H_0 \\ F_0 \\ \tilde{B}_0 \end{bmatrix},$$
$$C = \begin{bmatrix} C_0 & D_0 G_0 & -\tilde{C}_0 \end{bmatrix},\quad D_1 = D_0 H_0 - \tilde{D}_0.$$

Proof According to Lemmas 2.2 and 2.4, it can be seen that Ψ and Π can be selected as

$$\Psi = \begin{bmatrix} -1 & 0 \\ 0 & \omega_l^2 \end{bmatrix},\quad \Pi = \begin{bmatrix} 1 & 0 \\ 0 & -\gamma^2 \end{bmatrix}.$$

Then, it can be derived that

$$\left\| C(sI - A)^{-1}B + D_1 \right\|_\infty < \gamma, \ \forall \omega \in W_1. \tag{4.90}$$

The state-space realization of $G_s(s)$ is

$$G_s = \left[\begin{array}{ccc|c} A_0 & B_0G_0 & 0 & B_0H_0 \\ 0 & E_0 & 0 & F_0 \\ 0 & 0 & \tilde{A}_0 & \tilde{B}_0 \\ \hline C_0 & D_0G_0 & -\tilde{C}_0 & D_0H_0 - \tilde{D}_0 \end{array}\right].$$

It can be seen that (4.90) is equivalent to

$$\|G_s(s)\|_\infty < \gamma, \ \forall \omega \in W_1.$$

This completes the proof.

Let $p = \varepsilon s$, $\bar{\omega} = \varepsilon\omega$, and $p = j\bar{\omega}$. Similar results of fast subsystem can be given as follows.

Theorem 4.11 *Let $W_2 = \{\bar{\omega} \in \mathrm{R} : |\bar{\omega}| \geq \omega_h\}$ be given. Suppose $\det(j\omega I - A) \neq 0$, for any $\omega \in W_2$. Then, $\left\| G_f(p) \right\|_\infty < \gamma$, for any $\bar{\omega} \in W_2$ holds, if there exist real symmetric matrices P, Q, such that $Q > 0$, and*

$$\left[\begin{array}{ccc} AP + PA^T + AQA^T - \omega_h^2 Q & AQC^T + PC^T & B \\ CQA^T + CP & CQC^T - \gamma^2 & D_2 \\ B^T & D_2^T & -1 \end{array}\right] < 0,$$

where

$$A = \left[\begin{array}{ccc} A_{22} & B_2G_2 & 0 \\ 0 & E_{22} & 0 \\ 0 & 0 & \tilde{A}_{22} \end{array}\right], \quad B = \left[\begin{array}{c} B_2H \\ F_2 \\ \tilde{B}_2 \end{array}\right],$$
$$C = \left[\begin{array}{ccc} C_2 & DG_2 & -\tilde{C}_2 \end{array}\right], \quad D_2 = DH - \tilde{D}.$$

Proof The proof is similar to Theorem 4.10.

We have designed an H_∞ suboptimal controller to solve the model matching problem for SPSs in (semi)finite frequency ranges. Considering that the similar problem solved in [20], the results in this book can be compared with the existing ones through a simple example. The main difference is that results in [20] are established in the entire frequency range, whereas, our results are built in the (semi)finite frequency ranges.

Example 4.3 Consider the following systems, where

$$G_m(s) = \frac{s + 0.5}{(s + 2)(\varepsilon s + 2)}, \ G_p(s) = \frac{(s - 1)(\varepsilon s - 1)}{(s + 1)(\varepsilon s + 1)},$$

and $\varepsilon = 0.001$. Choose $\omega_1 = 0.2$ rad/s, $\omega_h = 5000$ rad/s, $T_d = \alpha = 0.05$, and $\gamma = 0.1$. Applying the design method formulated in this section, the controller can be obtained by

$$G_{c1}(s) = \frac{0.9363s^2 + 0.04707s + 0.055}{0.05s^2 + 1.002s + 0.05} + \frac{0.0001(\varepsilon s)^2 + 0.04704\varepsilon s + 0.9406}{0.05(\varepsilon s)^2 + 1.002\varepsilon s + 0.05} - 18.7293.$$

Following the algorithm developed in [20], the controller is obtained as follows,

$$G_{c2}(s) = -\frac{(s+1)(7s-5.5)}{6(s+2)(7s+1)} - \frac{\varepsilon s + 1}{3(\varepsilon s + 2)} + \frac{1}{6}.$$

Error functions in low and high-frequency ranges are depicted in Figs. 4.18 and 4.19, respectively.

Example 4.4 Consider the tracking problem, where

$$G_p(s) = \frac{(s+2)}{(s+3)(\varepsilon s + 1)},$$

and $\varepsilon = 0.001$. Select the parameters as $\omega_1 = 0.001$ rad/s, $T_d = \alpha = 0.05$ and $\tilde{k}_p = \tilde{k}_i = \tilde{k}_d = 0$.

In the following processes, we design two different controllers under different specifications.

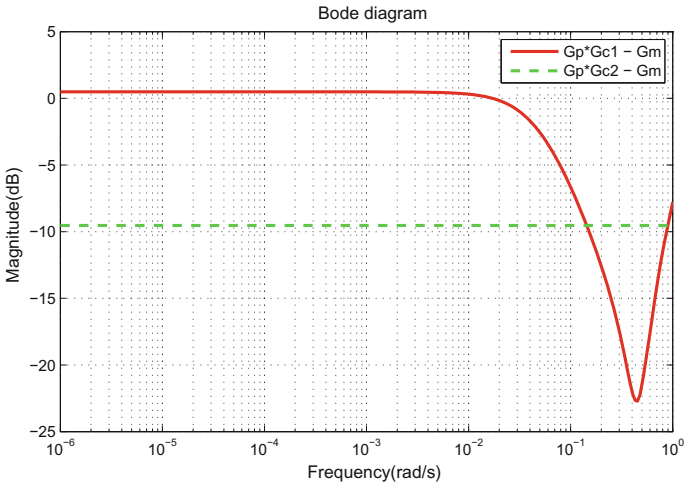

Fig. 4.18 Error functions in the low-frequency range

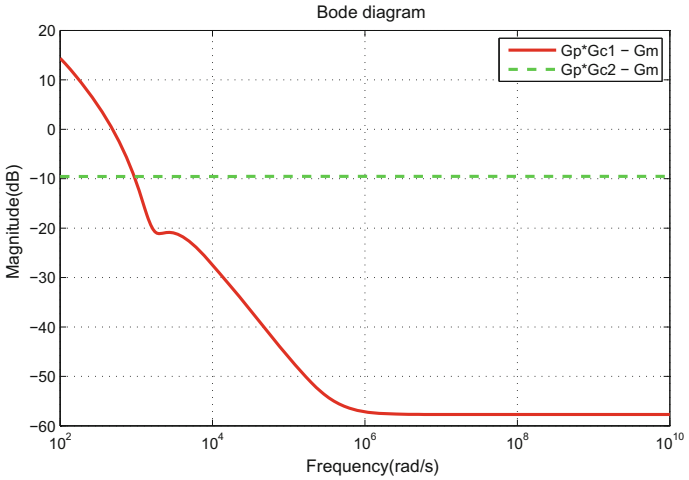

Fig. 4.19 Error functions in the hig-frequency range

1. When $\gamma = 0.1$ and $G_m(s) = \frac{1}{\gamma} + \gamma - 1$.
   Here, a controller is designed such that requirements

$$\|G_s(s)\|_\infty < \gamma, \quad \left\| \frac{1}{1 + G_p(s)G_c(s)} \right\|_\infty < \gamma,$$

   are satisfied.

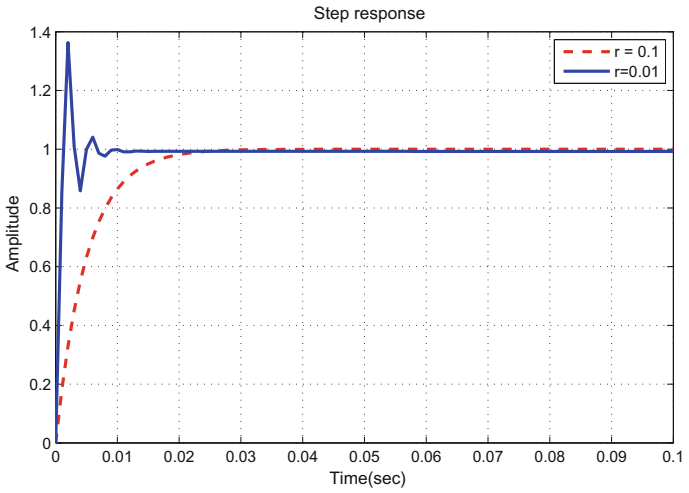

Fig. 4.20 Step responses

2. When $\gamma = 0.01$ and $G_m(s) = \gamma + 1/\gamma - 1$.
   In this case, the controller can be obtained,

$$G_c(s) = \frac{147.6s + 7.426}{0.05s^2 + 1.002s + 0.05}.$$

Step responses of the unity negative feedback system are plotted in Fig. 4.20.

4.7 Conclusion

In this chapter, we are mainly concerned with the FF H_∞ control problem of SPSs. The main theoretical results are given. First, the background knowledge of H_∞ control of SPSs are given to facilitate the understanding of readers, which are established in the entire frequency range. State feedback and output feedback synthesis of FF H_∞ control of SPSs are given in Sects. 4.2 and 4.3. A descriptor-system approach for H_∞ control of SPSs is demonstrated in Sect. 4.4, with the ill-conditioning of sufficient conditions much reduced. A special case of H_∞ control is shown in Sect. 4.5 to enable the plant track the given references. In Sect. 4.6, we have investigated the FF H_∞ model tracking issues. The validity of the proposed methods has been proven by the numerical results.

References

1. Chen, C.T.: Linear System Theory and Design. Holt Rinehart and Winston, New York (1984)
2. Dragan, V.: Asymptotic expansions for game-theoretic riccati equations and stabilization with disturbance attenuation for singularly perturbed systems. Syst. Control Lett. **20**(6), 455–463 (1993)
3. Dragan, V., Shi, P., Boukas, E.K.: Control of singularly perturbed system with markovian jump parameters: an H_∞ approach. Automatica **35**(8), 1359–1378 (1999)
4. Fridman, E.: Near-optimal H_∞ control of linear singularly perturbed systems. IEEE Trans. Autom. Control **41**(2), 236–240 (1996)
5. Fridman, E.: State-feedback H_∞ control of nonlinear singularly perturbed systems. Int. J. Robust Nonlinear Control **11**(12), 1115–1125 (2001)
6. Gong, C., Su, B.: Robust H_∞ filtering of convex polyhedral uncertain time-delay fuzzy systems. Int. J. Innov. Comput. Inf. Control **4**(4), 793–802 (2008)
7. Hara, S., Iwasaki, T.: Robust PID control using generalized KYP synthesis. IEEE Control Syst. Mag. **26**(1), 80–91 (2006)
8. Iwasaki, T., Hara, S.: Robust control synthesis with general frequency domain specifications: static gain feedback case. Proc. Am. Control Conf. **5**, 4613–4618 (2004)

9. Iwasaki, T., Hara, S.: Generalized KYP lemma: unified frequency domain inequalities with design applications. IEEE Trans. Autom. Control **50**(1), 41–59 (2005)
10. Iwasaki, T., Hara, S.: Feedback control synthesis of multiple frequency domain specifications via generalized KYP lemma. Int. J. Robust Nonlinear Control **17**(5–6), 415–434 (2007)
11. Iwasaki, T., Hara, S., Fradkov, A.L.: Time domain interpretations of frequency domain inequalities on finite ranges. Syst. Control Lett. **54**(7), 681–691 (2005)
12. Khail, H.K., Chen, F.C.: H_∞ control of two-time-scale systems. Proc. Am. Control Conf. **19**, 35–42 (1992)
13. Kokotovic, P.V., Khalil, H.K., OReilly, J.: Singular Perturbation Methods in Control: Analysis and Design. Academic Press, New York (1986)
14. Liang, C., Chen, B.: On the design of stabilizing controllers for singularly perturbed systems. IEEE Trans. Autom. Control **37**(11), 1828–1834 (1992)
15. Luse, D.W.: Frequency domain results for systems with multiple time scales. IEEE Trans. Autom. Control **31**(10), 918–924 (1986)
16. Luse, D.W., Ball, J.A.: Frequency-scale decomposition of H_∞ disk problems. SIAM J. Control Optim. **27**(4), 814–835 (1989)
17. Luse, D.W., Khail, H.K.: Frequency domain results for systems with slow and fast dynamics. IEEE Trans. Autom. Control **30**(12), 1171–1179 (1985)
18. Oloomi, H.M.: Nevanlinna-pick interpolation for two frequency scale systems. IEEE Trans. Autom. Control **40**(1), 369–377 (1995)
19. Oloomi, H.M., Sawan, M.E.: Suboptimal model-matching problem for two frequency scale transfer functions. In: Proceedings of the American Control Conference, pp. 2190–2191 (1989)
20. Oloomi, H.M., Sawan, M.E.: H_∞ model matching problem for singularly perturbed systems. Automatica **32**(3), 369–377 (1996)
21. Pan, Z., Basar, T.: H_∞ optimal control for singularly perturbed systems part I: Perfect state measurements. Automatica **29**(2), 401–423 (1992)
22. Pan, Z., Basar, T.: H_∞ optimal control for singularly perturbed systems part ii: imperfect state measurements. IEEE Trans. Autom. Control **39**(2), 280–299 (1994)
23. Rantzer, A.: On the Kalman-Yakubovich-Popov lemma. Syst. Control Lett. **28**(1), 7–10 (1996)
24. Shen, T.L.: H_∞ Control Theory and Applications. Tinghua University Press, Beijing (1996)
25. Shi, P., Dragan, V.: Asymptotic H_∞ control of singularly perturbed system with parametric uncertainties. IEEE Trans. Autom. Control **44**(9), 1738–1742 (1999)
26. Tan, W., Leung, T., Tu, Q.: H_∞ control for singularly perturbed systems. Automatica **34**, 255–260 (1998)
27. Wang, Y., Sun, Z.: H_∞ control of networked control system via LMI approach. Int. J. Innov. Comput. Inf. Control **3**(2), 343–352 (2007)

Chapter 5
Finite Frequency Positive Real Control for Singularly Perturbed Systems

With the development of high-performance mechatronics, the feedback control system is often required to exhibit some particular control system specifications such as high control bandwidth and FF disturbance suppression capability. Meanwhile, the integrated design of both mechanical plant and controller design is carried out to achieve performance specifications. In this chapter, a GKYP lemma-based algorithm is proposed for simultaneous finite frequency design of a mechanical SPS plant and controller through a convex separable parametrization. In Sect. 5.1, basic definitions and some related engineering background of passivity and positive real property are introduced. The design procedure using the classical slow-fast decomposition is represented in Sect. 5.2. To extend the results to nonstandard SPS, a descriptor-system method for SPSs are demonstrated in Sect. 5.3.

5.1 Passivity and Positive Real Property

In this section, we introduce the background knowledge of the passive theory, while the SPTs have been shown before. It has been mentioned in [28] that traditional passive system theory was a powerful tool for system analysis and synthesis. Passive system theory initially stemmed from electrical circuit theory, where networks of passive circuit components were known to be stable in various configurations. Using the traditional notion of energy, passivity theory had been applied in analysis and synthesis of many control systems. More generally speaking, the concept of passivity can be applied when there is no traditional notion of energy. In this case, we resort to define the generalized energy with the aid of an energy storage function. Note that, if the energy stored in a system can be bounded above by the energy supplied to the system, the system is passive.

As seen in [28], if passive systems have a special property that when connected in either a parallel or negative feedback manner as shown in Fig. 5.1(a) and (b),

C. Cai et al., *Finite Frequency Analysis and Synthesis for Singularly Perturbed Systems*, Studies in Systems, Decision and Control 78,
DOI 10.1007/978-3-319-45405-4_5

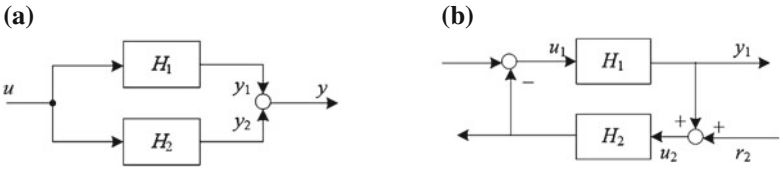

Fig. 5.1 Interconnections that preserve passivity

respectively, then the overall system remains passive. In other words, passive property can be preserved when the energy is stored in such interconnections, where a storage function that satisfies the passivity definition for the interconnected system can be calculated by the sum of the storage functions of the individual systems. With these results, we can see that large-scale systems can be stable through verifying passivity for each system component by following simple interconnection rules.

Definition 5.1 (*System Passivity*) Consider the following system,

$$\begin{aligned} \dot{x}(t) &= f(x(t), u(t)), \\ y(t) &= h(x(t), u(t)), \end{aligned} \tag{5.1}$$

where $x(t)$ is the process state, $u(t)$ is the control input, and $y(t)$ is the output of the system. System (5.1) is said to be **passive** if there exists a storage function $V(x(t)) > 0$ such that, for any time $t_1 > t_0$, t_0 be an initial time,

$$V(x(t_1)) - V(x(t_0)) < \int_{t_0}^{t_1} u^T(t) y(t) dt.$$

Note that if $V(x(t))$ is differentiable, we can alternatively write

$$\dot{V}(x(t)) < u^T(t) y(t), \quad t > 0.$$

Remark 5.1 Intuitively speaking, $V(x(t))$ can be referred to as the energy content of a control system, while $u^T(t)y(t)$ can be regarded as the power being fed to the system. Passivity implies that energy is being dissipated from the system. Notice that such an intuition holds exactly for electrical circuits. For more general systems, this can merely be used as a guidance.

It is worth pointing out that there are several variations of this definition in the literature, but essentially all definitions demonstrated that the output energy should be bounded such that the system did not produce more energy than the energy initially stored [6, 23].

As for the passive system theory, the following important definitions are given.

Definition 5.2 (*Positive Real*) The TFM

$$G(s) = C(sI - A)^{-1}B + D$$

is called **positive real**, if it is square and satisfies

$$G^*(s) + G(s) > 0, \quad s \in \mathbf{C}, \quad \mathrm{Re}(s) > 0 \tag{5.2}$$

Definition 5.3 (*Strict Positive Real*) A square TFM $G(s)$ is **strict positive real** if

1. $G(s)$ is analytic in the closed right half complex plane;
2. $G^*(j\omega) + G(j\omega) > 0$ for all $\omega \in (-\infty, \infty)$;
3. $G^*(\infty) + G(\infty) \geqslant 0$;
4. $\lim_{\omega\to\infty} \omega^2[G^*(j\omega) + G(j\omega)] > 0$, if $G^*(\infty) + G(\infty)$ is singular.

The concept of passivity and positive realness plays an important role in the analysis and controller design of linear systems, which actually represents the same property with the time-domain feature and frequency-domain feature, respectively.

As defined above, passivity is only a binary characterization of system behaviours, which depends on whether the system dissipates sufficient energy. Passive system theory provides a strong foundation for a composite framework for the stability of control systems [4, 23]. As mentioned in [4], it is easy to verify that passive systems have infinite gain margin and at least 90° of phase margin such that large loop gains can be tolerated. To conclude, passive control theory is very general and broad, which can be used in linear, nonlinear, continuous, and discrete-time control systems. In the following sections, we have investigated the FF positive real control of SPSs with the aid of some existing results in passive system theory.

5.2 Methods Based on Slow-Fast Decomposition

For a linear system, necessary and sufficient conditions for the existence of a stabilizing state feedback controller are given based on the GKYP lemma. Using the results to study SPSs, a composite state feedback controller is constructed, which preserves the stability and positive real property. It is well known that the mathematical treatment of systems with slow and fast dynamics has traditionally involved singularly perturbation theory, which have attracted much interest due to the great practical importance in recent years. There are many related research works such as [3, 9, 12, 15–17], which sub-controllers were designed for fast and modified slow subsystems, respectively, and then the composite controller was established. Whereas, most of the above-mentioned methods are based on the entire frequency, in fact, the fast and slow subsystems can be interpreted as descriptions of full system in the high-and low-frequency ranges [13]. The traditional methods did not consider the frequency characteristics of subsystems, and the conservatism tends to increase with the tedious design procedures. Positive realness appears in the field of system and control theories as an essential property, a well-known result is that when a positive real (PR)

dynamic system is connected to a strictly positive real (SPR) controller through negative feedback, the closed-loop system is internally stable [21]. The finite frequency positive real (FFPR) property was proposed in [22], and a variety of reasons to believe that FFPR is crucial for achieving good control performance was also provided. In decades, the KYP lemma has been recognized as one of the most important tools in the field of developing systems theory [18, 25, 27] such that the equivalence between FDIs and LMIs is established. However, the standard KYP lemma is not completely suitable when practical specifications are often given in different frequency ranges. Through generalizing the KYP lemma, Iwasaki et al. [5, 7, 8, 22] developed the GKYP lemma, which could convert a certain FDI in (semi)finite frequency range to a tractable LMI directly.

In this section, we consider SPR control for SPSs in (semi)finite frequency. First, we study the state feedback control for general linear systems in (semi)finite frequency, and use the results to study the finite frequency strictly positive real (FFSPR) control for SPSs.

Consider the following SPS, which is denoted by $G(s)$,

$$\begin{aligned} \dot{x}(t) &= A_{11}x_1(t) + A_{12}x_2(t) + B_1u(t), \\ \varepsilon\dot{x}_2(t) &= A_{21}x_1(t) + A_{22}x_2(t) + B_2u(t), \\ y(t) &= C_1x_1(t) + C_2x_2(t), \end{aligned} \tag{5.3}$$

where ε is a perturbation parameter satisfying $0 < \varepsilon \ll 1$, $x_1(t) \in \mathbf{R}^{n_1}$ and $x_2(t) \in \mathbf{R}^{n_2}$ are the slow and fast state vectors, respectively, $u(t) \in \mathbf{R}^p$ is the control input, $y(t) \in \mathbf{R}^q$ is the measurement output, and A_{22} is assumed to be nonsingular. Matrices A_{ij}, B_i and C_i $(i, j = 1, 2)$ are constant matrices of appropriate dimensions.

Consider a state feedback controller in the form of

$$u(t) = Kx(t).$$

Assume that the system $G(s)$ has no unstable lost poles.

Problem 5.1 Let $\bar{G}(s)$ denote the closed-loop TF of the system (5.3) from the control input $u(t)$ to the output $y(t)$. Our general goal is to find a stabilizing feedback controller K such that

1. $\bar{G}(j\omega) + \bar{G}^*(j\omega) > 0$, for all $|\omega| \le \omega_l$;
2. $\bar{G}(j\omega) + \bar{G}^*(j\omega) > 0$, for all $|\varepsilon\omega| \ge \omega_h$ and $\varepsilon\omega_l < \omega_h$.

In order to discuss the above problem for the SPS (5.3), let us first consider the state feedback control for general linear systems in the next subsection.

5.2.1 State Feedback Control for General Linear Systems

As mentioned before, using SPTs, the ill-conditioned LTI SPS can be decomposed into standard linear systems. The ill conditioning can be alleviated using time-scale

separation. Next, we give out methods for the state feedback control for linear systems, which can be applied in the reduced-order slow and fast subsystems directly.

Consider the linear system G_m as follows,

$$\begin{aligned} \dot{x}(t) &= Ax(t) + Bu(t), \\ y(t) &= Cx(t) + Du(t), \end{aligned} \tag{5.4}$$

where $x(t) \in \mathbf{R}^n$ is state vector, $u(t) \in \mathbf{R}^p$ is input vector, and $y(t) \in \mathbf{R}^q$ is output vector ($p = q$). The matrices A, B, C and D are constant matrices of appropriate dimensions.

Using the state feedback control $u(t) = Kx(t)$, the closed-loop TFM $\bar{G}_m$ of the system (5.4) is represented by

$$\begin{aligned} \dot{x}(t) &= (A + BK)x(t), \\ y(t) &= (C + DK)x(t). \end{aligned} \tag{5.5}$$

In order to achieve the PR property with the stability constraint of the closed-loop system $\bar{G}_m$, we obtain the necessary and sufficient conditions based on Lemmas 1.2 and 2.2 for the existence of a stabilizing state feedback controller, and develop a formula for all such state feedback controller K that can solve the problem mentioned above.

The main result is given as follows.

Theorem 5.1 *Let $\Phi, \Psi \in \mathbf{H}_2$, $\Pi \in \mathbf{H}_{p+q}$ and $\bar{G}_m(s)$ be given. Suppose that Λ represents curves on the complex plane. The following statements are equivalent.*

(1) *There exists a stabilizing state feedback gain K such that*

$$\bar{G}_m(s) + \bar{G}_m^*(s) > 0$$

holds for all $s \in \bar{\Lambda}(\Phi^T, \Psi^T)$.

(2) *There exist X, Y, H, $P = P^*$, $Q = Q^*$ and $P_a = P_a^*$ such that*

$$T \begin{bmatrix} \Phi \otimes P + \Psi \otimes Q & 0 \\ 0 & \Pi \end{bmatrix} T^* < \mathrm{He} \begin{bmatrix} -YZ \\ -XZ \\ AYZ + BHZ + BXZ \\ CYZ + DHZ + DXZ \end{bmatrix}, \tag{5.6}$$

$$\begin{bmatrix} 0 & P_a \\ P_a & 0 \end{bmatrix} < \mathrm{He} \begin{bmatrix} -YL \\ AYL + BHL \end{bmatrix}. \tag{5.7}$$

where

$$\Pi = \begin{bmatrix} 0 & -I_p \\ -I_q & 0 \end{bmatrix}, \ Z = \begin{bmatrix} I_{2n+p+q} \\ 0_{n\times(2n+p+q)} \end{bmatrix}, \ L = \begin{bmatrix} 0_{(2n+p+q)\times n} & 0 \\ -\hat{q}I_n & \hat{p}I_n \end{bmatrix},$$

scalars $\hat{p} \in \mathrm{C}$ and $\hat{q} \in \mathrm{C}$ are fixed vectors satisfying $\hat{p}\hat{q}^* + \hat{q}\hat{p}^* < 0$.

Furthermore, when (5.6) and (5.7) hold, all such solutions K are given by

$$K = HY^{\dagger} + RY^{\perp},$$

where R is an arbitrary $p \times (3n + p + q)$-dimensional matrix.

Proof Letting $\Pi = \begin{bmatrix} 0 & -I_p \\ -I_q & 0 \end{bmatrix}$, it is easy to verify that $\bar{G}_m(s) + \bar{G}_m^*(s) > 0$ is equivalent to

$$\sigma(\bar{G}_m^*(s), \Pi) = \begin{bmatrix} \bar{G}_m^*(s) \\ I_q \end{bmatrix}^* \begin{bmatrix} 0 & -I_p \\ -I_q & 0 \end{bmatrix} \begin{bmatrix} \bar{G}_m^*(s) \\ I_q \end{bmatrix} < 0.$$

According to Lemma 2.2, $\sigma(\bar{G}_m^*(s), \Pi) < 0$ for all $s \in \bar{\Lambda}(\Phi^T, \Psi^T)$ is equivalent to the existence of W, $P = P^*$, $Q = Q^* > 0$ such that

$$T \begin{bmatrix} \Phi \otimes P + \Psi \otimes Q & 0 \\ 0 & \Pi \end{bmatrix} T^* < \mathrm{He} \begin{bmatrix} -I_{n+q} \\ M \end{bmatrix} W,$$

where $P, Q \in \mathrm{C}^{n\times n}$, $W \in \mathrm{C}^{(n+q)\times(2n+p+q)}$ and $M = \begin{bmatrix} A + BK & B \\ C + DK & D \end{bmatrix}$.

Now write W as $W = \begin{bmatrix} W_a \\ W_b \end{bmatrix}$, which yields

$$T \begin{bmatrix} \Phi \otimes P + \Psi \otimes Q & 0 \\ 0 & \Pi \end{bmatrix} T^* < \mathrm{He} \begin{bmatrix} -I_n & 0 \\ 0 & -I_p \\ A + BK & B \\ C + DK & D \end{bmatrix} \begin{bmatrix} W_a \\ W_b \end{bmatrix}, \tag{5.8}$$

where $W_a \in \mathrm{C}^{n\times(2n+p+q)}$, $W_b \in \mathrm{C}^{p\times(2n+p+q)}$, and can be further represented by

$$T \begin{bmatrix} \Phi \otimes P + \Psi \otimes Q & 0 \\ 0 & \Pi \end{bmatrix} T^* < \mathrm{He} \begin{bmatrix} -W_a \\ -W_b \\ AW_a + BKW_a + BW_b \\ CW_a + DKW_a + DW_b \end{bmatrix}.$$

Remark 5.2 $\sigma(\bar{G}_m^*(s), \Pi) < 0$ can be regarded as the shaping of closed-loop TF $\bar{G}_m(s)$ in frequency domain, whereas, the stability is not included. In order to guarantee the stability of the closed-loop system, Lemmas 1.2 and 2.2 is taken into consideration.

The closed-loop system is stable if and only if the real part of each eigenvalue λ of $A + BK$ is negative. Set $\Phi = \begin{bmatrix} 0 & 1 \\ 1 & 0 \end{bmatrix}$, and we have

$$\sigma(\lambda, \Phi^T) = \lambda + \lambda^* < 0.$$

Based on this, the closed-loop system is stable if and only if there exist W_c, $P_a = P_a^* > 0$ such that

$$\begin{bmatrix} 0 & P_a \\ P_a & 0 \end{bmatrix} < \mathrm{He}\left\{ \begin{bmatrix} -I_n \\ A + BK \end{bmatrix} W_c \begin{bmatrix} -\hat{q} I_n & \hat{p} I_n \end{bmatrix} \right\}, \tag{5.9}$$

where $W_c \in \mathrm{C}^{n\times n}$, $P_a \in \mathrm{C}^{n\times n}$, $\begin{bmatrix} \hat{p} & \hat{q} \end{bmatrix} \begin{bmatrix} 0 & 1 \\ 1 & 0 \end{bmatrix} \begin{bmatrix} \hat{p} & \hat{q} \end{bmatrix}^* = \hat{p}\hat{q}^* + \hat{q}\hat{p}^* < 0$.

The condition (5.9) can be rewritten as

$$\begin{bmatrix} 0 & P_a \\ P_a & 0 \end{bmatrix} < \mathrm{He}\left\{ \begin{bmatrix} -W_c \\ AW_c + BKW_c \end{bmatrix} \begin{bmatrix} -\hat{q} I_n & \hat{p} I_n \end{bmatrix} \right\}. \tag{5.10}$$

Hence, there exists a stabilizing state feedback gain K such that

$$\bar{G}_m(s) + \bar{G}_m^*(s) > 0$$

holds for all $s \in \bar{\Lambda}(\Phi^T, \Psi^T)$ if and only if conditions (5.6) and (5.7) are both met.

Comparing (5.10) with (5.7), the two conditions are unfeasible because both the product terms and W_a, W_c are irrelative matrices with different dimension. In order to unify W_a and W_c, new variables are introduced. Now rewrite condition (5.7), and then we have

$$T \begin{bmatrix} \Phi \otimes P + \Psi \otimes Q & 0 \\ 0 & \Pi \end{bmatrix} T^* < \mathrm{He}\left(\begin{bmatrix} -I_n & 0 \\ 0 & -I_p \\ A + BK & B \\ C + DK & D \end{bmatrix} \begin{bmatrix} W_a & W_c \\ W_b & W_d \end{bmatrix} \begin{bmatrix} I_{2n+p+q} \\ 0_{n\times(2n+p+q)} \end{bmatrix} \right). \tag{5.11}$$

Here, it is obvious that condition (5.11) is independent of matrix variables W_c, W_d, which means W_c and W_d can be added to condition (5.11) as an additional matrix.

Similarly, condition (5.9) can be rewritten as

$$\begin{bmatrix} 0 & P_a \\ P_a & 0 \end{bmatrix} < \mathrm{He}\left(\begin{bmatrix} -I_n \\ A + BK \end{bmatrix} \begin{bmatrix} W_a & W_c \end{bmatrix} \begin{bmatrix} 0_{(2n+p+q)\times n} \\ I_n \end{bmatrix} \begin{bmatrix} -\hat{q} I_n & \hat{p} I_n \end{bmatrix} \right), \tag{5.12}$$

where W_a is independent of condition (5.12).

Until now, W_a and W_c have both appeared in the conditions (5.11) and (5.12).

Taking

$$\begin{bmatrix} W_a & W_c \end{bmatrix} = Y, \quad \begin{bmatrix} W_b & W_d \end{bmatrix} = X,$$

then the above conditions can be rewritten as

$$T\begin{bmatrix}\Phi\otimes P+\Psi\otimes Q & 0\\ 0 & \Pi\end{bmatrix}T^{*}<\mathrm{He}\left(\begin{bmatrix}-I_n & 0\\ 0 & -I_p\\ A+BK & B\\ C+DK & D\end{bmatrix}\begin{bmatrix}Y\\ X\end{bmatrix}\begin{bmatrix}I_{2n+p+q}\\ 0_{n\times(2n+p+q)}\end{bmatrix}\right) \tag{5.13}$$

$$\begin{bmatrix}0 & P_a\\ P_a & 0\end{bmatrix}<\mathrm{He}\left(\begin{bmatrix}-I_n\\ A+BK\end{bmatrix}Y\begin{bmatrix}0_{(2n+p+q)\times n}\\ I_n\end{bmatrix}\begin{bmatrix}-\hat{q}I_n & \hat{p}I_n\end{bmatrix}\right). \tag{5.14}$$

Furthermore, it can be seen that (5.13) and (5.14) can be simplified through matrix multiplying

$$T\begin{bmatrix}\Phi\otimes P+\Psi\otimes Q & 0\\ 0 & \Pi\end{bmatrix}T^{*}<\mathrm{He}\begin{bmatrix}-YZ\\ -XZ\\ AYZ+BKYZ+BXZ\\ CYZ+DKYZ+DXZ\end{bmatrix},$$

$$\begin{bmatrix}0 & P_a\\ P_a & 0\end{bmatrix}<\mathrm{He}\begin{bmatrix}-YL\\ AYL+BKYL\end{bmatrix},$$

where $Z=\begin{bmatrix}I_{2n+p+q}\\ 0_{n\times(2n+p+q)}\end{bmatrix}$, $L=\begin{bmatrix}0_{(2n+p+q)\times n} & 0\\ -\hat{q}I_n & \hat{p}I_n\end{bmatrix}$, which are equivalent to the following two inequalities by taking $KY=H$,

$$T\begin{bmatrix}\Phi\otimes P+\Psi\otimes Q & 0\\ 0 & \Pi\end{bmatrix}T^{*}<\mathrm{He}\begin{bmatrix}-YZ\\ -XZ\\ AYZ+BHZ+BXZ\\ CYZ+DHZ+DXZ\end{bmatrix},$$

$$\begin{bmatrix}0 & P_a\\ P_a & 0\end{bmatrix}<\mathrm{He}\begin{bmatrix}-YL\\ AYL+BHL\end{bmatrix}.$$

All the solutions satisfy $KY=H$ are given by

$$K=HY^{\dagger}+RY^{\perp}.$$

This completes the proof.

Remark 5.3 It is worth pointing out that Lemma 2.2 does not capture the closed-loop stability. Hence, an additional design specification, for example, regional poles constraints, which guarantees the stability is generally introduced.

Remark 5.4 It seems that the (5.11) and (5.13) are not needful, since they are equivalent to (5.8) and (5.9), respectively. However, the matrix variables W_a and W_c are irrelative matrices with different dimensions such that conditions (5.11) and (5.13)

could unify the W_a and W_c without introducing conservatism. Our results are necessary and sufficient conditions, which capture not only the frequency-domain shaping of closed-loop TFs but also the closed-loop stability.

5.2.2 *Finite Frequency Positive Real Control for Singularly Perturbed Systems*

Until now, we have derived the necessary and sufficient conditions for the existence of a stabilizing state feedback gain K. In the following discussion, we will use the results to study SPSs.

It is well known that SPSs have multiple time-scale properties, also with multiple frequency-scale properties. The decomposition of a control problem into slow and fast parts is very effective, and most of decomposition methods employ SPTs. Following the usual treatment, a scaling ratio of $p = \varepsilon s$ in the frequency domain is introduced. Hence, we decompose $G(s)$ with slow and fast subsystems expressed, respectively, as

$$G_s : \begin{cases} \dot{x}_s = A_s x_s + B_s u_s \\ y_s = C_s x_s + D_s u_s \end{cases}$$

and

$$G_f : \begin{cases} \varepsilon \dot{x}_f = A_{22} x_f + B_2 u_f \\ y_f = C_2 x_f, \end{cases}$$

where $A_s = A_{11} - A_{12}A_{22}^{-1}A_{21}$, $B_s = B_1 - A_{12}A_{22}^{-1}B_2$, $C_s = C_1 - C_2A_{22}^{-1}A_{21}$, $D_s = -C_2A_{22}^{-1}B_2$. Composite state feedback control for SPSs has been investigated in [4, 13], where a controller was constructed by designing controllers for slow and fast subsystems, respectively. In this subsection, we adopt the composite state feedback controller as follows:

$$u = \left[K_s + K_f A_{22}^{-1} A_{21} + K_f A_{22}^{-1} B_2 K_s \;\; K_f \right] \begin{bmatrix} x_1 \\ x_2 \end{bmatrix}.$$

Then, the slow and fast subsystems of closed-loop system $\bar{G}(s)$ are shown as follows:

$$\bar{G}_s : \begin{cases} \dot{x}_s = (A_s + B_s K_s) x_s + B_s T u_s \\ y_s = (C_s + D_s K_s) x_s + D_s T u_s \end{cases}$$

and

$$\bar{G}_f : \begin{cases} \varepsilon \dot{x}_f = (A_{22} + B_2 K_f) x_f + B_f u_f \\ y_f = C_2 x_f, \end{cases}$$

where $T = (I + K_2 A_{22}^{-1} B_2)^{-1}$. Also, as mentioned in [11], if $A_s + B_s K_s$ and $A_{22} + B_2 K_2$ are both Hurwitz stable, then the closed-loop systems $\bar{G}(s)$ are stable for sufficiently small ε.

Correspondingly, we can get the TFs of slow and fast subsystems in different frequency scales, respectively:

$$\bar{G}_s(s) = (C_s + D_s K_s)(sI - A_s - B_s K_s)^{-1} B_s T + D_s T, \tag{5.15}$$

$$\bar{G}_f(p) = C_2(pI - A_{22} - B_2 K_2)^{-1} B_2. \tag{5.16}$$

Moreover, it follows from [6] that the slow and fast subsystems can approximate the full system in the appropriate low- and high-frequency ranges, respectively. It means that, if $\bar{G}_s(s)$ and $\bar{G}_f(p)$ are both stable and SPR in low and high frequencies respectively, then $\bar{G}(s)$ will also be stable and SPR in the low and high frequencies for sufficiently small ε.

Set $\bar{\omega} = \varepsilon\omega$, then $p = j\bar{\omega}$. Now, the relevant result of fast subsystem is given as follows:

Theorem 5.2 *Let* $W_1 = \{\bar{\omega} \in \mathbf{R} : |\bar{\omega}| \geq \omega_h\}$ *and* $\bar{G}_f(p)$ *be given. The following statements are equivalent.*

(1) *There exists a stabilizing state feedback gain* K_f *such that*

$$\bar{G}_f(p) + \bar{G}_f^*(p) > 0$$

holds for all $\bar{\omega} \in W_1$.

(2) *There exist matrices* $X, Y, H, P = P^*,\ Q = Q^*$ *and* $P_a = P_a^* > 0$ *such that*

$$T \begin{bmatrix} Q & P & 0 & 0 \\ P & -\omega_h^2 Q & 0 & 0 \\ 0 & 0 & 0 & -I_p \\ 0 & 0 & -I_q & 0 \end{bmatrix} T^* < \mathrm{He} \begin{bmatrix} -YZ \\ -XZ \\ A_{22}YZ + B_2 HZ + B_2 XZ \\ C_2 YZ \end{bmatrix} \tag{5.17}$$

$$\begin{bmatrix} 0 & P_a \\ P_a & 0 \end{bmatrix} < \mathrm{He} \begin{bmatrix} -YL \\ A_{22}YL + B_2 HL \end{bmatrix} \tag{5.18}$$

where

$$Z = \begin{bmatrix} I_{2n_2+p+q} \\ 0_{n_2 \times (2n_2+p+q)} \end{bmatrix},\ L = \begin{bmatrix} 0_{(2n_2+p+q)\times n_2} & 0 \\ -\hat{q} I_{n_2} & \hat{p} I_{n_2} \end{bmatrix},\ \hat{p},\ \hat{q} \in \mathbf{C}$$

are fixed vectors satisfying $\hat{p}\hat{q}^* + \hat{q}\hat{p}^* < 0$, *and* T *is the permutation matrix. Furthermore, if (5.17) and (5.18) hold, then all such solutions* K_f *are given by* $K_f = HY^{\dagger} + RY^{\perp}$.

Proof Setting $\Phi = \begin{bmatrix} 0 & 1 \\ 1 & 0 \end{bmatrix}$, $\Psi = \begin{bmatrix} 1 & 0 \\ 0 & -\omega_h^2 \end{bmatrix}$, and the frequency set can be given by

$$\Lambda(\Phi, \Psi) = \{j\bar{\omega} \,||\bar{\omega}| \geq \omega_h\}$$

The remaining is similar as the proof of Theorem 5.1.

Similar result of slow subsystem is given as follows:

Theorem 5.3 *Let $W_2 = \{\omega \in \mathbf{R} : |\omega| \leq \omega_l\}$ and $\bar{G}_s(s)$ be given. The following statements are equivalent.*

(1) *There exists a stabilizing state feedback gain K_s such that*

$$\bar{G}_s(s) + \bar{G}_s^*(s) > 0$$

holds for all $\omega \in W_2$.

(2) *There exist X, Y, H, $P = P^*$, $Q = Q^* > 0$, and $P_a = P_a^* > 0$ such that*

$$T \begin{bmatrix} -Q & P & 0 & 0 \\ P & \omega_l^2 Q & 0 & 0 \\ 0 & 0 & 0 & -I_p \\ 0 & 0 & -I_q & 0 \end{bmatrix} T^* < \mathrm{He} \begin{bmatrix} -YZ \\ -XZ \\ A_0YZ + B_0HZ + B_0TXZ \\ C_0YZ + D_0HZ + D_0TXZ \end{bmatrix} \tag{5.19}$$

$$\begin{bmatrix} 0 & P_a \\ P_a & 0 \end{bmatrix} < \mathrm{He} \begin{bmatrix} -YL \\ A_0YL + B_0HL \end{bmatrix} \tag{5.20}$$

where

$$Z = \begin{bmatrix} I_{2n_1+p+q} \\ 0_{n_1 \times (2n_1+p+q)} \end{bmatrix}, \; L = \begin{bmatrix} 0_{(2n_1+p+q)\times n_1} & 0 \\ -\hat{q}I_{n_1} & \hat{p}I_{n_1} \end{bmatrix}, \; \text{and } \hat{p}, \; \hat{q} \in \mathbf{C}, \hat{p}\hat{q}^* + \hat{q}\hat{p}^* < 0,$$

and T is the permutation matrix. Furthermore, all such solutions K_s are given by

$$K_s = HY^{\dagger} + RY^{\perp}.$$

Proof Setting $\Phi = \begin{bmatrix} 0 & 1 \\ 1 & 0 \end{bmatrix}$, $\Psi = \begin{bmatrix} -1 & 0 \\ 0 & \omega_l^2 \end{bmatrix}$, we have

$$\Lambda(\Phi, \Psi) = \{j\omega \,||\omega| \leq \omega_l\}.$$

Note that $\bar{G}_s(s)$ is a slightly different from $\bar{G}_m(s)$ in the form. Let us recall the procedure of proving Theorem 5.1, and we make a simple change of (5.8), namely

$$T \begin{bmatrix} \Phi \otimes P + \Psi \otimes Q & 0 \\ 0 & \Pi \end{bmatrix} T^* < \mathrm{He} \left(\begin{bmatrix} -I_{n_1} & 0 \\ 0 & -I_p \\ A + BK & BT \\ C + DK & DT \end{bmatrix} \begin{bmatrix} Y \\ X \end{bmatrix} \begin{bmatrix} I_{2n_1+p+q} \\ 0_{n_1 \times (2n_1+p+q)} \end{bmatrix} \right)$$

which is equivalent to

$$T\begin{bmatrix}\Phi\otimes P+\Psi\otimes Q & 0\\ 0 & \Pi\end{bmatrix}T^{*}<\mathrm{He}\begin{bmatrix}-YZ\\ -XZ\\ AYZ+BKYZ+BTXZ\\ CYZ+DKYZ+DTXZ\end{bmatrix}.$$

The following proof is similar to that of Theorem 5.1, which is omitted here.

Remark 5.5 If we set

$$\Pi=\begin{bmatrix}I_p & 0\\ 0 & -\gamma^2 I_q\end{bmatrix},$$

Theorems 5.2 and 5.3 can be applied to (semi)finite frequency H_∞ control, and the composite state feedback controller is also

$$K=\begin{bmatrix}K_s+K_f A_{22}^{-1}A_{21}+K_f A_{22}^{-1}B_2K_s & K_f\end{bmatrix}.$$

SPR control for SPSs in (semi)finite frequency ranges has been investigated in this section. Necessary and sufficient conditions for the existence of a stabilizing state feedback controller for the general linear systems are derived based on GKYP lemma, and the related results are used to study SPSs. Through designing controllers for the fast and modified slow subsystems, a composite feedback controller for SPSs is constructed, which preserves the stability and positive real property.

5.3 A Descriptor-System Method for Strictly Positive Real Control of Singularly Perturbed Systems

As mentioned before, the dynamics of SPSs contain the interaction of the slow and fast phenomena so that the feedback design often suffers from high dimension and ill-posed problem [10, 11]. SPTs are used in analytical investigations of robustness of system properties at the cost of model accuracy [2, 11, 14]. The stability and control specifications of the original system can be inferred from the analysis of lower-order subsystems in separate time scales. Despite the great practical significance for analysis and design, there are still restrictions and limitations with classical methods because only a small group of SPSs are capable for slow-fast decomposition.

Contrast with the existing methods, a descriptor-system method of SPSs will be introduced to avoid the slow-fast decomposition, which can also be easily applied into both standard and nonstandard SPSs. Nowadays, the theory of singular systems is well developed to pave the way to find a new synthesis approach to SPSs. In [24, 26], many results previously known only for regular state-space systems have been extended to the singular systems. It has been pointed out that the singular systems are limiting forms of SPSs. Via constraint of the algebraic condition that the limiting solution is available to approach that of the SPSs, the limiting models are employed to design controllers for the original SPSs. In [29], the problems of

robust stability analysis and robust stabilization for a class of linear SPSs with norm-bounded time-varying uncertainties were solved with the aid of the existing results for singular systems under certain conditions. Singular method to nonlinear singularly perturbed optimal control problem has been proposed in [1, 19, 20, 30], which also illustrated that the optimal (ε-independent) regulators for the singular systems were near-optimal regulators for the corresponding SPSs.

In this section, we adopt the singular method to design the ε-dependent or ε-independent state feedback controller to realize the PR property of the SPS.

Consider the SPS $G(s)$ as follows:

$$\begin{aligned} \dot{x}_1 &= A_{11}x_1 + A_{12}x_2 + B_1u, \\ \varepsilon\dot{x}_2 &= A_{21}x_1 + A_{22}x_2 + B_2u, \\ y &= C_1x_1 + C_2x_2. \end{aligned} \tag{5.21}$$

Define a new variable as $\eta(t) := \begin{bmatrix} x_1(t) \\ x_2(t) \end{bmatrix}$, and then $G(s)$ can be rewritten in a more concise and explicit form as follows:

$$\begin{aligned} E\dot{\eta} &= A\eta + Bu \\ y &= C\eta \end{aligned} \tag{5.22}$$

where

$$E = \begin{bmatrix} I_{n_1} & 0 \\ 0 & \varepsilon I_{n_2} \end{bmatrix},\ A = \begin{bmatrix} A_{11} & A_{12} \\ A_{21} & A_{22} \end{bmatrix},\ B = \begin{bmatrix} B_1 \\ B_2 \end{bmatrix},\ C = \begin{bmatrix} C_1 & C_2 \end{bmatrix}.$$

Then, the open-loop TFM from the input u to the measurement output y is

$$G_{yu}(s) = C(sE - A)^{-1}B,$$

which can be viewed as a matrix function about small parameter ε. Let a state feedback controller with the form of $u = K\eta + r$. The closed-loop system of $G(s)$ is written as

$$\begin{aligned} E\dot{\eta} &= (A + BK)\eta + Br, \\ y &= C\eta, \end{aligned} \tag{5.23}$$

where $r(t)$ is the reference input vector. Hence the TFM of the reference input $r(t)$ to the measurement output $y(t)$ is

$$T_{yr}(s) = C(sE - (A + BK))^{-1}B,$$

or represented in the standard form in Lemma 2.2,

$$M = \begin{bmatrix} A & B \\ C & 0 \end{bmatrix} + \begin{bmatrix} B \\ 0 \end{bmatrix} K \begin{bmatrix} I_n & 0 \end{bmatrix}.$$

The qualitative analysis of TF properties and its relationship with stability analysis have a long history back to the year 1892. Control performance of mechanical structure design can be significantly improved when the system structure has certain specifications such as PR property. Based on the following theorem, both ε-dependent and ε-independent controllers can be designed.

For sake of representation, three target frequency sets are defined, respectively, in the low-, middle- and high-frequency range:

1. the low-frequency range: $\Lambda_l = \{\omega : |\omega| < \omega_l\}$;
2. the middle-frequency range: $\Lambda_m = \{\omega : \omega_1 < \omega < \omega_2\}$;
3. the high-frequency range: $\Lambda_h = \{\omega : |\omega| > \omega_h\}$.

Theorem 5.4 *For given matrices R_l, R_m, R_h and scalar $\gamma > 0$, the closed-loop system (5.23) satisfies PR property in the low-frequency range,*

$$T_{yr}{}^*(j\omega) + T_{yr}(j\omega) > 0,\ \omega \in \Lambda_l,$$

if there exist symmetric matrices $Q > 0$, W and matrices $P_\varepsilon = \begin{bmatrix} P_{11} & 0 \\ P_{21} & P_{22} \end{bmatrix}$, V_2, κ and scalar ε^* such that for any $\varepsilon \in (0, \varepsilon^*]$, the following LMI holds:

$$\begin{bmatrix} -Q & 0 & P_\varepsilon & 0 \\ 0 & 0 & 0 & -I_p \\ P_\varepsilon & 0 & \omega_l^2 Q & 0 \\ 0 & -I_p & 0 & 0 \end{bmatrix} < \mathrm{He} \begin{bmatrix} -I_n & 0 & 0 \\ 0 & -I_p & 0 \\ A & B & B \\ C & 0 & 0 \end{bmatrix} \begin{bmatrix} WR_l \\ V_2 \\ \kappa R_l \end{bmatrix}, \tag{5.24}$$

where ω_l, defined in Λ_l, is given in advance.

Or, the closed-loop system (5.23) achieves the PR property in the middle-frequency range,

$$T_{yr}{}^*(j\omega) + T_{yr}(j\omega) > 0,\ \omega \in \Lambda_m,$$

if the following LMI holds:

$$\begin{bmatrix} -Q & 0 & P_\varepsilon + j\omega_c Q & 0 \\ 0 & 0 & 0 & -I_p \\ P_\varepsilon + j\omega_c Q & 0 & -\omega_1\omega_2 Q & 0 \\ 0 & -I_p & 0 & 0 \end{bmatrix} < \mathrm{He} \begin{bmatrix} -I_n & 0 & 0 \\ 0 & -I_p & 0 \\ A & B & B \\ C & 0 & 0 \end{bmatrix} \begin{bmatrix} WR_m \\ V_2 \\ \kappa R_m \end{bmatrix}, \tag{5.25}$$

where $\omega_c = (\omega_1 + \omega_2)/2$ is defined in Λ_m and given in advance.

Or, the closed-loop system (5.23) satisfies the PR property in the high-frequency range,

$$T_{yr}{}^*(j\omega) + T_{yr}(j\omega) > 0,\ \omega \in \Lambda_h,$$

which is equal to the feasibility of LMI below:

$$\begin{bmatrix} Q & 0 & P_\varepsilon & 0 \\ 0 & 0 & 0 & -I_p \\ P_\varepsilon & 0 & -\omega_h^2 Q & 0 \\ 0 & -I_p & 0 & 0 \end{bmatrix} < \mathrm{He} \begin{bmatrix} -I_n & 0 & 0 \\ 0 & -I_p & 0 \\ A & B & B \\ C & 0 & 0 \end{bmatrix} \begin{bmatrix} WR_h \\ V_2 \\ \kappa R_h \end{bmatrix}, \tag{5.26}$$

where ω_h is determined beforehand.

Furthermore, the gain of the state feedback controller is shown as $K = \kappa W^{-1}$.

Proof Given $\Pi = \begin{bmatrix} 0 & I_p \\ I_p & 0 \end{bmatrix}$, then the finite frequency inequality

$$\begin{bmatrix} T_{yr}(j\omega) \\ I_p \end{bmatrix}^* \Pi \begin{bmatrix} T_{yr}(j\omega) \\ I_p \end{bmatrix} < 0, \quad \omega \in (-\infty, \ +\infty)$$

becomes

$$T_{yr}^*(j\omega) + T_{yr}(j\omega) > 0, \tag{5.27}$$

and the closed-loop system (5.24) has the passive property.

Based on Lemma 2.2, we can obtain the sufficient conditions for the establishment of (5.27) as follows,

$$\begin{bmatrix} A & B \\ I_n & 0 \end{bmatrix}^* \Xi \begin{bmatrix} A & B \\ I_n & 0 \end{bmatrix} + \begin{bmatrix} C & 0 \\ 0 & I_p \end{bmatrix}^* \Pi \begin{bmatrix} C & 0 \\ 0 & I_p \end{bmatrix} < 0, \tag{5.28}$$

where $\Xi = \begin{bmatrix} -Q & PE \\ EP & \omega_l^2 Q \end{bmatrix}$, which is equivalent to

$$\begin{bmatrix} A & I_n \\ C & 0 \end{bmatrix} \Xi \begin{bmatrix} A & I_n \\ C & 0 \end{bmatrix}^* + \begin{bmatrix} B & 0 \\ 0 & I_p \end{bmatrix} \Pi \begin{bmatrix} B & 0 \\ 0 & I_p \end{bmatrix}^* < 0. \tag{5.29}$$

Based on Lemma 2.2, it gives that (5.29) can be rewritten by

$$\begin{bmatrix} -Q & 0 & PE & 0 \\ 0 & 0 & 0 & -I_p \\ EP & 0 & \omega_l^2 EQE & 0 \\ 0 & -I_p & 0 & 0 \end{bmatrix} < \mathrm{He} \begin{bmatrix} -I_n & 0 & 0 \\ 0 & -I_p & 0 \\ A & B & B \\ C & 0 & 0 \end{bmatrix} \begin{bmatrix} WR_m \\ V_2 \\ \kappa R_m \end{bmatrix}, \tag{5.30}$$

where $P = \begin{bmatrix} P_{11} & P_{21} \\ P_{21} & \varepsilon P_{22} \end{bmatrix}$.

Taking $PE = \begin{bmatrix} P_{11} & 0 \\ P_{21} & P_{22} \end{bmatrix} := P_\varepsilon$ and $EQE = \begin{bmatrix} Q_{11} & 0 \\ 0 & 0 \end{bmatrix}$, we can derive that (5.30) is equivalent to

$$\begin{bmatrix} -Q & 0 & \begin{bmatrix} P_{11} & \varepsilon P_{12} \\ P_{21} & P_{22} \end{bmatrix} & 0 \\ 0 & 0 & 0 & -I_p \\ \begin{bmatrix} P_{11} & P_{21}^* \\ \varepsilon P_{21} & P_{22} \end{bmatrix} & 0 & \omega_l^2 \begin{bmatrix} Q_{11} & 0 \\ 0 & 0 \end{bmatrix} & 0 \\ 0 & -I_p & 0 & 0 \end{bmatrix} < \mathrm{He} \begin{bmatrix} -I_n & 0 & 0 \\ 0 & -I_p & 0 \\ A & B & B \\ C & 0 & 0 \end{bmatrix} \begin{bmatrix} WR_l \\ V_2 \\ \kappa R_l \end{bmatrix}, \quad (5.31)$$

which gives

$$\begin{bmatrix} -Q & 0 & \begin{bmatrix} P_{11} & 0 \\ P_{21} & P_{22} \end{bmatrix} & 0 \\ 0 & 0 & 0 & -I_p \\ \begin{bmatrix} P_{11} & P_{21}^* \\ 0 & P_{22} \end{bmatrix} & 0 & \omega_l^2 \begin{bmatrix} Q_{11} & 0 \\ 0 & 0 \end{bmatrix} & 0 \\ 0 & -I_p & 0 & 0 \end{bmatrix} < \mathrm{He} \begin{bmatrix} -I_n & 0 & 0 \\ 0 & -I_p & 0 \\ A & B & B \\ C & 0 & 0 \end{bmatrix} \begin{bmatrix} WR_l \\ V_2 \\ \kappa R_l \end{bmatrix}, \quad (5.32)$$

for the continuity of the function about ε.

For the middle-frequency case and high-frequency case, Ξ_m and Ξ_h are, respectively

$$\Xi_m = \begin{bmatrix} -Q & PE + j\omega_c Q \\ EP - j\omega_c Q & -\omega_1\omega_2 EQE \end{bmatrix}, \ \Xi_h = \begin{bmatrix} Q & PE \\ EP & -\omega_h^2 EQE \end{bmatrix}.$$

The proofs are the similar as the case of low-frequency one.

In the end, we derive sufficient conditions for the SPSs to achieve the PR property in different frequency ranges via a novel method inspiring from singular systems. It should be pointed out that the method in this section can be applied to both standard and nonstandard SPSs, which have broader application perspectives.

5.4 Conclusion

Finite frequency positive real control for SPSs has been investigated in this chapter. In Sect. 5.1, basic background knowledge for passivity and positive realness has been given. The high order and ill-conditioning characteristics of SPSs make it difficult to apply the existing results in SPSs directly. Two methods are demonstrated. In Sect. 5.2, SPAs are employed with slow and fast subsystems constructed, respectively. Sufficient conditions for the finite frequency PR control of slow and fast subsystems are given, and a composite controller is given by composing the slow and fast control law. To avoid the degradation of the model accuracy, a descriptor-system method for PR control of SPSs is given in Sect. 5.3. Finally, conclusions are given here.

References

1. Dragan, V., Morozan, T., Shi, P.: Asymptotic properties of input-output operators norm associated with singularly perturbed systems with multiplicative white noise. SIAM J. Control Optim. **41**(1), 141–163 (2002)
2. Dragan, V., Mukaidani, H., Shi, P.: The linear quadratic regulator problem for a class of controlled systems modeled by singularly perturbed ito differential equations. SIAM J. Control Optim. **50**(1), 448–470 (2012)
3. Fridman, E.: Near-optimal H_∞ control of linear singularly perturbed systems. IEEE Trans. Autom. Control **41**(2), 236–240 (1996)
4. Haddad, W.M., Chellaboina, V.S.: Nonlinear Dynamical Systems and Control: A Lyapunov-Based Approach. Princeton University Press, Princeton (2008)
5. Hara, S., Iwasaki, T.: Robust PID control using generalized KYP synthesis. IEEE Control Syst. Mag. **26**(1), 80–91 (2006)
6. Hill, D., Moylan, P.: Stability results for nonlinear feedback systems. Automatica **13**(4), 377–382 (1977)
7. Iwasaki, T., Hara, S., Fradkov, A.L.: Time domain interpretations of frequency domain inequalities on (semi) finite ranges. Syst. Control Lett. **54**(7), 681–691 (2005)
8. Iwasaki, T., Hara, S.: Generalized KYP lemma: unified frequency domain inequalities with design applications. IEEE Trans. Autom. Control **50**(1), 41–59 (2005)
9. Khail, H.K., Chen, F.C.: H_∞ control of two-time-scale systems. Proc. Am. Control Conf. **19**, 35–42 (1992)
10. Kokotovic, P.V., O'Malley, R.E., Sannuti, P.: Singular perturbations and order reduction in control theory-an overview. Automatica **12**(2), 123–132 (1976)
11. Kokotovic, P.V., Khalil, H.K., OReilly, J.: Singular Perturbation Methods in Control: Analysis and Design. Academic Press, New York (1986)
12. Luse, D.W., Ball, J.A.: Frequency-scale decomposition of H_∞ disk problems. SIAM J. Control Optim. **27**(4), 814–835 (1989)
13. Luse, D.W., Khalil, H.K.: Frequency domain results for systems with slow and fast dynamics. IEEE Trans. Autom. Control **AC–30**(12), 1171–1179 (1985)
14. Naidu, D.S., Calise, A.J.: Singular perturbation methods and time scales in guidance and control of aerospace systems: a survey. AIAA J. Guid. Control Dyn. **24**(6), 1057–1078 (2001)
15. Oloomi, H.M., Sawan, M.E.: Suboptimal model-matching problem for two frequency scale transfer functions. In: Proceedings of the American Control Conference, pp. 2190–2191 (1989)
16. Pan, Z., Basar, T.: H_∞ optimal control for singularly perturbed systems Part I: perfect state measurements. In: Proceedings of American Control Conference, pp. 1850–1854 (1992)
17. Pan, Z., Basar, T.: H_∞ optimal control for singularly perturbed systems Part II: perfect state measurements. IEEE Trans. Autom. Control **39**(2), 280–300 (1994)
18. Rantzer, A.: On the Kalman–Yakubovich–Popov lemma. Syst. Control Lett. **28**(1), 7–10 (1996)
19. Shi, P., Shue, S., Agarwal, R.: Robust disturbance attenuation with stability for a class of uncertain singularly perturbed systems. Int. J. Control **70**(6), 873–891 (1998)
20. Shi, P., Dragan, V.: Asymptotic H_∞ control for singularly perturbed systems with parametric uncertainties. IEEE Trans. Autom. Control **44**(9), 1738–1742 (1999)
21. Sun, W., Khargonekar, P.P., Shim, D.: Solution to the positive real control problem for linear time-invariant systems. IEEE Trans. Autom. Control **39**(10), 2034–2046 (1994)
22. Sun, W., Khargonekar, P.P., Shim, D.: Robust control synthesis with general frequency domain specifications: static gain feedback case. Proc. Am. Control Conf. **5**, 4613–4618 (2004)
23. van der Schaft, A.J.: L_2-Gain and Passivity in Nonlinear Control. Springer, New York (1999)
24. Verghese, G.C., Levy, B.C., Kailath, T.: A generalized state-space for singular systems: a survey. IEEE Trans. Autom. Control **AC–26**(4), 811–831 (1981)
25. Willems, J.C.: Least squares stationary optimal control and the algebraic Riccati equation. IEEE Trans. Autom. Control **AC–16**(6), 621–634 (1971)
26. Xu, S., Lam, J.: Robust Control and Filtering of Singular Systems. Springer, Berlin (2006)

27. Yakubovich, V.A.: A frequency theorem for the case in which the state and control spaces are Hilbert spaces with an application to some problems in the synthesis of optimal controls.I. Sib. Math. J. **15**(3), 457–476 (1974)
28. Zames, G.: On the input-output stability of time-varying nonlinear feedback systems, part one: conditions derived using concepts of loop gain, conicity, and positivity. IEEE Trans. Autom. Control **AC–11**(2), 228–238 (1966)
29. Zhong, N., Sun, M., Zou, Y.: Robust stability and stabilization for singularly perturbed control systems: method based on singular systems. Int. J. Innov. Comput. Appl. **4**(7), 1761–1770 (2008)
30. Zhou, L., Lu, G.: Robust stability of singularly perturbed descriptor systems with nonlinear perturbation. IEEE Trans. Autom. Control **56**(4), 858–863 (2011)

Chapter 6
The Sensitivity-Shaping Problem for Singularly Perturbed Systems

In this chapter, a design technique is carried out by applying robustness criteria to obtain stability and satisfy some performances. A loop-shaping technique has been researched by selecting a suitable open-loop TF and then the robust controller is constructed. This chapter is arranged as follows: the basic definitions are presented in Sect. 6.1. The loop-shaping design procedure for SISO SPSs via using the finite frequency strategy is demonstrated in Sect. 6.2. Such method has been extended to be applied in MIMO SPSs in Sect. 6.3. Using observer-based controllers, the fault detection (FD) issue for SPSs based on finite frequency methods has been investigated in Sect. 6.4. Simulation examples are given respectively to show the validity and effectiveness of the design procedure.

6.1 Sensitivity Function and Complementary Sensitivity Function

The design specifications, such as tracking performance, bandwidth and robustness to model uncertainty, are expressed by constraints on the gain responses of the closed-loop TFs. These problems of the closed-loop TFs are called loop shaping. One typical example of loop-shaping is called the sensitivity-shaping problem, which aims at realizing good tracking performance and disturbance attenuation ability.

Suppose that the feedback system is designed, and the level of sensitivity reduction is given by

$$|S(j\omega)| = |\frac{1}{1 + G_p(j\omega)G_c(j\omega)}| \leqslant \varepsilon < 1, \ \forall \omega \in [0, \ \omega_l],$$

C. Cai et al., *Finite Frequency Analysis and Synthesis for Singularly Perturbed Systems*, Studies in Systems, Decision and Control 78,
DOI 10.1007/978-3-319-45405-4_6

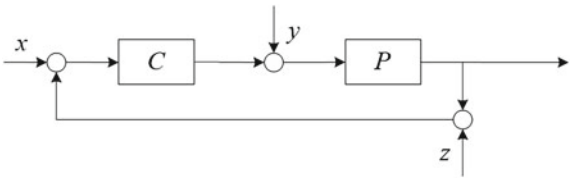

Fig. 6.1 Unity feedback plant with controller

where G_p and G_c are TFs of the plant and corresponding controller, respectively, $\varepsilon > 0$ is a given constant.

Bandwidth constraints in feedback design typically require that the open-loop TF is small above a specified frequency. These constraints are commonly needed to ensure stability robustness despite the presence of modeling uncertainty in the plant model, particularly at high frequencies. One way of quantifying such bandwidth constraints is via requiring the open-loop TF to satisfy

$$|L(j\omega)| \leqslant \frac{M_h}{\omega^{1+\beta}} \leqslant \tilde{\varepsilon} < 1, \ \forall \omega \in [\omega_h, \infty),$$

where $\omega_h > \omega_l$, and $M_h > 0, \ \beta > 0$ are some given constants.

Consider a control system given in Fig. 6.1. A controller C provides stability if it provides internal stability for every plant in the uncertainty set P. If L denotes the open-loop TF ($L = PC$), then the sensitivity function S can be written as

$$S = \frac{1}{1+L},$$

while the complimentary sensitivity function or the input-output TF can be represented as

$$T = 1 - S = \frac{L}{1+L}.$$

To make the closed loops with desired shapes, one must choose appropriate weighting functions, such as $W_1, \ W_2$ as follows to shape the closed-loop TF using control technique.

For a multiplicative perturbation model, robust stability condition is met if and only if $\|W_2 T\|_\infty < 1$ [1, 4], which implies that

$$\left|\frac{W_2(j\omega)L(j\omega)}{1+L(j\omega)}\right| < 1,$$

or

$$|\Omega(j\omega)W_2(j\omega)L(j\omega)| < |1+L(j\omega)|, \ \ \omega \in (-\infty, +\infty), \ \ \|\Omega\|_\infty < 1.$$

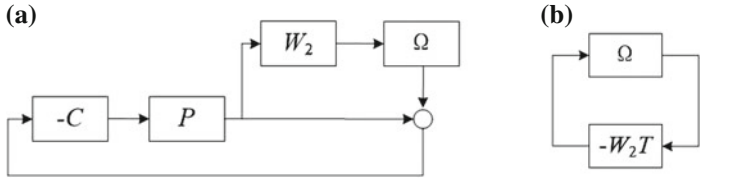

Feedback loop with uncertainty representation.

Feedback loop in standard reduced form.

Fig. 6.2 Interconnections that preserve passivity

The block diagram of a typical perturbed system, ignoring all inputs, is shown in Fig. 6.2(a). The TF from output of Ω to the input of Ω equals $-W_2T$. The properties of the block diagram can be reduced to those of the configuration given in Fig. 6.2(b) [1, 3].

The maximum loop gain $\|-W_2T\|_\infty$ is less than 1 for all allowable Ω if and only if the small gain condition $\|W_2T\|_\infty < 1$ holds. The nominal performance condition for an internally stable system is given as $\|W_1S\|_\infty < 1$, where W_1 is a real-rational, stable, minimum phase TF, also called a weighting function. If the plant P is perturbed by some uncertainties, there is $\tilde{P} = (1 + \Omega W_2)P$, similarly, S will be

$$\tilde{S} = \frac{1}{1 + (1 + \Omega W_2 L)} = \frac{S}{1 + \Omega W_2 T}.$$

The robust performance condition should thereby be

$$\|W_2T\|_\infty < 1, \text{ and } \|\frac{W_1S}{1 + \Omega W_2T}\|_\infty < 1, \ \forall \|\Omega\| < 1.$$

Combining all the above, it can be shown that a necessary and sufficient condition for robust stability and performance is [4]:

$$\||W_1S| + |W_2T|\|_\infty < 1.$$

Overall, loop shaping is a graphical procedure to design a proper controller C satisfying robust stability and performance criteria given above. The basic idea of the method is to construct the loop TF L to satisfy the robust performance criterion approximately, and then to obtain the controller from the relationship $C = L/P$. Internal stability of the plants and properness of C constitute the constraints of the method. Condition $L = PC$ should not have any pole zero cancellation. Different from the existing results mentioned before, the GKYP lemma is used as the frequency division tool to replace the use of the weighing functions, from which new results are obtained.

6.2 Finite Frequency S/T Mixed Sensitivity Design for SISO Singularly Perturbed Systems

The section derives sufficient conditions for the feasibility of a kind of non-convex problem based on GKYP lemma approach. A controller for the SPS is designed in detail to satisfy frequency domain loop-shaping specifications which are given in terms of H_∞ norm. It has been further shown that this controller is obtained by designing its fast and slow parts, respectively. The effectiveness of the proposed method is demonstrated through being compared with traditional H_∞ design method.

For engineering applications, this section aims at investigating the mixed sensitivity problems of SISO SPSs via finite frequency strategy. We extract the dominant frequency components in FF ranges from the the dynamics of SPSs, and design a controller to achieve frequency domain loop-shaping specifications. Based on the GKYP lemma, the controller for the full system is designed, which has the similar singularly perturbed structure with the full system. Furthermore, the parameters of this controller can be derived through designing its fast and slow parts. Finally, the example comparison with traditional H_∞ method shows the superiority of our results. The main feature of this method is that the controller for the full system is designed directly, without the composition of the suboptimal controllers.

Loop-shaping is a typical control design, which requires small sensitivity in a low-frequency range and small complementary sensitivity in a high-frequency range [23]. Simultaneously, the stability margin specification should be satisfied in a middle frequency range.

An SISO singularly perturbed system $G_p(s)$ is given:

$$\begin{aligned} \dot{x}_1 &= A_{11}x_1 + A_{12}x_2 + B_1u, \\ \varepsilon\dot{x}_2 &= A_{21}x_1 + A_{22}x_2 + B_2u, \\ y &= C_1x_1 + C_2x_2 + Du, \end{aligned} \tag{6.1}$$

where $x_1 \in \mathbf{R}^{n_1}$, $x_2 \in \mathbf{R}^{n_2}$, $u \in \mathbf{R}$, $y \in \mathbf{R}$, and A_{22} is assumed to be non-singular.

Problem 6.1 A controller $G_c(s)$ is designed to achieve the following specifications:

(1) $\left|\frac{1}{1+G_p(j\omega)G_c(j\omega)}\right| < \gamma_1, |\omega| \le \omega_l$;
(2) $\left|1 + G_p(j\omega)G_c(j\omega)\right| > \gamma_0, \omega_l \le |\omega| \le \omega_h$;
(3) $\left|\frac{G_p(j\omega)G_c(j\omega)}{1+G_p(j\omega)G_c(j\omega)}\right| < \gamma_3, \omega_h \le |\omega|$,

where $\omega_l < \omega_h$.

Specification (1) represents good tracking performance with small γ_1. The specification (2) ensures a reasonable stability margin with large γ_0. The specification (3) represents robustness against unmodeled dynamics of the plant in high-frequency range with small γ_3. Specifications (1) and (2) will lead to non-convex regions on the complex plane such that the GKYP lemma can not be directly applied to them.

In addition, the three specifications above will be rewritten in other forms, which are more rigorous. Based on the GKYP lemma, we obtain the sufficient conditions for the feasibility of the non-convex problem, and the results and some relevant propositions will be applied to the loop-shaping control design based on the GKYP lemma. The similar specifications are presented in [6, 9], the main difference is that the specifications they introduced were based on the real and imaginary parts of open-loop TF.

Through classical slow-fast decomposition methods, the slow subsystem $G_{ps}(s)$ and fast subsystem $G_{pf}(s)$ of $G_p(s)$ can be expressed as

$$\begin{aligned} \dot{x}_s &= A_s x_s + B_s u_s, \\ y_s &= C_s x_s + D_s u_s, \end{aligned} \tag{6.2}$$

and

$$\begin{aligned} \varepsilon \dot{x}_f &= A_{22} x_f + B_2 u_f, \\ y_f &= C_2 x_f + D u_f, \end{aligned} \tag{6.3}$$

where $A_s = A_{11} - A_{12}A_{22}^{-1}A_{21}$, $B_s = B_1 - A_{12}A_{22}^{-1}B_2$, $C_s = C_1 - C_2A_{22}^{-1}A_{21}$, $D_s = D - C_2A_{22}^{-1}B_2$.

To solve the numerical stiffness in $G_p(s)$, we design a controller $G_c(s)$ which has a similar structure as the original system:

$$\begin{aligned} \dot{p} &= E_{11}p + E_{12}q + F_1 e, \\ \varepsilon \dot{q} &= E_{21}p + E_{22}q + F_2 e, \\ u &= G_1 p + G_2 q + He, \end{aligned}$$

where $p \in \mathbf{R}^{\tilde{n}_1}$, $q \in \mathbf{R}^{\tilde{n}_2}$, $e \in \mathbf{R}$, $u \in \mathbf{R}$ and E_{22} is non-singular.

Decomposing the controller, the slow part $G_{cs}(s)$ and fast part $G_{cf}(s)$ are obtained:

$$\begin{aligned} \dot{p}_s &= E_s p_s + F_s e_s, \\ u_s &= G_s p_s + H_s e_s, \end{aligned}$$

and

$$\begin{aligned} \varepsilon \dot{p}_f &= E_{22} p_f + F_2 e_f, \\ u_f &= G_2 p_f + H e_f, \end{aligned}$$

where $E_s = E_{11} - E_{12}E_{22}^{-1}E_{21}$, $F_s = F_1 - E_{12}E_{22}^{-1}F_2$, $G_s = G_1 - G_2E_{22}^{-1}E_{21}$ and $H_s = H - G_2E_{22}^{-1}F_2$.

Since loop-shaping design problem requires small sensitivity in a low-frequency range and small complementary sensitivity in a high-frequency range, we define

sensitivity function $S(s)$ and complementary sensitivity function $T(s)$ as follows:

$$S(s) = \frac{1}{1 + G_{ps}G_{cs}},\ T(s) = \frac{G_{pf}G_{cf}}{1 + G_{pf}G_{cf}}.$$

Problem 6.2 Taking the definition of H_∞ norm in finite frequency range into consideration, the following specifications are obtained:

(1) $\|S(j\omega)\|_\infty < \gamma_1, |\omega| \le \omega_l$;
(2) $\left\|1 + G_{ps}(j\omega)G_{cs}(j\omega)\right\|_\infty > \gamma_2, |\omega| \le \omega_h$;
(3) $\|T(j\omega)\|_\infty < \gamma_3, \omega_h \le |\omega|$;
(4) $\left\|1 + G_{pf}(j\omega)G_{cf}(j\omega)\right\|_\infty > \gamma_4, \omega_l \le |\omega|$,

where $\omega_l < \omega_h$.

Specifications (1) and (3) ensure the small sensitivity and small complementary sensitivity with small γ_1 and γ_3 in low-and high-frequency ranges respectively, and the specifications (2) and (4) guarantee a certain stability margin with large γ_2 and γ_4.

According to results of Iwasaki [19], the relevant result of slow subsystem is given as follows:

Theorem 6.1 *Let* $W_1 = \{\omega \in \mathbf{R} : |\omega| \le \omega_l\}$, $W_2 = \{\omega \in \mathbf{R} : |\omega| \le \omega_h\}$ *be given, where* $\omega_l < \omega_h$. *Suppose* $\det(j\omega I - A) \ne 0$ $(\omega \in W_2)$. *Then, the constraints,* $\|S(s)\|_\infty < \gamma_1$ *for any* $\omega \in W_1$ *and* $\left\|1 + G_{ps}G_{cs}\right\|_\infty > \gamma_2$ *for any* $\omega \in W_2$, *hold if there exist real symmetric matrices* P_1, P_2 *and* $Q_1 > 0$, $Q_2 > 0$, *such that the following inequalities are satisfied,*

$$\begin{bmatrix} AP_1 + P_1A^T - AQ_1A^T + \omega_l^2 Q_1 & -AQ_1C^T + P_1C^T & B \\ -CQ_1A^T + CP_1 & -CQ_1C^T - {\gamma_1}^2 I & D_1 \\ B^T & {D_1}^T & -I \end{bmatrix} < 0 \tag{6.4}$$

and

$$\begin{bmatrix} AP_2 + P_2A^T - AQ_2A^T + \omega_h^2 Q_2 - BB^T & -AQ_2C^T + P_2C^T - BD_2^T \\ -CQ_2A^T + CP_2 - D_2B^T & -CQ_2C^T - D_2{D_2}^T + {\gamma_2}^2 I \end{bmatrix} < 0, \tag{6.5}$$

where

$$A = \begin{bmatrix} A_s & B_sG_s \\ 0 & E_s \end{bmatrix},\ B = \begin{bmatrix} B_sH_s \\ F_s \end{bmatrix},\ C = \begin{bmatrix} C_s & D_sG_s \end{bmatrix},$$

$$D_1 = D_sH_s - \left(\frac{1}{\gamma_1} + \gamma_1 - 1\right),\ D_2 = D_sH_s + 1.$$

Proof Combining Lemma 2.2 with SCL 2.4 and taking

$$\Psi = \begin{bmatrix} -1 & 0 \\ 0 & \omega_l^2 \end{bmatrix},\ \pi = \begin{bmatrix} I & 0 \\ 0 & -\gamma_1^2 I \end{bmatrix},\ D = D_1,$$

we have

$$\begin{bmatrix} A & I \\ C & 0 \end{bmatrix} \left(\begin{bmatrix} 0 & P \\ P & 0 \end{bmatrix} + \Psi^T \otimes Q \right) \begin{bmatrix} A & I \\ C & 0 \end{bmatrix}^T + \begin{bmatrix} B & 0 \\ D & I \end{bmatrix} \pi \begin{bmatrix} B & 0 \\ D & I \end{bmatrix}^T < 0,$$

which gives

$$\left\| C(sI - A)^{-1}B + D_1 \right\|_\infty < \gamma_1, \ \forall \omega \in W_1. \tag{6.6}$$

Defining

$$\Psi = \begin{bmatrix} -1 & 0 \\ 0 & \omega_l^2 \end{bmatrix}, \ \pi = \begin{bmatrix} I & 0 \\ 0 & -\gamma_1^2 I \end{bmatrix}, \ D = D_2,$$

then (6.5) is equivalent

$$\left\| C(sI - A)^{-1}B + D_2 \right\|_\infty > \gamma_2, \ \forall \omega \in W_2 \tag{6.7}$$

The state space realization of $G_{ps}(s)G_{cs}(s)$ is

$$\begin{bmatrix} \dot{x}_s \\ \dot{p}_s \end{bmatrix} = \begin{bmatrix} A_s & B_s G_s \\ 0 & E_s \end{bmatrix} \begin{bmatrix} x_s \\ p_s \end{bmatrix} + \begin{bmatrix} B_s H_s \\ F_s \end{bmatrix} e_s$$
$$y_s = \begin{bmatrix} C_s & D_s G_s \end{bmatrix} \begin{bmatrix} x_s \\ p_s \end{bmatrix} + D_0 H_0 e_s.$$

Then, the inequality (6.6) is equivalent to

$$\left\| G_{ps}G_{cs} - \left(\frac{1}{\gamma_1} + \gamma_1 - 1 \right) \right\|_\infty < \gamma_1, \ \forall \omega \in W_1.$$

Remark 6.1 It can be seen that $G_p(s)$ and $G_c(s)$ are SISO systems, and the sensitivity problem can be specified with a scalar $\gamma_1 < 1$ such that

$$\|S(s)\|_\infty = \left\| \frac{1}{1 + G_{ps}G_{cs}} \right\|_\infty < \gamma_1, \ \forall \omega \in W_1.$$

Inequality (6.7) is equivalent to

$$\left\| 1 + G_{ps}G_{cs} \right\|_\infty > \gamma_2, \ \forall \omega \in W_2.$$

Similar result of fast subsystem is given as follows:

Theorem 6.2 *Let* $W_1 = \{\omega \in \mathbf{R} : |\omega| \geqslant \omega_h\}$, $W_2 = \{\omega \in \mathbf{R} : |\omega| \geqslant \omega_l\}$ *be given, where* $\omega_l < \omega_h$. *Suppose* $\det(j\omega I - A) \neq 0 (\omega \in W_2)$. *Then, the requirements,* $\|T(s)\|_\infty < \gamma_3$ *for any* $\omega \in W_1$ *and* $\left\| 1 + G_{ps}G_{cs} \right\|_\infty > \gamma_4$ *for any* $\omega \in W_2$, *hold if there exist real symmetric matrices* P_1, P_2 *and* $Q_1 > 0$, $Q_2 > 0$, *such that the following inequalities are satisfied,*

$$\begin{bmatrix} AP_1 + P_1A^T - AQ_1A^T + \omega_l^2 Q_1 & -AQ_1C^T + P_1C^T & B \\ -CQ_1A^T + CP_1 & -CQ_1C^T - \beta^2 I & D_1 \\ B^T & {D_1}^T & -I \end{bmatrix} < 0, \tag{6.8}$$

and

$$\begin{bmatrix} AP_2 + P_2A^T - AQ_2A^T + \omega_h^2 Q_2 - BB^T & -AQ_2C^T + P_2C^T - BD_2^T \\ -CQ_2A^T + CP_2 - D_2B^T & -CQ_2C^T - D_2{D_2}^T + {\gamma_2}^2 I \end{bmatrix} < 0, \tag{6.9}$$

where $\beta = \frac{\gamma_3}{1+\gamma_3}$, $A = \begin{bmatrix} A_{22}/\varepsilon & B_2G_2/\varepsilon \\ 0 & E_{22}/\varepsilon \end{bmatrix}$, $B = \begin{bmatrix} B_2H/\varepsilon \\ F_2/\varepsilon \end{bmatrix}$, $C = \begin{bmatrix} C_2 & DG_2 \end{bmatrix}$ *and* $D_1 = DH$, $D_2 = DH + 1$.

Proof Similar to the proof of Theorem 6.1.

It has been shown how to design a controller for a SPS to satisfy loop-shaping specifications. Since similar problem has been discussed in [10], the results obtained are compared with theirs in the following examples. The main difference is that they consider the problem in the entire frequency range, whereas our results are built in the finite frequency ranges.

Example 6.1 Consider the following SISO SPS,

$$G_p(s) = \frac{s+1}{(s+2)(\varepsilon s+1)},$$

where $\varepsilon = 0.0001$.

In order to make the comparison clearly, we choose $\omega_l = 2 \times 10^{-5}$, $\omega_h = 2 \times 10^5$. Applying the design method, we obtain the controller as follows:

$$G_c(s) = \frac{284.7s + 5.691 \times 10^6}{s^2 + 10002s + 1 \times 10^4}.$$

The composite controller is obtained (Fig. 6.3),

$$G_c(s) = \frac{0.0001949s^4 + 1.952s^3 + 23.86s^2 + 90.95s + 102.1}{1 \times 10^{-11}s^5 + 2.051 \times 10^{-5}s^4 + 0.1025s^3 + 0.6659s^2 + 0.8195s + 0.2561}.$$

The sensitivity functions and the step response are depicted in Fig. 6.4.

Example 6.2 Let the plant with the small parameter $\varepsilon = 0.001$ be

$$G_p(s) = \frac{s+0.5}{(s+2)(\varepsilon s+2)}.$$

A controller will be designed such that both γ_2 and γ_4 will approach 1, and $\gamma_1 \leq 0.1$, $\gamma_3 \leq 0.1$.

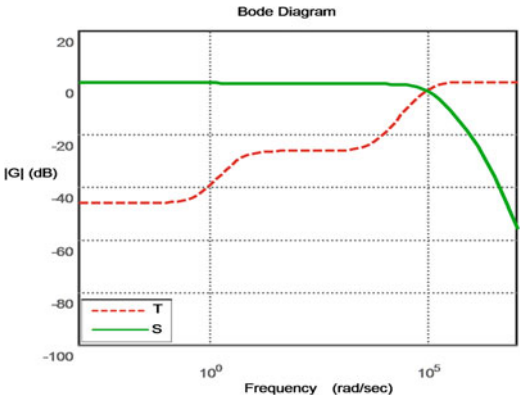

Fig. 6.3 Sensitivity functions in the finite frequency ranges

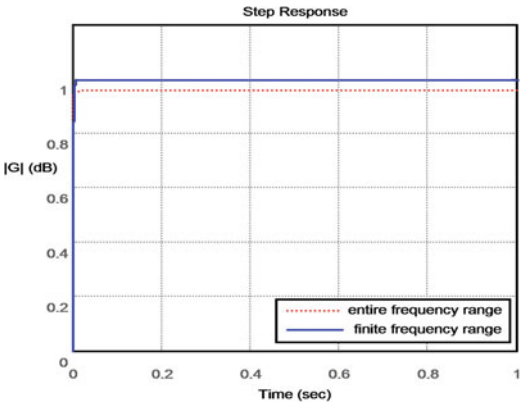

Fig. 6.4 Sensitivity functions in the finite frequency ranges

In this example, select parameters $\omega_l = 2 \times 10^{-4}$, $\omega_h = 2 \times 10^4$ and $G_2 = 1$, $E_{22} = -1$, $E_{11} = -2$, $E_{12} = E_{21} = G_1 = 1$, $H = 0$. To make our results more convincing, we provide two groups of specifications, and then design two different controllers according to the different specifications:

(1) $\gamma_1 = 0.1$, $\gamma_3 = 0.01$
Using the design procedure in this subsection, a controller is developed as

$$G_c(s) = \frac{413.1s + 7.282 \times 10^4}{s^2 + 1002s + 1000}.$$

(2) $\gamma_1 = 0.01$, $\gamma_3 = 0.01$

Similarly, another controller to satisfy specification (2) is obtained:

$$G_c(s) = \frac{772.8s + 7.921 \times 10^5}{s^2 + 1002s + 1000}.$$

It is easily to verify that the parameters selected meet $\gamma_4 = 0.97$ and $\gamma_2 = 1.18$ that means a certain stability margin has been guaranteed. The sensitivity functions and the step response are depicted in Fig. 6.4.

Loop-shaping design for SPSs has been investigated in these examples. A singularly perturbed form controller is also constructed. The most remarkable is that the controller can be design directly without the composition of the suboptimal controllers.

6.3 Finite Frequency H_-/H_∞ Control for MIMO Singularly Perturbed Systems

There are many research results along the H_∞ control problem for singularly perturbed. Oloomi and Sawan [15] studied the suboptimal matching problem for SISO two frequency-scale systems and obtained a suboptimal H_∞ solution through solving the model matching problems for low-and high-frequency models. Tan et al. [20] have derived a set of ε-independent sufficient and necessary conditions for the existence of an H_∞ suboptimal controller in a different and simple way. Pan and Basar [16, 17] have solved the H_∞ control problem for the MIMO SPS using the theory of differential games, and presented an ε-independent two-stage procedure for the construction of a suboptimal solution. Luse and Ball [12] studied a weighted sensitivity problem and derived an approximate solution in which the problem is decomposed into slow and fast subproblems. However, their results are based on the entire frequency, without considering the frequency characteristics of subsystems sufficiently.

One of the most fundamental results relation frequency domain and time domain is the KYP lemma, which establishes the equivalence between the FDI and the LMI [18, 21]. As the extension of the standard KYP lemma, the GKYP lemma was introduced by Iwasaki et al., which provided an LMI characterization of FDIs in (semi)finite frequency range [6, 8, 19]. Finite frequency control of SPS were developed in [13, 14]. Mei et al. [14] studied for H_∞ Control of SPS by a GKYP lemma based approach. Huang et al. [7] discussed finite frequency positive real control for SPS.

In this section, the H_-/H_∞ control issue are considered for MIMO SPS in (semi)finite frequency ranges, and a singularly perturbed form controller is designed to satisfy different FF specifications. Introducing H_- index and H_∞ norm of TFM in different frequency set, the SPS can achieve desired robustness and good sensor noise rejection capability. Finally, a example is given to demonstrate the superiority of our results.

Consider the following SPS $G(s)$:

$$\begin{aligned} \dot{x}_1(t) &= A_{11}x_1(t) + A_{12}x_2(t) + B_1u(t), \\ \varepsilon\dot{x}_2(t) &= A_{21}x_1(t) + A_{22}x_2(t) + B_2u(t), \\ y(t) &= C_1x_1(t) + C_2x_2(t) + Du(t), \end{aligned} \tag{6.10}$$

where $x_1(t) \in \mathbf{R}^{n_1}$ and $x_2(t) \in \mathbf{R}^{n_2}$ $(n = n_1 + n_2)$ are the states vectors, $u(t) \in \mathbf{R}^p$ is the input vector, $y(t) \in \mathbf{R}^q$ is the output vector and $0 < \varepsilon \ll 1$ is a small real parameter. The TFM is represented by

$$G(s) = C(sI_n - A)^{-1}B + D := \left[\begin{array}{cc} A & B \\ C & D \end{array}\right] \in \mathbf{RH}_\infty,$$

where $A = \left[\begin{array}{cc} A_{11} & A_{12} \\ \frac{A_{21}}{\varepsilon} & \frac{A_{22}}{\varepsilon} \end{array}\right]$, $B = \left[\begin{array}{c} B_1 \\ \frac{B_2}{\varepsilon} \end{array}\right]$, $C = \left[\begin{array}{cc} C_1 & C_2 \end{array}\right]$, and D are constant matrices of appropriate dimensions.

As $r(t) = 0$, the desired disturbance rejection capability of $G(s)$ with good dynamic characteristics would require designing a controller $G_c(s)$ such that the following requirement is satisfied

$$\bar{\sigma}\left(\left(I_q + G(s)G_c(s)\right)^{-1}\right) < \gamma_1, \quad |\omega| \le \omega_l. \tag{6.11}$$

As $d(t) = 0$, the desired disturbance rejection capability of $G(s)$ with good dynamic characteristics would require designing a controller $G_c(s)$ such that the following requirement is satisfied

$$\bar{\sigma}\left(G(s)G_c(s)\left(I_q + G(s)G_c(s)\right)^{-1}\right) < \gamma_2, \quad |\omega| \ge \omega_h, \tag{6.12}$$

where γ_1 and γ_2 are two small real constants.

Remark 6.2 The output sensitivity matrix $S_o(s) = \left(I_q + G(s)G_c(s)\right)^{-1}$, shown in Fig. 6.5, is defined as the TF from the disturbance d to measurement output y, and the output complementary sensitivity matrix is denoted by

$$T_o(s) = I_q - S_o(s) = G(s)G_c(s)\left(I_q + G(s)G_c(s)\right)^{-1}.$$

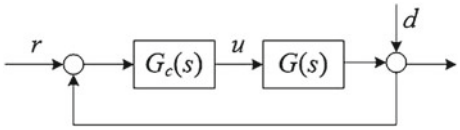

Fig. 6.5 The residual output subject to the low-frequency noise

Remark 6.3 It should be noted that the inequality (6.11) has reveal that the singular value of $S_0(s)$ is supposed small for good dynamic performance of the plant output in the low-frequency range $[-\omega_l, \omega_l]$, while inequality (6.12) has shown that the singular value of $G(s)$ is supposed small to guarantee desired robustness and sufficient sensor noise rejection capability in the high-frequency range $(-\infty, -\omega_h] \cup [\omega_h, \infty)$.

Based on Lemma 2.1, we can obtain the following lemmas in the equivalent form.

Lemma 6.1 *Define the rational function $G(\lambda) = (\lambda I_n - A)^{-1}B$, where $A \in \mathbf{C}^{n\times n}$, $B \in \mathbf{C}^{n\times p}$. Given Hermitian matrix $\Pi \in \mathbf{C}^{(n+p)\times(n+p)}$, the complex frequency set Λ can be defined by*

$$\Lambda(\Phi, \Psi) = \left\{\lambda \in \mathbf{C} : \begin{bmatrix}\lambda \\ 1\end{bmatrix}^* \Phi \begin{bmatrix}\lambda \\ 1\end{bmatrix} = 0,\ \begin{bmatrix}\lambda \\ 1\end{bmatrix}^* \Psi \begin{bmatrix}\lambda \\ 1\end{bmatrix} \geqslant 0\right\}, \tag{6.13}$$

where λ is the frequency variable (s for continuous-time and z for discrete-time cases), and Hermitian matrices $\Phi, \Psi \in \mathbf{C}^{2\times 2}$. The following statements are equivalent,

(1) $\begin{bmatrix}G(\lambda) \\ I_p\end{bmatrix}^* \Pi \begin{bmatrix}G(\lambda) \\ I_p\end{bmatrix} < 0 (>0)$, *for any $\lambda \in \Lambda(\Phi, \Psi)$;*

(2) There exist Hermitian matrices P and $Q > 0$, such that

$$\begin{bmatrix}A & B \\ I_n & 0\end{bmatrix}^* (\Phi \otimes P + \Psi \otimes Q) \begin{bmatrix}A & B \\ I_n & 0\end{bmatrix} + \Pi < 0 (> 0).$$

For clarity of explanation, the dual version of the GKYP lemma is introduced.

Lemma 6.2 *Define the rational function $G(\lambda) = C(\lambda I_n - A)^{-1}$, where $A \in \mathbf{C}^{n\times n}$, $C \in \mathbf{C}^{q\times n}$. Given Hermitian matrix $\Gamma \in \mathbf{C}^{(n+q)\times(n+q)}$, the complex frequency set $\Lambda(\Phi, \Psi)$ can be denoted by (6.13). The following statements are equivalent,*

(1) $\begin{bmatrix}G(\lambda) & I_q\end{bmatrix} \Gamma \begin{bmatrix}G(\lambda) & I_q\end{bmatrix}^* < 0 (> 0)$, *for any $\lambda \in \Lambda(\Phi, \Psi)$.*

(2) There exist Hermitian matrices P and $Q > 0$, such that the following inequality is satisfied

$$\begin{bmatrix}A & I_n \\ C & 0\end{bmatrix} (\Phi \otimes P + \Psi \otimes Q) \begin{bmatrix}A & I_n \\ C & 0\end{bmatrix}^* + \Gamma < 0 (> 0).$$

As an extension of Lemmas 6.1 and 6.2, the following lemma is given.

Lemma 6.3 *Let* $W = \left\{\omega \in \mathbf{R} : \begin{bmatrix}j\omega \\ 1\end{bmatrix}^* \Psi \begin{bmatrix}j\omega \\ 1\end{bmatrix} \geq 0\right\}$, *with the relationship between W and Ψ shown in Table 6.1. Assume* $\det(j\omega I_n - A) \neq 0$ $(\omega \in W)$.

The constraint condition $\|G(s)\|_-^W = \left\|C(sI_n - A)^{-1}B + D\right\|_-^W > \beta$ holds if and only if exist Hermitian matrices P_1 and $Q_1 > 0$, such that

Table 6.1 Comparison of $W - \Psi$

W	Ψ
$\lvert\omega\rvert \le \omega_l$	$\begin{bmatrix} -1 & 0 \\ 0 & \omega_l^2 \end{bmatrix}$
$0 \le \omega \le \omega_l$	$\begin{bmatrix} -1 & -j\omega_l/2 \\ j\omega_l/2 & 0 \end{bmatrix}$
$\omega_l \le \omega \le \omega_h$	$\begin{bmatrix} -1 & j(\omega_l+\omega_h)/2 \\ -j(\omega_l+\omega_h)/2 & -\omega_l\omega_h \end{bmatrix}$
$\lvert\omega\rvert \ge \omega_h$	$\begin{bmatrix} 1 & 0 \\ 0 & -\omega_h^2 \end{bmatrix}$
$\omega \ge \omega_h$	$\begin{bmatrix} 0 & j \\ -j & -2\omega_h \end{bmatrix}$
$0 \le \omega < \infty$	$\begin{bmatrix} 0 & 0 \\ 0 & 0 \end{bmatrix}$

$$\begin{bmatrix} A & B \\ I_n & 0 \end{bmatrix}^* \left(\begin{bmatrix} 0 & P_1 \\ P_1 & 0 \end{bmatrix} + \Psi \otimes Q_1 \right) \begin{bmatrix} A & B \\ I_n & 0 \end{bmatrix} + \begin{bmatrix} C^*C & C^*D \\ D^*C & D^*D - \beta^2 I_p \end{bmatrix} > 0. \quad (6.14)$$

Similarly, the constraint condition $\|G(s)\|_\infty^W = \left\|C(sI_n - A)^{-1}B + D\right\|_\infty^W < \gamma$ *holds if and only if exist Hermitian matrices* P_2 *and* $Q_2 > 0$*, such that*

$$\begin{bmatrix} A & I_n \\ C & 0 \end{bmatrix} \left(\begin{bmatrix} 0 & P_2 \\ P_2 & 0 \end{bmatrix} + \Psi \otimes Q_2 \right) \begin{bmatrix} A & I_n \\ C & 0 \end{bmatrix}^* + \begin{bmatrix} BB^* & BD^* \\ DB^* & DD^* - \gamma^2 I_q \end{bmatrix} < 0. \quad (6.15)$$

Proof According to definition of H_- index, $\|G(s)\|_-^W > \beta$ is equivalent to $\inf\limits_{\omega \in W} [G(j\omega)] > \beta$, which is rewritten by $G^*(j\omega)G(j\omega) > \beta^2 I_p$, for any $\omega \in W$, i.e.,

$$\left(C(j\omega I_n - A)^{-1}B + D\right)^* \left(C(j\omega I_n - A)^{-1}B + D\right) - \beta^2 I_p > 0, \ \forall \omega \in W, \quad (6.16)$$

based on the minimum singular value definition.

It can be seen that (6.16) can be further represented by

$$\begin{bmatrix} (j\omega I_n - A)^{-1}B \\ I_p \end{bmatrix}^* \begin{bmatrix} C^*C & C^*D \\ D^*C & D^*D - \beta^2 I_p \end{bmatrix} \begin{bmatrix} (j\omega I_n - A)^{-1}B \\ I_p \end{bmatrix} > 0, \ \forall \omega \in W.$$

Hence, according to Lemma 6.1, the inequality (6.15) holds if and only if there exist Hermitian matrices, P_1 and $Q_1 > 0$, such that

$$\begin{bmatrix} (j\omega I_n - A)^{-1}B \\ I_p \end{bmatrix}^* (\Phi \otimes P_1 + \Psi \otimes Q_1) \begin{bmatrix} (j\omega I_n - A)^{-1}B \\ I_p \end{bmatrix} + \Pi > 0, \ \forall \omega \in W,$$

where $\Pi = \begin{bmatrix} C^*C & C^*D \\ D^*C & D^*D - \beta^2 I_p \end{bmatrix}$.

Here, we define $\lambda = j\omega$, which means the real part of λ is zero, i.e., $\lambda^* + \lambda = 0$ with its matrix form

$$\begin{bmatrix} \lambda \\ 1 \end{bmatrix}^* \begin{bmatrix} 0 & 1 \\ 1 & 0 \end{bmatrix} \begin{bmatrix} \lambda \\ 1 \end{bmatrix} = 0. \tag{6.17}$$

The frequency variable $\omega \in \lambda$ can be characterized by $\lambda \in \Lambda(\Phi, \Psi), \Phi = \begin{bmatrix} 0 & 1 \\ 1 & 0 \end{bmatrix}$, and Ψ can be used in the frequency division. The proof of the equivalence between $\|G(s)\|_\infty^W < \gamma$ and inequality (6.15) is similar to the above proof, which is omitted here [8].

According to the Table 6.1, in the low-frequency range $|\omega| \le \omega_l$, one can obtain that (6.14) is equivalent to

$$\begin{bmatrix} A & B \\ I_n & 0 \end{bmatrix}^* \begin{bmatrix} -Q_1 & P_1 \\ P_1 & \omega_l^2 Q_1 \end{bmatrix} \begin{bmatrix} A & B \\ I_n & 0 \end{bmatrix} + \begin{bmatrix} C^*C & C^*D \\ D^*C & D^*D - \beta^2 I_p \end{bmatrix} > 0.$$

In the high-frequency range $|\omega| \ge \omega_h$, one can achieve that inequality (6.15) is equivalent to

$$\begin{bmatrix} A & I_n \\ C & 0 \end{bmatrix} \begin{bmatrix} Q_2 & P_2 \\ P_2 & -\omega_h^2 Q_2 \end{bmatrix} \begin{bmatrix} A & I_n \\ C & 0 \end{bmatrix}^* + \begin{bmatrix} BB^* & BD^* \\ DB^* & DD^* - \gamma^2 I_q \end{bmatrix} < 0.$$

Using the tradition singularly perturbed method, slow subsystem $G_s(s)$ and fast subsystem $G_f(\varepsilon s)$ are obtained

$$\begin{aligned} \dot{x}_s &= A_s x_s + B_s u_s, \\ y_s &= C_s x_s + D_s u_s, \end{aligned} \tag{6.18}$$

and

$$\begin{aligned} \varepsilon \dot{x}_f &= A_{22} x_f + B_2 u_f, \\ y_f &= C_2 x_f + D u_f, \end{aligned} \tag{6.19}$$

where $A_s = A_{11} - A_{12}A_{22}^{-1}A_{21}$, $B_s = B_1 - A_{12}A_{22}^{-1}B_2$, $C_s = C_1 - C_2 A_{22}^{-1}A_{21}$, $D_s = D - C_2 A_{22}^{-1}B_2$. Throughout this subsection, the following assumptions are required.

Assumption 6.1 *A_s is stable matrix.*

Assumption 6.2 *A_{22} has no eigenvalues on the imaginary axis.*

It has been shown in [5] that the TF of a SPS can be written as sum of two TFs in two different frequency-scales, s and εs, corresponding to the time-scales t and $\tau = t/\varepsilon$:

$$G(s) = G_s(s) + G_f(\varepsilon s),$$

which means that $G_s(s)$ and $G_f(\varepsilon s)$ can approximate $G(s)$ in low and high frequencies, respectively. Then, let $G_{cs}(s)$ be a controller for slow subsystem $G_s(s)$ and $G_{cf}(\varepsilon s)$ be a controller for fast subsystem $G(\varepsilon s)$.

It can be assumed that the controllers have the following state-space realizations

$$G_{sc}(s) : \begin{cases} \dot{x}_{sc} = A_{sc}x_{sc} + B_{sc}(\rho)y_{sc}, \\ u_{sc} = C_{sc}x_{sc} + D_{sc}(\rho)y_{sc}, \end{cases}$$

$$G_{fc}(\varepsilon s) : \begin{cases} \varepsilon\dot{x}_{fc} = A_{fc}x_{fc} + B_{fc}(\zeta)y_{fc}, \\ u_{fc} = C_{fc}x_{fc} + D_{fc}(\zeta)y_{fc}, \end{cases}$$

where $x_{sc} \in \mathbf{R}^{n_s}$ and $x_{fc} \in \mathbf{R}^{n_f}$ $(n_k = n_s + n_f)$.

Assumption 6.3 *$B_{sc}(\rho)$, $D_{sc}(\rho)$, $B_{fc}(\zeta)$ and $D_{fc}(\zeta)$ are proper dimension affinely function of ρ and ζ, respectively. A_{sc}, C_{sc}, A_{fc} and C_{fc} are constant proper dimension matrices.*

It means that $G_s(s)$ and $G_f(\varepsilon s)$ depend affinely on the design parameters ρ and ζ, respectively, which also shows that the poles of $G_s(s)$ and $G_f(\varepsilon s)$ are fixed, and the zeros are designed through the choice of ρ and ζ [6].

Assumption 6.4 *A_{sc} is stable matrix.*

The following theorem is one of our main results, and formally states the sufficient conditions of SPS controller to satisfy the performance of the plant output in the low-frequency range $[-\omega_l, \omega_l]$ and noise rejection in the high-frequency range $(-\infty, -\omega_h] \cup [\omega_h, \infty)$.

Theorem 6.3 *Suppose Assumptions 6.3 and 6.4 are satisfied. Inequalities (6.14) and (6.15) hold if there exist small constants $\beta > 0$, $\gamma > 0$ and $\varepsilon > 0$, Hermitian matrices P_1, P_2 and $Q_1 > 0$, $Q_2 > 0$ such that the following LMIs hold*

$$\begin{bmatrix} P_1\hat{A} + \hat{A}^*P_1 + \hat{C}^*\hat{C} & \hat{C}^*\hat{D} & P_1 & 0 & \hat{A}^* \\ \hat{D}^*\hat{C} & (1-\beta^2)I_{n_1+n_s} + D_sD_{sc} + D_{sc}^*D_s^* & 0 & \hat{B}^* & \hat{B}^* \\ P_1 & 0 & I_{n_1+n_s} & 0 & 0 \\ 0 & \hat{B} & 0 & I_p & 0 \\ \hat{A} & \hat{B} & 0 & 0 & Q_1^{-1} \end{bmatrix} > 0, \tag{6.20}$$

$$\begin{bmatrix} P_2\bar{A}^* + \bar{A}P_2 - \omega_h^2 Q_2 & P_2\bar{C}^* & \bar{B} & \bar{A}Q_2 \\ \bar{C}P_2 & -\gamma^2 I_p & \bar{D} & \bar{C}Q_2 \\ \bar{B}^* & \bar{D}^* & -I_l & 0 \\ Q_2\bar{A}^* & Q_2\bar{C}^* & 0 & -Q_2 \end{bmatrix} < 0, \tag{6.21}$$

where

$$\hat{A} = \begin{bmatrix} A_s & B_s C_{sc} \\ 0 & A_{sc} \end{bmatrix},\ \hat{B} = \begin{bmatrix} B_s D_{sc} \\ B_{sc} \end{bmatrix},\ \hat{C} = \begin{bmatrix} C_s & D_s C_{sc} \end{bmatrix},\ \hat{D} = D_s D_{sc} + I_p,$$

$$\bar{A} = \varepsilon^{-1}\begin{bmatrix} A_{22} & B_2 C_{fc} \\ 0 & A_{fc} \end{bmatrix},\ \bar{B} = \varepsilon^{-1}\begin{bmatrix} B_2 D_{fc} \\ B_{fc} \end{bmatrix},\ \bar{C} = \begin{bmatrix} C_2 & DC_{fc} \end{bmatrix},\ \textit{and}\ \bar{D} = DD_{fc}.$$

Proof Considering that

$$\bar{\sigma}\left(\left(I_p + G(s)G_c(s)\right)^{-1}\right) = \frac{1}{\left(I_p + G(s)G_c(s)\right)} < \gamma_1 :\ \ |\omega| \le \omega_l$$

and

$$\bar{\sigma}\left(G(s)G_c(s)\left(I_p + G(s)G_c(s)\right)^{-1}\right) = \frac{1}{\frac{1}{\bar{\sigma}(G(s)G_c(s))} + 1} < \gamma_2 :\ \ |\omega| \ge \omega_h,$$

i.e.,

$$\left(I_p + G(s)G_c(s)\right) > \beta :\ \ |\omega| \le \omega_l, \tag{6.22}$$

$$\bar{\sigma}\left(G(s)G_c(s)\right) < \gamma :\ \ |\omega| \ge \omega_h, \tag{6.23}$$

where $\beta = \frac{1}{\gamma_1}$ and $\gamma = \frac{\gamma_2}{1-\gamma_2} \approx \gamma_2$, it can be seen that inequalities (6.22) and (6.23) are, respectively, equivalent to

$$\left\| I_p + G(s)G_c(s) \right\|_{-}^{[-\omega_l, \omega_l]} > \beta, \tag{6.24}$$

$$\left\| G(s)G_c(s) \right\|_{\infty}^{(-\infty, -\omega_h] \cup [\omega_h, \infty)} < \gamma. \tag{6.25}$$

Hence, for the slow subsystem $G_s(s)$ and its controller $G_{cs}(s)$, condition (6.24) is equivalent to

$$\left\| I_p + G_s(s)G_{sc}(s) \right\|_{-}^{[-\omega_l, \omega_l]} > \beta. \tag{6.26}$$

Similarly, for the fast subsystem $G_f(\varepsilon s)$ along with its controller $G_{cf}(\varepsilon s)$, condition (6.25) is equivalent to

$$\left\| G_f(\varepsilon s)G_{fc}(\varepsilon s) \right\|_{\infty}^{(-\infty, -\omega_h] \cup [\omega_h, \infty)} < \gamma. \tag{6.27}$$

Moreover, we have

$$I_p + G_s(s)G_{sc}(s) = I_p + \left[\begin{array}{c|c} A_s & B_s \\ \hline C_s & D_s \end{array}\right]\left[\begin{array}{c|c} A_{sc} & B_{sc} \\ \hline C_{sc} & D_{sc} \end{array}\right]$$
$$= \left[\begin{array}{cc|c} A_s & B_sC_{sc} & B_sD_{sc} \\ 0 & A_{sc} & B_{sc} \\ \hline C_s & D_sC_{sc} & D_sD_{sc}+I \end{array}\right] := \left[\begin{array}{c|c} \hat{A} & \hat{B} \\ \hline \hat{C} & \hat{D} \end{array}\right]$$

and

$$G_f(\varepsilon s)G_{fc}(\varepsilon s) = \left[\begin{array}{c|c} A_{22}/\varepsilon & B_2/\varepsilon \\ \hline C_2 & D \end{array}\right]\left[\begin{array}{c|c} A_{fc}/\varepsilon & B_{fc}/\varepsilon \\ \hline C_{fc} & D_{fc} \end{array}\right]$$
$$= \left[\begin{array}{cc|c} A_{22}/\varepsilon & B_2C_{fc}/\varepsilon & B_2D_{fc}/\varepsilon \\ 0 & A_{fc}/\varepsilon & B_{fc}/\varepsilon \\ \hline C_2 & DC_{fc} & DD_{fc} \end{array}\right] := \left[\begin{array}{c|c} \bar{A} & \bar{B} \\ \hline \bar{C} & \bar{D} \end{array}\right].$$

According to Lemma 6.2, in the low-frequency range $[-\omega_l, \omega_l]$, the inequality (6.26) holds if and only if there exist symmetric matrices P_1 and $Q_1 > 0$ such that

$$\begin{bmatrix} \hat{A} & \hat{B} \\ I_{n_1+n_s} & 0 \end{bmatrix}^T \begin{bmatrix} -Q_1 & P_1 \\ P_1 & \omega_l^2 Q_1 \end{bmatrix} \begin{bmatrix} \hat{A} & \hat{B} \\ I_{n_1+n_s} & 0 \end{bmatrix} + \begin{bmatrix} \hat{C}^T\hat{C} & \hat{C}^T\hat{D} \\ \hat{D}^T\hat{C} & \hat{D}^T\hat{D} - \beta^2 I_p \end{bmatrix} > 0,$$

i.e.,

$$\begin{bmatrix} -\hat{A}^*Q_1\hat{A} + P_1\hat{A} + \hat{A}^*P_1 + \omega_l^2 Q_1 + \hat{C}^*\hat{C} & -\hat{A}^*Q_1\hat{B} + P_1\hat{B} + \hat{C}^*\hat{D} \\ \star & -\hat{B}^*Q_1\hat{B} + \hat{D}^*\hat{D} - \beta^2 I_p \end{bmatrix} > 0. \tag{6.28}$$

However, $\begin{bmatrix} -P_1^2 & -P_1\hat{B} \\ \star & -\hat{B}^*\hat{B} \end{bmatrix} \le 0$, and the inequality (6.28) can be rewritten by

$$\begin{bmatrix} -\hat{A}^*Q_1\hat{A} + P_1\hat{A} + \hat{A}^*P_1 + \omega_l^2 Q_1 + \hat{C}^*\hat{C} - P_1^2 & -\hat{A}^*Q_1\hat{B} + \hat{C}^*\hat{D} \\ \star & -\hat{B}^*Q_1\hat{B} + \hat{D}^*\hat{D} - \beta^2 I_p - \hat{B}^*\hat{B} \end{bmatrix} > 0.$$

Based on Schur complementary Lemma, inequality (6.28) can be written equivalently as

$$\begin{bmatrix} P_1\hat{A} + \hat{A}^*P_1 + \omega_l^2 Q_1 + \hat{C}^*\hat{C} & \hat{C}^*\hat{D} & P_1 & 0 & \hat{A}^* \\ \star & \hat{D}\hat{D}^* - \beta^2 I_p & 0 & \hat{B}^* & \hat{B}^* \\ \star & \star & I_{n_1+n_s} & 0 & 0 \\ \star & \star & \star & I_{n_1+n_s} & 0 \\ \star & \star & \star & \star & Q_1^{-1} \end{bmatrix} > 0 \tag{6.29}$$

Due to the constraints $Q_1 > 0$ and $(D_s D_{sc})^* D_s D_{sc} \geq 0$, the (1, 1) element and (2, 2) element of left matrix of inequality (6.29) are

$$P_1\hat{A} + \hat{A}^* P_1 + \omega_l^2 Q_1 + \hat{C}^*\hat{C} > P_1\hat{A} + \hat{A}^* P_1 + \hat{C}^*\hat{C}$$

and

$$\hat{D}^*\hat{D} = (D_s D_{sc} + I_p)^*(D_s D_{sc} + I_p) \geq I_p + D_s D_{sc} + D_{sc}^* D_s^*.$$

In the high-frequency range, $(-\infty, -\omega_h] \cup [\omega_h, \infty)$, the control performance (6.27) holds if and only if there exist symmetric matrices P_2 and $Q_2 > 0$ such that

$$\begin{bmatrix} \bar{A} & I_{n_2+n_f} \\ \bar{C} & 0 \end{bmatrix} \begin{bmatrix} Q_2 & P_2 \\ P_2 & -\omega_h^2 Q_2 \end{bmatrix} \begin{bmatrix} \bar{A} & I_{n_2+n_f} \\ \bar{C} & 0 \end{bmatrix}^* + \begin{bmatrix} \bar{B}\bar{B}^* & \bar{B}\bar{D}^* \\ \bar{D}\bar{B}^* & \bar{D}\bar{D}^* - \gamma^2 I_p \end{bmatrix} < 0,$$

i.e.,

$$\begin{bmatrix} \bar{A}Q_2\bar{A}^* + P_2\bar{A}^* + \bar{A}P_2 - \omega_h^2 Q_2 + \bar{B}\bar{B}^* & \bar{A}Q_2\bar{C}^* + P_2\bar{C}^* + \bar{B}\bar{D}^* \\ \star & \bar{C}Q_2\bar{C}^* + \bar{D}\bar{D}^* - \gamma^2 I_p \end{bmatrix} < 0.$$

Based on Schur complementary Lemma, inequality (6.29) can be written equivalently as (6.21).

Next, we discuss the stability of slow control subsystem. Take $\hat{A} = \begin{bmatrix} A_s & B_s C_{sc} \\ 0 & A_{sc} \end{bmatrix}$, where A_{sc} and C_{sc} be constant matrices in the controller $G_{sc}(s)$, and the stability of $\hat{A}$ is equivalent to the that of A_s and A_{sc}.

Theorem 6.4 *Consider a SPS described by $G(s)$, with the subsystems controllers $G_{sc}(s)$ and $G_{fc}(s)$. Suppose that Assumptions 6.3 and 6.4 are satisfied, and the closed-loop system G_s is stable. Control performances (6.11) and (6.12) hold, if exist Hermitian matrices P_1, P_2 and $Q_1 > 0$, $Q_2 > 0$ such that LMIs (6.20) and (6.21) hold. Then, the controller can be formulated by*

$$G_c(s) = G_{cs}(s) + G_{cf}(\varepsilon s).$$

Example 6.3 Consider the one-link robotic manipulator with flexible joint illustrated in [5],

$$\begin{aligned} \dot{x}_1 &= x_2, \\ \dot{x}_2 &= J_2^{-1}(mgl\sin x_1 - \beta_s z_3 - \beta_d z_4), \\ \varepsilon\dot{z}_1 &= -z_1 + x_1, \\ \varepsilon\dot{z}_2 &= -z_2 + x_2, \\ \varepsilon\dot{z}_3 &= z_4, \\ \varepsilon\dot{z}_4 &= J_2^{-1} mgl\sin x_1 - (J_1 + J_2)J_2^{-1}J_1^{-1}(\beta_s z_3 + \beta_d z_4) + J_1^{-1}u, \\ y_1 &= x_1, \\ y_2 &= z_2, \end{aligned} \tag{6.30}$$

Table 6.2 Physical parameters of one-link robotic manipulator with flexible joint

Physical description	Parameter	Value	Unit
Angular displacements of the rotor	θ_1	–	rad
Angular displacements of the link	θ_2	–	rad
Real small parameter	μ	–	–
Moment of inertia of the rotor	J_1	1	$\mathrm{kg \cdot m^2}$
Moment of inertia of the link	J_2	1.333	$\mathrm{kg \cdot m^2}$
Mass of the link	m	1	kg
Half length of link	l	1	m
Gravitational acceleration constant	g	1.62	$\mathrm{m/s^2}$
Spring constant of linear torsional spring	β_s	3	N/m
Damping coefficient of linear torsional damper	β_d	3	Ns /m

where $x_1 := \theta_2,\ x_2 := \dot{\theta}_2,\ \varepsilon\dot{z}_1 = -z_1 + \theta_2,\ \varepsilon\dot{z}_2 = -z_2 + \dot{\theta}_2, z_3 := \varepsilon^{-2}(\theta_2 - \theta_1)$, $z_4 := \varepsilon^{-1}(\dot{\theta}_2 - \dot{\theta}_1)$. Some parameters in (6.30) are listed in Table 6.2.

Letting $\sin x_1 \approx x_1$ and substituting the related parameters into (6.30) can yield

$$\begin{aligned}
\dot{x}_1 &= x_2,\\
\dot{x}_2 &= 1.215x_1 - 2.15z_3 - 2.15z_4,\\
\varepsilon\dot{z}_1 &= -z_1 + x_1,\\
\varepsilon\dot{z}_2 &= -z_2 + x_2,\\
\varepsilon\dot{z}_3 &= z_4,\\
\varepsilon\dot{z}_4 &= 1.215x_1 - 5.25z_3 - 5.25z_4 + u,\\
y_1 &= z_1,\\
y_2 &= z_2,
\end{aligned}$$

where

$$A_{11} = \begin{bmatrix} 0 & 1 \\ 1.215 & 0 \end{bmatrix},\ A_{12} = \begin{bmatrix} 0 & 0 & 0 & 0 \\ 0 & 0 & -2.25 & -2.25 \end{bmatrix},$$

$$A_{21} = \begin{bmatrix} 1 & 0 \\ 0 & 1 \\ 0 & 0 \\ 1.215 & 0 \end{bmatrix},\ A_{22} = \begin{bmatrix} -1 & 0 & 0 & 0 \\ 0 & -1 & 0 & 0 \\ 0 & 0 & 0 & 1 \\ 0 & 0 & -5.25 & -5.25 \end{bmatrix},$$

$$B_1 = \begin{bmatrix} 0 \\ 0 \end{bmatrix},\ B_2 = \begin{bmatrix} 0 & 0 & 0 & 1 \end{bmatrix}^T,\ C_1 = \begin{bmatrix} 0 & 0 \\ 0 & 0 \end{bmatrix},\ C_2 = \begin{bmatrix} 1 & 0 & 0 & 0 \\ 0 & 1 & 0 & 0 \end{bmatrix},\ D = \begin{bmatrix} 0 \\ 0 \end{bmatrix}$$

Related parameters of the slow and fast subsystems of (6.30) are listed as follows

$$A_s = \begin{bmatrix} 0 & 1 \\ 0.7174 & 1 \end{bmatrix},\ B_s = \begin{bmatrix} 0 \\ -0.4095 \end{bmatrix},\ C_s = \begin{bmatrix} 1 & 0 \\ 0 & 1 \end{bmatrix},\ D_s = \begin{bmatrix} 0 \\ 0 \end{bmatrix},$$

$$A_{22}=\begin{bmatrix}-1 & 0 & 0 & 0\\ 0 & -1 & 0 & 0\\ 0 & 0 & 0 & 1\\ 0 & 0 & -5.25 & -5.25\end{bmatrix},\ B_2=\begin{bmatrix}0\ 0\ 0\ 1\end{bmatrix}^T,\ C_2=\begin{bmatrix}1\ 0\ 0\ 0\\ 0\ 1\ 0\ 0\end{bmatrix},\ D=\begin{bmatrix}0\\ 0\end{bmatrix}.$$

The PID strategy is adopted in this example. For the slow subsystem $G_s(s)$, it is obtained

$$G_{sc}(s)=\begin{bmatrix}K_{s1}(s)\ K_{s2}(s)\end{bmatrix},$$

where

$$K_{s1}(s)=k_{p1}+\frac{k_{i1}}{s}+\frac{k_{d1}}{1+T_{d1}s},$$

$$K_{s2}(s)=k_{p2}+\frac{k_{i2}}{s}+\frac{k_{d2}}{1+T_{d2}s},$$

in which $T_{d1}>0$ and $T_{d2}>0$ are small time constants, and parameters k_{pj}, k_{ij} and k_{dj} $(j=1,2)$ are designed parameters. We can obtain its state-space realization as

$$\left[\begin{array}{cc}A_{sc} & B_{sc}(\rho)\\ C_{sc} & D_{sc}(\rho)\end{array}\right]=\left[\begin{array}{cccc|cc}0 & 0 & 0 & 0 & k_{i1} & 0\\ 1 & -1/T_{d1} & 0 & 0 & k_{i1}-k_{d1}/T_{d1}^2 & 0\\ 0 & 0 & 0 & 0 & 0 & k_{i2}\\ 0 & 0 & 1 & -1/T_{d2} & 0 & k_{i2}-k_{d2}/T_{d2}^2\\ \hline 0 & 1 & 0 & 1 & k_{p1}+k_{d1}/T_{d1} & k_{p2}+k_{d2}/T_{d2}\end{array}\right]$$

Similarly, for fast subsystem $G_f(s)$, the state-space realization controller $G_{fc}(\varepsilon s)$ can be represented by

$$\left[\begin{array}{cc}A_{fc}/\varepsilon & B_{fc}(\zeta)/\varepsilon\\ C_{fc} & D_{fc}(\zeta)\end{array}\right]=\left[\begin{array}{cccc|cc}0 & 0 & 0 & 0 & \bar{k}_{i1}/\varepsilon & 0\\ 1 & -1/\varepsilon\bar{T}_{d1} & 0 & 0 & \bar{k}_{i1}/\varepsilon-\bar{k}_{d1}/\varepsilon\bar{T}_{d1}^2 & 0\\ 0 & 0 & 0 & 0 & 0 & \bar{k}_{i2}/\varepsilon\\ 0 & 0 & 1 & -1/\varepsilon\bar{T}_{d2} & 0 & \bar{k}_{i2}/\varepsilon-\bar{k}_{d2}/\varepsilon\bar{T}_{d2}^2\\ \hline 0 & 1 & 0 & 1 & \bar{k}_{p1}+\bar{k}_{d1}/\bar{T}_{d1} & \bar{k}_{p2}+\bar{k}_{d2}/\bar{T}_{d2}\end{array}\right]$$

where $\bar{T}_{d1}>0$ and $\bar{T}_{d2}>0$ are small time constants, and $\bar{k}_{pj}$, $\bar{k}_{ij}$ and $\bar{k}_{dj}$ $(j=1,2)$ are designed parameters.

Overall, H_-/H_∞ control for MIMO SPSs in the finite frequency ranges has been investigated in this section. Sufficient conditions for the existence of an H_-/H_∞ suboptimal controller are derived based on GKYP lemma. A singularly perturbed form controller is constructed through designing its fast and slow parts. The result is applied to deal with the H_-/H_∞ control problem in different frequency ranges to achieve the desired robustness and better sensor noise rejection.

6.4 Fault Detection for Singularly Perturbed Systems

This section addresses the FD synthesis for a class of linear SPSs with disturbances. The observer is designed via using a singular method, in which the SPSs could be processed within a uniform framework instead of the classical slow-fast decomposition. The problem of robust FD is converted into a standard H_∞ model-matching. Based on the GKYP lemma and parameter-dependent Lyapunov functions, a full-order observer is designed such that the corresponding error dynamic system is asymptotically stable and satisfies a prescribed finite frequency H_-/H_∞ performance index. A novel three-step design procedure is then proposed to extract the fault feature from strong background disturbances. An illustrative example is given to demonstrate the validity and applicability of the proposed approaches in the simulation part.

The main contributions of this method are outlined as follows.

1. Different from the existing slow-fast decomposition method, a novel approach stemming from singular systems based on the matrix inequality machinery is utilized, which enjoys great potential and vast application prospects because they are also effective for the widespread non-standard SPSs. With the aid of these new approaches, both ε-dependent and ε-independent FD observers can be designed.
2. The frequency nature of SPSs is considered in design of a well-conditioned FD observer to reduce the conservatism of design procedure. It is noted that the slow modes are sensitive to oscillators associated with low-frequency signals while the fast modes are more easily affected by the high-frequency power source. On this basis, the window H_∞ specification index from the external disturbance to measurement output is particularly fixed in the low or high frequency ranges to obtain stable resistance to various of unknown disturbances. The window H_- index from the fault input to measurement output is specified in the middle frequency range to improve the fault-sensitivity capability of the overall system.
3. To best of our knowledge, it is the first time that finite frequency issues have been investigated for the FD of SPSs, and the results can be extended to more sophisticated systems with multi time-scale property. Due to the existence of modes with distinctive rates of convergence, the control specifications such as H_-/H_∞ specification index can be further loosen combined with the frequency characteristics of the whole system.

Consider the SPS as follows:

$$\begin{aligned} \dot{x}_1(t) &= A_{11}x_1(t) + A_{12}x_2(t) + B_{w_1}w(t) + B_{u_1}u(t) + B_{f_1}f(t), \\ \varepsilon\dot{x}_2(t) &= A_{21}x_1(t) + A_{22}x_2(t) + B_{w_2}w(t) + B_{u_2}u(t) + B_{f_2}f(t), \\ y(t) &= C_1x_1(t) + C_2x_2(t) + D_1u(t) + D_2f(t) + D_3w(t), \end{aligned} \tag{6.31}$$

where $x_1(t) \in \mathbf{R}^{n_1}$ and $x_2(t) \in \mathbf{R}^{n_2}$ $(n = n_1 + n_2)$ are the slow and fast state vectors, $y(t) \in \mathbf{R}^q$ is the measured output, $u(t) \in \mathbf{R}^p$ is the control input, $w(t) \in \mathbf{R}^r$ reveals the disturbance vector, $f(t) \in \mathbf{R}^s$ represents the fault input vector. It should

be noted that A_{ij}, B_{w_i}, B_{u_i}, B_{f_i}, C_i, D_k $(i, j = 1, 2;\ k = 1, 2, 3)$ are constant matrices of appropriate dimensions. The perturbed parameter ε, $0 < \varepsilon \ll 1$, serves as a measurement of the separation in "scale" of the slow and fast dynamics.

For convenience of development in the sequel, define a new variable as

$$\eta(t) := \begin{bmatrix} x_1(t) \\ x_2(t) \end{bmatrix},$$

and then (6.31) can be rewritten in a more concise and explicit form,

$$\begin{aligned} E_\varepsilon \dot{\eta}(t) &= A\eta(t) + B_w w(t) + B_u u(t) + B_f f(t), \\ y(t) &= C\eta(t) + D_1 u(t) + D_2 f(t) + D_3 w(t), \end{aligned} \tag{6.32}$$

where

$$E_\varepsilon = \begin{bmatrix} I_{n_1} & 0 \\ 0 & \varepsilon I_{n_2} \end{bmatrix},\ A = \begin{bmatrix} A_{11} & A_{12} \\ A_{21} & A_{22} \end{bmatrix},\ B_w = \begin{bmatrix} B_{w_1} \\ B_{w_2} \end{bmatrix},$$
$$B_u = \begin{bmatrix} B_{u_1} \\ B_{u_2} \end{bmatrix},\ B_f = \begin{bmatrix} B_{f_1} \\ B_{f_2} \end{bmatrix},\ C = \begin{bmatrix} C_1 & C_2 \end{bmatrix}.$$

To detect the fault, a FD observer in the form of SPS is constructed as

$$\begin{aligned} E_\varepsilon \dot{\breve{\eta}}(t) &= A\breve{\eta}(t) + B_u u(t) + L(y(t) - \breve{y}(t)), \\ \breve{y}(t) &= C\breve{\eta}(t) + D_1 u(t), \\ r(t) &= y(t) - \breve{y}(t), \end{aligned} \tag{6.33}$$

where $\breve{\eta}(t) \in \mathbf{R}^n (n = n_1 + n_2)$ and $\breve{y}(t) \in \mathbf{R}^q$ denote the state and output estimation vectors, respectively; and $r(t)$ is the residual signal, which relies on the fault input $f(t)$ and the external disturbance $w(t)$. The design parameter is the observer gain matrix $L = \begin{bmatrix} L_1 \\ L_2 \end{bmatrix}$.

Remark 6.4 It is clear that if a system is controllable and the system states are available for feedback, then the system closed-loop poles can be assigned arbitrarily through a constant feedback. However, for most practical applications, the system states are not completely accessible and all the designer knows are the input–output data, which brings in increasingly more attention on observer-based controllers.

Denoting a new variable as $\hat{\eta}(t) = \eta(t) - \breve{\eta}(t)$, the following state error dynamic SPS is then obtained,

$$\begin{aligned} E_\varepsilon \dot{\hat{\eta}}(t) &= \bar{A}\hat{\eta}(t) + \bar{B}_w w(t) + \bar{B}_f f(t), \\ r(t) &= C\hat{\eta}(t) + D_2 f(t) + D_3 w(t), \end{aligned} \tag{6.34}$$

where

$$\bar{A} = A - LC = \begin{bmatrix} A_{11} - L_1C_1 & A_{12} - L_1C_2 \\ A_{21} - L_2C_1 & A_{22} - L_2C_2 \end{bmatrix} := \begin{bmatrix} \hat{A}_{11} & \hat{A}_{12} \\ \hat{A}_{21} & \hat{A}_{22} \end{bmatrix},$$
$$\bar{B}_w = B_w - LD_3 = \begin{bmatrix} B_{w_1} - L_1D_3 \\ B_{w_2} - L_2D_3 \end{bmatrix} := \begin{bmatrix} \hat{B}_{w_1} \\ \hat{B}_{w_2} \end{bmatrix},$$
$$\bar{B}_f = B_f - LD_2 = \begin{bmatrix} B_{f_1} - L_1D_2 \\ B_{f_2} - L_2D_2 \end{bmatrix} := \begin{bmatrix} \hat{B}_{f_1} \\ \hat{B}_{f_2} \end{bmatrix}.$$

Remark 6.5 We aim to detect the occurrence of a fault in the presence of unknown disturbances. Nominally, the residual process $r(t)$ is zero in the absence of a fault and non-zero otherwise. However, when driven by unknown disturbing sources with high amplitudes, the residual process can fail to go to zero even in the absence of a fault. If this happens, the FD observer detects but cannot isolate the fault. In this case, the state error dynamic system (6.34) is constructed to convert the FD issue into the H_∞ model matching problem.

On this basis, the corresponding TFMs from fault signal $f(t)$ to the residual $r(t)$ and from the external disturbances $w(t)$ to the residual $r(t)$, denoted by $G_{rf}(s)$ and $G_{rw}(s)$ respectively, are derived.

$$G_{fr}(s) = C(sE_\varepsilon - \bar{A})^{-1}\bar{B}_f + D_2,$$
$$G_{wr}(s) = C(sE_\varepsilon - \bar{A})^{-1}\bar{B}_w + D_3.$$

To investigate H_-/H_∞ performance of continuous-time control systems in local frequency ranges, a new conception of window H_-/H_∞ norm is presented, and it is stated that traditional H_-/H_∞ norm is a special case of window H_-/H_∞ norm.

Remark 6.6 The H_- index of a TFM $G(s)$ over the finite frequency range $[\omega_1, \omega_2]$ and its H_∞ norm over the finite frequency range $[0, \omega_l] \cup [\omega_h, +\infty)$ are defined as Definition 2.4.

Remark 6.7 H_- norm is used as the worst-case fault sensitivity measure. To indicate the dependency on the finite frequency range $[\omega_1, \omega_2]$, we define the window H_- norm as $\|G(s)\|_-^{[\omega_1,\omega_2]}$, which is simplified into $\|G(s)\|_-$ when the frequency range is made with certainty.

Problem 6.3 Based on the above motivation, the design problem of a robust FD observer for the linear SPS (6.31) should satisfy, for any $\varepsilon \in (0, \varepsilon^*]$, as follows:

1. The internal stability constraint: $(E_\varepsilon, \bar{A})$ is stable.
2. The disturbance attenuation ability:

$$\|G_{rw}(s)\|_\infty^{[0,\omega_l]\cup[\omega_h,+\infty)} < \beta. \tag{6.35}$$

3. The fault sensitivity capability:

$$\|G_{rf}(s)\|_-^{[\omega_1,\omega_2]} > \gamma. \tag{6.36}$$

Remark 6.8 The internal stability requirement ensures the asymptotical stability of the error dynamic SPS (6.34) in the absence of unknown disturbances. Condition (6.35) is used to reduce the norm of the closed-loop TFM from the disturbance to the control output to a preserved level. To some extent, the suppression of low- or high-frequency disturbances, divided by trade-off frequencies ω_l and ω_h, can reduce conservatism than the suppression of the disturbances in the entire frequency ranges. In addition, the constraint (6.36) is a FF performance index which increases the fault sensitivity in the fixed frequency range because the frequency characteristics of the fault input, imposed artificially, is known in advance. The frequencies ω_1 and ω_2 given beforehand are used to reflect the general frequency range of the fault input. The noise-signal gain ratio is defined as

$$\delta = \frac{\beta}{\gamma},$$

which can be used to evaluate the FD observers. A better FD observer ought to achieve smaller δ.

Then, a reliable FD mechanism is required to make the system capable of detecting the occurrence of a fault, identifying the faulty component and determining a course of action that restores safe operation of the system. The threshold detection mechanism is utilized in this section, described in Fig. 6.6, which announces a fault when the size of a residual exceeds some prescribed value [2, 11]. This prescribed value could be determined to balance a rate of fault alarm against a rate of miss alarm. Hence, the following logical relationship for FD is in Fig. 6.7.

Here

$$\| r(t) \|_{2,T} = \left[\int_{t_1}^{t_2} r^T(t) r(t) dt \right]^{1/2}, \ T = t_2 - t_1,$$

$t \in (t_1, t_2]$ is the finite-time window, and $J_{th} > 0$ is setted threshold [22].

Remark 6.9 The following useful remarks are given.

1. In a FD progress, a residual signal should be constructed and a residual evaluation function be computed, which is then compared with a predefined threshold. If the

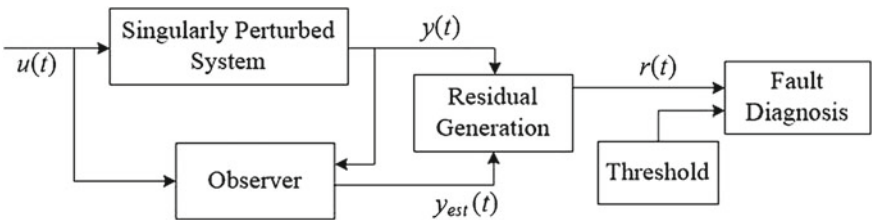

Fig. 6.6 Fault identification scheme for SPSs

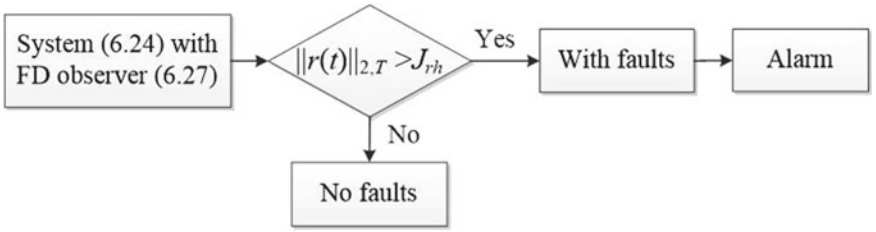

Fig. 6.7 Fault judgment for SPSs

residual exceeds the setted threshold, the fault will be detected and an alarm of fault be generated.

2. As mentioned before, a configurable threshold is used to extract fault features from strong background disturbances. To avoid the false alarm caused by external disturbance, the scalar β in the requirement (6.35) should be set not larger than the threshold J_{th}. Similarly, the parameter γ in (6.36), representing the fault sensitivity capability, should be imposed larger than J_{th} to improve accuracy and efficiency of alarm. The noise-signal gain ratio J is used to optimize the solutions to get more effective FD observer.
3. The threshold mechanism can also be viewed as the smooth filtering device. Due to the existence of the external noise, especially for the high-frequency ones, there exist many glitches in the residual outputs. The threshold mechanism can make the residual evaluation process smoothly when the finite-time window length T is chosen appropriately.

The following lemma is used throughout this section.

Lemma 6.4 *Given matrices* $T_1,\ T_2,\ T_3 \in \mathbf{C}^{n\times n}$, $T_3 < 0$ *holds, if there exists a constant* $0 < \varepsilon^* \ll 1$ *such that*

$$\varepsilon^2 T_1 + \varepsilon T_2 + T_3 \leqslant 0$$

holds for all $\varepsilon \in (0, \varepsilon^*]$.

Proof Consider the following function:

$$\begin{aligned} f(\varepsilon) &= \nu^*(\varepsilon^2 T_1 + \varepsilon T_2 + T_3)\nu \\ &= \varepsilon^2 \nu^* T_1 \nu + \varepsilon \nu^* T_2 \nu + \nu^* T_3 \nu, \end{aligned} \tag{6.37}$$

where $\nu \in \mathbf{C}^n$. Using property of the quadratic function $f(\varepsilon)$, we have

$$f(\varepsilon) \leqslant 0,\ \varepsilon \in (0, \varepsilon^*], \tag{6.38}$$

where $f(\varepsilon)$ is a continue function about ε, and ε^* is a small positive parameter. The sufficient condition for the existence of (6.38) is

$$f(0) = \nu^* T_3 \nu < 0.$$

According to the definition of negative definite matrix, $T_3 < 0$ is derived. This completes the proof.

6.4.1 Internal Stability Conditions

Internal stability is an essential system requirement in control system design, which guarantee smooth operation of all dynamics in the absence of external disturbances. In this subsection, a parameter-dependent Lyapunov functions is adopted to alleviate the stiffness of SPSs, which can be converted to LMIs to obtain feasible solutions.

Theorem 6.5 *For given real constants $\hat{p}$ and $\hat{q}$ satisfying $\hat{p}\hat{q} > 0$, if there exist a matrix κ_s, and symmetric matrices $P_s = \begin{bmatrix} P_{s11} & P_{s12} \\ \star & \frac{1}{\varepsilon} P_{s22} \end{bmatrix} > 0$, and W_s such that the LMI below is established,*

$$\begin{bmatrix} 0 & 0 & P_{s_{11}} & 0 \\ \star & 0 & P_{s_{12}}^* & P_{s_{22}} \\ \star & \star & 0 & 0 \\ \star & \star & \star & 0 \end{bmatrix} < \mathrm{He} \begin{bmatrix} -W_s \\ A^* W_s + C^* \kappa_s \end{bmatrix} \begin{bmatrix} \hat{p} I_n & \hat{q} I_n \end{bmatrix}, \tag{6.39}$$

then there exists a scalar $0 < \varepsilon^* \ll 1$ such that for any $\varepsilon \in (0, \varepsilon^*]$, the closed-loop error dynamic system (6.34) is internally stable. The state feedback gain can then be given by $L = (\kappa_s W_s^{-1})^*$.

Proof Select the Lyapunov function related with the parameter ε as

$$V(\hat{\eta}(t)) = \hat{\eta}^*(t) P_{s\varepsilon} \hat{\eta}(t),$$

where

$$P_{s\varepsilon} = E_\varepsilon P_s E_\varepsilon = \begin{bmatrix} P_{s_{11}} & \varepsilon P_{s_{12}} \\ \star & \varepsilon P_{s_{22}} \end{bmatrix}.$$

According to the SCL 2.4, $P_{s\varepsilon} > 0$ can be guaranteed by $P_{s_{11}} - \varepsilon P_{s_{12}} P_{s_{22}}^{-1} P_{s_{12}}^* > 0$.

Denote a quadratic function as

$$f(\varepsilon) = \nu^* P_{s_{11}} \nu - \varepsilon \nu^* P_{s_{12}} P_{s_{22}}^{-1} P_{s_{12}}^* \nu,$$

where ν is a vector. Thus, $f(\varepsilon)$ is a unary function about ε. From Lemma 2.2, we can obtain that there exists $0 < \varepsilon^* \ll 1$ such that $f(\varepsilon) > 0$ is established, for any $\varepsilon \in (0, \varepsilon^*]$. So it has $f(0) = \nu^* P_{s_{11}} \nu > 0$. According to the definition of positive definite matrix, we have $P_{s_{11}} > 0$. Then, the derivative of $V(\hat{\eta}(t))$ along the trajectories of (6.34) with no external inputs is

$$\dot{V}(\hat{\eta}(t)) = \hat{\eta}^*(t)[(A - LC)^* P_s E_\varepsilon + E_\varepsilon P_s (A - LC)]\hat{\eta}(t) < 0,$$

which is equivalent to

$$(A^* - C^* L^*) P_s E_\varepsilon + E_\varepsilon P_s (A - LC) < 0,$$

or it is written in the standard form in Lemma 2.2,

$$\begin{bmatrix} \bar{A}_n^* & I \end{bmatrix} \begin{bmatrix} 0 & P_s E_\varepsilon \\ E_\varepsilon P_s & 0 \end{bmatrix} \begin{bmatrix} \bar{A} \\ I_n \end{bmatrix} < 0, \tag{6.40}$$

where $\bar{A}^* = A^* + C^*(-L^*) I_n$.

According to Lemma 2.2, (6.40) can be converted into the following LMI:

$$\begin{bmatrix} 0 & P_s E_\varepsilon \\ E_\varepsilon P_s & 0 \end{bmatrix} < \mathrm{He} \begin{bmatrix} -I_n \\ \bar{A}^* \end{bmatrix} W_s R_s. \tag{6.41}$$

Substituting $P_s = \begin{bmatrix} P_{s11} & P_{s12} \\ \star & \frac{1}{\varepsilon} P_{s22} \end{bmatrix}$ into (6.41), we have

$$\begin{bmatrix} 0 & 0 & P_{s_{11}} & \varepsilon P_{s_{12}} \\ \star & 0 & P_{s12}^* & P_{s_{22}} \\ \star & \star & 0 & 0 \\ \star & \star & \star & 0 \end{bmatrix} < \mathrm{He} \begin{bmatrix} -W_s \\ A^* W_s + C^* \kappa_s \end{bmatrix} R_s, \tag{6.42}$$

where $\kappa_s = -L^* W_s$.

Plugging $R_s = \begin{bmatrix} \hat{p} I_n & \hat{q} I_n \end{bmatrix}$ into (6.42) yields that

$$\begin{bmatrix} 0 & 0 & P_{s_{11}} & \varepsilon P_{s_{12}} \\ \star & 0 & P_{s12}^* & P_{s_{22}} \\ \star & \star & 0 & 0 \\ \star & \star & \star & 0 \end{bmatrix} < \mathrm{He} \begin{bmatrix} -W_s \\ A^* W_s + C^* \kappa_s \end{bmatrix} \begin{bmatrix} \hat{p} I_n & \hat{q} I_n \end{bmatrix}, \tag{6.43}$$

where $\hat{p}$ and $\hat{q}$ are scalars which satisfy the constraint $\hat{p}\hat{q} > 0$.

Based on Lemma 6.4, it can be seen that (6.43) holds for any $\varepsilon \in (0, \varepsilon^*]$, if

$$\begin{bmatrix} 0 & 0 & P_{s_{11}} & 0 \\ \star & 0 & P_{s12}^* & P_{s_{22}} \\ \star & \star & 0 & 0 \\ \star & \star & * & 0 \end{bmatrix} < \mathrm{He} \begin{bmatrix} -W_s \\ A^* W_s + C^* \kappa_s \end{bmatrix} \begin{bmatrix} \hat{p} I_n & \hat{q} I_n \end{bmatrix} \tag{6.44}$$

is true. This completes the proof.

6.4.2 Disturbance Attenuation Conditions

This subsection presents a solution to the problem of disturbance attenuation constraint (6.35) via FD observer (6.33) for a linear SPS (6.31). The frequency nature of SPSs, active disturbance attenuation ability in the middle frequency range, is taken into consideration. The H_∞ norm in the low-and high-frequency ranges for the SPS (6.31) is specified to ensure the good resistance ability against all kinds of disturbances.

Theorem 6.6 *For given matrices R_l, R_h and a positive scalar $\beta > 0$, if there exist matrices V_{12} and κ_1, and symmetric matrices*

$$P_1 = \begin{bmatrix} P_{111} & P_{112} \\ \star & \frac{1}{\varepsilon} P_{122} \end{bmatrix}, \; Q_1 = \begin{bmatrix} Q_{111} & Q_{112} \\ \star & Q_{122} \end{bmatrix} > 0,$$

and W_1 such that the error dynamic SPS (6.34) satisfies the system performance (6.35) for any $\varepsilon \in (0, \varepsilon^*]$, then the following LMIs hold:

$$\begin{bmatrix} -Q_{111} & -Q_{112} & 0 & P_{111} & 0 & 0 \\ \star & -Q_{122} & 0 & P_{112}^* & P_{122} & 0 \\ \star & \star & I_q & 0 & 0 & 0 \\ \star & \star & \star & \omega_l^2 Q_{111} & 0 & 0 \\ \star & \star & \star & \star & 0 & 0 \\ \star & \star & \star & \star & \star & -\beta^2 I_p \end{bmatrix} < \mathrm{He} \begin{bmatrix} -I_n & 0 & 0 \\ 0 & -I_q & 0 \\ A^* & C^* & C^* \\ B_w^* & D_3^* & D_3^* \end{bmatrix} \begin{bmatrix} W_1 R_l \\ V_{12} \\ \kappa_1 R_l \end{bmatrix} \tag{6.45}$$

and

$$\begin{bmatrix} Q_{111} & Q_{112} & 0 & P_{111} & 0 & 0 \\ \star & Q_{122} & 0 & P_{112}^* & P_{122} & 0 \\ \star & \star & I_q & 0 & 0 & 0 \\ \star & \star & \star & -\omega_h^2 Q_{111} & 0 & 0 \\ \star & \star & \star & \star & 0 & 0 \\ \star & \star & \star & \star & \star & -\beta^2 I_p \end{bmatrix} < \mathrm{He} \begin{bmatrix} -I_n & 0 & 0 \\ 0 & -I_q & 0 \\ A^* & C^* & C^* \\ B_w^* & D_3^* & D_3^* \end{bmatrix} \begin{bmatrix} W_1 R_h \\ V_{12} \\ \kappa_1 R_h \end{bmatrix}, \tag{6.46}$$

where ω_l and ω_h are cut-off frequencies. Then, the FD observer gain of (6.33) can be calculated by $L_1 = (-\kappa_1 W_1^{-1})^*$.

Proof Condition (6.36) can be represented as follows:

$$G_{wr}^*(s) G_{wr}(s) < \beta^2 I_r,$$

which gives

$$\begin{bmatrix} B_w{}^* (s E_\varepsilon - \bar{A}^*)^{-1} & I_r \end{bmatrix} \Theta_1 \begin{bmatrix} (s E_\varepsilon - \bar{A})^{-1} B_w \\ I_r \end{bmatrix} < 0, \tag{6.47}$$

where $\Theta_1 = \begin{bmatrix} C^* & 0 \\ D_3^* & I_r \end{bmatrix} \begin{bmatrix} I_q & 0 \\ 0 & -\beta^2 I_r \end{bmatrix} \begin{bmatrix} C & D_3 \\ 0 & I_r \end{bmatrix}$.

Based on the Lemma 2.2, the inequality (6.47) can be converted into

$$\begin{bmatrix} \bar{A}^* & E_\varepsilon & C^* & 0 \\ B_w^* & 0 & D_3^* & I_r \end{bmatrix} \Theta_2 \begin{bmatrix} \bar{A} & B_w \\ E_\varepsilon & 0 \\ C & D_3 \\ 0 & I_r \end{bmatrix} < 0, \tag{6.48}$$

where $\Theta_2 = \begin{bmatrix} \Phi \otimes P_1 + \Psi \otimes Q_1 & 0 & 0 \\ 0 & I_q & 0 \\ 0 & 0 & -\beta^2 I_r \end{bmatrix}$.

Leading in the elementary transformation T, it can be seen that (6.48) can be simplified into

$$\begin{bmatrix} \bar{A}^* & C^* & E_\varepsilon & 0 \\ B_w^* & D_3^* & 0 & I_r \end{bmatrix} T \Theta_2 T^* \begin{bmatrix} \bar{A} & B_w \\ C & D_3 \\ E_\varepsilon & 0 \\ 0 & I_r \end{bmatrix} < 0. \tag{6.49}$$

Defining a new variable as $N_1 = \begin{bmatrix} \bar{A}^* & C^* & E_\varepsilon & 0 \\ B_w^* & D_3^* & 0 & I_r \end{bmatrix}$, it is obtained that

$$\begin{aligned} M_1 &= \begin{bmatrix} \bar{A}^* & C^* \\ B_w^* & D_3^* \end{bmatrix} = \begin{bmatrix} A^* & C^* \\ B_w^* & D_3^* \end{bmatrix} + \begin{bmatrix} C^* \\ D_3^* \end{bmatrix} (-L^*) \begin{bmatrix} I_n & 0 \end{bmatrix} \\ &:= \mathscr{A}_1 + \mathscr{B}_1 (-L^*) \mathscr{C}_1, \end{aligned}$$

which is represented in the standard form of Lemma 2.2. Hence, (6.49) can be rewritten as

$$N_1 \begin{bmatrix} I_n & 0 & 0 & 0 \\ 0 & I_q & 0 & 0 \\ 0 & 0 & E_\varepsilon & 0 \\ 0 & 0 & 0 & I_r \end{bmatrix} T \Theta_2 T^* \begin{bmatrix} I_n & 0 & 0 & 0 \\ 0 & I_q & 0 & 0 \\ 0 & 0 & E_\varepsilon & 0 \\ 0 & 0 & 0 & I_r \end{bmatrix} N_1^* < 0, \tag{6.50}$$

Plugging the matrices characterizing $\Phi = \begin{bmatrix} 0 & 1 \\ 1 & 0 \end{bmatrix}$, $\Psi = \begin{bmatrix} -1 & 0 \\ 0 & \omega_l^2 \end{bmatrix}$ of the low-frequency range into (6.50), it yields

$$\begin{bmatrix} -Q_1 & 0 & P_1 E_\varepsilon & 0 \\ \star & I_q & 0 & 0 \\ \star & \star & \omega_l^2 E_\varepsilon Q_1 E_\varepsilon & 0 \\ \star & \star & \star & -\beta^2 I_r \end{bmatrix} < \mathrm{He} \begin{bmatrix} -I_{(n+q)\times(n+r)} \\ M_1 \end{bmatrix} \chi_1, \tag{6.51}$$

where

$$\chi_1 = \mathscr{C}_1^\dagger W_1 R_l + (I_{n+r} - \mathscr{C}_1^\dagger \mathscr{C}_1) \begin{bmatrix} V_{11} \\ V_{12} \end{bmatrix} = \begin{bmatrix} W_1 R_1 \\ V_{12} \end{bmatrix}.$$

Substituting the symmetric matrices $P_1 = \begin{bmatrix} P_{111} & P_{112} \\ \star & \frac{1}{\varepsilon} P_{122} \end{bmatrix}$ and $Q_1 = \begin{bmatrix} Q_{111} & Q_{112} \\ \star & Q_{122} \end{bmatrix}$ into (6.51), we have

$$\delta_1(\varepsilon) < 0, \tag{6.52}$$

where

$$\delta_1(\varepsilon) = \begin{bmatrix} -Q_{111} & -Q_{112} & 0 & P_{111} & \varepsilon P_{112} & 0 \\ \star & -Q_{122} & 0 & P_{112}^* & P_{122} & 0 \\ \star & \star & I_q & 0 & 0 & 0 \\ \star & \star & \star & \omega_l^2 Q_{111} & \varepsilon\omega_l^2 Q_{112} & \\ \star & \star & \star & \star & \varepsilon^2\omega_l^2 Q_{122} & 0 \\ \star & \star & \star & \star & \star & -\beta^2 I_r \end{bmatrix} - \mathrm{He}\begin{bmatrix} -I_n & 0 & 0 \\ 0 & -I_q & 0 \\ A^* & C^* & C^* \\ B_w^* & D_3^* & D_3^* \end{bmatrix}\begin{bmatrix} W_1 R_l \\ V_{12} \\ \kappa_1 R_l \end{bmatrix},$$

$$\kappa_1 = -L^* W_1.$$

From Lemma 2.2, we can obtain that if there exists $0 < \varepsilon^* \ll 1$ such that (6.52) is set up for any $\varepsilon \in (0, \varepsilon^*]$, it is established

$$\delta_1(0) < 0,$$

which is equivalent to

$$\begin{bmatrix} -Q_{111} & -Q_{112} & 0 & P_{111} & 0 & 0 \\ \star & -Q_{122} & 0 & P_{112}^* & P_{122} & 0 \\ \star & \star & I_q & 0 & 0 & 0 \\ \star & \star & \star & \omega_l^2 Q_{111} & 0 & 0 \\ \star & \star & \star & \star & 0 & 0 \\ \star & \star & \star & \star & \star & -\beta^2 I_r \end{bmatrix} < \mathrm{He}\begin{bmatrix} -I_n & 0 & 0 \\ 0 & -I_q & 0 \\ A^* & C^* & C^* \\ B_w^* & D_3^* & D_3^* \end{bmatrix}\begin{bmatrix} W_1 R_l \\ V_{12} \\ \kappa_1 R_l \end{bmatrix}. \tag{6.53}$$

Similarly, it is established for the high-frequency case that

$$\begin{bmatrix} Q_{111} & Q_{112} & 0 & P_{111} & 0 & 0 \\ \star & Q_{122} & 0 & P_{112}^* & P_{122} & 0 \\ \star & \star & I_q & 0 & 0 & 0 \\ \star & \star & \star & -\omega_h^2 Q_{111} & 0 & 0 \\ \star & \star & \star & \star & 0 & 0 \\ \star & \star & \star & \star & \star & -\beta^2 I_r \end{bmatrix} < \mathrm{He}\begin{bmatrix} -I_n & 0 & 0 \\ 0 & -I_q & 0 \\ A^* & C^* & C^* \\ B_w^* & D_3^* & D_3^* \end{bmatrix}\begin{bmatrix} W_1 R_h \\ V_{12} \\ \kappa_1 R_h \end{bmatrix}, \tag{6.54}$$

in which the matrices characterizing the high-frequency range are selected as

$$\Phi = \begin{bmatrix} 0 & 1 \\ 1 & 0 \end{bmatrix}, \Psi = \begin{bmatrix} 1 & 0 \\ 0 & -\omega_h^2 \end{bmatrix}.$$

This completes the proof.

Corollary 6.1 *If the error dynamic SPS (6.34) satisfies the system performance (6.35) for any $\varepsilon \in (0, \varepsilon^*]$ in the entire frequency range, then the following LMI is established:*

$$\begin{bmatrix} 0 & 0 & \mathscr{P}_1 & 0 \\ \star & I_q & 0 & 0 \\ \star & \star & 0 & 0 \\ \star & \star & \star & -\beta^2 I_r \end{bmatrix} < \mathrm{He} \begin{bmatrix} -I_n & 0 & 0 \\ 0 & -I_q & 0 \\ A^* & C^* & C^* \\ B_w^* & D_3^* & D_3^* \end{bmatrix} \begin{bmatrix} W_1 R_l \\ V_{12} \\ \kappa_1 R_l \end{bmatrix}, \tag{6.55}$$

where $\mathscr{P}_1 = \begin{bmatrix} P_{111} & 0 \\ P_{112}^* & P_{122} \end{bmatrix}$.

Proof Let $Q = 0$, condition (6.35) is equal to

$$\begin{bmatrix} 0 & 0 & 0 & P_{111} & 0 & 0 \\ \star & 0 & 0 & P_{112}^* & P_{122} & 0 \\ \star & \star & I_q & 0 & 0 & 0 \\ \star & \star & \star & 0 & 0 & 0 \\ \star & \star & \star & \star & 0 & 0 \\ \star & \star & \star & \star & \star & -\beta^2 I_r \end{bmatrix} < \mathrm{He} \begin{bmatrix} -I_n & 0 & 0 \\ 0 & -I_q & 0 \\ A^* & C^* & C^* \\ B_w^* & D_3^* & D_3^* \end{bmatrix} \begin{bmatrix} W_1 R_l \\ V_{12} \\ \kappa_1 R_l \end{bmatrix}, \tag{6.56}$$

which is the corresponding full frequency condition, and a special case of the finite frequency condition in Theorem 6.6.

Substituting $\mathscr{P}_1 = \begin{bmatrix} P_{111} & 0 \\ P_{112}^* & P_{122} \end{bmatrix}$ into (6.56), we have

$$\begin{bmatrix} 0 & 0 & \mathscr{P}_1 & 0 \\ \star & I_q & 0 & 0 \\ \star & \star & 0 & 0 \\ \star & \star & \star & -\beta^2 I_r \end{bmatrix} < \mathrm{He} \begin{bmatrix} -I_n & 0 & 0 \\ 0 & -I_q & 0 \\ A^* & C^* & C^* \\ B_w^* & D_3^* & D_3^* \end{bmatrix} \begin{bmatrix} W_1 R_l \\ V_{12} \\ \kappa_1 R_l \end{bmatrix}. \tag{6.57}$$

This completes the proof.

6.4.3 *Fault Sensitivity Conditions*

In this subsection, fault sensitivity is analyzed for the error dynamic SPS (6.34), which can provide a health monitoring and maintenance system of smooth operation. The worst case fault sensitivity measure is formulated in terms of LMIs to provide sufficient conditions for (6.36).

Theorem 6.7 *For a given matrix R_m and a positive scalar $\gamma > 0$, if there exist matrices V_{22}, κ_2 and symmetric matrices $P_2 = \begin{bmatrix} P_{211} & P_{212} \\ \star & \frac{1}{\varepsilon} P_{222} \end{bmatrix}$, $Q_2 = \begin{bmatrix} Q_{211} & Q_{212} \\ \star & Q_{222} \end{bmatrix} > 0$, W_2 such that the error dynamic SPS (6.34) satisfies the system performance (6.36) for any $\varepsilon \in (0, \varepsilon^*]$, where $0 < \varepsilon^* \ll 1$. Then the following LMI holds:*

$$\begin{bmatrix} -Q_{211} & -Q_{212} & 0 & P_{211}+j\omega_c Q_{211} & 0 & 0 \\ \star & -Q_{222} & 0 & P_{212}^T+j\omega_c Q_{212}^* & P_{222} & 0 \\ \star & \star & -I_q & 0 & 0 & 0 \\ \star & \star & \star & -\omega_1\omega_2 Q_{211} & 0 & 0 \\ \star & \star & \star & \star & 0 & 0 \\ \star & \star & \star & \star & \star & \gamma^2 I_s \end{bmatrix} < \mathrm{He}\begin{bmatrix} -I_n & 0 & 0 \\ 0 & -I_q & 0 \\ A^* & C^* & C^* \\ B_f^* & D_2^* & D_2^* \end{bmatrix}\begin{bmatrix} W_2 R_m \\ V_{22} \\ \kappa_2 R_m \end{bmatrix}, \tag{6.58}$$

where ω_1 and ω_2 are cut-off frequencies, $\omega_c = (\omega_1+\omega_2)/2$. The FD observer gain of (6.33) is $L_2 = (-\kappa_2 W_2^{-1})^*$.

Proof According to Lemma 2.2, the finite frequency FDI (6.36) holds, if there exist Hermitian matrices P_2 and $Q_2 > 0$ such that

$$\begin{bmatrix} \bar{A}^* & E \\ \bar{B}_f^* & 0 \end{bmatrix} \Xi \begin{bmatrix} \bar{A} & \bar{B}_f \\ E & 0 \end{bmatrix} + \begin{bmatrix} C^* & 0 \\ D_2^* & I_s \end{bmatrix} \Pi \begin{bmatrix} C & D_2 \\ 0 & I_s \end{bmatrix} < 0, \tag{6.59}$$

where $\Xi = \begin{bmatrix} -Q_2 & P_2+j\omega_c Q_2 \\ P_2 - j\omega_c Q_2 & -\omega_1\omega_2 Q_2 \end{bmatrix}$, $\Pi = \begin{bmatrix} -I_q & 0 \\ 0 & \gamma^2 I_s \end{bmatrix}$.

To improve the solvability of (6.59), P_2 and Q_2 are set in the forms as follows to alleviate the numerical stiffness of (6.59)

$$P_2 = \begin{bmatrix} P_{211} & P_{212} \\ \star & \frac{1}{\varepsilon} P_{222} \end{bmatrix}, \quad Q_2 = \begin{bmatrix} Q_{211} & Q_{212} \\ \star & Q_{222} \end{bmatrix}.$$

Leading in the transformation matrix T, it is apparent that (6.59) can be written in a more simplified way as follows,

$$N_2 \begin{bmatrix} I_n & 0 & 0 & 0 \\ 0 & I_q & 0 & 0 \\ 0 & 0 & E_\varepsilon & 0 \\ 0 & 0 & 0 & I_s \end{bmatrix} T\Theta_3 T^* \begin{bmatrix} I_n & 0 & 0 & 0 \\ 0 & I_q & 0 & 0 \\ 0 & 0 & E_\varepsilon & 0 \\ 0 & 0 & 0 & I_s \end{bmatrix} N_2^* < 0, \tag{6.60}$$

where

$$\begin{aligned} N_2 &= \begin{bmatrix} M_2 & I_{n+s} \end{bmatrix} = \begin{bmatrix} \bar{A}^* & C^* & I_n & 0 \\ \bar{B}_f^* & D_2^* & 0 & I_s \end{bmatrix}, \\ M_2 &= \begin{bmatrix} \bar{A}^* & C^* \\ \bar{B}_f^* & D_2^* \end{bmatrix} = \begin{bmatrix} A^* & C^* \\ B_f^* & D_2^* \end{bmatrix} + \begin{bmatrix} C^* \\ D_2^* \end{bmatrix} (-L^*) \begin{bmatrix} I_n & 0 \end{bmatrix} \\ &= \mathscr{A}_2 + \mathscr{B}_2(-L^*)\mathscr{C}_2, \\ \Theta_3 &= \begin{bmatrix} \Xi & 0 \\ 0 & \Pi \end{bmatrix} = \begin{bmatrix} -Q_2 & P_2+j\omega_c Q_2 & 0 & 0 \\ P_2 - j\omega_c Q_2 & -\omega_1\omega_2 Q_2 & 0 & 0 \\ 0 & 0 & -I_q & 0 \\ 0 & 0 & 0 & \gamma^2 I_s \end{bmatrix}. \end{aligned}$$

Then, we have that (6.60) can be represented as the standard form in Lemma 2.2, namely

$$N_2 \begin{bmatrix} -Q_2 & 0 & P_2E_\varepsilon + j\omega_c Q_2 E_\varepsilon & 0 \\ \star & -I_q & 0 & 0 \\ \star & \star & -\omega_1\omega_2 E_\varepsilon Q_2 E_\varepsilon & 0 \\ \star & \star & \star & \gamma^2 I_s \end{bmatrix} N_2^* < 0,$$

which can be converted into the feasible LMI as follows

$$\delta_2(\varepsilon) < 0, \tag{6.61}$$

where

$$\delta_2(\varepsilon) = \begin{bmatrix} -Q_{211} & -Q_{212} & 0 & P_{211} + j\omega_c Q_{211} & \varepsilon(P_{212} + j\omega_c Q_{212}) & 0 \\ \star & -Q_{222} & 0 & P_{212}^* + j\omega_c Q_{212}^* & P_{222} + \varepsilon j\omega_c Q_{222} & 0 \\ \star & \star & -I_q & 0 & 0 & 0 \\ \star & \star & \star & -\omega_1\omega_2 Q_{211} & -\varepsilon\omega_1\omega_2 Q_{212} & 0 \\ \star & \star & \star & \star & -\varepsilon^2\omega_1\omega_2 Q_{222} & 0 \\ \star & \star & \star & \star & \star & \gamma^2 I_s \end{bmatrix}$$
$$-\mathrm{He}\begin{bmatrix} -I_n & 0 & 0 \\ 0 & -I_q & 0 \\ A^* & C^* & C^* \\ B_f^* & D_2^* & D_2^* \end{bmatrix}\begin{bmatrix} W_2 R_m \\ V_{22} \\ \kappa_2 R_m \end{bmatrix}.$$

From Lemma 6.4, one can derive that (6.61) is set up for any $\varepsilon \in (0, \varepsilon^*]$, where $0 < \varepsilon^* \ll 1$, if and only if $\delta_2(0) < 0$, which gives

$$\begin{bmatrix} -Q_{211} & -Q_{212} & 0 & P_{211} + j\omega_c Q_{211} & 0 & 0 \\ \star & -Q_{222} & 0 & P_{212}^* + j\omega_c Q_{212}^* & P_{222} & 0 \\ \star & \star & -I_q & 0 & 0 & 0 \\ \star & \star & \star & -\omega_1\omega_2 Q_{211} & 0 & 0 \\ \star & \star & \star & \star & 0 & 0 \\ \star & \star & \star & \star & \star & \gamma^2 I_s \end{bmatrix}$$
$$< \mathrm{He}\begin{bmatrix} -I_n & 0 & 0 \\ 0 & -I_q & 0 \\ A^* & C^* & C^* \\ B_f^* & D_2^* & D_2^* \end{bmatrix}\begin{bmatrix} W_2 R_m \\ V_{22} \\ \kappa_2 R_m \end{bmatrix}. \tag{6.62}$$

This completes the proof.

Corollary 6.2 *If the error SPS (6.34) satisfies the system performance (6.36) for any $\varepsilon \in (0, \varepsilon^*]$ in the entire frequency range, where $0 < \varepsilon^* \ll 1$, then the following LMI is established:*

$$\begin{bmatrix} 0 & 0 & \mathscr{P}_2 & 0 \\ \star & -I_q & 0 & 0 \\ \star & \star & 0 & 0 \\ \star & \star & \star & \gamma^2 I_s \end{bmatrix} < \mathrm{He} \begin{bmatrix} -I_n & 0 & 0 \\ 0 & -I_q & 0 \\ A^* & C^* & C^* \\ B_f^* & D_2^* & D_2^* \end{bmatrix} \begin{bmatrix} W_2 R_m \\ V_{22} \\ \kappa_2 R_2 \end{bmatrix}, \tag{6.63}$$

where $\mathscr{P}_2 = \begin{bmatrix} P_{211} & 0 \\ P_{212}^* & P_{222} \end{bmatrix}$.

Proof It can be worked out along the same line as that in the proof of Corollary 6.1.

Finally, we demonstrate the usefulness of the results by developing a new algorithm that can stabilize the whole error dynamic system (6.34) and detect the occurrence of fault in presence of background disturbances. To design a well-conditioned FD observer (6.33) for the SPS (6.31) to achieve internal stability and constraints (6.35), (6.36) simultaneously. The noise-signal gain ratio J is utilized as performance index to stop the step-by-step process.

Algorithm 6.1 *Given system matrices* $A,\ B_w,\ B_u,\ B_f,\ C,\ D_1,\ D_2,\ D_3$ *and the desired noise-to-signal ratio* α. *Let* $\mu_1 \geqslant 0$ *and* $\mu_2 \geqslant 0$ *be sufficiently small parameters, which are the adjustable step-sizes. Set* $i = 0,\ j = 0$ *and* $m \in Z^+$.

Step 1. *Choose the initial performance indexes* $\beta,\ \gamma\ (\beta < J_{th} < \gamma)$ *and the required trade-off frequencies* $\omega_l,\ \omega_h,\ \omega_1,\ \omega_2$.

Step 2. *Main iterative steps:*
(i) *Solve (6.39), (6.45), (6.46) and (6.58) and get the feasible solutions* P_s, $P_1,\ Q_1,\ P_2,\ Q_2$ *and* L
(ii) *Put* $i = i + 1$. *With* P, Q *obtained in Step 2(a) and with*

$$\gamma = \gamma + \mu_1 > \|D_3\|,\ \beta = \beta - \mu_2 < \|D_2\|,\ J_i = \frac{\beta}{\gamma},$$

find a feasible L *for LMIs (6.39), (6.45), (6.46) and (6.58). Store* $L_i = L$ *and* J_i. *If a feasible solution cannot be found, then* $L_i = L_{i-1}$.
(iii) *If the performance* $J_i < \alpha$, *then a desired observer gain* $L = L_i$ *is found. Stop.*

Step 3. *Set* $j = j + 1$. *If* $j < p$, *repeat Step 2, else Stop (the feasible solution cannot be found).*

Example 6.4 Simulations were carried out on MATLAB® based on the LMI toolbox to test the efficacy of the proposed approaches. MATLAB provides a numerical computing platform to observe the theoretical validation of the algorithm. Consider the system in the form of SPS:

$$\begin{aligned} \dot{x}_1(t) &= x_1(t) + 2x_2(t) + w(t) + u(t) + 2f(t), \\ \varepsilon\dot{x}_2(t) &= x_1(t) + 5x_2(t) + 3w(t) + u(t) + 2f(t), \\ y(t) &= x_1(t) + x_2(t) + w(t) + u(t) + f(t). \end{aligned}$$

1. Generalized stability criterion:

Solving (6.39), $\hat{p} = 1$, $\hat{q} = 1$, the following feasible solutions is obtained to guarantee the internal stability property of all dynamics in the absence of background disturbances

$$W_s = \begin{bmatrix} -355.6168 & -34.7736 \\ -34.7736 & -61.9120 \end{bmatrix}, \; P_s = \begin{bmatrix} 708.8443 & 0 \\ 530.1923 & 285.8950 \end{bmatrix}.$$

It's noted that $P_{s11} = 708.8443 > 0$, which satisfies the stability constraint $P_{s11} > 0$. The corresponding robust FD observer gain matrix L is obtained as

$$L = \begin{bmatrix} 0.8666 \\ 8.8659 \end{bmatrix}.$$

From Fig. 6.8, both the slow and fast modes, originally radiating outward, reach the steady states with aid of the robust FD observer in the form of (6.33). From the frequency domain perspective, the poles in the s-plane are moved from the right half plane to the left half one to achieve the internal property of the whole system.

2. Disturbance attenuation ability:

Given $\beta = 0.4$, we set the trade-off frequencies as $\omega_l = 5$ rad/s and $\omega_h = 40$ rad/s according to the open-loop system frequency characteristic of the SPS. In other words, the SPS, itself, achieves active disturbance ability in the frequency band $\Lambda_m = [\omega_l, \omega_h]$. To solve the disturbance attenuation constraint (6.45) and (6.46) in the band-elimination region $\Lambda_n = \{\omega | \omega \in (0, \omega_l] \cup [\omega_h, +\infty)\}$, the feasible solutions

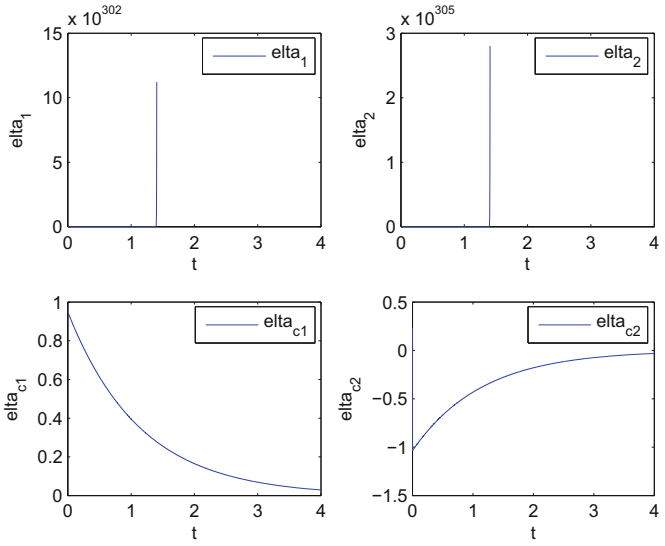

Fig. 6.8 The stabilization of the continuous-time SPS

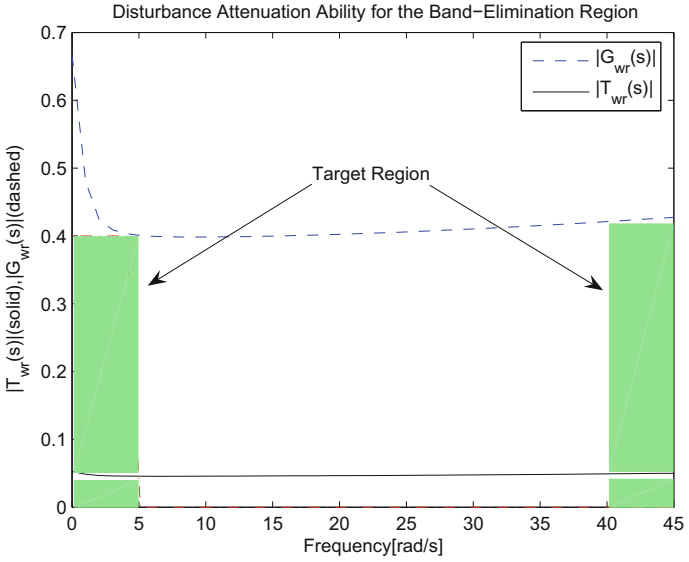

Fig. 6.9 The disturbance attenuation ability of the continuous-time SPS

are listed as follows:

$$W_1 = \begin{bmatrix} -3.3930 & 0.0970 \\ 0.0970 & -0.0115 \end{bmatrix}, P_1 = \begin{bmatrix} 0.2069 & 0 \\ -0.4053 & 0.3816 \end{bmatrix},$$
$$Q_1 = \begin{bmatrix} 0.0031 & -0.0095 \\ -0.0095 & 16.4503 \end{bmatrix} > 0,$$
$$V_{12} = \begin{bmatrix} -1.2930 & -0.1566 & -19.1343 & 3.0767 & 3.7886 & 2.8808 \end{bmatrix}.$$

It is obvious that the amplitude–frequency characteristic of the error dynamic system (6.34) is shown Fig. 6.9, where the colored parts represent the target region Λ_n. The amplitude of (6.34) in the required region Λ_n is restricted below β, so that the good disturbance attenuation ability is achieved in the entire frequency range. This method is particularly suitable for SPSs due to the unique frequency nature, that is active disturbance attenuation ability in the middle frequency range. The disturbance attenuation ability is satisfied originally outside the target region Λ_n. Through solving the finite frequency constraints (6.45) and (6.46), the disturbance attenuation ability can be realized in the full-frequency spectrum which reduces the conservatism.

Remark 6.10 Based on the unique frequency nature of SPS, finite frequency system specifications can lead to the establishment of entire-frequency ones, which have some theory basis. The trade-off frequencies ω_l, ω_h, characterizing the target frequency Λ_n, are also the start point and end point of the region Λ_m. In the band-elimination region Λ_n, the disturbance attenuation constraint is guaranteed. Considering the continuity of the amplitude–frequency characteristic curve from the

disturbance $w(t)$ to the residual output $r(t)$, the disturbance attenuation constraint in Λ_m can be guaranteed to a certain extent by the start point ω_l and the end point ω_h.

3. Fault sensitivity ability:

The frequency characteristics of the fault signal, imposed artificially, is known beforehand, which are the foundation of the values of ω_l, ω_h. It is assumed that the general frequency range of faults are set as $\Lambda_f = \{\omega|\omega \in [80 \text{ rad/s}, 100 \text{ rad/s}]\}$ by engineers. Given the worst fault-sensitivity index $\gamma = 1.5$ and trade-off frequencies $\omega_1 = 80$ rad/s, $\omega_2 = 100$ rad/s, we get the following feasible solutions by solving (6.58):

$$W_2 = \begin{bmatrix} 21.3246 & 0.9399 \\ 0.9399 & 0.1613 \end{bmatrix}, \quad P_2 = \begin{bmatrix} 9.5369 & 0 \\ -0.7965 & -0.0206 \end{bmatrix},$$
$$Q_1 = \begin{bmatrix} 0.2399 & -0.0465 \\ -0.0465 & 272.0003 \end{bmatrix} > 0,$$
$$V_{22} = \begin{bmatrix} 130.1518 & 22.7187 & -79.9690 & -211.7720 & 13.8318 & 63.7811 \end{bmatrix}.$$

From Fig. 6.10, the amplitude of the frequency response from the fault input $f(t)$ to the residual output $r(t)$ in Λ_f is adjusted larger than the index γ with aid of FD observer, in which the colored region is used to represent Λ_f.

Solving (6.39), (6.45), (6.46), (6.58) simultaneously based on Algorithm 6.1, the observer gain matrix is calculated

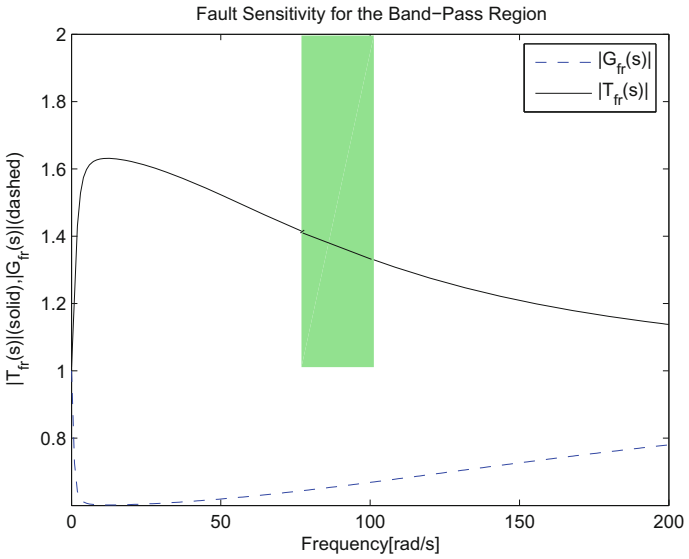

Fig. 6.10 The fault sensitivity of the continuous-time SPS

$$L = \begin{bmatrix} 5.3097 \\ 4.6047 \end{bmatrix},$$

where the threshold is chosen as $J_{th} = 1$.

In order to further explain the effectiveness of our results, we have conducted a series of time-domain simulations. To analyze the effects of faults and disturbances on the residual of detection observer simultaneously, we consider the faults as

$$f(t) : \begin{cases} = 1, \ t > 0.5 \text{ s}, \\ = 0, \ 0 < t < 0.5 \text{ s}. \end{cases}$$

The disturbances are selected as sinusoidal signals: $w_1(t) = 0.8\sin(t)$ (low-frequency noises) and $w_2(t) = \sin(400t)$ (high-frequency noises). The corresponding residual outputs in presence of both fault signals and external disturbances are demonstrated in Figs. 6.11 and 6.12. It is obvious that fault features can be extracted from disturbances. In addition, residual outputs can trace the desired faults accurately with fast response rate. To better alarm when the faults occur, the threshold $J_t h = 1$ is adopted to detect the occurrence of faults by comparing the residual evaluation with the threshold. From Fig. 6.13, it can be found that the fault can easily be detected at the point $t = 0.5$ s. To demonstrate the superiority of our method, it is apparent that the finite frequency approaches achieve better performance in Fig. 6.14, where the dot-dash line denotes the residual output of the finite frequency approach and the solid line denotes the residual output of the full frequency one.

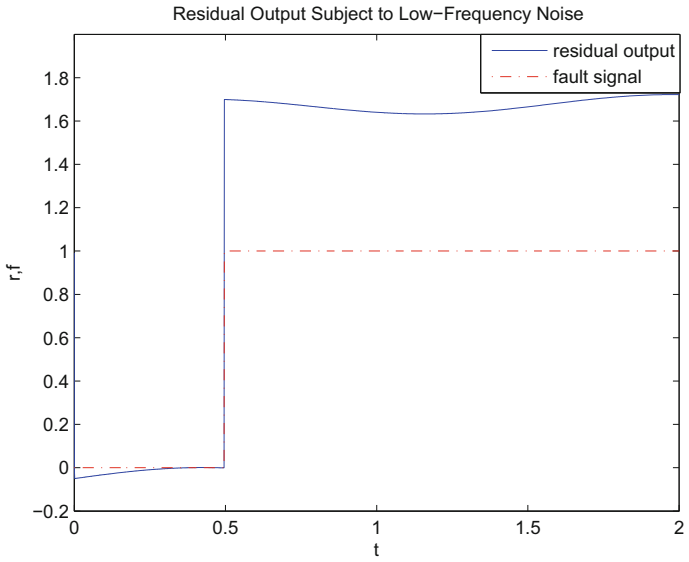

Fig. 6.11 The residual output subject to the low-frequency noise

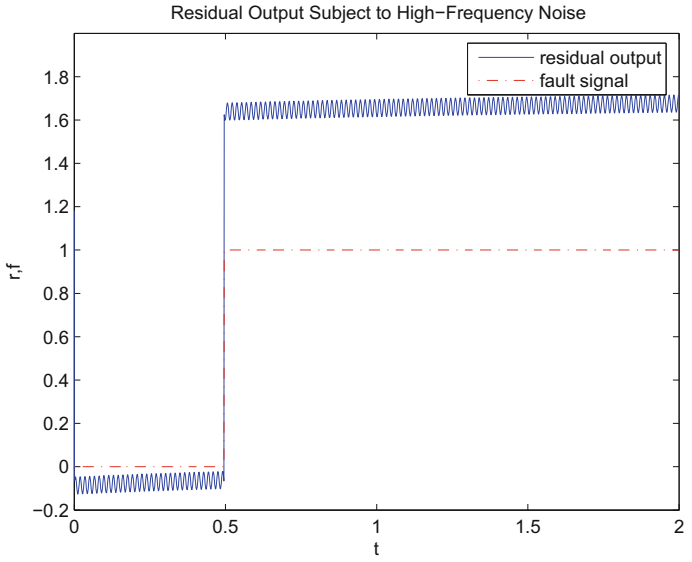

Fig. 6.12 The residual output subject to the high-frequency noise

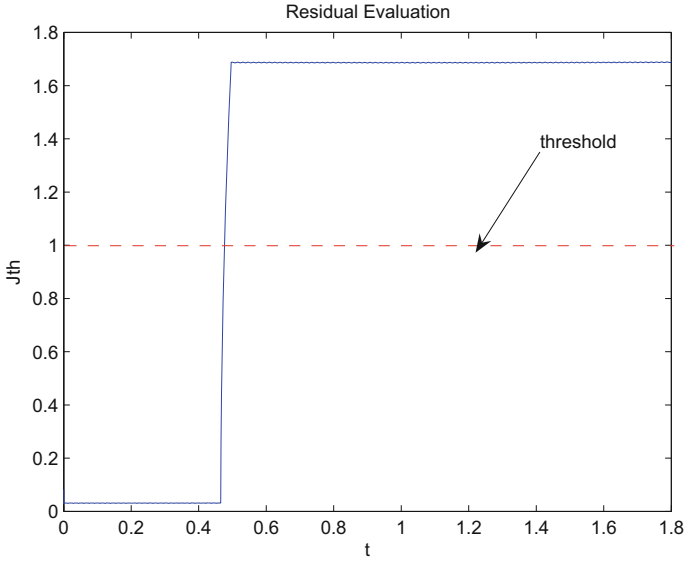

Fig. 6.13 Residual evaluation

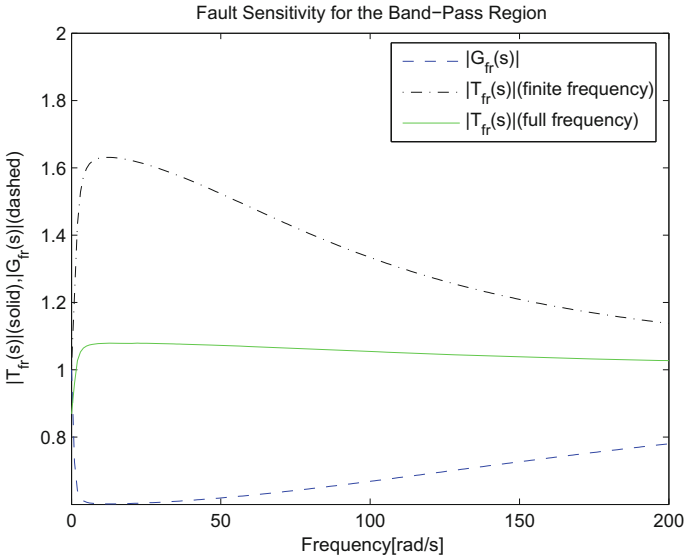

Fig. 6.14 Comparison between the finite frequency approaches and the full frequency approaches

Remark 6.11 It is apparent that finite frequency approaches usually have less conservatism than the full frequency ones because the constraints should only be kept in the specified frequency ranges. By employing finite frequency approaches, the smaller β and larger γ can be designed a well-conditioned FD observer.

6.5 Conclusion

To sum up, we have developed new methodologies in this section for synthesizing a robust FD observer to achieve $H_\infty/H\_$ performance in the finite frequency ranges. Sufficient conditions for the existence of the feasible robust FD observers are presented in terms of LMIs via the existing results from the singular systems. A literature LMI design procedure is proposed to optimize the noise-signal ratio in this paper. From the numerical examples, our design methods are seen to be more applicable and less conservable.

References

1. Chao, A., Athans, M.: Stability robustness to unstructured uncertainty for linear time invariant systems. In: Levine, W.S. (ed.) The Control Handbook. CRC Press and IEEE Press, Boca Raton (1996)

2. Chen, C.X., Wang, X.J., Niu, D.Z., Ren, X.Y., Qu, K.: A hierarchical fault detection method based on IS-SVM in integrated navigation system. Sens. Transducers **175**(7), 111–116 (2014)
3. Dahleh, M.A.: L_1 Robust control: theory, computation and design. In: Levine, W.S. (ed.) The Control Handbook. CRC Press and IEEE Press, Boca Raton (1996)
4. Doyle, J.C., Francis, B.A., Tannenbaum, A.R.: Feedback Control Theory. MacMillan Publishing Co, New York (1992)
5. Glielmo, L., Corless, M.: On output feedback control of singularly perturbed systems. Appl. Math. Comput. **217**(3), 1053–1070 (2010)
6. Hara, S., Iwasaki, T., Shiokata, D.: Robust PID control using generalized KYP synthesis: direct open-loop shaping in multiple frequency ranges. IEEE Control Syst. **26**(1), 80–91 (2006)
7. Huang, Y., Cai, C., Zou, Y.: Finite frequency positive real control for singularly perturbed systems. Int. J. Control Autom. Syst. **9**(2), 376–383 (2011)
8. Iwasaki, T., Hara, S.: Generalized KYP lemma: unified frequency domain inequalities with design applications. IEEE Trans. Autom. Control **50**(1), 41–59 (2005)
9. Iwasaki, T., Hara, S., Fradkov, A.L.: Time domain interpretations of frequency domain inequalities on (semi) finite ranges. Syst. Control Lett. **57**(7), 681–691 (2005)
10. Khail, H.K., Chen, F.C.: H_∞ control of two-time-scale systems. Proc. Am. Control Conf. **19**, 35–42 (1992)
11. Li, T., Zhang, Y.: Fault detection and diagnosis for stochastic systems via output PDFs. J. Frankl. Inst. **384**(6), 1140–1152 (2011)
12. Luse, D.W., Ball, J.A.: Frequency-scale decomposition of H_∞ disk problems. SIAM J. Control Optim. **27**(4), 814–835 (1989)
13. Mei, P., Cai, C., Zou, Y.: Robust fuzzy control of nonlinear singularly perturbed systems with parametric uncertainties. Int. J. Innov. Comput. **4**(8), 2079–2086 (2008)
14. Mei, P., Cai, C., Zou, Y.: A generalized KYP lemma based approach for H_∞ control of singularly perturbed systems. Circuits Syst. Signal Process. **28**(6), 945–957 (2009)
15. Oloomi, H.M., Sawan, M.E.: Suboptimal model-matching problem for two frequency scale transfer functions. In: Proceedings of the American Control Conference, pp. 2190–2191, Pittsburgh, PA (1989)
16. Pan, Z., Basar, T.: H_∞ optimal control for singularly perturbed systems Part I: Perfect state measurements. IEEE Trans. Autom. Control **29**(2), 401–423 (1993)
17. Pan, Z., Basar, T.: H_∞ optimal control for singularly perturbed systems Part II: Imperfect state measurements. IEEE Trans. Autom. Control **39**(2), 280–299 (1994)
18. Rantzer, A.: On the Kalman-Yakubovich-Popov lemma. Syst. Control Lett. **28**(1), 7–10 (1996)
19. Sun, W., Khargonekar, P.P., Shim, D.: Robust control synthesis with general frequency domain specifications: static gain feedback case. Proc. Am. Control Conf. **5**, 4613–4618 (2004)
20. Tan, W., Leung, T., Tu, Q.: H_∞ control for singularly perturbed systems. Automatica **34**(2), 255–260 (1998)
21. Willems, J.C.: Least squares stationary optimal control and the algebraic Riccati equation. IEEE Trans. Autom. Control AC **16**(6), 621–634 (1971)
22. Zhang, J., Lyu, M., Karimi, H.R., Zuo, J., Bo, Y.: Fault detection for network control systems with multiple communication delays and stochastic missing measurements. Math. Probl. Eng. Article ID 690461, 1–9 (2014)
23. Zhou, K., Doyle, J., Glover, K.: Robust and optimal control. Prentice-Hall, Upper Saddle River (1996)

Part III
Applications

In this part, the engineering backgrounds and the applications for finite frequency control of SPSs are introduced. It includes aerospace, machinery, electronic and electrical, chemical kinetics problem, biology and so on. The wind turbines model is set up using the slow-fast decomposition method and the corresponding controller is researched using linear parameter varying SPM. Another typical application is robust H_∞ control of miniature quadrotors in hovering given to show the effectiveness and merits of our methods from practical point of view.

Chapter 7
Applications

7.1 Background of Applications of Singular Perturbation Methods

7.1.1 Applications of Singular Perturbation Methods in Aerospace

The theory of SPM originated from fluid dynamics and applied widely in the area of aerospace systems [110]. In [134], a design method was proposed for the manual flight control system corresponding to the lateral motion of the aircraft based on SPaTSs. In [108], genetic algorithm was used to minimize the flight time using SPMs, and the optimal flight guidance law was obtained.

In [125], SPM was used to design a reduced-order controller with high accuracy for two-time-scale aircraft dynamics systems. Diagnosis and modelling were considered for multiple time-scale nonlinear flight mechanics in [87]. In [49], an aircraft Auxiliary Power Unit turbine system was modelled as an SPS. The least-square optimal estimation of the fault parameter vector was obtained, and a finite impulse response differentiator was designed for the system.

SPMs were utilized to separate the nonlinear model of super manoeuverable aircraft into slow and fast subsystems, and dynamic inversion was applied to design the control laws [155]. A singular perturbation control strategy was proposed for regulating the longitudinal flight dynamics of an unmanned air vehicle based on the four-time-scale decomposition in [36].

In [12], considering a class of nonlinear systems actuated by actuators whose actuator dynamics were assumed to be fast, baseline controller was designed, and SPM was applied to prove that the closed loop system achieved the control objective.

A postbuckling analysis was presented for nano-composite cylindrical shells reinforced by single-walled carbon nano-tubes subjected to combined axial and radial mechanical loads in thermal environment in [124], and a boundary layer theory and

C. Cai et al., *Finite Frequency Analysis and Synthesis for Singularly Perturbed Systems*, Studies in Systems, Decision and Control 78,
DOI 10.1007/978-3-319-45405-4_7

associated singular perturbation technique were employed to determine the buckling loads and postbuckling equilibrium paths.

A singular perturbation-like approach was proposed in [54] to compensate the effects of fin-actuator dynamics in the nonlinear missile system. SPT was applied to obtain a two-loop mathematical model of a nonlinear multivariate model of air-to-air missile in [34] and to obtain a near-optimal midcourse guidance law for medium-range air-to-air missile in [109].

7.1.2 Applications of Singular Perturbation Methods in Mechanical Systems

Another interesting area of the application of SPM was mechanical dynamics and control. For a multi-link flexible robot with uncertainties, an improved composite controller was designed based on singular perturbation theory in [26]. In [120], a new control strategy for flexible-joint manipulators with joint friction was proposed. The proposed controller includes two main components: a friction compensating torque and a composite controller torque which was designed using SPM.

A finite-dimensional model of a flexible arm was presented in [80] with its approximate representation through the slow and fast decomposition, and a combined PD-H_∞ control strategy was developed. See [18, 27, 28, 32, 33, 102, 104, 123, 135, 136, 138, 141] for more results about applications of SPaTSs technique to flexible robots.

In [86], a group of robotic systems were modelled as two coupled systems represented by dynamics of the centre of mass and dynamics of the formation. Using high gain feedback, asymptotic decoupling was gained and singular perturbation analysis was studied. Velocity field control of uncertain robotic manipulators was studied in [21]. Based on modelling error compensation ideas and singular perturbation theory, a PI-type controller was drived which guaranteed the closed-loop was semi-global practical stable, namely "given any compact set of initial velocity field errors, there exist PI control gains which guarantee that the robot tracks a desired velocity field with arbitrary accuracy".

It was considered walking system of a power transmission line inspection robot in [145]. The closed-loop systems was devided into fast and slow subsystems using SPM and a composite controller was designed that contains an adaptive PD controller applied to slow subsystem and optimal controller applied to fast subsystem. In [31], closed kinematic chains (CKC) were modelled as DAEs which are transferred to SPSs and the properties of singular perturbation model were analyzed. The validity domain and the error characterization of the singular perturbation formulation of CKC were presented compared with the DAEs model in [150]. In [146], conditions of locally asymptotically stability were derived based on the SPM.

In [38], results on partial stability of differential form of speed-gradient control for SPS were generalized to the case of speed-gradient control in finite form. A new

wave-net controller was designed based on SPM for the bilateral teleoperation of robots through the internet in [46]. According to SPTs, direct torque control (DTC) was derived in [129] and a link between DTC and feedback linearization was presented. An explicit relationship between DTC performance and machine characteristics has been revealed, which can used to improve DTC performance by designing an induction motor.

In [147], the singular perturbation formulation was compared to control based on input-output linearization. Their advantages and disadvantages of each method are described. Travelling wave solutions of viscous conservation laws were studied in [1]. The eigenvalue problem corresponding to the linearization around a viscous shock wave were viewed as a singularly perturbed problem, and geometric singular perturbation theory was used for the analysis of the Evans function. And the Gardnerand Zumbrun result about the first derivative of the Evans function were proved at the origin.

A new coming correction algorithm, basing on the SPTs, was proposed for the attitude update computation with non-ideal angular rate information [43]. Singular perturbation theory was applied to show that the Boltzmann-Enskog equation results in the Navier-Stokes equation for incompressible fluids together with two different Boussinesq relations and temperature fluctuation equations in [58] and the proof of a rigorous result was given in [59].

In addition to the above applications, singular perturbation theory was also applied to air-conditioning systems [111], an axially moving cable with large sag [115], a four-wheeled steering and four-wheeled drive vehicle [106], early detection systems with multiple-bottleneck links [150], harmonic drive systems [45], pneumatic vibration isolators [50], the voice coil motor [103], hypersonic vehicles [92], hydraulic systems, a flexible beam used in underwater exploration [93], infinite-dimensional mechanics of fluids and plasmas [160], dual-loop exhaust gas recirculation air-path systems [158], underactuated biped robots [29], hydrostatic drive or cylinder [84], single-axis rate gyro [24], bimolecular association mechanism [39], 2D thermal convection loop [142], and so on.

7.1.3 Applications of Singularly Perturbed Methods in Electrical and Electronic Circuits Systems

Neglecting dynamic saliency in synchronous machines of power systems is a common simplified way [83]. This section [23] is a summary to explain how to model power systems using SPM through neglecting the fast dynamics to obtain a simplified power system model. The error associated with neglecting dynamic saliency was eliminated by inserting a singularly perturbed term into the machine model [105]. In [130, 140], SPM was used to synchronous generator systems to study free-chattering composite control and sliding mode control. In [73], a doubly-fed induction generator was considered to design a controller based on multi-time-scale theory. In [131, 132],

sliding mode control and variable structure control were applied to synchronous generator systems based on singular perturbation theory.

For singularly perturbed relay systems [40, 41], a theorem about existence and stability of the periodic solutions was proved and an algorithm of asymptotic representation for this periodic solutions was presented using boundary layer method. Forced singular perturbations were proposed to reduce computations of mutilate strapdown terrestrial navigation algorithm in [144]. The transmission problem was studied for the system of piezoelectricity having piecewise constant coefficients in [63].

For a class of direct-current-direct-current (DC-DC) power converters, current-mode control problem was studied in [2]. Singular perturbation was used to separate the fast and slow states of DC-DC converters systems in [68], and a relationship between inductance, capacitance, load resistance and loss resistances was obtained from analysis of an approximate model. Compared with [68], discrete-time analysis was added in [69].

For a wind power system, a fifth-order precise model was obtained using segmentation method in [42]. The art wind power generators systems were modelled in [119], and SPM was used to simplify the differential equations. Considering the wind energy conversion systems in [113], a novel control structure was introduced to explore the delivered power as a control input. The new structure was based on the two reduced subsystems obtained by singular perturbation theory. Papers such as [96, 97] studied the singular perturbation analysis and synthesis of wind energy conversion systems. Singular perturbation theory was used to analyzed wind energy conversion systems in [60], and then time-scale method and model predictive control (MPC) were combined to control wind energy conversion systems in [161].

For servomotor systems [163], a general line voltage controller controller was taken into the original system, and then the closed loop system was decomposed to two subsystems using SPaTSs to represent the position control loop and the high frequency dynamics, respectively. Singular perturbation theory was used to design an observer of sliding mode type for the flux estimation of an induction machine in [139]. In order to provide insight into the connections between the different nodes of a power network, a method based on differential geometric control theory was obtained in [5]. In [53], circuit-averaging techniques were applied to simplify a lumped-parameter model of the cardiovascular system.

Considering the non-coherent digital delay lock loops on chip timing synchronization in [51], the mean time to lose lock was calculated using diffusion approximation and SPMs. Loop bandwidth was optimized for the first order loop. The stability of a large-scale power system was analyzed by Jacobian analysis based on singular perturbation in [154]. Considering the converter-interfaced wind turbines in [114], singular perturbation theory was used to decompose the system dynamics based on which a controller was designed to isolate wind-power fluctuations from the power grid.

In [148], a singularly perturbed model was developed for additive increase and multiplicative decrease/random early detection systems with multiple bottlenecks and feedback delays, and then stability was analyzed. The delay-dependent LMIs

conditions for the stability were established, and sufficiently small parameters were selected to guarantee the asymptotic stability of the system.

In [85], SPTs were applied to the permanent magnet synchronous machine system. Based on the decoupled subsystems, the control speed and the I_d current were carried out by neuro-fuzzy regulators. Based on the combination of permanent-magnet synchronous generator and super sparse matrix converter, a novel variable-speed wind energy generation scheme was developed in [159]. Emitter-coupled multivibrators were modelled and analyzed using the singular perturbation theory in [107]. A sampled-data strategy for a boundary control problem of a heat conduction system modelled as partial differential equation was developed in [25]. Using singular perturbation theory, the reduced subsystems are presented.

Considering the power system model in [77], SPM was used to decompose the system into slow and fast subsystems and the relationship between the stability of reduced-order system and original system was analyzed. In [156], a class of power systems with detailed excitation and power system stabilizer controller was modelled as an SPS. A LMI-based approach was developed to estimate the stability region. Considering multi-machine power systems with matched additive uncertainty and input multiplicative uncertainty in [22], several time-scale separation designs were used for robust stabilization and performance recovery.

A complementary controller was designed to improve power systems stability in [137] based on singular perturbation theory. Considering an oscillator model which was composed of a fast membrane potential dynamics and a slow recovery dynamics in [95], phase response curves for both the dynamics and plausibility of feedback inputs to the slow dynamics rather than the fast dynamics were shown using singular perturbation theory.

7.1.4 Applications of Singular Perturbation Methods in Chemical Reactions and Reactors

Two different reducing order methods were compared to singularly perturbed form for chemical kinetics equations in [62]. An SPM was applied for model reduction of stiff chemical Langevin equations and chemical kinetics problems in [30, 72]. Global Quasi-Linearization method which was based on TTS theory was presented for an automatic reduction of chemical kinetics models in [15]. Equations for the description of chemical reactions of dissociation and recombination were transformed into singularly perturbed equations in [44]. A new concept of critical simplification for chemical kinetics was proposed which was valid in the presence of a dominant competitive reaction and critical phenomena in [157].

An SPM was used to analyzed and synthesize the model of thermal explosion in a gas-droplets mixture [14], and a chemical reactor and a feed effluent heat exchanger in [61]. Viewing the prompt jump approximation nuclear reactor dynamics as

the zeroth-order approximation of an asymptotic expansion to SPSs of ordinary differential equations, [6] derived the equations describing its first-order approximation.

Two-point linear controllers for binary distillation columns were designed based on singular perturbation theory in [19]. Considering a singularly perturbed convection-diffusion equation with constant coefficients in a half plane, with Dirichlet boundary conditions [66], precise pointwise bounds for the derivatives of the solution were obtained.

7.1.5 Applications of Singular Perturbation Methods in Biology

Models describing the biotechnical process behaviour were usually high order, nonlinear with time-varying parameters. In [64], decomposition techniques based on singular perturbation analysis or batch phase analysis were used to simplify the model.

Considering a host-vector model for a disease without immunity in [118], the stability of the steady states using the contracting-convex-sets technique was studied using the geometric singular perturbation method, and the existence of travelling wavesolutions was established.

The work of [162] revealed that travelling wave solutions existed for a modified vector-disease model using the geometric singular perturbation theory. Models that incorporated local and individual interactions were introduced in [128], in addition, epidemiological time-scales were used to reduce the dimensionality of the model and SPMs were used to corroborate the results of time-scale approximations.

In [112] a mathematical model was proposed for the differentiation of osteoblastic and osteoclastic populations in bone, and singular perturbation theory was used to analyze the highly diversified dynamics. Considering the model describing the growth of microalgae, the authors of [20] maximized the specific growth rate of microalgae by manipulating the irradiance using singular perturbation theory.

The topic of [122] focused on the analysis of a nonlinear dynamical model of a class of bioprocesses in order to obtain reduced order models, and SPMs and quasi-steady state assumption were used.

A novel ion channel biosensor was modelled in [90], and singular perturbation theory was used to designed an optimal input voltage to the biosensor to minimize the covariance of the estimation error.

A mechanism was proposed in bio-molecular systems to attenuate retroactivity in [**?**]. By coordinating transforms and singular perturbation theory, retroactivity can be arbitrarily attenuated by internal system gains.

In [71], the model was analyzed to predict the performance of the biosensor in transient and steady-state regimes. Singular perturbation was used to determine the conditions for globally uniformly stability of a class of biological networks with different time-scales under parameter perturbations in [89].

Based on singular perturbation theory, dynamical system theory and DAEs, a mathematical framework was developed to analyze and design on-line schemes for fixed point recur-rent neural learning in [116].

7.1.6 *Applications of Singular Perturbation Methods in Other Areas*

In [127], the moisture-induced deformation in an elastic panel was modelled as SPSs. Compared with experimental results, the solution was analyzed based on the material of the elastic panel. Optimal climate control problem was studied for a potato storage facility to exploit the favourable weather conditions in [65].

A upper bound for the fast time-scale was derived. Using SPM and based on Fenichel's theorems, extensions of Hirsch's generic convergence theorem for monotone systems were studied in [149]. Considering a large-scale nonlinear network system, singular perturbation was used to decompose the states into fast and slow subsystems in [9, 10], and the validity of the reduced-model approximation was proved on the infinite time interval.

Notion of TTS distributions was introduced [101] and TTS distribution was analyzed in two different time-scales. Singular perturbation was applied to choose the PageRank factor in a bow-tie web graph [3]. Boundary value theory was applied to analyze the gravitational-tidal evolution of planetary subsystems in [11]. The topic of [4] was about the spectral properties of the Neumann-Laplacian on the singularly perturbed periodic quasi-cylinder. Singular perturbation theory was used to analyze the global asymptotic stability of positive equilibria of ratio-dependent predator-prey models with stage structure for the prey in [100].

In [47], singular perturbation theory was applied to analyzed the quadratic family with multiple poles. The author of [117] analyzed the stokes flow in a singularly perturbed exterior domain. Considering static and dynamic behaviour of two-dimensional droplets in [121], an evolution equation for the droplet thickness was obtained using singular perturbation theory. In [133], "vorticity distributions over the diffracted shock both from Lighthill's theory applicable for small bends and Sakurai and Takayama's theory applicable for larger bends have been investigated for Mach numbers 1.80 and 1.95" using singular perturbation theory.

7.2 Wind Turbines Control Using Linear Parameter Varying Singularly Perturbed Model

The rotor speed tracking problem of variable-speed wind turbine systems operating below rated wind speed is studied in this section. A linear parameter varying (LPV) model is used to approximate the nonlinear SPM. Following, stability and robust

properties of the open-loop linear SPS are analyzed using LMI and LPV. An algorithm to design a stabilizing state feedback controller is proposed, which can guarantee the robust property of the closed-loop system.

In this section, the mathematical model of wind turbine systems with permanent magnet synchronous generators is developed. Note that the electrical part of the system changes much faster than the mechanical part, namely, the states of the wind energy conversion systems have two different time-scales. Based on the TTS property of wind turbine systems, stretching transformation is used to obtain the singularly perturbed nonlinear model. LPV techniques are then used to linearize the singularly perturbed nonlinear system.

Our consideration is focused on partial load, which is the optimal tip-speed ratio of the wind rotor speed with respect to the wind speed changing. For this control purpose, all the concluding aerodynamics, drive train dynamics, and generator dynamics are considered.

Commonly, the aerodynamic torque T_r is given as follows [126, 151]:

$$T_r = \frac{1}{2}\rho\pi R^3 C_Q(\lambda) V^2, \tag{7.1}$$

where ρ is the air density, V is the wind speed, and R is the radius of the wind rotor plane. Power coefficient $C_Q(\lambda)$ is approximated by a second-order polynomial of tip-speed ratio λ [8],

$$C_Q(\lambda) = C_{Q\max} - k_Q(\lambda - \lambda_{Q\max})^2, \tag{7.2}$$

where $C_{Q\max}$ is the maximum power coefficient, $\lambda_{Q\max}$ is the optimal tip-speed ratio corresponding to $C_{Q\max}$, and λ is defined by

$$\lambda = \frac{\omega_r R}{V}, \tag{7.3}$$

with ω_r as the wind rotor speed.

The drive train block has the model as below [91, 99]:

$$\dot{\omega}_r = -\frac{i}{\eta J_r} T_H + \frac{1}{J_r} T_r, \tag{7.4}$$

$$\dot{\omega}_g = \frac{1}{J_g} T_H - \frac{1}{J_g} T_g, \tag{7.5}$$

$$\dot{T}_H = iK_g\omega_r - K_g\omega_g - B_g\left(\frac{1}{J_g} + \frac{i^2}{\eta J_r}\right) T_H + \frac{iB_g}{J_r} T_r + \frac{B_g}{J_g} T_g, \tag{7.6}$$

where ω_g is the generator speed, T_H is the internal torque, J_r is the wind rotor inertia, J_g is the generator inertia, K_g is the stiffness coefficient of the high-speed shaft (the generator shaft), B_g is the damping coefficient of the high-speed shaft (the generator shaft), i is the gearbox ratio, and η is the gearbox efficiency.

Then, the generator dynamics are modelled as follows [99, 151]:

$$\dot{i}_d = -\frac{R_s}{L_d} i_d + \frac{pL_q}{L_d} i_q \omega_g - \frac{1}{L_d} u_d, \tag{7.7}$$

$$\dot{i}_q = -\frac{R_s}{L_q} i_q - \frac{p}{L_q}(L_d i_d - \phi_m)\omega_g - \frac{1}{L_q} u_q, \tag{7.8}$$

$$T_g = p\phi_m i_q$$

where T_g is the generator electromagnetic torque, i_d, L_d, u_d and i_q, L_q, u_q are the d and q components of the stator current, inductance, voltage, respectively, R_s is the stator resistance, p is the number of pole pairs, and ϕ_m is the flux. Combining (7.4)–(7.8), the complete nonlinear model of the wind energy conversion system is obtained.

Considering the order of magnitude of L_d and L_q, we select the singular perturbation parameter as $\varepsilon = 1 \times 10^{-2}$, and obtain:

$$\varepsilon \dot{i}_d = -\frac{R_s}{\overline{L}_d} i_d + \frac{pL_q}{\overline{L}_d} i_q \omega_g - \frac{1}{\overline{L}_d} u_d, \tag{7.9}$$

$$\varepsilon \dot{i}_q = -\frac{R_s}{\overline{L}_q} i_q - \frac{p}{L_q}(L_d i_d - \phi_m)\omega_g - \frac{1}{\overline{L}_q} u_q, \tag{7.10}$$

where $\overline{L}_d = L_d \times 10^2$ and $\overline{L}_q = L_q \times 10^2$. Then, the singularly perturbed nonlinear system is obtained by uniting (7.4)–(7.6) and (7.9)–(7.10).

Now we are ready to derive the linear model using LPV method. Choose an operating point $\theta_1 = [\hat{\omega}_r \ \hat{V} \ \hat{\omega}_g \ \hat{i}_d \ \hat{i}_q]^T$, and linearize the nonlinear parts in the singularly perturbed nonlinear system at point θ_1:

$$T_r(\lambda, V) - T_r(\hat{\lambda}, \hat{V}) = -B_r(\theta_1)\delta\omega_r + K_{rv}(\theta_1)\delta V, \tag{7.11}$$

$$\omega_g i_q - \hat{\omega}_g \hat{i}_q = B_{gq}(\theta_1)\delta i_q + B_{qg}(\theta_1)\delta\omega_g, \tag{7.12}$$

$$\omega_g i_d - \hat{\omega}_g \hat{i}_d = B_{gd}(\theta_1)\delta i_d + B_{dg}(\theta_1)\delta\omega_g, \tag{7.13}$$

where

$$\delta\omega_r = \omega_r - \hat{\omega}_r, \ \delta V = V - \hat{V}, \ \delta i_q = i_q - \hat{i}_q,$$

$$\delta i_d = i_d - \hat{i}_d, \ \delta\omega_g = \omega_g - \hat{\omega}_g, \ \hat{\lambda} = R\hat{\omega}_r / \hat{V},$$

$$B_r(\theta_1) = -\frac{\partial T_r}{\partial \omega_r}\Big|_{(\hat{\omega}_r, \hat{V})} = -\frac{T_r(\hat{\lambda}, \hat{V})}{\hat{\omega}_r} \frac{\partial C_Q/\partial\lambda}{C_Q/\lambda}\Big|_{(\hat{\lambda}, \hat{V})}$$

$$= \rho\pi R^4 k_Q \big(R\hat{\omega}_r - \lambda_{Q\max}\hat{V}\big), \tag{7.14}$$

$$
\begin{aligned}
K_{rv}(\theta_1) &= \frac{\partial T_r}{\partial V}\,|_{(\hat{\omega}_r,\hat{V})} = \frac{T_r(\hat{\lambda},\hat{V})}{\hat{V}}\Big(2-\frac{\partial C_Q/\partial\lambda}{C_Q/\lambda}\Big|_{(\hat{\lambda},\hat{V})}\Big)\\
&= \rho\pi R^4 k_Q\Big(R\hat{\omega}_r-(1-\frac{C_{Q\max}}{k_Q\lambda_{Q\max}^2})\lambda_{Q\max}\hat{V}\Big),\qquad (7.15)\\
B_{gq}(\theta_1) &= \hat{\omega}_g,\ B_{qg}(\theta_1)=\hat{i}_q,\ B_{gd}(\theta_1)=\hat{\omega}_g,\ B_{dg}(\theta_1)=\hat{i}_d.
\end{aligned}
$$

Substituting (7.11)–(7.13) into (7.4)–(7.6) and (7.9)–(7.10) yields the following singularly perturbed linear system at the operating point θ_1:

$$
\begin{bmatrix}\dot{\delta}\omega_r\\ \dot{\delta}\omega_g\\ \dot{\delta}T_H\\ \varepsilon\dot{\delta}i_d\\ \varepsilon\dot{\delta}i_q\end{bmatrix}=A(\theta_1)\begin{bmatrix}\delta\omega_r\\ \delta\omega_g\\ \delta T_H\\ \delta i_d\\ \delta i_q\end{bmatrix}+B(\theta_1)\begin{bmatrix}\delta V\\ \delta u_d\\ \delta u_q\end{bmatrix},\qquad (7.16)
$$

where

$$
A(\theta_1)=\begin{bmatrix}
-\frac{B_r(\theta_1)}{J_r} & 0 & -\frac{i}{\eta J_r} & 0 & 0\\
0 & 0 & \frac{1}{J_g} & 0 & -\frac{1}{J_g}P\phi_m\\
iK_g-\frac{iB_gB_r(\theta_1)}{J_r} & -K_g & -B_g\big(\frac{1}{J_g}+\frac{i^2}{\eta J_r}\big) & 0 & \frac{B_g}{J_g}P\phi_m\\
0 & \frac{PL_q}{L_d}B_{qg}(\theta_1) & 0 & -\frac{R_s}{L_d} & \frac{PL_q}{L_d}B_{gq}(\theta_1)\\
0 & \frac{P}{L_q}(\phi_m-L_dB_{dg}(\theta_1)) & 0 & -\frac{P}{L_q}L_dB_{gd}(\theta_1) & -\frac{R_s}{L_q}
\end{bmatrix},
$$

$$
B(\theta_1)=\begin{bmatrix}
\frac{1}{J_r}K_{rv}(\theta_1) & 0 & 0\\
0 & 0 & 0\\
\frac{iB_gK_{rv}(\theta_1)}{J_r} & 0 & 0\\
0 & -\frac{1}{L_d} & 0\\
0 & 0 & -\frac{1}{L_q}
\end{bmatrix}.
$$

Furthermore, denoting $x=[\delta\omega_r\ \ \delta\omega_g\ \ \delta T_H]^T$, $z=[\delta i_d\ \ \delta i_q]^T$ and $u=[\delta u_d\ \ \delta u_q]^T$, rewrite (7.16) as

$$
\begin{aligned}
E_\varepsilon\begin{bmatrix}\dot{x}\\ \dot{z}\end{bmatrix} &= A(\theta_1)\begin{bmatrix}x\\ z\end{bmatrix}+B(\theta_1)\begin{bmatrix}\delta V(t)\\ \delta u_d\\ \delta u_q\end{bmatrix}\\
&= A(\theta_1)\begin{bmatrix}x\\ z\end{bmatrix}+B_1(\theta_1)\delta V+B_2u,\qquad (7.17)
\end{aligned}
$$

where

$$E_\varepsilon = \begin{bmatrix} I_3 & 0 \\ 0 & \varepsilon I_2 \end{bmatrix}, \quad B(\theta_1) = \begin{bmatrix} B_1(\theta_1) & B_2 \end{bmatrix}.$$

Then, by appropriately choosing operating points θ_i as a convex polytope with θ_i being vertices

$$\Theta = \mathrm{Co}\{\theta_1, \theta_2, \theta_3, \theta_4, \theta_5\} \tag{7.18}$$

with $i = 1, \ldots, 5$. Note that the LPV model (7.17), with $B_r(\theta)$ and $K_{rv}(\theta)$ approximated by (7.14) and (7.15), is affine in parameters. There exist scalars a, b, c, and d such that $B_r(\theta) = a\theta + b$ and $K_{rv}(\theta) = c\theta + d$. Hence, it is easy to verify that, for any $\theta \in \Theta$, there exist a set of positive numbers $\alpha_i > 0$ with $i = 1, \ldots, 5$ such that

$$A(\theta) = \sum_{i=1}^{5} \alpha_i A(\theta_i), \quad B_1(\theta) = \sum_{i=1}^{5} \alpha_i B_1(\theta_i), \tag{7.19}$$

where $\sum_{i=1}^{5} \alpha_i = 1$. Therefore, for any $\theta \in \Theta$, we have derived the singularly perturbed LPV model as below:

$$E_\varepsilon \begin{bmatrix} \dot{x} \\ \dot{z} \end{bmatrix} = A(\theta) \begin{bmatrix} x \\ z \end{bmatrix} + B_1(\theta)\delta V + B_2 u. \tag{7.20}$$

Remark 7.1 For the details of skills to choose operating points appropriately, please refer to [8].

7.2.1 Stability Analysis of Open-Loop System

In this subsection, our objective is to hold the optimal tip-speed ratio by adjusting wind rotor speed with respect to the wind speeds. The operating points are chosen such that the tip-speed ratio is optimal. States x and z in (7.20) are required to decay to zero, which indicates that errors between the actual states and the desired states tend to zero. In this sense, the wind turbine runs to extract all the available power.

Therefore, we will analyze the stability of the SPS (7.20) when the control input $u = 0$ based on LMI techniques. If $u = 0$, from (7.20), we can obtain the SPS as follows:

$$E_\varepsilon \begin{bmatrix} \dot{x} \\ \dot{z} \end{bmatrix} = A(\theta) \begin{bmatrix} x \\ z \end{bmatrix} + B_1(\theta)\delta V(t). \tag{7.21}$$

Theorem 7.1 *For an SPS in the form (7.21) and a given positive scalar $\gamma > 0$, if there exist positive symmetrical matrices $P_i > 0,\ i = 1, \ldots, 5$, satisfying that*

$$\begin{bmatrix} A^T(\theta_i)P_iE_\varepsilon + E_\varepsilon^T P_i A(\theta_i) & \star & \star \\ B_1^T(\theta_i)P_iE_\varepsilon & -\gamma^2 I & \star \\ C & 0 & -I \end{bmatrix} < 0 \tag{7.22}$$

where

$$\theta = \sum_{i=1}^{5} \alpha_i\theta_i,\ \sum_{i=1}^{5} \alpha_i = 1,\ A(\theta) = \sum_{i=1}^{5} \alpha_i A(\theta_i),\ B_1(\theta) = \sum_{i=1}^{5} \alpha_i B_1(\theta_i)$$

and $\alpha_i > 0$, then the equilibrium point of system (7.21) at θ is asymptotically stable, and the condition that $\|C(sE_\varepsilon - A)^{-1}B_1\| < \gamma$ is satisfied.

Proof Construct a Lyapunov function as

$$W(X) = X^T E_\varepsilon^T P E_\varepsilon X, \tag{7.23}$$

where $X = \begin{bmatrix} x & z \end{bmatrix}^T$ and $P = \sum_{i=1}^{5} \alpha_i P_i$. Since $P_i > 0$ and $\alpha_i > 0$, we have $P > 0$ such that $W(X) > 0$ holds.

Firstly, the asymptotically stability of the system is proved under conditions in Theorem 7.1, when the disturbance $\delta V(t)$ is zero. With $\delta V(t) = 0$, differentiating $W(X)$ with the respect to t along the trajectory of (7.21) yields

$$\frac{dW(X)}{dt} = X^T\{A^T(\theta)PE_\varepsilon + E_\varepsilon^T PA(\theta)\}X. \tag{7.24}$$

According to the LMI (7.22), we have

$$A^T(\theta_i)P_iE_\varepsilon + E_\varepsilon^T P_i A(\theta_i) < 0. \tag{7.25}$$

Then, adding the weight values (i.e., α_i) of θ_i to (7.25) yields

$$\begin{aligned} &\left\{\sum_{i=1}^{5} \alpha_i A^T(\theta_i)\right\}\left\{\sum_{i=1}^{5} \alpha_i P_i\right\}E_\varepsilon + E_\varepsilon^T\left\{\sum_{i=1}^{5} \alpha_i P_i\right\}\left\{\sum_{i=1}^{5} \alpha_i A(\theta_i)\right\} \\ &= A^T(\theta)PE_\varepsilon + E_\varepsilon^T PA(\theta) < 0. \end{aligned} \tag{7.26}$$

Therefore, $\dot{W}(X) < 0$. Hence, the system of (7.21) at point θ is asymptotically stable when $\delta V(t) = 0$.

Next, we prove the robust property of the system (7.21) when the disturbance $\delta V(t) \neq 0$.

Considering $\alpha_i > 0$ and using the LMI (7.22), it yields

$$\sum_{i=1}^{5}\alpha_i \sum_{i=1}^{5}\alpha_i \begin{bmatrix} A^T(\theta_i)PE_\varepsilon + E_\varepsilon^T PA(\theta_i) & \star & \star \\ B_1^T(\theta_i)PE_\varepsilon & -\gamma^2 I & \star \\ C & 0 & -I \end{bmatrix} < 0, \tag{7.27}$$

which leads to

$$\begin{bmatrix} A^T(\theta)PE_\varepsilon + E_\varepsilon^T PA(\theta) & \star & \star \\ B_1^T(\theta)PE_\varepsilon & -\gamma^2 I & \star \\ C & 0 & -I \end{bmatrix} < 0. \tag{7.28}$$

Then, by using SCL twice, LMI (7.28) can be transformed into

$$A^T(\theta)PE_\varepsilon + E_\varepsilon^T P^T A(\theta) + C^T C + \frac{1}{\gamma^2}E_\varepsilon^T P^T B_1(\theta)B_1^T(\theta)PE_\varepsilon < 0. \tag{7.29}$$

Differentiating $W(X)$ along the trajectory of (7.21) and using (7.29) yield

$$\begin{aligned} \frac{dW(X)}{dt} &= X^T\{A^T(\theta)PE_\varepsilon + E_\varepsilon^T PA(\theta)\}X + \delta V^T B_1^T(\theta)PE_\varepsilon X + X^T E_\varepsilon^T PB_1(\theta)\delta V \\ &< X^T\{-C^T C - \frac{1}{\gamma^2}E_\varepsilon^T P^T B_1(\theta)B_1^T(\theta)PE_\varepsilon\}X \\ &\quad + \delta V^T B_1^T(\theta)PE_\varepsilon X + X^T E_\varepsilon^T PB_1(\theta)\delta V \\ &= -y^T y + \gamma^2 \delta V^T \delta V - \gamma^2\big(\delta V - \frac{1}{\gamma^2}B_1^T PE_\varepsilon X\big)^T\big(\delta V - \frac{1}{\gamma^2}B_1^T PE_\varepsilon X\big). \end{aligned} \tag{7.30}$$

Based on the asymptotically stability proved at the first part of this proof, we have $X(\infty) = 0$. Provided that $X(0) = 0$, integrating both sides of (7.30) from $t = 0$ to $t = \infty$ yields

$$\begin{aligned} 0 < &-\int_0^\infty y^T(t)y(t)dt + \int_0^\infty \gamma^2 \delta V^T(t)\delta V(t)dt \\ &-\int_0^\infty \gamma^2(\delta V - \gamma^{-2}B_1^T(\theta)PE_\varepsilon X)^T(\delta V - \gamma^{-2}B_1^T(\theta)PE_\varepsilon X)dt \end{aligned} \tag{7.31}$$

Then, one can obtain that

$$\begin{aligned} &\int_0^\infty y^T(t)y(t)dt - \int_0^\infty \gamma^2 \delta V^T(t)\delta V(t)dt \\ &< -\int_0^\infty \gamma^2(\delta V - \gamma^{-2}B_1^T(\theta)PE_\varepsilon X)^T \\ &\quad (\delta V - \gamma^{-2}B_1^T(\theta)PE_\varepsilon X)dt. \end{aligned} \tag{7.32}$$

Therefore,

$$\int_0^\infty y^T(t)y(t)dt - \int_0^\infty \gamma^2 V^T(t)V(t)dt < 0. \tag{7.33}$$

It is obvious that $\|C(sE_\varepsilon - A(\theta))^{-1}B_1(\theta)\| < \gamma$ holds. This completes the proof.

Remark 7.2 Even though Theorem 7.1 can guarantee the stability and robust property of the system (7.21), LMI (7.22) is dependent on small parameter ε.

The following result improves the ill-conditioned condition in Theorem 7.1.

Theorem 7.2 *For an SPS in the form of (7.21) and a given positive scalar $\gamma > 0$, if there exist symmetrical matrices $P_i,\ i = 1, \ldots, 5$, satisfying*

$$E_\varepsilon^T P_i = P_i^T E_\varepsilon > 0, \tag{7.34}$$

$$\begin{bmatrix} A^T(\theta_i)P_i + P_i A(\theta_i) & \star & \star \\ B_1^T(\theta_i)P_i & -\gamma^2 I & \star \\ C & 0 & -I \end{bmatrix} < 0, \tag{7.35}$$

where

$$\theta = \sum_{i=1}^5 \alpha_i\theta_i,\ \sum_{i=1}^5 \alpha_i = 1,\ A(\theta) = \sum_{i=1}^5 \alpha_i A(\theta_i),\ B_1(\theta) = \sum_{i=1}^5 \alpha_i B_1(\theta_i)$$

and $\alpha_i > 0$, then the equilibrium point of the system (7.21) at point θ is asymptotically stable and $\|C(sE_\varepsilon - A(\theta))^{-1}B_1(\theta)\| < \gamma$ holds.

Proof Define a Lyapunov function as

$$W(X) = X^T E_\varepsilon^T P X, \tag{7.36}$$

where $X = \begin{bmatrix} x & z \end{bmatrix}^T$ and $P = \sum_{i=1}^5 \alpha_i P_i$. According to the condition (7.34), we have

$$E_\varepsilon^T P = P^T E_\varepsilon > 0. \tag{7.37}$$

As a consequence, $W(X) > 0$ is satisfied. Then, the time-derivative of $W(X)$ along the solution of (7.20) is given by

$$\dot{W}(X) = X^T\{A^T(\theta)P + P^T A(\theta)\}X + \delta V^T B_1^T(\theta)PX + X^T P^T B_1(\theta)\delta V. \tag{7.38}$$

The following part is similar to the proof of Theorem 7.1 and is omitted here.

7.2.2 Controller Design

In this subsection, we will design a robust state-feedback controller for the system (7.20), and analyze the stability property of its closed-loop system.

Since the coefficients of the system (7.20) depend on the θ, it is reasonable to design a controller whose feedback gain matrix also depends on θ.

From (7.19) and (7.21), for any point $\theta \in \Theta$, the dynamic equation of the nonlinear SPS can be expressed as a weight-sum of the dynamic equations at the vertices θ_i $(i = 1, \ldots, 5)$ of Θ. Therefore, we will design controllers for the LTI systems operating at the vertices θ_i $(i = 1, \ldots, 5)$ of Θ and use a weight-sum of the controllers at vertices as the control input to the system at point $\theta \in \Theta$.

At the vertex point θ_i, $i \in \{1, 2, 3, 4, 5\}$, design a robust state feedback controller as below:

$$u_i = K(\theta_i)X. \tag{7.39}$$

The closed-loop system of (7.21) at the vertex point θ_i with (7.39) as control input is of the following form,

$$E_\varepsilon \dot{X} = A_c(\theta_i)X + B_1(\theta_i)\delta V, \tag{7.40}$$

where $A_c(\theta_i) = A(\theta_i) + B_2K(\theta_i)$.

Then, for a nonlinear SPS (7.20) at θ, the state-feedback controller is given by

$$u(\theta) = K(\theta)X = \sum_{i=1}^{5} \alpha_i K(\theta_i)X, \tag{7.41}$$

where $\alpha_i > 0$ and $\sum_{i=1}^{5} \alpha_i = 1$.

Applying (7.41) in system (7.20), the closed-loop system is obtained as

$$E_\varepsilon \begin{bmatrix} \dot{x} \\ \dot{z} \end{bmatrix} = (A(\theta) + B_2K(\theta)) \begin{bmatrix} x \\ z \end{bmatrix} + B_1(\theta)V. \tag{7.42}$$

The properties of closed-loop system of (7.42) are analyzed in the next Theorem 7.3. To develop Theorem 7.3, the following lemma from [48] is needed.

Lemma 7.1 [48] *For matrices $X, Y \in \mathbf{R}^{m\times n}$ and $H > 0$, and a scalar $\delta > 0$, then we have*

$$X^THY + Y^THX \leqslant \delta X^THX + \delta^{-1}Y^THY. \tag{7.43}$$

Theorem 7.3 *The closed-loop system of (7.20) with (7.41) as control input is asymptotically stable, and*

$$\|C(sE_\varepsilon - A_c(\theta))^{-1}B_1(\theta)\| < \gamma$$

is satisfied for a given $\gamma > 0$, if there exist matrices P_i and $K(\theta_i)$ of appropriate dimension, such that the following LMIs hold

$$E_\varepsilon^T P_i = P_i^T E_\varepsilon > 0, \tag{7.44}$$

$$\begin{bmatrix} A^T(\theta_i)P_i + P_i^T A(\theta_i) & \star & \star & \star & \star \\ B_2K(\theta_i) & -I & \star & \star & \star \\ P_i & 0 & -I & \star & \star \\ B_1^T(\theta_i)P_i & 0 & 0 & -\gamma^2 I & \star \\ C & 0 & 0 & 0 & -I \end{bmatrix} < 0. \tag{7.45}$$

Proof Similar to the proof of Theorem 7.1, because

$$A(\theta) = \sum_{i=1}^{n} \alpha_i A(\theta_i),\ B_1(\theta) = \sum_{i=1}^{n} \alpha_i B_1(\theta_i),\ K(\theta) = \sum_{i=1}^{n} \alpha_i K_1(\theta_i),\ \sum_{i=1}^{n} \alpha_i = 1$$

and $\alpha_i > 0$. According to (7.45), we have

$$\begin{bmatrix} A^T(\theta)P_i + P_i^T A(\theta) & \star & \star & \star & \star \\ B_2K(\theta) & -I & \star & \star & \star \\ P_i & 0 & -I & \star & \star \\ B_1^T(\theta)P_i & 0 & 0 & -\gamma^2 I & \star \\ C & 0 & 0 & 0 & -I \end{bmatrix} < 0. \tag{7.46}$$

Setting $P = \sum_{i=1}^{n} \alpha_i P_i$, from (7.44) and (7.46), the following inequalities hold

$$E_\varepsilon^T P = P^T E_\varepsilon > 0, \tag{7.47}$$

$$\begin{bmatrix} A^T(\theta)P + P^T A(\theta) & \star & \star & \star & \star \\ B_2K(\theta) & -I & \star & \star & \star \\ P & 0 & -I & \star & \star \\ B_1^T(\theta)P & 0 & 0 & -\gamma^2 I & \star \\ C & 0 & 0 & 0 & -I \end{bmatrix} < 0. \tag{7.48}$$

According to SCL 2.4, inequality (7.48) is equivalent to

$$\begin{aligned} &A^T(\theta)P + P^T A(\theta) + (B_2K(\theta))^T(B_2K(\theta)) + P^T P \\ &+C^T C + \frac{1}{\gamma^2} P^T B_1(\theta)B_1^T(\theta)P < 0 \end{aligned} \tag{7.49}$$

From Lemma 7.1, it is easy to obtain

$$(B_2K(\theta))^T P + P^T(B_2K(\theta)) \leqslant (B_2K(\theta))^T(B_2K(\theta)) + P^T P. \tag{7.50}$$

Hence, from (7.49) and (7.50), we have

$$\begin{aligned} &A^T(\theta)P + P^TA(\theta) + (B_2K(\theta))^TP + P^T(B_2K(\theta)) \\ &+C^TC + \frac{1}{\gamma^2}P^TB_1(\theta)B_1^T(\theta)P < 0, \end{aligned} \tag{7.51}$$

which is equivalent to

$$\begin{aligned} &(A(\theta) + B_2K(\theta))^TP + P^T(A(\theta) + B_2K(\theta)) \\ &+C^TC + \frac{1}{\gamma^2}P^TB_1(\theta)B_1^T(\theta)P < 0. \end{aligned} \tag{7.52}$$

Define a Lyapunov function as

$$W(X) = X^TE_\varepsilon^TPX, \tag{7.53}$$

where $X = \begin{bmatrix} x & z \end{bmatrix}^T$. Then, the time-derivative of $W(X)$ along the solution of (7.20) is given by

$$\begin{aligned} \dot{W}(X) = X^T\{(A(\theta) + B_2K(\theta))^TP + P^T(A(\theta) + B_2K(\theta))\}X \\ + V^TB_1^T(\theta)PX + X^TP^TB_1(\theta)V. \end{aligned}$$

The following part is similar to the proof of Theorem 7.1 and is omitted here.

7.2.3 *Algorithm of Synthesis*

In order to clarify the whole process of designing a parameter-dependent controller for the original nonlinear system (7.4)–(7.8), the following algorithm is presented.

Step 1. Choose five operating points $\theta_1, \ldots, \theta_5$.
Step 2. Determine singular perturbation parameter ε, and get the nonlinear SPSs (7.4)–(7.6) and (7.9)–(7.10).
Step 3. Linearize the nonlinear SPSs (7.4)–(7.6), (7.9)–(7.10) at θ_i, and obtain the linear parameter-dependent coefficient $A(\theta_i)$ and $B(\theta_i)$ $(i = 1, \ldots, 5)$.
Step 4. For a given γ, at each operating point θ_i, LMIs (7.44) and (7.45) are solved to obtain control gain matrices K_i $(i = 1, \ldots, 5)$.
Step 5. At time t_k, the variable $\theta(t_k) = \theta_k$ is measured, and the weighting coefficients α_i satisfying

$$\theta_k = \sum_{i=1}^{5} \alpha_i(t_k)\theta_i \tag{7.54}$$

are computed with $0 \leqslant \alpha_i \leqslant 1$ and $\sum_{i=1}^{5} \alpha_i = 1$.

Step 6. The control gain matrix at time t_k is obtained as below:

$$K(\theta(t_k)) = \sum_{i=1}^{5} \alpha_i(t_k) K_i \tag{7.55}$$

Step 7. Apply the controller (7.55) to the original nonlinear system (7.4)–(7.8).
Step 8. At time t_{k+1}, repeat Step 5 to Step 8.

Remark 7.3 This algorithm can only be applied to the point $\theta \in \Theta$, where Θ is defined by (7.18). If $\theta \notin \Theta$, it can not be guaranteed that we can computed $\alpha_i > 0$, $i = 1, \ldots, 5$, with $\sum_{i=1}^{5} \alpha_i = 1$ satisfied.

Remark 7.4 Since the operating point $\theta = [\hat{\omega}_r \ \hat{V} \ \hat{\omega}_g \ \hat{i}_d \ \hat{i}_q]^T$ involves wind speed V, Θ implies the range of the wind speed within which our algorithm is effective.

7.2.4 Simulation Examples

In this subsection, our goal is to track the desired wind rotor speed and maintain the optimal tip-speed ratio with the wind speed changing. The simulation study is performed to verify the effectiveness of the proposed control algorithms. The parameters of the wind turbine from [98] are used in the next examples as given in Table 7.1.

Example 7.1 Consider a wind turbine system with the parameters depicted in Table 7.1. The wind speed is assumed as a constant 13 m/s in this example. Using the developed Algorithm, the wind rotor tracking is shown in Fig. 7.1. It can be seen that the tracking error between actual rotor speed and the desired rotor speed decays to zero.

Example 7.2 In this example, the wind input file is selected as the mean wind speed 15 m/s changing within a range of 5 m/s. The wind file is based on data collected at 100 Hz. The other parameters are the same as Table 7.1. Figure 7.2 shows the wind input file.

Our objective is to track the desired rotor speed $\omega_{\text{ref}}(t) = \lambda_{\text{opt}} * V(t)/R$. Because of the slow response characteristics of wind turbine systems, it is impossible to track the high frequency part of the wind rotor reference. We aim to track the desired rotor speed at low frequency part, and reduce the tracking error at the high frequency part. Figure 7.3 shows the wind rotor tracking performance. It can be seen that the controlled rotor speed can track the desired rotor speed accurately after four seconds, and the control scheme achieves the desired tracking performance.

Table 7.1 Parameters of wind turbine [98]

Physical description	Parameter	Value	Unit
Cut-in wind speed	V	4	m/s
Mean wind speed	V_R	15	m/s
Optimal tip-speed ratio	λ_{Qmax}	6.2	–
Rotor radius	R	2.5	m
Optimal power coefficient	C_{Pmax}	0.4633	–
Air density	ρ	0.98	kg/m^3
Gearbox efficiency	η	1	–
Wind rotor inertia	J_r	3.88	kg $\cdot$ m^2
Generator inertia	J_g	0.22	kg $\cdot$ m^2
Number of pole pairs	P	3	–
Gearbox ratio	i	6	–
Flux linkage	ϕ_m	0.4382	wb
Shaft damping coefficient	B_g	0.3	kg $\cdot$ m^2/s
Shaft stiffness coefficient	K_g	75	N m/rad
Stator d-axis inductance	L_d	41.56	mH
Stator q-axis inductance	L_q	41.56	mH
Stator resistance	R_s	3.3	Ω

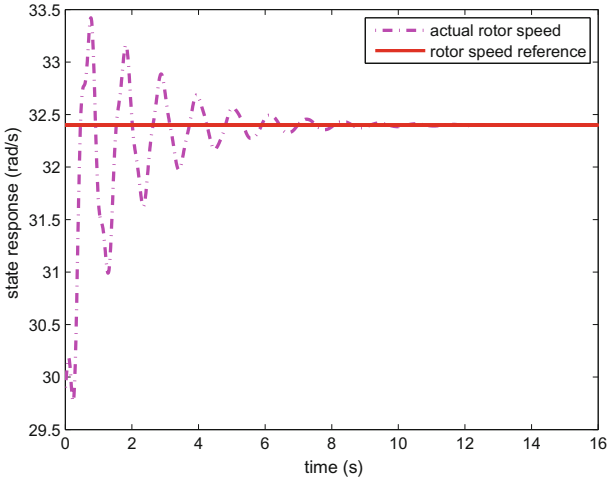

Fig. 7.1 Rotor speed constant tracking

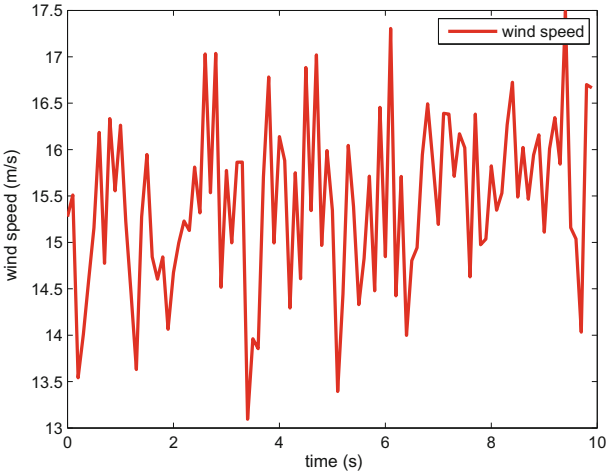

Fig. 7.2 Wind speed

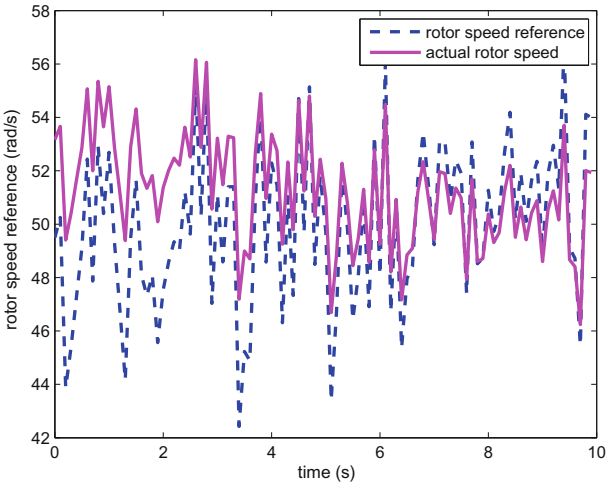

Fig. 7.3 Rotor speed tracking

7.3 Robust H_∞ Controller for Miniature Quad-Rotors in Hovering

This section is concerned with the H_∞ control synthesis of miniature quad-rotors to improve its hovering capability in presence of wind disturbances. With aid of SPaTSs, the six-degree-freedom flight dynamics can be decoupled into two subsystems: one for translational motion corresponding to the low-frequency subsystem and the other for the orientational motion referred to as the high-frequency subsystem. To avoid the unnecessary frequency overlap, the GKYP lemma is employed in the irrelevant dominant frequency ranges of the related subsystems. Sub-controllers are designed to stabilize the low- and the high-frequency subsystems and satisfy the associated H_∞ performance specifications, respectively. The composite controller composed of sub-controllers is applied directly to the overall flight system of miniature quad-rotors. The characteristics of wind are considered, and different composite controllers are designed in various flight regimes to ensure an adequate response in all flight modes. Based on this, a novel switch strategy is then put forward to guarantee desired hovering capability under different weather conditions. Detail analysis of the performance achieved by the piece-wise controller is provided when it is applied to the original system. The effectiveness and merits of the proposed switch strategy are illustrated with a numerical result.

There has been an exponential increase in the prevalence of miniature UAVs over past decades. To date, both miniature fixed-wing and rotary-wing aircraft are extensively used in numerous military and civil applications [16]. Due to some unique features such as low cost, small size, good manoeuverability and hover capability, miniature UAVs are well suited for missions such as fire detection, victims localization, etc. A precise model plays an important role in prediction for the behaviours of various dynamic systems. The significance for modelling a quad-rotor vehicle dynamics has been addressed in the documented research results such as [13, 56, 75]. The flight dynamic model for miniature UAV is derived using well-established aircraft and rotorcraft theories, and the related model parameters are estimated through system identification using practical input-output data collected from particular experiments. To achieve autonomous flight, miniature UAVs are equipped with microcomputers such that control laws can be executed onboard to replace the action of a human pilot [16, 17]. Control strategy is formulated according to various flight regimes to guarantee satisfactory performance over the full flight envelope.

Many dynamical systems such as aircraft and racket systems and electric power systems feature TTS characteristics, namely, an interaction of fast and slow dynamics [78, 94, 153]. Such systems are governed by both fast and slow dynamics, and customarily referred to as SPSs. For miniature UAVs, translational dynamics are regarded as slow dynamics, whereas orientation dynamics are considered to be fast. Feedback design for SPSs commonly suffers from high dimensionality and ill-posed problems. Consequently, the design based on the overall system or some simplified models may cause the closed-loop system far from its desired performance or even unstable. SPTs have been proven to be common tools for modelling, analysis and

design of flight control systems, and the numerical stiffness is much alleviated. Engineers usually separate states into two parts, and introduce a small parameter ε to determine the degree of separation between the slow and fast modes. In [153], the nature of multi-time-scale systems is presented, and it is possible to obtain controllers that are independent of ε. The success of perturbation techniques involving multiple time-scales shed light on the research of the frequency-domain approaches which characterize the frequency behaviours of slow and fast subsystems, repsectively. In [81, 82], transfer-function matrices for SPSs are considered, and conditions that guarantee system behaviours are decomposed into several frequency scales.

In the literature, a variety of SPTs have been applied into the controller design of UAVs to achieve their missions not only with increasing efficiency, but also with more safety and security. A Lyapunov-based control in [37] using singular perturbation theory is proposed and applied in a miniature UAV. The research work presented in [7] addressed the stability analysis of a hierarchical controller of a UAV. More superficially, position and attitude control laws were successively designed via a time-scale separation between the translational dynamics and orientational dynamics of a six degrees-of-freedom vertical take off and landing UAV model. In [35], Esteban and Rivas proposed a singular perturbation control strategy for regulating the longitudinal flight dynamics of a UAV, where control strategy was based on a time-scale decomposition that included the altitude, velocity, pitch, and flight path angle dynamics. SPTs were used in [52] to develop a full-authority trajectory controller for an autonomous helicopter. In [143], time-controlled optimal flight-trajectory generation methods, which included the effects of risk caused by threat environment, had been proposed, and singular perturbation method was used to obtain reduced-order airplane models that allow static rather than dynamic optimization.

Good hovering capability is a key system specification for missions such as vision inspection of buildings for maintenance and post-disaster relief. In the content of H_∞ control of SPSs, over the past decades, a variety of singularly perturbed models have been proposed and investigated. Combined with the distinctive behaviours between slow and fast states, the concept of H_∞ control of SPSs was raised in [67] with H_∞ properties of the two subsystems established, respectively. In [79], a fuzzy model was used to represent the SPSs, and both the state feedback and SOFCs were developed to achieve the H_∞ disturbance attenuation performance. Li, Wang and Liang proposed a new methodology to design sub-optimal controllers for SPSs, which can be further extended to other robust and multi-objective control problems for SPSs [76]. Considering that the system commonly works in some specific frequency ranges under certain operating conditions, it is, thus, too strict and unpractical to keep H_∞ performance index established in the full frequency range, which leads to the research of the finite frequency H_∞ control (FF H_∞ control). During the past few years, some good results of the FF H_∞ control of SPSs have been documented in the literature. In [88], a method to design a composite state feedback controller was constructed to realize the FF H_∞ control of SPSs based on the GKYP lemma. Huang et al. extended this method to realize positive real control of SPSs [57]. In [55], an output feedback controller for SISO SPSs was designed to meet frequency-domain loop-shaping specifications. Despite its theoretical significance and engineering importance, the

Fig. 7.4 Quad-rotor aerial vehicle developed at the Khalifa University

concept of frequency dividing control for SPSs, however, has not attracted much research attention yet, not to mention the composite design on the SPSs.

In this section as shown in Fig. 7.4, a miniature UAV is formulated into an SPS to meet the requirements of high precision and quality in modern engineering, and a positive parameter ε is served as a measurement of "speed" to separate the translational dynamics and orientational dynamics. H_∞ control is then conducted based on the unique frequency nature of SPSs.

The main contributions of this section are outlined as follows.

(1) We present the stability and control performance analysis of the miniature UAV using singular perturbation theory. The flight control system, represented in the form of an SPS, is decoupled into two reduced-order subsystems in separate time-scales: the translational subsystem (slow subsystem) in the slow time-scale and the orientational subsystem (fast subsystem) in the fast time-scale. The flight system of the miniature UAV is modelled in terms of SPS such that the model accuracy is increased to a large extent.
(2) Sub-controllers are designed, respectively, for the corresponding slow and fast subsystems to increase their robustness to different types of external disturbances. Advantage is thereby taken of the singularly perturbed nature of the problem to design a well-conditioned composite feedback controller to solve the original SPS within a specified order-of-ε accuracy.
(3) The frequency nature of SPSs is considered in the design of H_∞ hovering controller for miniature UAVs. Note that the slow modes are sensitive to oscillators associated with low-frequency signals, while the fast modes are more easily affected by high-frequency power sources. Thus, slow and fast subsystems are constructed, separately, in the low and high frequency ranges to avoid the unnecessary frequency band overlap, and referred to as the low-frequency cut-off

subsystem and high-frequency cut-off subsystem in the literature. Such cut-off frequency subsystems with lower system order can characterize the frequency characteristic of the high-dimensional flight system in disjoint frequency ranges.

(4) The conservatism of the H_∞ performance index is highly reduced with the aid of finite frequency H_∞ control. Contrast with the existing method, finite frequency control is put forward, and the H_∞ index for the related cut-off frequency subsystem is established in the corresponding dominant frequency range.

(5) Wind gust contains abundant frequency components, and is thus regarded as the external disturbance. Due to this, we adopt a novel control strategy based on switch between different composite controllers to meet the requirements of different flight regimes. More specifically, an index switching function is used to select the candidate sub-controller according to different weather conditions.

7.3.1 Modelling

In this section, a six-degree-of-freedom (6-DOF) miniature UAV developed at the Khalifa University, SAQER, is used as an example for the controller design with state variables and parameters shown in Tables 7.2 and 7.3, respectively.

Motion equations are derived from Newton's second law. The force equation is given by

$$\begin{aligned} \dot{u} &= -(wq - vr) + X/m - g\sin\theta, \\ \dot{v} &= -(ur - wp) + Y/m + g\cos\theta\sin\phi, \\ \dot{w} &= -(vp - qu) + Z/m + g\cos\theta\cos\phi, \end{aligned} \tag{7.56}$$

Table 7.2 Body frame variables

Physical description	x axis	y axis	z axis
Angular rates	p	q	r
Velocity components	u	v	w
Force components	X	Y	Z
Moment components	L	M	N
Moment of inertia	I_{xx}	I_{yy}	I_{zz}
Product of inertia	I_{yz}	I_{xz}	I_{xy}

Table 7.3 Motor variables

Physical description	Parameter
Thrust of i-th motor	T_i
Torque of i-th motor	M_i
Total mass of the vehicle	m
Length between a motor and the centre	l

where forces acting on the vehicle are given by

$$\begin{aligned} X &= mX_u u + mX_\theta \theta + mX_q q, \\ Y &= mY_v v + mY_\phi \phi + mY_p p, \\ Z &= mZ_w w + T_1 + T_2 + T_3 + T_4. \end{aligned}$$

The moment equation is given by

$$\begin{aligned} I_{xx}\dot{p} &= (I_{yy} - I_{zz})qr + I_{xz}(\dot{r} + pq) + L, \\ I_{yy}\dot{q} &= (I_{zz} - I_{xx})rp + I_{xz}(r^2 - p^2) + M, \\ I_{zz}\dot{r} &= (I_{xx} - I_{yy})pq + I_{xz}(\dot{p} - qr) + N, \end{aligned} \tag{7.57}$$

where

$$\begin{aligned} L &= I_{xx}L_u u + I_{xx}L_v v + I_{xx}L_p p + 2(T_4 - T_2)l, \\ M &= I_{yy}M_u u + I_{yy}M_v v + I_{yy}M_q q + 2(T_1 - T_3)l, \\ N &= I_{zz}N_r r - M_1 - M_3 + M_2 + M_4. \end{aligned}$$

Due to the symmetric structure of the vehicle, all products of inertias are zero: $I_{xy} = I_{xz} = I_{yz} = 0$. The following relationship is considered,

$$\begin{bmatrix} p \\ q \\ r \end{bmatrix} = \begin{bmatrix} 1 & 0 & -\sin\theta \\ 0 & \cos\phi & \sin\phi\cos\theta \\ 0 & -\sin\phi & \cos\phi\cos\theta \end{bmatrix} \begin{bmatrix} \dot{\phi} \\ \dot{\theta} \\ \dot{\psi} \end{bmatrix},$$

which can be rewritten as

$$\begin{aligned} \dot{\phi} &= p + p\sin\phi\tan\theta + r\cos\phi\tan\theta, \\ \dot{\theta} &= q\cos\phi - r\sin\phi, \\ \dot{\psi} &= q\sin\phi\sec\theta + r\cos\phi\sec\theta. \end{aligned} \tag{7.58}$$

The complete system is composed of the translational dynamics (7.56) and the orientation dynamics (7.57)–(7.58). Then, we aim to design the H_∞ controller to improve the hovering capability of the complete system.

Current practice in the design of H_∞ hovering controller for miniature UAVs is to linearize the aircraft dynamics near the operating point with several trim conditions to reduce the coupling among related aircraft dynamics. We assume that the vehicle operates at hover, and the trimmed states are given by

$$u = 0,\ v = 0,\ w = 0,\ p = 0,\ q = 0,\ r = 0.$$

With regard to the fact that the variation range of angles $\phi,\ \theta,\ \psi$ near the operating point is not larger than 5°, we have

$$\sin\phi = 0,\ \ \cos\phi = 1,\ \ \sin\theta = 0,$$
$$\cos\theta = 1,\ \ \sin\psi = 0,\ \ \cos\psi = 1,$$

which can be further used in model simplification.

If the linearization of the system (7.56)–(7.57) is conducted near the operating point, the following 6-DOF model can be obtained as

$$\begin{bmatrix} \dot{\delta}_u \\ \dot{\delta}_v \\ \dot{\delta}_p \\ \dot{\delta}_q \\ \dot{\delta}_w \\ \dot{\delta}_r \end{bmatrix} = \begin{bmatrix} X_u & 0 & 0 & X_q & 0 & 0 \\ 0 & Y_v & Y_p & 0 & 0 & 0 \\ L_u & L_v & L_p & 0 & 0 & 0 \\ M_u & M_v & 0 & M_q & 0 & 0 \\ 0 & 0 & 0 & 0 & Z_w & 0 \\ 0 & 0 & 0 & 0 & 0 & N_r \end{bmatrix} \begin{bmatrix} \delta u \\ \delta v \\ \delta p \\ \delta q \\ \delta w \\ \delta r \end{bmatrix} + \begin{bmatrix} 0 & 0 & 0 & 0 \\ 0 & 0 & 0 & 0 \\ L_{lat} & 0 & 0 & 0 \\ 0 & M_{lon} & 0 & 0 \\ 0 & 0 & Z_{col} & 0 \\ 0 & 0 & 0 & N_{ped} \end{bmatrix} \begin{bmatrix} \delta_{lat} \\ \delta_{lon} \\ \delta_{col} \\ \delta_{ped} \end{bmatrix} \tag{7.59}$$

Taking the effects of the wind into consideration, additional items are added into (7.59) to represent the external disturbances,

$$\begin{bmatrix} \dot{\delta}_u \\ \dot{\delta}_v \\ \dot{\delta}_p \\ \dot{\delta}_q \\ \dot{\delta}_w \\ \dot{\delta}_r \end{bmatrix} = \begin{bmatrix} X_u & 0 & 0 & X_q & 0 & 0 \\ 0 & Y_v & Y_p & 0 & 0 & 0 \\ L_u & L_v & L_p & 0 & 0 & 0 \\ M_u & M_v & 0 & M_q & 0 & 0 \\ 0 & 0 & 0 & 0 & Z_w & 0 \\ 0 & 0 & 0 & 0 & 0 & N_r \end{bmatrix} \begin{bmatrix} \delta u \\ \delta v \\ \delta p \\ \delta q \\ \delta w \\ \delta r \end{bmatrix} + \begin{bmatrix} B_{wu} \\ B_{wv} \\ B_{ww} \\ B_{wp} \\ B_{wq} \\ B_{wr} \end{bmatrix} \varpi + \begin{bmatrix} 0 & 0 & 0 & 0 \\ 0 & 0 & 0 & 0 \\ L_{lat} & 0 & 0 & 0 \\ 0 & M_{lon} & 0 & 0 \\ 0 & 0 & Z_{col} & 0 \\ 0 & 0 & 0 & N_{ped} \end{bmatrix} \begin{bmatrix} \delta_{lat} \\ \delta_{lon} \\ \delta_{col} \\ \delta_{ped} \end{bmatrix} \tag{7.60}$$

where ϖ is considered as the wind, the constant matrices B_{wu}, B_{wv}, B_{ww}, B_{wp}, B_{wq} and B_{wr} are used as the weighing matrices to characterize the components of wind on related dynamics in different directions. The related parameters of SAQER's bare flight dynamics model after system identification is given in Table 7.4. On this basis, we obtain three reduced subsystems, one of which can be modelled in the singularly perturbed form,

(1) w subsystem in the slow time-scale t:

$$\dot{\delta}w = Z_{col}\delta_{col}, \tag{7.61}$$

Table 7.4 Parameters of SAQER's bare flight dynamics model after linearization

Variable	Value	Variable	Value
X_u	−0.02	M_u	0.05
X_θ	−9.8	M_v	0
X_q	0.21	M_q	−0.58
Y_v	0.02	Z_w	0
Y_ϕ	9.8	N_r	0
Y_p	0.21	L_{lat}	141.21
L_u	0	M_{lon}	138.71
L_v	0.05	Z_{col}	11.12
L_p	0.59	N_{ped}	7.83

(2) r subsystem in the fast time-scale τ:

$$\dot{\delta} r = \mathscr{N}_{ped}\delta_{ped}, \tag{7.62}$$

where $\mathscr{N}_{ped} = \varepsilon N_{ped}$,

(3) $uvpq$ subsystem:

$$\begin{aligned}\begin{bmatrix}\dot{\delta u}\\ \dot{\delta v}\\ \dot{\delta p}\\ \dot{\delta q}\end{bmatrix} &= \begin{bmatrix}X_u & 0 & 0 & X_q\\ 0 & Y_v & Y_p & 0\\ L_u & L_v & L_p & 0\\ M_u & M_v & 0 & M_q\end{bmatrix}\begin{bmatrix}\delta u\\ \delta v\\ \delta p\\ \delta q\end{bmatrix} + \begin{bmatrix}0 & 0\\ 0 & 0\\ L_{lat} & 0\\ 0 & M_{lon}\end{bmatrix}\begin{bmatrix}\delta_{lat}\\ \delta_{lon}\end{bmatrix}\\ &:= P\begin{bmatrix}\delta u\\ \delta v\\ \delta p\\ \delta q\end{bmatrix} + B\begin{bmatrix}\delta_{lat}\\ \delta_{lon}\end{bmatrix}.\end{aligned} \tag{7.63}$$

Using the local linearization method, the whole flight system can be decoupled into three subsystems: the w subsystem, r subsystem, and $uvpq$ subsystem. Apparently, the value of velocity component w is determined merely by the voltage δ_{col}, and the control input δ_{ped} is a decisive factor for the flight dynamic r. Note that the $uvpq$ subsystem can be represented in the singularly perturbed form (7.63) because the eigenvalues of the state matrix P cluster into two groups

$$\lambda(P) = \{-0.0018,\ -0.5982,\ 0.0021,\ 0.6079\}.$$

The presence of two separate sets of eigenvalues of P is an inherent property of SPSs.

The design of H_∞ controller for w subsystem and r subsystem can use the classical H_∞ control approaches, which has already been intensively researched in the literature. To highlight the key point of this section, that is, the following work is mainly focused on the reduced TTS subsystem.

Denoting the slow part as $\xi = \begin{bmatrix}\delta_u & \delta_v\end{bmatrix}^T$, the fast part as $\varsigma = \begin{bmatrix}\delta_p & \delta_q\end{bmatrix}^T$ and the control input u as $u = \begin{bmatrix}\delta_{lat} & \delta_{lon}\end{bmatrix}^T$, the singularly perturbed form of the reduced system (1.36) is derived,

$$\begin{bmatrix}\dot{\xi}\\ \varepsilon\dot{\varsigma}\end{bmatrix} = \begin{bmatrix}\mathscr{A}_{11} & \mathscr{A}_{12}\\ \mathscr{A}_{21} & \mathscr{A}_{22}\end{bmatrix}\begin{bmatrix}\xi\\ \varsigma\end{bmatrix} + \begin{bmatrix}\mathscr{B}_1\\ \mathscr{B}_2\end{bmatrix}u + \begin{bmatrix}\mathscr{B}_{w1}\\ \mathscr{B}_{w2}\end{bmatrix}w, \tag{7.64}$$

where

$$\mathscr{A}_{11} = \begin{bmatrix} X_u & 0 \\ 0 & Y_v \end{bmatrix}, \ \mathscr{A}_{12} = \begin{bmatrix} 0 & X_q \\ Y_p & 0 \end{bmatrix},$$
$$\mathscr{A}_{21} = \begin{bmatrix} \varepsilon L_u & \varepsilon L_v \\ \varepsilon M_u & \varepsilon M_v \end{bmatrix}, \ \mathscr{A}_{22} = \begin{bmatrix} \varepsilon L_p & 0 \\ 0 & \varepsilon M_q \end{bmatrix},$$
$$\mathscr{B}_1 = \begin{bmatrix} 0 & 0 \\ 0 & 0 \end{bmatrix}, \ \mathscr{B}_2 = \begin{bmatrix} \varepsilon L_{lat} & 0 \\ 0 & \varepsilon M_{lon} \end{bmatrix}.$$

Remark 7.5 Wind is the external disturbance in the SPS model (7.64), which affects the position and attitude of the UAV. Wind can be divided into different classifications based on time or geography. Despite complex weather conditions, weighing matrices $\mathscr{B}_{w1}$ and $\mathscr{B}_{w2}$ are used to characterize wind components in different directions. In [74], it can be seen that wind dynamics are the combination of short-, medium- and long-term wind speed fluctuations, but the power of wind is mainly concentrated in low frequency range. Turbulence such as wind dust, a special type of wind occurring frequently in real life, is the main contributor to high-frequency components of wind.

Applying the SPA into the SPS (7.64), we have the following subsystems, that is translational subsystem in the slow time-scale t, denoted as Σ_{uv},

$$\begin{aligned} \dot{\xi}_s &= (\mathscr{A}_s + \mathscr{B}_{us}K_s)\xi_s + \mathscr{B}_{ws}w, \\ y_s &= (\mathscr{C}_s + \mathscr{D}_{us}K_s)\xi_s + \mathscr{D}_{ws}w, \end{aligned} \tag{7.65}$$

$$\begin{aligned} &\mathscr{A}_s = \mathscr{A}_{11} + \mathscr{A}_{12}\mathscr{A}_{22}^{-1}\mathscr{A}_{21}, \ \mathscr{B}_{us} = \mathscr{B}_1 + \mathscr{A}_{12}\mathscr{A}_{22}^{-1}\mathscr{B}_2, \\ &\mathscr{B}_{ws} = \mathscr{B}_{w1} + \mathscr{A}_{12}\mathscr{A}_{22}^{-1}\mathscr{B}_{w2}, \ \mathscr{C}_s = \mathscr{C}_1 + \mathscr{C}_2\mathscr{A}_{22}^{-1}\mathscr{A}_{21}, \\ &\mathscr{D}_{us} = \mathscr{D}_1 + \mathscr{C}_2\mathscr{A}_{22}^{-1}\mathscr{B}_2, \ \mathscr{D}_{ws} = \mathscr{D}_2 + \mathscr{C}_2\mathscr{A}_{22}^{-1}\mathscr{B}_{w2}, \end{aligned}$$

and orientational subsystem in the fast time-scale τ, denoted as Σ_{pq},

$$\begin{aligned} \dot{\varsigma}_f &= (\mathscr{A}_{22} + \mathscr{B}_2K_f)\varsigma_f + \mathscr{B}_{w2}w, \\ y_f &= (\mathscr{C}_2 + \mathscr{D}_1K_f)\varsigma_f + \mathscr{D}_2w, \end{aligned} \tag{7.66}$$

TTS characteristic of system (7.64) implies that

$$\max |\lambda(\mathscr{A}_{22})| \ll \min |\lambda(\mathscr{A}_s)|,$$

where $\mathscr{A}_s$ and $\mathscr{A}_{22}$ are the slow and fast subsystem state matrices. Based on this, the parameter ε can be determined by

$$\varepsilon = \min |\lambda(\mathscr{A}_s)| / \max \lambda|(\mathscr{A}_{22})|.$$

Using SPTs in (7.65) and (7.66), cut-off frequency subsystems for (7.64) are constructed with the closed-loop transfer-function matrices as

$$T_{\text{low}}(s) = \mathscr{C}_{sc}(sI_n - \mathscr{A}_{sc})^{-1}\mathscr{B}_{ws} + \mathscr{E}_{ws},$$

where $\mathscr{E}_{ws} = \mathscr{D}_{ws} - \mathscr{C}_2\mathscr{A}_{22}^{-1}\mathscr{B}_{w2} + \mathscr{D}_2$, $\mathscr{A}_{sc} = \mathscr{A}_s + \mathscr{B}_{us}K_l, \mathscr{C}_{sc} = \mathscr{C}_s + \mathscr{D}_{us}K_l$, and

$$T_{\text{high}}(p) = \mathscr{C}_{fc}(pI_m - \mathscr{A}_{fc})^{-1}\mathscr{B}_{w2} + \mathscr{E}_{wf},$$

where $\mathscr{E}_{wf} = \mathscr{D}_{ws} + \mathscr{D}_2$, $\mathscr{A}_{fc} = \mathscr{A}_{22} + \mathscr{B}_{u2}K_h, \mathscr{C}_{fc} = \mathscr{C}_2 + \mathscr{D}_1K_h$.

7.3.2 Design of H_∞ Controller for Miniature UAVs in Hovering

Waving with wind is a good status for the flight system rather than staying stationary in the air, which requires less input energy. Stability and disturbance attenuation capability of orientational dynamics is a necessary requirement for the hovering task to keep the sustainable flight of the UAV while the position (the translational dynamics) of the UAV is not that important for such task. Based on this concept, we present methods to design the H_∞ controller in hovering for the miniature UAV.

Theorem 7.4 (Design of Normal Controller) *For a given cut-off frequency ω_c, scalars $\gamma_1 > 0$, p_1, q_1, p_2 and q_2 satisfying $p_1q_1 > 0$ and $p_2q_2 > 0$, and matrices R_l, the closed-loop SPS (7.64) achieves H_∞ property to resist the effects of low-frequency wind,*

1. *the closed-loop subsystem (7.64) is internally stable for $\varepsilon \in (0, \varepsilon^*]$,*
2. $\|T_{low}(s)\|_\infty^{\Lambda_l} < \gamma_1$,

if there exist symmetric matrices W_s, $P_s > 0$, $P_f > 0$, P_l and $Q_l > 0$ such that the following LMIs hold:

$$\begin{bmatrix} 0 & P_s \\ P_s & 0 \end{bmatrix} < \mathbf{He}\begin{bmatrix} -W_s \\ \mathscr{A}_sW_s + \mathscr{B}_{us}\kappa_s \end{bmatrix}\begin{bmatrix} q_1I_n & p_1I_n \end{bmatrix}, \tag{7.67}$$

$$\begin{bmatrix} 0 & P_f \\ P_f & 0 \end{bmatrix} < \mathbf{He}\begin{bmatrix} -W_f \\ \mathscr{A}_{22}W_f + \mathscr{B}_2\kappa_f \end{bmatrix}\begin{bmatrix} q_2I_m & p_2I_m \end{bmatrix}, \tag{7.68}$$

$$\begin{bmatrix} -Q_l & 0 & P_l & 0 \\ \star & I_r & 0 & 0 \\ \star & \star & \omega_c^2Q_l & 0 \\ \star & \star & \star & -\gamma_1^2I_q \end{bmatrix} < \mathbf{He}\begin{bmatrix} -I_n & 0 & 0 \\ 0 & -I_r & 0 \\ \mathscr{A}_s & \mathscr{B}_{ws} & \mathscr{B}_{us} \\ \mathscr{C}_s & \mathscr{E}_{ws} & \mathscr{D}_{us} \end{bmatrix}\begin{bmatrix} W_sR_l \\ V_{l2} \\ \kappa_sR_l \end{bmatrix}. \tag{7.69}$$

Feasible state feedback sub-controller gains are then given by $K_l = \kappa_sW_s^{-1}$ and $K_h = \kappa_fW_h^{-1}$ such that the composite state feedback controller gain is

$$K_p = \begin{bmatrix} K_l + K_hA_{22}^{-1}A_{21} + K_hA_{22}^{-1}B_2K_l & K_h \end{bmatrix}.$$

Proof Under normal weather conditions, the major energy of wind is concentrated in the low frequency range, and the slow modes (translational dynamics) are more easily affected by the external disturbance compared with the fast modes (orientational dynamics). Low frequency characteristic of the whole fight system can be represented by the low-frequency cut-off subsystem Σ_l. In other words, fast modes have the high-pass property, and they can resist the low-frequency disturbance without input control. In this case, the following requirement should be satisfied:

1. The internal stability property of the whole system (7.64) should be satisfied.
2. The H_∞ norm index for the low-frequency cut-off subsystem Σ_l should be kept,

$$\|T_{\text{low}}(s)\|_\infty < \gamma_1.$$

State feedback controller gains K_l and K_h are designed, respectively. Next, we present methods to design the composite state feedback controller which can be applied to the original ill-conditioned system (7.64).

It follows from Lemma 1.3 that, for sufficiently small ε, $u = K_p x$ is an internally stabilizing controller, and $\|G(s,\varepsilon)\|_{zw} < \gamma + O(\varepsilon)$ is satisfied for singularly perturbed system (3.5). From [70], a composite controller in the normal weather conditions is formulated as

$$K_p = \left[K_l + K_h A_{22}^{-1} A_{21} + K_h A_{22}^{-1} B_2 K_l \;\; K_h \right].$$

Theorem 7.5 (Design of Wind Dust Controller) *For given cut-off frequency ω_c, given scalars $\gamma_1 > 0$, $\gamma_2 > 0$, p_1, q_1, p_2 and q_2 satisfying $p_1 q_1 > 0$, $p_2 q_2 > 0$ and $\gamma_1 \gg \gamma_2$, and matrices R_l and R_h, the closed-loop SPS (7.64) achieves H_∞ property in the entire frequency range, namely*

1. *the closed-loop subsystem (7.64) is internally stable for $\varepsilon \in (0, \varepsilon^*]$,*
2. *$\|T_{low}(s)\|_\infty^{\Lambda_l} < \gamma_1$, $\|T_{high}(p)\|_\infty^{\Lambda_h} < \gamma_2$,*

if there exist symmetric matrices W_s, W_f, $P_s > 0$, $P_f > 0$, P_l, P_h and $Q_l > 0$, $Q_h > 0$ such that the following LMIs hold:

$$\begin{bmatrix} 0 & P_s \\ P_s & 0 \end{bmatrix} < \mathbf{He} \begin{bmatrix} -W_s \\ \mathscr{A}_s W_s + \mathscr{B}_{us} \kappa_s \end{bmatrix} \begin{bmatrix} q_1 I_n \\ p_1 I_n \end{bmatrix}^T, \tag{7.70}$$

$$\begin{bmatrix} 0 & P_f \\ P_f & 0 \end{bmatrix} < \mathbf{He} \begin{bmatrix} -W_f \\ \mathscr{A}_{22} W_f + \mathscr{B}_2 \kappa_f \end{bmatrix} \begin{bmatrix} q_2 I_m \\ p_2 I_m \end{bmatrix}^T, \tag{7.71}$$

$$\begin{bmatrix} -Q_l & 0 & P_l & 0 \\ \star & I_r & 0 & 0 \\ \star & \star & \omega_c^2 Q_l & 0 \\ \star & \star & \star & -\gamma_1^2 I_q \end{bmatrix} < \mathbf{He} \begin{bmatrix} -I_n & 0 & 0 \\ 0 & -I_r & 0 \\ \mathscr{A}_s & \mathscr{B}_{ws} & \mathscr{B}_{us} \\ \mathscr{C}_s & \mathscr{E}_{ws} & \mathscr{D}_{us} \end{bmatrix} \begin{bmatrix} W_s R_l \\ V_{l2} \\ \kappa_s R_l \end{bmatrix}, \tag{7.72}$$

$$\begin{bmatrix} Q_h & 0 & P_h & 0 \\ \star & I_r & 0 & 0 \\ \star & \star & -(\omega_c/\varepsilon)^2 Q_l & 0 \\ \star & \star & \star & -\gamma_2^2 I_q \end{bmatrix} < \mathbf{He} \begin{bmatrix} -I_m & 0 & 0 \\ 0 & -I_r & 0 \\ \mathscr{A}_{22} & \mathscr{B}_{w2} & \mathscr{B}_{u2} \\ \mathscr{C}_2 & \mathscr{E}_{wf} & \mathscr{D}_1 \end{bmatrix} \begin{bmatrix} W_f R_h \\ V_{h2} \\ \kappa_f R_h \end{bmatrix}. \tag{7.73}$$

Feasible state feedback sub-controller gains are given by $K_l = \kappa_s W_s^{-1}$ *and* $K_h = \kappa_f W_h^{-1}$ *such that the composite state feedback controller gain subject to wind dust turbulence is*

$$K_t = \left[K_l + K_h A_{22}^{-1} A_{21} + K_h A_{22}^{-1} B_2 K_l \; K_h \right].$$

Proof Wind dust is a special type of wind, which contains abundant high frequency components. The attitudes corresponding to fast modes are easily affected at the existence of wind dust. Under these conditions, the following constraints should be satisfied:

1. the closed-loop subsystem (7.64) is internally stable for $\varepsilon \in (0, \varepsilon^*]$,
2. $\|T_{\text{low}}(s)\|_\infty^{\Lambda_l} < \gamma_1$, $\|T_{\text{high}}(p)\|_\infty^{\Lambda_h} < \gamma_2$, $\gamma_1 > \gamma_2$.

Note that Requirement 2 balances the input energy saving with hovering capability of the UAV. The following proof is similar as that of Theorem 7.4, which is omitted here.

7.3.3 The Flexible Strategy

Next, we introduce the control strategy for the miniature UAV. Contrast with the existing H_∞ hovering control, external disturbance characteristics are taken into consideration to achieve better disturbance attenuation capability and save the energy of control input u. Different types of disturbances are handled by different composite controllers.

- Under normal weather conditions, the miniature UAV hovers in the air with external disturbances such as breeze and background noises. Under this circumstance, the power spectrum of wind is mainly fixed in the low frequency range such that translational dynamics corresponding to slow modes are easily affected. According to Theorem 7.4, the proper controller K_p is adopted to restrain the low-frequency disturbances.
- Under severe weather conditions such as wind gusts, the H_∞ hovering control should also play a role to guarantee the desired hovering capability of the UAV. In this case, there is a significant power bump in the high frequency ranges with the main power spectrum still in the low frequency range. Effects from high-frequency disturbances to orientational dynamics cannot be neglected directly. Thus, we design a particular controller K_t based on Theorem 7.5 to restrain both low- and high-frequency disturbances.
- We set the stop frequency w_{stop} to protect the aircraft health. If wind frequency exceeds w_{stop}, a UAV should not execute the associated flight task.

The composite state feedback algorithm is

$$K = \begin{cases} K_p & 0 < \omega < \omega_c \\ K_t & \omega_c < \omega < \omega_{\text{stop}} \end{cases}$$

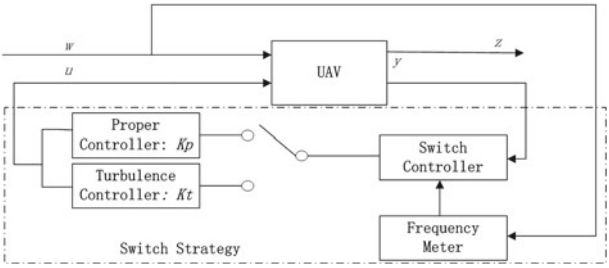

Fig. 7.5 The switch strategy for H_∞ hovering control

which aims at balancing hardware cost with system performances, and the switch strategy is illustrated in Fig. 7.5.

Remark 7.6 We found that the finite frequency control is well suited for the miniature UAV which have abundant dynamics due to the unique frequency nature of SPSs. Moreover, wind disturbances are considered to avoid the unnecessary frequency overlap of reduced-order subsystems. The key feature of the switching strategy is stated:

1. Frequency division in states: the construction of the low- and high-frequency subsystems is realized through slow-fast decomposition, and sub-controllers are designed based on these subsystems. The dominant frequency components in related frequency ranges are extracted.
2. Frequency division in external disturbance: wind is taken into consideration due to the distinctive disturbance sensitivity of low- and high-frequency components. Turbulence is a special type of wind whose power spectrum is focused in the high frequency range. We set the trade-off frequency ω_c to detect the existence of turbulence flows. In this sense, we design the control law K_p and K_t to retrain different types of disturbances.

7.3.4 Numerical Examples

Prior to the practical implementation, we have carried out a series of MATLAB®-based simulations to demonstrate the validity of the proposed method. For given parameters in Table 7.4, trade-off frequencies are selected as $\omega_c = 50\,\text{rad/s}$ and $\omega_{\text{stop}} = 100\,\text{rad/s}$.

With aid of SPTs, a miniature UAV modelled in (7.64) can be decoupled into slow and fast subsystems, and the related low- and high-frequency cut-off subsystems Σ_l, Σ_h are constructed based on them.

Based on Theorem 7.4, we have designed the H_∞ controller for the system Σ_l, and the frequency responses of the open-loop and closed-loop transfer-function matrices are shown in Fig. 7.6, respectively. From the left picture of Fig. 7.6, we can see that the low-frequency components have been extracted because all these modes have

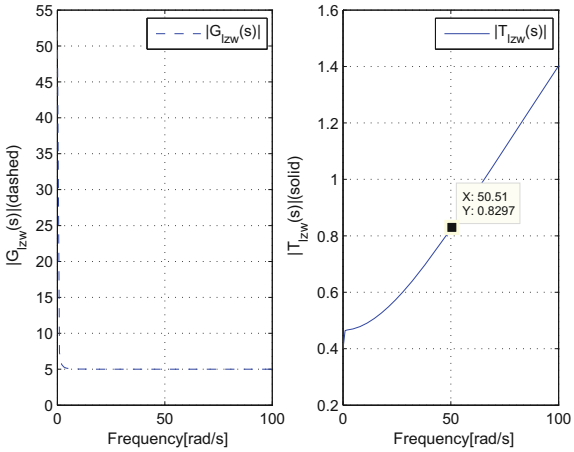

Fig. 7.6 The frequency response of low-frequency subsystem

low-pass property. In other words, for the high-frequency external disturbances, these slow states, themselves, can restrain such disturbances to some extent without the help of state feedback controllers. The right side of Fig. 7.6 has shown that the amplitude response from the external disturbance to the measurement output after introduction of K_l has been restrained below γ_1 in which $\gamma_1 = 1.266$. The LMI solutions are shown below:

$$P_s = \begin{bmatrix} 7333 & 6387 \\ 6387 & 10949 \end{bmatrix} > 0,\ \kappa_s = \begin{bmatrix} 130.9524 & 209.4434 \\ -148.8170 & -120.9878 \end{bmatrix},$$
$$Q_l = \begin{bmatrix} 0.3908 & -0.4800 \\ -0.4800 & 1.7243 \end{bmatrix} > 0,\ P_l = \begin{bmatrix} 2440 & -5289 \\ -5289 & 11470 \end{bmatrix},\ W_s = \begin{bmatrix} -2453 & 5268 \\ 5268 & -11496 \end{bmatrix}.$$

The sub-controller K_l is formulated as

$$K_l = \begin{bmatrix} -5.8379 & -2.6936 \\ -2.6936 & 2.4186 \end{bmatrix}.$$

Similarly, the frequency responses of the open-loop and closed-loop high-frequency subsystems, are demonstrated in Fig. 7.7. The high-frequency oscillators are totally extracted which have the high pass property and achieve high speed of state variation than the low-frequency ones. In the high frequency range $\Lambda_h = |\bar{w}| > 50$ rad/s, the effects from the external disturbances to the measurement output has been restrained under 0.13. In this sense, the orientational dynamics can be viewed as keeping unchanged.

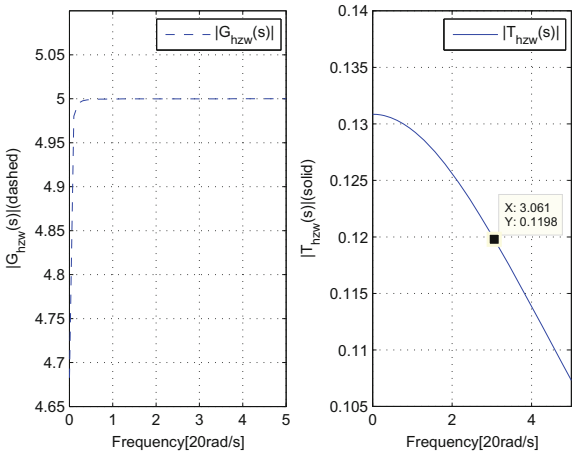

Fig. 7.7 The frequency response of high-frequency subsystem

The related solutions for Theorem 7.5 are shown below,

$$P_s = \begin{bmatrix} 1.6632 & -0.3798 \\ -0.3798 & 1.2179 \end{bmatrix} > 0,\ \kappa_f = \begin{bmatrix} 0.2514 & -0.0598 \\ -0.0598 & 0.1834 \end{bmatrix},$$
$$Q_h = \begin{bmatrix} 0.2030 & -0.0158 \\ -0.0158 & 0.2473 \end{bmatrix} > 0,\ P_h = \begin{bmatrix} 0.2249 & -0.0071 \\ -0.0071 & 0.2151 \end{bmatrix},\ W_s = \begin{bmatrix} -0.2249 & 0.0071 \\ 0.0071 & -0.2151 \end{bmatrix}.$$

The sub-controller K_h is formulated as

$$K_h = \begin{bmatrix} -1.1100 & 0.2414 \\ 0.2379 & -0.8448 \end{bmatrix}.$$

Based on the composite strategy, the composite state feedback control which is applied into the whole system (7.64) is

$$K = \begin{bmatrix} 1700.6 & 573.2 & -1.1 & 0.2 \\ -879.2 & 337.7 & 0.2 & -0.8 \end{bmatrix}.$$

The effectiveness of the composite controller K is depicted in Fig. 7.8. The comparison between Figs. 7.6, 7.7 and 7.8 indicates that the frequency characteristics of the original flight system in the low (high) frequency range can be described by that of its low-frequency subsystem Σ_l (high-frequency subsystem Σ_h).

Based on Theorems 7.4–7.5, we design the normal controller K_p and the turbulence controller K_t to restrain different types of disturbances.

$$K_p = \begin{bmatrix} 456.6 & -434.2 & 1.6 & 0.8 \\ -79.2 & 304.7 & 0.2 & -0.7 \end{bmatrix},\quad K_t = \begin{bmatrix} -56.6 & 34.2 & -1.55 & 0.8 \\ 78.2 & -44.7 & 0.8 & -1.7 \end{bmatrix}.$$

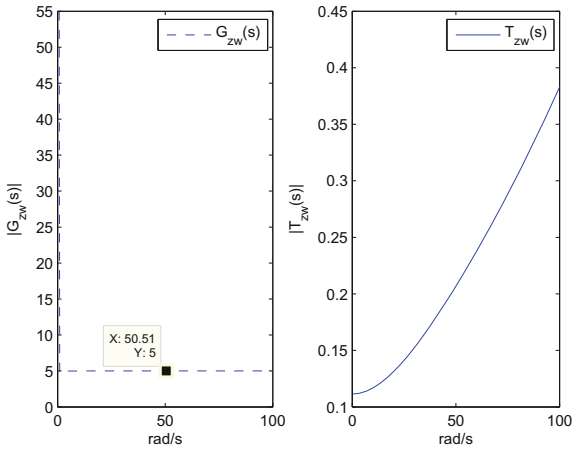

Fig. 7.8 The frequency response of the whole system (7.64)

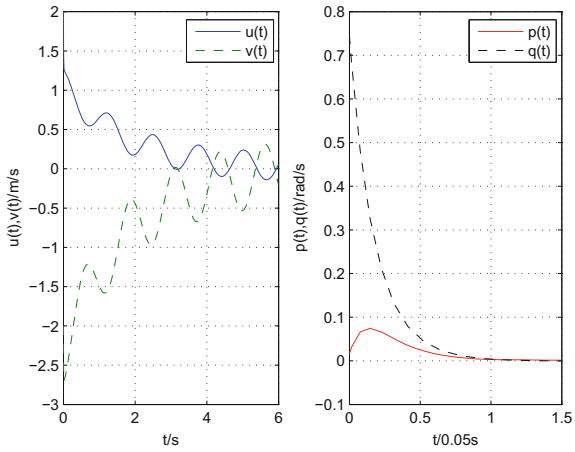

Fig. 7.9 The disturbance attenuation ability of u, v, p, q under basic wind

To further explain the effectiveness of our results, we have conducted a series of time-domain simulations. From the frequency domain perspective, the wind can be viewed as a combination of multiple frequency components. The first simulation assumes a UAV is subject to a constant but relatively mild wind disturbance with the amplitude of $V = 0.8$ m/s and $w = 3$ rad/s. Figure 7.9 demonstrates the effectiveness of our proposed method in terms of disturbance rejection for both translational and oriental dynamics. It can be observed that the velocities u and v are restrained to 0.4 m/s so that the UAV slightly wave with the wind. In this case, there is almost no affects from the wind disturbances to the orientational dynamics p, q. In other words, the disturbance attenuation ability of the translational dynamics is undemanding to save the input energy whereas we should improve the disturbance attenuation ability of the orientational dynamics to guarantee the UAV maintains its steady state.

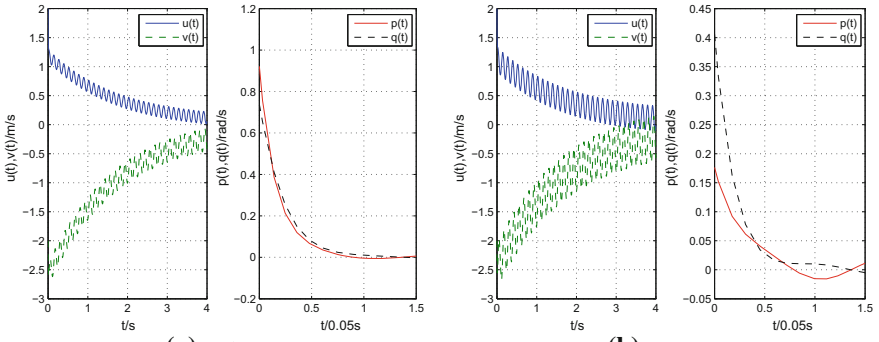

(a) V=5 m/s **(b)** V=12 m/s

Fig. 7.10 The disturbance attenuation ability of u, v, p, q under wind gust

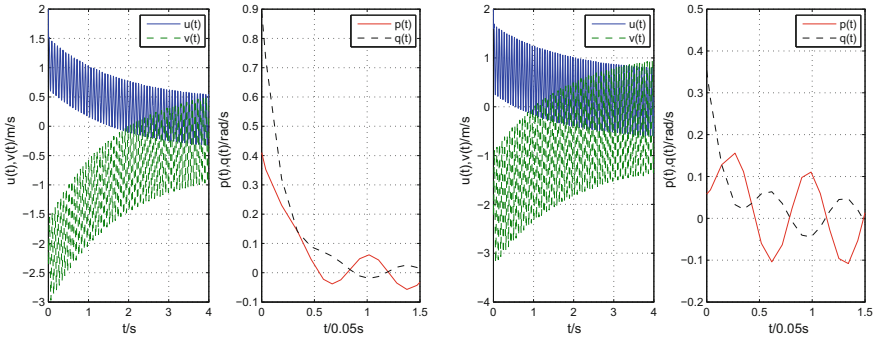

(a) V=19 m/s **(b)** V=26 m/s

Fig. 7.11 The disturbance attenuation ability of u, v, p, q under wind gust

As mentioned in the previous sections, wind gust causes sudden increase in speed or frequency, and thus cannot be neglected in miniature UAV control at hover. To demonstrate the effectiveness of the turbulence controller in presence of wind dust, have carried out simulations for wind gusts with different amplitudes. More specifically, wind gusts ranging from 5 to 26 m/s with the increment of 7 m/s are studied in Figs. 7.10 and 7.11. Note that disturbances have more effects on the translational dynamics u, v than the orientational dynamics p, q to save the input energy and keep the attitude of the UAV. Via the comparison of Figs. 7.10 and 7.11 with Fig. 7.9, we observe that the wind dust (high-frequency component) makes UAV shake more frequently. Through the turbulence controller, the status of the UAV is restricted in a small neighbourhood of the operating point (i.e., $u = v = 0$ m/s, $p = q = 0$ rad/s) so that the UAV will not lose its balance in the presence of different wind.

In this section, we have investigated the H_∞ control synthesis of miniature UAVs to improve its hovering capability by reduce the effects from wind to the measurement output. First and foremost, low- and high-frequency subsystems are constructed,

respectively, in the disjoint frequency ranges. Robust control specifications for subsystems are given in terms of multiple frequency domain inequalities in (semi)finite ranges, which can be converted into feasible LMIs by aid of the GKYP lemma. The composite controller, which consists of multiple sub-controllers, can be directly applied to stabilize the whole flight system and achieve the H_∞ control specification. A novel switch strategy is also proposed to guarantee good hovering capability under different weather conditions. A numerical example has been provided to show the usefulness of the proposed results.

7.4 Conclusion

In this chapter, we have investigated the engineering background of finite frequency control of SPSs. A detailed overview is given in Sect. 7.1. Two typical application examples are presented with wind turbines control using linear parameter varying singularly perturbed model given in Sect. 7.2 and robust H_∞ control of miniature quad-rotors in hovering given in Sect. 7.3 to show the effectiveness and merits of our methods from practical point of view.

References

1. Achleitner, F., Szmolyan, P.: Saddle-node bifurcation of viscous profiles. Phys. D **241**(20), 1703–1717 (2012)
2. Alvarez-Ramirez, J., Espinosa-Perez, G., Noriega-Pineda, D.: Current-mode control of DC-DC power converters: a backstepping approach. Int. J. Robust Nonlinear Control, pp. 421–442 (2003)
3. Avrachenkov, K., Litvak, N., Pham, K.S.: A singular perturbation approach for choosing the pagerank damping factor. Internet Mathematics **5**(1), 47–69 (2008)
4. Bakharev, F.L., Nazarov, S.A., Ruotsalainen, K.M.: A gap in the spectrum of the Neumann-Laplacian on a periodic waveguide. Appl. Anal. **92**(9), 1–27 (2012)
5. Barany, E., Schaffer, S., Wedeward, K., Ball, S.: Nonlinear controllability of singularly perturbed models of power flow networks. In: 43rd IEEE Conference on Decision and Control, vol. 5, pp. 4826–4832 (2004)
6. Beauwens, R., Mika, J.: The improved prompt jump approximation. Transp. Theory Stat. Phys. **36**(1–3), 211–225 (2007)
7. Bertrand, S., Hamel, T., Piet-Lahanier, H.: Stability analysis of an UAV controller using singular perturbation theory. In: The 17th International Federation of Automatic Control World Congress, pp. 5706–5711 (2008)
8. Bianchi, F.D., Battista, H.D., Mantz, R.J.: Wind Turbine Control Systems Principles. Modelling and Gain Scheduling Design. Springer, London (2007)
9. Biyik, E., Arcak. M.: Area aggregation and time scale modeling for sparse nonlinear networks. In: 45th IEEE Conference on Decision and Control, pp. 4046–4051 (2006)
10. Biyik, E., Arcak, M.: Area aggregation and time-scale modeling for sparse nonlinear networks. Syst. Control Lett. **57**(2), 142–149 (2008)
11. Bondarenko, V.V., Markov, Y.G., Mikisha, A.M., Rykhlova, L.V., Skorobogatykh, I.V.: Gravitational-tidal evolution of planetary subsystems of the Sun. Astron. Astrophys. Trans. **25**(4), 275–290 (2006)

12. Boskovic, J.D., Mehra, R.K.: A decentralized fault-tolerant control system for accommodation of failures in higher-order flight control actuators. IEEE Trans. Control Syst. Technol. **18**(5), 1103–1115 (2010)
13. Bristeau, P.J., Martin, P., Salaun, E., Petit, N.: The role of propeller aerodynamics in the model of a quadrotor UAV. In: Proceedings of the European Control Conference, pp. 683–688 (2009)
14. Bykov, V., Goldfarb, I., Goldshtein, V., Barry Greenberg, J.: Thermal explosion in a hot gas mixture with fuel droplets: a two reactant model. Combust. Theor. Model. **6**, 339–359 (2002)
15. Bykov, V., Goldshtein, V., Maas, U.: Simple global reduction technique based on decomposition approach. Combust. Theor. Model. **12**(2), 389–405 (2008)
16. Cai, G., Chen, B.M., Lee, T.H.: Unmanned Rotorcraft Systems. Springer, New York (2011)
17. Cai, G., Wang, B., Chen, B.M., Lee, T.H.: Design and implementation of a flight control system for an unmanned rotorcraft using RPT control approach. Asian J. Control **15**(1), 95–119 (2013)
18. Cao, X.T., Li, Y.C.: Distributed parameter singular perturbation model and cooperative control of flexible manipulators. Proceedings of 2005 International Conference on Machine Learning and Cybernetics **2**, 1009–1014 (2005)
19. Castellanos-Sahagun, E., Alvarez, J.: Synthesis of two-point linear controllers for binary distillation columns. Chem. Eng. Commun. **193**(2), 206–232 (2006)
20. Celikovsky, S., Papacek, S., Cervantes Herrera, A., Ruiz Leon, J.: Singular perturbation based solution to optimal microalgal growth problem and its infinite time horizon analysis. In: 47th IEEE Conference on Decision and Control, pp. 2662–2667 (2008)
21. Cervantes, I., Kelly, R., Alvarez-Ramirez, J., Moreno, J.: A robust velocity field control. IEEE Trans. Control Syst. Technol. **10**(6), 888–894 (2002)
22. Chakrabortty, A., Scholtz, E.: Time-scale separation designs for performance recovery of power systems with unknown parameters and faults. IEEE Trans. Control Syst. Technol. **19**(2), 382–390 (2011)
23. Chen, Y., Liu, Y.Q.: Summary of singular perturbation modeling of multi-time scale power systems. In: 2005 IEEE/PES Transmission and Distribution Conference and Exhibition: Asia and Pacific, pp. 1–4 (2005)
24. Chen, H.H.: Stability and chaotic dynamics of a rate gyro with feedback control under uncertain vehicle spin and acceleration. J. Sound Vib. **273**(4–5), 949–968 (2004)
25. Cheng, M.B., Radisavljevic, V., Chang, C.C., Lin, C.F., Su, W.C.: A sampled-data singularly perturbed boundary control for a heat conduction system with noncollocated observation. IEEE Trans. Autom. Control **54**(6), 1305–1310 (2009)
26. Cheong, J., Youm, Y., Chung, W.K.: Joint tracking controller for multi-link flexible robot using disturbance observer and parameter adaptation scheme. J. Robotic Syst. **19**(8), 401–417 (2002)
27. Cheong, J., Chung, W.K., Youm, Y.: PID composite controller and its tuning for flexible link robots. Proc. IEEE Int. Conf. Intell. Robots Syst. **19**(8), 2122–2127 (2002)
28. Cheong, J., Chung, W.K., Youm, Y.: Inverse kinematics of multilink flexible robots for high-speed applications. IEEE Trans. Robot. Autom. **20**(2), 269–282 (2004)
29. Chevallereau, C.: Time-scaling control for an underactuated biped robot. IEEE Trans. Robot. Autom. **19**(2), 362–368 (2003)
30. Contou-Carrere, M.N., Sotiropoulos, V., Kaznessis, Y.N., Daoutidis, P.: Model reduction of multi-scale chemical Langevin equations. Syst. Control Lett. **60**(1), 75–86 (2011)
31. Dabney, J.B., Ghorbel, F.H., Wang, Z.Y.: Modeling closed kinematic chains via singular perturbations. Proc. Am. Control Conf. **5**, 4104–4110 (2002)
32. Dai, J.H., Gu, E.: Trajectory-tracking control of a multiple flexible joint robot based on singular perturbation. Proc. 5th Biannual World Autom. Congr. **14**, 77–82 (2002)
33. Dai, J.H., Gu, E.: Singular perturbation method in control of multiple flexible-joint robots. Intell. Autom. Soft Comput. **9**(2), 121–128 (2003)
34. Duan, C.Y., Zhang, Y.X., Dong, C.Y., Sun, R.: Adaptive sliding mode control for bank-to-turn missiles. In: 9th International Conference on Electronic Measurement and Instruments, pp. 3512–3517 (2009)

35. Esteban, S., Rivas, D.: Singular perturbation control of the longitudinal flight dynamics of a UAV. In: UKACC International Conference on Control, pp. 310–315 (2012)
36. Esteban, S., Rivas, D.: Singular perturbation control of the longitudinal flight dynamics of an UAV. In: 2012 UKACC International Conference on Control, pp. 310–315 (2012)
37. Flores, G., Lozano, R.: Lyapunov-based controller using singular perturbation theory: an application on a mini-UAV. Proc. Am. Control Conf. **45**, 1596–1601 (2013)
38. Fradkov, A., Andrievsky, B.: Singular perturbations of systems controlled by energy-speed-gradient method. In: 43rd IEEE Conference on Decision and Control, vol. 4, pp. 3441–3446 (2004)
39. Fraser, S.J.: Slow manifold for a bimolecular association mechanism. J. Chem. Phys. **120**(7), 3075–3085 (2004)
40. Fridman, L.M.: Slow periodic motions with internal sliding modes in variable structure systems. Int. J. Control **75**(7), 524–537 (2002)
41. Fridman, L.: Slow periodic motions in variable structure systems. Int. J. Syst. Sci. **33**(14), 1145–1155 (2002)
42. Fu, D.F., Xing, Y.: Study on linear dynamic model and analysis of operating characteristics of high-power VSCF wind energy conversion system. In: World Non-Grid-Connected Wind Power and Energy Conference, pp. 1–6 (2009)
43. Fu, L., Wang, L.L., Hu, J.H.: Coning algorithm based on singular perturbation. Aircr. Eng. Aerosp. Technol. **85**(3), 178–185 (2013)
44. Galli, M., Groppi, M., Riganti, R., Spiga, G.: Singular perturbation techniques in the study of a diatomic gas with reactions of dissociation and recombination. Appl. Math. Comput. **146**(2–3), 509–531 (2003)
45. Gandhi, P.S., Ghorbel, F.: High-speed precision tracking with harmonic drive systems using integral manifold control design. Int. J. Control **78**(2), 112–121 (2005)
46. Ganjefar, S.: Adaptive wavenet controller design for teleoperation systems with variable time delays using singular perturbation method. Int. J. Control Autom. Syst. **11**(3), 597–607 (2013)
47. Garijo, A., Marotta, S.M., Russell, E.D.: Singular perturbations in the quadratic family with multiple poles. J. Differ. Equ. Appl. **19**(1), 124–145 (2013)
48. Ghaoui, L.E., Feron, E., Balakrishnan, V.: Linear Matrix Inequalities in System and Control Theory. Philadelphia: Society for industrial and applied mathematics (1994)
49. Gorinevsky, D., Nwadiogbu, E., Mylaraswamy, D.: Model-based diagnostics for small-scale turbomachines. In: Proceedings of the 41st IEEE Conference on Decision and Control, vol. 4, pp. 1–5 (2002)
50. Han, D.K., Chang, P.H.: A robust two-time-scale control design for a pneumatic vibration isolator. In: 46th IEEE Conference on Decision and Control, pp. 1666–1672 (2007)
51. Hasson, J., Bobrovsky, B.Z.: Optimal design of an all-digital chip timing recovery loop for direct-sequence spreads pectrum systems. Eur. Trans. Telecommun. **16**(6), 509–520 (2004)
52. Heiges, M.W., Menon, P.K.A., Achrage, D.P.: Synthesis of a helicoptor full-authority controller. J. Guidance **15**(1), 222–227 (1989)
53. Heldt, T., Chang, J.L., Chen, J.J.S., Verghese, G.C., Mark, R.G.: Cycle-averaged dynamics of a periodically driven, closed-loop circulation model. Control Eng. Pract. **13**(9), 1163–1171 (2005)
54. Hong, J.W., Yeom, J.H., Song, S.H., Ha, I.J.: A singular perturbation-like method to compensate the effect of fin-actuator dynamics in nonlinear missile control. In: SICE-ICASE International Joint Conference, pp. 837–841 (2006)
55. Huang, Y., Cai, C., Zou, Y.: Output feedback finite frequency H_∞ control for SISO singularly perturbed systems. In: Asian Control Conference, pp. 1188–1192 (2009)
56. Huang, H., Hoffman, G.M., Waslander, S.L., Tomlin, C.J.: Aerodynamics and control of autonumous quadrotor helicopters in aggressive maneuvering. In: Proceedings of the IEEE International Conference on Robotics and Automation, pp. 3277–3282 (2009)
57. Huang, Y., Cai, C., Zou, Y.: Finite frequency positive real control for singularly perturbed systems. Int. J. Control Autom. Syst. **9**(2), 376–383 (2011)

58. Jagodzinski, S., Lachowicz, M.: On two incompressible hydrodynamic limits of the Boltzmann-Enskog Equation. I. formal derivations. Transp. Theory Stat. Phys. **33**(2), 157–181 (2004)
59. Jagodzinski, S., Lachowicz, M.: On two incompressible hydrodynamic limits of the Boltzmann-Enskog Equation II: a rigorous result. Transp. Theory Stat. Phys. **34**(6), 447–474 (2004)
60. Jaison, S., Naidu, D.S., Zydek, D.: Time scale analysis and synthesis of wind energy conversion systems. In: Proceedings of the WSEAS-NAUN 4th International Conference on Circuits, Systems, Control and Signals, pp. 21–26 (2013)
61. Jogwar, S.S., Baldea, M., Daoutidis, P.: Dynamics and control of reactor- feed effluent heat exchanger networks. In: Proceedings of the American Control Conference, pp. 1481–1486 (2008)
62. Kaper, H.G., Kaper, T.J.: Asymptotic analysis of two reduction methods for systems of chemical reactions. Phys. D **165**(1–2), 66–93 (2002)
63. Kapitonov, B.V., Raupp, M.A.: Boundary observation and exact control of multilayered piezoelectric body. Math. Methods Appl. Sci. **26**(5), 431–452 (2003)
64. Keesman, K.J.: State and parameter estimation in biotechnical batch reactors. Control Eng. Pract. **10**(2), 219–225 (2002)
65. Keesman, K.J., Peters, D., Lukasse, L.J.S.: Optimal climate control of a storage facility using local weather forecasts. Control Eng. Pract. **11**(5), 505–516 (2003)
66. Kellogg, R.B., Stynes, M.: A singularly perturbed convection-diffusion problem in a half-plane. Appl. Anal. **85**(12), 1471–1485 (2006)
67. Khalil, H.K., Chen, F.: H_∞ control of two-time-scale systems. Proc. Am. Control Conf. **19**, 1151–1152 (1992)
68. Kimball, J.W., Krein, P.T.: Singular perturbation theory for DC-DC converters and application to PFC converters. In: IEEE Power Electronics Specialists Conference, pp. 882–887 (2007)
69. Kimball, J.W., Krein, P.T.: Singular perturbation theory for DC-DC converters and application to PFC converters. IEEE Trans. Power Electron. **23**(6), 2970–2981 (2008)
70. Kokotovic, P., Khalil, H., O'Reilly, J.: Singular Perturbation Methods in Control: Analysis and Design. Academic Press, New York (1986)
71. Krishnamurthy, V., Monfared, S.M., Cornell, B.: Ion channel biosensors–part II: dynamic modeling, analysis, and statistical signal processing. IEEE Trans. Nanotechnol. **9**(3), 313–321 (2010)
72. Lam, S.H.: Model reductions with special CSP data. Combust. Flame **160**(2), 2707–2711 (2013)
73. Li, X.Y., Chen, X.H., Tang, G.Q.: Output feedback control of doubly-fed induction generator based on multi-time scale model. In: Third International Conference on Electric Utility Deregulation and Restructuring and Power Technologies, pp. 2798–2802 (2008)
74. Li, D., Chen, C.: Wind speed model for dynamic simulation of wind power generation system. In: Proceedings of the CSEE (November 2005)
75. Li, K., Phang, S.K., Chen, B.M., Lee, T.H.: Platform design and mathematical modeling of an ultralight quadrotor helicopters in aggressive maneuvering. In: Proceedings of the International Conference on Unmanned Aircraft Systems, pp. 1066–1075 (2013)
76. Li, Y., Wang, J., Yang, G.: Sub-optimal linear quadratic control for singularly perturbed systems. In: Proceedings of the 40th IEEE Conference on Decision and Control, vol. 2, pp. 3698–3703 (2001)
77. Li, P., Zhang, B.H., Shu, J., Bo, Z.Q., Klimek, A.: Research on order reduction of power system modeling for dynamic voltage stability analysis. In: IEEE PES Transmission and Distribution Conference and Exposition, pp. 1–5 (2010)
78. Liu, H., Sun, F., He, K., Sun, Z.: Survey of singularly perturbed control systems: theory and applications. Control Theory Appl. **20**(1), 1–7 (2003)
79. Liu, H., Sun, F., Hu, Y.: H_∞ control for fuzzy singularly perturbed systems. J. Fuzzy Sets Syst. **155**(2), 272–291 (2005)

80. Lizarraga, I., Etxebarria, V.: Combined PD-H_∞ approach to control of flexible link manipulators using only directly measurable variables. Cybern. Syst. **34**(1), 19–31 (2003)
81. Luse, D.W.: Frequency domain results for systems with multiple time scales. IEEE Trans. Autom. Control **31**(10), 918–924 (1986)
82. Luse, D.W., Khail, H.K.: Frequency domain results for systems with slow and fast dynamics. IEEE Trans. Autom. Control **30**(12), 1171–1179 (1985)
83. Ma, F., Fu, L.J.: Principle of multi-time scale order reduction and its application in AC/DC hybrid power systems. In: International Conference on Electrical Machines and Systems, pp. 3951–3956 (2008)
84. Manhartsgruber, B.: Stability analysis of the servohydraulic equations with linear state feedback and harmonic reference signal. Nonlinear Dyn. Eng. Syst. **3**(1), 92–95 (2003)
85. Massoum, A., Fellah, M.K., Meroufel, A., Wira, P., Bendaoud, A.: Neuro-fuzzy control of a singularly perturbed permanent magnet synchronous machine fed by a three levels inverter. In: IEEE International Symposium on Industrial Electronics, pp. 1867–1872 (2008)
86. Mastellone, S., Stipanovic, D.M., Spong, M.W.: Multi-agent formation control and trajectory tracking via singular perturbation. In: IEEE International Conference on Control Applications, pp. 557–562 (2007)
87. Mease, K.: Multiple time-scales in nonlinear flight mechanics: diagnosis and modeling. Appl. Math. Comput. **164**(2), 627–648 (2005)
88. Mei, P., Cai, C., Zou, Y.: A generalized KYP lemma based approach for H_∞ control of singularly perturbed systems. Circuits Syst. Signal Proc. **28**(6), 945–957 (2009)
89. Meyer-Baese, A., Cappendijk, S., Althaus, E.: Global uniform stability analysis of biological networks with different time-scales under perturbations. In: International Joint Conference on Neural, pp. 2098–2102 (2009)
90. Monfared, S.M., Krishnamurthy, V., Cornell, B.: Stochastic modeling and signal processing of nano-scale protein-based biosensors. In: IEEE International Workshop on Genomic Signal Processing and Statistics, pp. 1–6 (2009)
91. Munteanu, I., Bratcu, A., Cutululis, N., Ceanga, E.: Optimal Control of Wind Energy Systems: Towards a Global Approach. Springer, London (2008)
92. Naidu, D.S.: Analysis of non-dimensional forms of singular perturbation structures for hypersonic vehicles. Acta Astronaut. **66**(3–4), 577–586 (2010)
93. Naidu, D.S.: Singular perturbation analysis of a flexible beam used in underwater exploration. Int. J. Syst. Sci. **42**(1), 183–194 (2011)
94. Naidu, D.S., Calise, A.J.: Singular perturbation methods and time scales in guidance and control of aerospace systems: a survey. AIAA J. Guidance Control Dyn. **24**(6), 1057–1078 (2001)
95. Nakada, K., Sato, Y.D., Matsuoka, K.: Theoretical analysis of phase resetting on matsuoka oscillators. In: Advances in Cognitive Neurodynamics (III), pp. 531–536. Springer, Netherlands (2013)
96. Nguyen, H.M., Naidu, D.S.: Singular perturbation analysis and synthesis of wind energy conversion systems under stochastic environments. In: Advances in Systems Theory, Signal Processing and Computational Science, pp. 283–288 (2012)
97. Nguyen, H.M., Naidu, D.S.: Time scale analysis and control of wind energy conversion systems. In: 5th International Symposium on Resilient Control Systems, pp. 149–154 (2012)
98. Nguyen, H.M.: Advanced Control Strategies for Wind Energy Conversion Systems, Ph.D. thesis, Idaho State University, USA (2013)
99. Nguyenn, H.M., Naidu, D.S.: Time scale anal-ysis and control of wind energy conversion systems. In: Proceedings of the 5th International Symposium on Resilient Control Systems, pp. 149–154 (2012)
100. Nie, L., Teng, Z.D.: Singular perturbation method for global stability of ratio-dependent predator-prey models with stage structure for the prey. Electron. J. Differ. Equ. **2013**(86), 1–9 (2013)
101. Oloomi, H., Shafai, B.: Two-time-scale distributions and singular perturbations. Int. J. Control **77**(11), 1040–1049 (2004)

102. Ott, C., Albu-Schaffer, A., Hirzinger, G.: Comparison of adaptive and nonadaptive tracking control laws for a flexible joint manipulator. IEEE/RSJ Int. Conf. Intell Robots Syst. **2**, 2018–2024 (2002)
103. Pang, C.K., Lewis, F.L., Ge, S.S., Guo, G.X., Chen, B.M., Lee, T.H.: Singular perturbation control for vibration rejection in HDDs using the PZT active suspension as fast subsystem observer. IEEE Trans. Industr. Electron. **54**(3), 1375–1386 (2007)
104. Park, No-Cheol, Yang, Hyun-Seok, Park, Hyung-Wug, Park, Young-Pil: Position/vibration control of two-degree-of-freedom arms having one flexible link with artificial pneumatic muscle actuators. Robotics Auton. Syst. **40**(4), 239–253 (2002)
105. Pekarek, S.D., Lemanski, M.T., Walters, E.A.: On the use of singular perturbations to neglect the dynamic saliency of synchronous machines. IEEE Trans. Energy Convers. **17**(3), 385–391 (2002)
106. Peng, S.T., Sheu, J.J., Chang, C.C.: A control scheme for automatic path tracking of vehicles subject to wheel slip constraint. Proc. Am. Control Conf. **1**, 804–809 (2004)
107. Prochaska, M., Probst, F.A., Mathis, W.: Analysis of emitter-coupled multivibrators by singularly perturbed systems. Math. Comput. Model. Dyn. Syst. **13**(6), 531–543 (2007)
108. Qi, Z.Q., Hu, G.D., Yang, Z.H., Zhang, F.E.: Flight guidance control using genetic algorithm combined with singular perturbation technique. Int. Conf. Mach. Learn. Cybern. **2**, 1034–1038 (2003)
109. Qiao, Q.Q., Chen, W.C.: A near optimal midcourse guidance law for air-to-air missile. Appl. Mech. Mater. **336–338**, 833–838 (2013)
110. Ramnath, R.V.: Multiple Scales Theory and Aerospace Applications. AIAA, Reston (2010)
111. Rasmussen, B., Alleyne, A., Shah, R.: Reduced order modeling of transcritical AC system dynamics using singular perturbation. Proc. Am. Control Conf. **3**, 2264–2269 (2003)
112. Rattanakul, C., Lenbury, Y., Krishnamara, N., Wollkind, D.J.: Modeling of bone formation and resorption mediated by parathyroid hormone: response to estrogen/PTH therapy. Biosyst. **70**, 55–72 (2003)
113. Rawn, B.G., Lehn, P.W., Maggiore, M.: Toward controlled wind farm output: adjustable power filtering. In: IEEE Power Engineering Society General Meeting, pp. 1–6 (2006)
114. Rawn, B.G., Lehn, P.W., Maggiore, M.: Control methodology to mitigate the grid impact of wind turbines. IEEE Trans. Energ. Convers. **22**(2), 431–438 (2007)
115. Renezeder, H.C., Steindl, A., Troger, H.: On the dynamics of axially moving strings. Proc. Appl. Math. Mech. **4**(1), 201–202 (2004)
116. Riaza, R., Zufiria, P.J.: Differential-algebraic equations and singular perturbation methods in recurrent neural learning. Dyn. Syst. **18**(1), 89–105 (2003)
117. Riva, M.D.: Stokes flow in a singularly perturbed exterior domain. Complex Variables Elliptic Equ. **58**(2), 231–257 (2013)
118. Ruan, S.G., Xiao, D.M.: Stability of steady states and existence of travelling waves in a vector-disease model. In: Proceedings of the Royal Society of Edinburgh, pp. 991–1011 (2004)
119. Runge, J., Oswald, B.R.: Modelling of a controlled doubly fed induction machine for the use in offshore wind power plants. In: 39th International Universities Power, Engineering Conference, pp. 1155–1159 (2004)
120. Salmasi, H., Fotouhi, R., Nikiforuk, P.N.: On the stability of a friction compensation strategy for flexible-joint manipulators. Adv. Robot. **24**(15), 2059–2086 (2010)
121. Savva, N., Kalliadasis, S.: Droplet motion on inclined heterogeneous substrates. J. Fluid Mech. **725**, 462–491 (2013)
122. Selisteanu, D., Petre, E., Roman, M., Bobasu, E.: Structural properties and reduced order modeling of a class of bioprocesses. In: Proceedings of the 2010 International Conference on Modeling, Identification and Control, pp. 88–93 (2010)
123. Shao, Z.Y., Zhang, X.D.: Intelligent control of flexible-joint manipulator based on singular perturbation. In: IEEE International Conference on Automation and Logistics, pp. 243–248 (2010)
124. Shen, H.S., Xiang, Y.: Postbuckling of nanotube-reinforced composite cylindrical shells under combined axial and radial mechanical loads in thermal environment. Compos. Part B Eng. **52**, 311–322 (2013)

125. Shim, K.H., Sawan, M.E.: Approximate controller design for singularly perturbed aircraft systems. Aircr. Eng. Aerosp. Technol. Int. J. **77**(4), 311–316 (2005)
126. Shirazi, F.A., Grigoriadis, K.M., Viassolo, B.: Wind turbine integrated structural and LPV control design for improved closed-loop performance. Int. J. Control **85**(8), 1178–1196 (2012)
127. Smith, W.R., Gramberg, H.J.J.: Mathematical modelling of moisture-induced panel deformation. J. Eng. Math. **43**, 347–366 (2002)
128. Song, B.J., Castillo-Chavez, C., Aparicio, J.P.: Tuberculosis models with fast and slow dynamics: the role of close and casual contacts. Math. Biosci. **180**(1–2), 187–205 (2002)
129. Sorchini, Z., Krein, P.T.: Formal derivation of direct torque control for induction motors using the singular perturbation method. In: IEEE 36th Power Electronics Specialists Conference, pp. 2422–2428 (2005)
130. Soto-Cota, A., Fridman, L.M., Loukianov, A.G., Canedo, J.M.: Power system singularly perturbed discontinuous control. In: Proceedings of the American Control Conference, vol. 3, pp. 2580–2585 (2004)
131. Soto-Cota, A., Loukianov, A.G., Canedo, J.M., Fridman, L.M.: Variable structure control of synchronous generator: singularly perturbed analysis. In: Proceedings of the 42nd IEEE Conference on Decision and Control, vol. 4, pp. 3513–3518 (2003)
132. Soto-Cota, A., Fridman, L.M., Loukianov, A.G., Canedo, J.M.: Variable structure control of synchronous generator: singularly perturbed analysis. Int. J. Control **79**(1), 1–13 (2006)
133. Srivastava, R.S.: On the vorticity distribution over a normal diffracted shock for small and large bends. Shock Waves **23**(5), 1–4 (2013)
134. Stoica, A., Berbente, S., Condurache, A.: Optimal flight control system for the lateral motion of a fighter aircraft. Rev. Roum. des Sci. Tech., Serie de Mecani. Appl. **45**, 277–293 (2002)
135. Subudhi, B., Morris, A.S.: Dynamic modelling, simulation and control of a manipulator with flexible links and joints. Robotics Auton. Syst. **41**(4), 257–270 (2002)
136. Subudhi, B., Morris, A.S.: Singular perturbation approach to trajectory tracking of flexible robot with joint elasticity. Int. J. Syst. Sci. **34**(3), 167–179 (2003)
137. Sun, M.J., Yan, G.G., Zhang, Y.J.: A design method of the complementary controller for multi-infeed hvdc transmission systems using singular perturbation theory. Adv. Mater. Res., pp. 766–770 (2013)
138. Taghirad, H.D., Khosravi, M.A.: Stability analysis and robust composite controller synthesis for flexible joint robots. IEEE/RSJ Int. Conf. Intell. Robots Syst. **3**, 2073–2078 (2002)
139. Touhami, O., Mezouar, A.E.K., Ibtiouen, R., Mekhtoub, S.: Sliding mode control and flux observer for a singularly perturbed model of an induction machine. IEEE Int. Conf. Ind. Technol. **1**, 108–114 (2004)
140. Tsang, K.M., Wang, J.: Design of second order sliding mode controller for synchronous generators based on singular perturbation method. Int. Conf. Power Syst. Technol. **1**, 333–338 (2002)
141. Vakil, M., Fotouhi, R., Nikiforuk, P.N.: End-effector trajectory tracking of a flexible link manipulator using integral manifold concept. Int. J. Syst. Sci. **42**(12), 2057–2069 (2011)
142. Vazquez, R., Krstic, M.: Thermal convection loop control by continuous backstepping and singular perturbations. Proc. Am. Control Conf. **6**, 3882–3887 (2005)
143. Vian, J.L., Moore, J.R.: Trajectory optimization with risk minimization for military aircraft. J. Guidance **12**(3), 311–317 (1989)
144. Waldmann, J.: Forced singular perturbations as theoretical background to a split-coordinate frame multirate strapdown terrestrial navigation algorithm. In: 4th International Conference on Control and Automation, pp. 28–32 (2003)
145. Wang, L.D., Cheng, S., Zhang, J.W., Hu, Y.: Control of a redundantly actuated power line inspection robot based on a singular perturbation model. In: IEEE International Conference on Robotics and Biomimetics, pp. 198–203 (2009)
146. Wang, Z.Y., Ghorbel, F.H.: Control of closed kinematic chains using a singularly perturbed dynamic model. In: 43rd IEEE Conference Decision and Control, vol. 1, 317–322 (2004)
147. Wang, Z.Y., Ghorbel, F.H.: Control of closed kinematic chains: a comparative study. In: Proceedings of the American Control Conference, pp. 2498–2503 (2006)

148. Wang, L.J., Mukaidani, H., Shen, X.M., Liu, X.Z.: Delay-dependent stability analysis for large-scale multiple-bottleneck systems using singular perturbation approach. In: IEEE Global Telecommunications Conference, pp. 1–5 (2008)
149. Wang, L.M., Sontag, E.D.: A remark on singular perturbations of strongly monotone systems. In: 45th IEEE Conference on Decision and Control, pp. 989–994 (2006)
150. Wang, Z.Y., Ghorbel, F.H., Dabney, J.B.: On the domain and error characterization in the singular perturbation modeling of closed kinematic chains. Proc. Am. Control Conf. **1**, 493–498 (2004)
151. Wang, C., Lin, W., Le, X.: Modelling of a PMSG wind turbine with autonomous control. Math. Prob. Eng. **2014**(1), 1–9 (2014)
152. Wilde, R.R., Kokotovic, P.V.: Stability of singularly perturbed systems and networks with parasitiecs. IEEE Trans. Autom. Control **17**(4), 245–246 (1972)
153. Winkelman, J.R., Chow, J.H., Allemong, J.J., et al.: Multi-time-scale analysis of a power system. Automatica **16**(1) 35–43 (1980)
154. Xia, J.K., Xin, M.: Bifurcation analysis for power system voltage stability based on singular perturbation method. In: International Conference on Electrical Machines and Systems, pp. 1811–1814 (2007)
155. Xie, R., Wang, X.M., Li, Y.: Neural network adaptive inversion control law design for a super-maneuverable aircraft. In: The 4th IEEE Conference on Industrial Electronics and Applications, pp. 3434–3437 (2009)
156. Xin, H., Gan, D., Huang, M., Wang, K.: Estimating the stability region of singular perturbation power systems with saturation nonlinearities: an linear matrix inequality based method. IET Control Theory Appl. **4**(3), 351–361 (2010)
157. Yablonsky, G.S., Mareels, I.M.Y., Lazman, M.: The principle of critical simplification in chemical kinetics. Chem. Eng. Sci. **58**(21), 4833–4842 (2003)
158. Yan, F.J., Wang, J.M.: Control of diesel engine dual-loop EGR air-path systems by a singular perturbation method. Control Eng. Pract. **21**(7), 981–988 (2013)
159. Yao, S., Mei, S., Hua, G.W.: One novel variable-speed wind energy system based on pmsg and super sparse matrix converter. In: International Conference on Electrical Machines and Systems, pp. 2384–2389 (2008)
160. Yoshida, Z., Morrison, P.J.: Unfreezing casimir invariants: singular perturbations giving rise to forbidden instabilities, e-prints, March 2013. arXiv:1303.0887
161. Zhang, Y., Nguyen, H., Naidu, D.S., Zou, Y., Cai, C.: Time scale analysis and synthesis for model predictive control. In: Proceedings of the WSEAS-NAUN 4th International Conference on Circuits, Systems, Control and Signals, pp. 27–32 (2013)
162. Zhang, J.M.: Existence of travelling waves in a modified vector-disease model. Appl. Math. Model. **33**(2), 626–632 (2009)
163. Zhang, R.J., Chen, Y.B.: Dual-loop feedback control of servo motor systems using singular perturbation method. Proc. Am. Control Conf. **6**, 4657–4662 (2003)

Index

C. Cai et al., *Finite Frequency Analysis and Synthesis for Singularly Perturbed Systems*, Studies in Systems, Decision and Control 78,
DOI 10.1007/978-3-319-45405-4